Double strand break repair within constitutive heterochromatin

Aikaterini Tsouroula

▶ **To cite this version:**

Aikaterini Tsouroula. Double strand break repair within constitutive heterochromatin. Genomics [q-bio.GN]. Université de Strasbourg, 2017. English. NNT : 2017STRAJ036 . tel-01737626

HAL Id: tel-01737626

https://theses.hal.science/tel-01737626v1

Submitted on 19 Mar 2018

HAL is a multi-disciplinary open access archive for the deposit and dissemination of scientific research documents, whether they are published or not. The documents may come from teaching and research institutions in France or abroad, or from public or private research centers.

L'archive ouverte pluridisciplinaire **HAL**, est destinée au dépôt et à la diffusion de documents scientifiques de niveau recherche, publiés ou non, émanant des établissements d'enseignement et de recherche français ou étrangers, des laboratoires publics ou privés.

UNIVERSITÉ DE STRASBOURG

ÉCOLE DOCTORALE DES SCIENCES DE LA VIE ET DE LA SANTE DE STRASBOURG

IGBMC – CNRS UMR 7104 – Inserm U 964

THÈSE présentée par :

Aikaterini TSOUROULA

soutenue le : **07 juillet 2017**

pour obtenir le grade de : **Docteur de l'université de Strasbourg**

Discipline/ Spécialité : Aspects moléculaires et cellulaires de la biologie

Double Strand Break Repair within constitutive heterochromatin

THÈSE dirigée par :

Dr. SOUTOGLOU Evi	DR, IGBMC, université de Strasbourg

RAPPORTEURS :

Dr. POLO Sophie	CR, Epigenetics and Cell Fate Center, Paris VII University, France
Dr. VAN ATTIKUM Haico	Professor, Leiden University Medical Center, The Netherlands

---

AUTRES MEMBRES DU JURY :

Dr. TARSOUNAS Madalena	Professor, CRUK/MRC Oxford Institute for Radiation Oncology
Dr. TORA Laszlo	DR, IGBMC, université de Strasbourg

To my grandmother...

Table of Contents

ADDENDIX

Kring Hansen, R.*[1], Mund, A.*[1], Lund Poulsen*[1], S., Sandoval, M., Klement, K., **Tsouroula, K.,** Tollenaere, M., Räschle, M., Soria, R., Offermanns, S., Worzfeld, T., Grosse, R., Brandt, D.T., Rozell, B., Mann, M., Cole, F., Soutoglou, E., Goodarzi, A.A., Daniel, J.A., Mailand, N., Bekker-Jensen, S. (2016). SCAI promotes DNA double-strand break repair in distinct chromosomal contexts. *Nature Cell Biology* 18, 1357-1366. doi: 10.1038/ncb3436.

Lemaitre, C., Grabarz, A.*[2], **Tsouroula, K.***[2], Andronov, L., Furst, A., Pankotai, T., Heyer, V., Rogier, M., Attwood, K.M., Kessler, P., Dellaire, G., Klaholz, B., Reina-San-Martin, B., Soutoglou, E. (2014). Nuclear position dictates DNA repair pathway choice. *Genes & development*. doi: 10.1101/gad.248369.114.

Acknowledgements

I would like to thank several people who have contributed to the conception, execution and writing of my thesis.

Firstly I would like to express my sincere gratitude to my supervisor Evi Soutoglou for giving me the chance to be part of her laboratory, working on challenging projects. Her motivation and immense knowledge as well as our fruitful discussions contributed to my personal and scientific improvement. I had the great opportunity to work with a woman like Evi having a brilliant professional career while being a great mother.

Besides my supervisor, I would like to thank the rest of my committee members Haico Van Attikum, Sophie Polo, Madalena Tarsounas and Laszlo Tora for their helpful suggestions and advice. My sincere thanks also go to Bernardo Reina-San-Martin for his great contribution to my project and his precious support. Moreover, I thank Niels Mailand for giving me the opportunity to participate in an interdisciplinary collaboration.

Furthermore, I am grateful to all current and past lab members for advice, criticism, reagents and their sense of humor. A special mention to my colleagues/friends Audrey, Luyba and Ioanna for their unconditional support, encouragement and help in scientific and non-scientific moments. My days in the lab would not have been the same without you.

I would like to give special credit to my friends Despoina, Christiana, Dimitris, Aineias and Thanasis that are by my side for many years, supporting me in good and bad moments. In particular, I'm grateful to Despoina and Christiana because, without their support and love, I wouldn't have successfully completed my Ph.D. I also feel extremely lucky that during these years of my Ph.D, I had the chance to meet people that I consider as new family members and truly good friends. There are no words to express my gratitude to Cathy and Kostas Hatzidiakos for always being by my side. I would also like to thank Adam, Federica, Federico and Alex for supporting me in my everyday life inside and outside of the lab.

Last but not least, I would like to thank my mom Maria, my aunt Niki, my uncle Vaggelis and my cousins Marialena and Konstantinos for their support but also criticism that has contributed to my self-improvement. Most of all, I want to thank my grandmother Katerina who is no longer with us. Without her unconditional love, support and trust I wouldn't have accomplished any goals in my life including the Ph.D.

My sincere thanks go to all these people who made my days with a smile during these years …

Abbreviations

53BP1	p53-Binding Protein 1
ACF1	ATP-utilizing Chromatin assembly and remodeling Factor 1
AID	Activation-Induced cytidine Deaminase
ALT	Alternative Lengthening of Telomeres
Alt-EJ	Alternative End-Joining
ANP32e	Acidic Nuclear Phosphoprotein 32 Family Member E
ATM	Ataxia - Telangiectasia Mutated
ATR	Ataxia Telangiectasia and Rad3 related
ATRIP	ATR Interacting Protein
BACH1	BTB domain and CNC Homolog 1
BBAP	B-Lymphoma- And BAL-Associated Protein
BIR	Break-Induced Replication
BLM	Bloom helicase
BMI1	B lymphoma Mo-MLV insertion region 1 homolog
BRCA1	Breast Cancer 1
BRCA2	Breast Cancer 2
BRCT	BRCA1 C Terminus
BRIT1	BRCT-repeat inhibitor of hTERT expression
CAF-1	Chromatin Assembly Factor 1
CBP	cAMP-regulated-enhancer (CRE) - Binding Protein
CD	ChromoDomain
CDK	Cyclin-Dependent-Kinase
CENP-A	Centromere Protein A
CHD	Chromodomain-Helicase-DNA binding
Chk1	Checkpoint kinase 1
Chk2	Checkpoint kinase 2
cNHEJ	classical NHEJ
CRISPR	Clustered Regularly Interspaced Short Palindromic Repeats
CSD	Chromo-Shadow Domain
CSR	Class Switch Recombination
DDR	DNA Damage Response
D-loop	Displacement-loop
DNAPK	DNA-dependent Protein Kinase
DNAPKcs	DNAPK catalytic subunit
DSB	Double Strand Break
DUBs	Deubiquitinating enzymes
ERCC1	Excision repair cross-complementing 1
ETTA1	Ewing tumor-associated antigen 1
EXD2	Exonuclease 3’-5’ domain-containing protein 2
EXO1	Exonuclease 1
FANCD2	Fanconi Anemia Complementation Group D2

FANCI	Fanconi Anemia Complementation Group I
FANCJ	Fanconi Anemia Complementation group J
FBH1	F-Box DNA Helicase 1
FLIP	Fluorescent loss in Photobleaching
FRAP	Fluorescent recovery after Photobleaching
GCN5	General Control Of Amino-Acid Synthesis 5
GO	Gene Ontology
gRNA	guide RNA
HATs	Histone Acetyltransferases
HC	Heterochromatin
HDACs	histone deacetylases
HELB	DNA Helicase B
HJ	Holliday-Junction
HJURP	Holliday Junction Recognition Protein
HMGN1	High Mobility Group Nucleosome Binding Domain 1
HP1	Heterochromatin Protein 1
HR	Homologous recombination
Igs	Immunoglobulins
IR	Ionizing Radiation
IRIF	Ionizing Radiation-Induced Foci
ISWI	Imitation Switch
KAP1	KRAB-associated protein-1
KDM2A	Lysine Demethylase 2A
LEDGF	Lens epithelium-derived growth factor
LINC	Linker of Nucleoskeleton and cytoskeleton
MBTD1	MBT domain containing 1
MDC1	Mediator of DNA damage checkpoint protein 1
MMSET	Multiple Myeloma SET domain
Mps3	Monopolar spindle 3
MRN	Mre11-RAD50-NBS1
MRX	Mre11-RAD50-XRS2
MSD	Mean Squared Displacement
MTA1	Metastasis Associated 1
NBS1	Nijmegen Breakage Syndrome 1
NHEJ	Non-Homologous End Joining
NuMA	Nuclear Mitotic Apparatus Protein 1
NuRD	Nucleosome Remodeling Deacetylase
PALB2	Partner and localizer of BRCA2
PAM	Protospacer Adjacent Motif
PARGs	poly-ADP-ribose glycohydrolases
PARPs	poly-ADP-ribosyl polymerases
PAXX	Paralog of XRCC4 and XLF
PcG	Polycomb Group

PHF11	Plant Homeodomain Finger 11
PNKP	Polynucleotide Kinase/Phosphatase
PP4C	Protein Phosphatase 4 catalytic subunit
PRMT5	Protein Arginine Methyltransferase 5
PTIP	PAX Transactivation activation domain- Interacting Protein
PTMs	Post-Translational Modifications
RECQ5	RecQ Like helicase 5
RIF1	RAP1-interacting factor 1
RNF20	Ring Finger Protein 20
RNF40	Ring Finger Protein 40
RNF8	Ring Finger protein 8
ROS	Reactive Oxygen Species
RPA	Replication Protein A
RSC	Chromatin structure remodeling
RSF1	Remodeling And Spacing Factor 1
RUVBL1	RuvB Like AAA ATPase 1
SCAI	Suppressor Of Cancer Cell Invasion
SDSA	Synthesis-Dependent Strand Annealing
SETD2	SET domain containing 2
SETDB1	SET Domain Bifurcated 1
SHM	Somatic hypermutation
SIRT6	Sirtuin 6
SIRT7	Sirtuin 7
SMARCAD1	SWI/SNF-related, matrix-associated actin-dependent regulator of chromatin, subfamily a, containing DEAD/H box 1
SMC	Structural Maintenance of Chromosome
SSA	Single Strand Annealing
ssDNA	single-stranded DNA
SWI/SNF	Switching defective/sucrose non-fermenting
TADs	Topologically Associated Domains
TCR	T cell receptors
TIP60	Tat interactive protein 60 kDa
TIRR	Tudor Interacting Repair Regulator
TopBP1	Topoisomerase II Binding Protein 1
TSS	Transcriptional Start Site
UBC16	Ubiquitin-Conjugating Enzyme 16
UCHL3	Ubiquitin carboxyl-terminal hydrolase isozyme L3
UHRF1	Ubiquitin-like PHD and RING finger protein 1
UIM	Ubiquitin Interaction Motif
USP11	Ubiquitin specific peptidase 11
USP26	Ubiquitin specific peptidase 26
USP37	Ubiquitin specific peptidase 37
UV	Ultraviolet

WRN	Werner syndrome helicase/exonuclease
WSTF	WITCH ATP-dependent chromatin remodeling complex
XLF	XRCC4-like factor
XRCC1	X-ray repair cross-complementing protein 1
XRCC3	X-ray repair cross-complementing protein 3
XRCC4	X-ray repair cross-complementing protein 4

Figures Index

Thesis Summary

DNA damage represents a very frequent event during cell cycle, occurring at a rate of 10^3 to 10^6 molecular lesions per cell per day. It can be subdivided into two main categories: endogenous damage occurring via normal metabolic processes inside cells and exogenous damage caused by external DNA damaging agents. Double-strand breaks (DSBs), in which both strands in the double helix are severed, are particularly hazardous to the cell because they can lead to genomic instability, chromosomal translocations, cellular transformation and cancer. DSBs activate the DNA Damage Response (DDR) pathway, a complex network of processes that allows recognition of the break and activation of the checkpoints, which pauses cell cycle progression, leaving time for the cell to repair the breaks before dividing. Cells repair DSBs via two major pathways: Homologous recombination (HR) and Non Homologous End Joining (NHEJ). HR requires the presence of an identical or nearly identical sequence to be used as a template for repair of the break, and it functions mainly during S and G2 phases, taking advantage of the information coded by homologous template to eliminate the DSB in an error-free manner. In this pathway, after break recognition, 3' single stranded DNA overhangs are generated by resection and subsequently bound by the heterotrimeric Replication Protein A (RPA), facilitating RAD51 loading, the key molecule for strand invasion, D-loop and Holliday-junction formation. DNA is synthetized according to the homologous template and thus genetic information, disrupted by the DSB, is restored. On the other hand, NHEJ is considered as an error-prone repair mechanism compared to HR, leading to re-ligation of the free DNA ends without the presence of a non-damaged template. In this case, breaks are recognized by the Ku80-Ku70 heterodimer, followed by the activation of a quick signaling cascade resulting in the rejoining of the broken ends. Ultimately, both HR and NHEJ lead to checkpoint activation and cell-cycle arrest. In case of persistent damage, apoptotic or senescence pathways are activated.

DNA repair occurs in the context of highly structured chromatin. Two structurally different types of chromatin can be distinguished: euchromatin (EC) and heterochromatin (HC), the latter being highly condensed and restricting DNA transactions. Thus DSB repair within heterochromatin is challenging. It has been shown that global and α-particle induced DNA damage results in heterochromatin expansion and re-localization of the breaks outside of the heterochromatin core domain. More specifically, in *Drosophila melanogaster* DSBs move outside of the HC domain to be repaired by HR that is finally completed at the nuclear pores. Although these studies have set the basis for understanding how DNA repair proceeds in chromatin dense regions, the underlying

mechanisms of DNA repair of heterochromatic breaks are not well understood. The goal of my PhD was to investigate DSB repair within heterochromatin in mammalian cells.

To address this question, we took advantage of the CRISPR (Clustered Regularly Interspaced Short Palindromic Repeats) system from *S. pyogenes* that consists of two components: Cas9, an endonuclease that generates DSBs and a guide RNA (gRNA) driving it to its target locus. Upon binding to its DNA target, Cas9 can induce one DSB three base pairs before the Protospacer Adjacent Motif (PAM) sequence, another determinant factor for its target specificity. In this case, we engineered a CRISPR/Cas9 system in which DSBs can be efficiently and specifically induced in heterochromatin of NIH3T3 mouse fibroblasts. More specifically, we have designed a gRNA targeting major satellite repeats of pericentric heterochromatin, which in mouse cells corresponds to the DAPI-dense regions known as chromocenters. Using high-resolution imaging and 3D reconstruction we find that in G1, both DDR and NHEJ (but not HR) are activated within the HC core domain, exemplified by the recruitment of Ku80 and several DDR markers. In G2, however, we find that both NHEJ and HR are activated. Nevertheless, contrary to NHEJ (occurring exclusively at the core), HR activity is spatially restricted. While RPA recruitment is observed at the core HC domain, RAD51 is entirely peripheral. This indicates that DNA-end resection and the search for homology are spatially separated and suggests that resected DNA ends re-localize to the HC periphery to perform the late steps of HR. Mechanistically, we show that DSB re-localization does not involve relaxation of the core HC structure, or the release of HP1s, but rather requires DNA end-resection and the active exclusion of RAD51 from the core HC domain.

To investigate whether the above results are specific to pericentric heterochromatin, we also used the CRISPR/Cas9 system to induce DSBs in centromeric heterochromatin, corresponding to centromeres of NIH3T3 mouse fibroblasts. In this case, we designed a gRNA against centromeric minor satellite repeats and we induced specifically DSBs in centromeres. In contrast to DSBs induced in pericentric heterochromatin, we showed that RAD51 is efficiently recruited at centromeric lesions both in G1 and G2, suggesting that in this case HR is active throughout the cell cycle. On the other hand, Ku80 is recruited in the same way as in pericentric heterochromatin. These results were published on the July 7th 2016 issue of *Molecular Cell*. Based on these data, we have provided insight into the temporal and spatial regulation of DSB repair pathways within heterochromatin in mammalian cells and we have shown striking differences in the mode of repair between centromeric and pericentric heterochromatin.

Following these recently published data, we are particularly interested in understanding the difference in the repair between centromeric and pericentromeric lesions. Although these two structures are highly condensed as typical examples of constitutive heterochromatin, they are characterized by different DNA sequence, chromatin modifications and histone variant composition. These differences could have an impact on the DNA repair outcome. More specifically, pericentric heterochromatin is enriched in H3K9me3 and HP1s that are considered the key markers of constitutive heterochromatin. On the other hand, nucleosomes of centromeres are enriched in CENP-A, an H3 histone variant (specific for centromeres) as well as in H3K36me2 and H3K4me2 that represent a more active chromatin environment. Our goal is to investigate if and how this unique structure of centromeric heterochromatin could allow RAD51 recruitment and thus HR activation throughout the cell cycle in comparison with pericentric heterochromatin where HR is inhibited in G1. To address this question, we are using two approaches: a candidate gene approach and an unbiased proteomics approach. For the candidate approach, we express different HR proteins in the cells and we check their recruitment at the Cas9-induced centromeric versus pericentromeric lesions in G1. Our previous finding that RAD51 is recruited in G1 in centromeres but not in pericentromeres suggesting differential activation of HR between these two structures is also supported by our new preliminary data since other HR proteins are mainly recruited at centromeres after damage induction. Moreover, the unique centromeric features seem to affect positively HR in G1 since RAD51 recruitment is decreased under *CENP-A* knockdown conditions. Similar results are obtained after knockdown of the specific for CENP-A histone chaperone *HJURP*.

Apart from the candidate approach and in order to identify novel factors that allow HR in centromeres in G1, we have performed unbiased proteomics experiments using the Bio-ID technology. In this technology, BirA* is used that is the promiscuous *E. coli* biotin ligase which biotinylates proteins in close proximity with it, in the presence of biotin. This allows for the efficient isolation of biotinylated proteins by using streptavidin-coupled beads that will then be submitted to identification by mass spectrometry. For our experiments, we have created an NIH3T3 cell line that stably expresses Cas9 fused to BirA*. This Cas9-BirA* is efficiently targeted to centromeres or pericentromeres upon expression of the corresponding gRNA, induces DSBs and biotinylates proteins in proximity as we have detected by immunofluorescence and western blot analysis experiments checking for different DDR factors and streptavidin staining respectively. These biotinylated proteins have been isolated using streptavidin-coupled beads and submitted to identification by mass spectrometry, revealing some interesting candidates that could be

implicated in HR activation in centromeres in G1. This project will shed light on the differences in DSB repair between two heterochromatic structures with different characteristics highlighting how the chromatin environment and not only the compaction can affect the outcome of the repair.

Apart from my own project, I also contributed to the project of another PhD student in the laboratory working on DNA repair pathway choice in different nuclear compartments. To test if the location of the break affects the repair outcome, we compared the repair of DSBs induced at the nuclear lamina or the nuclear pores versus the nuclear interior and we showed that breaks induced at the lamina fail to rapidly activate DDR and repair by HR in contrast to the other two nuclear compartments. They are also positionally stable, not moving to an HR permissive environment like the pores or the nuclear interior but instead they are repaired *in situ* by a highly mutagenic pathway. For this project, I performed all experiments related to the nuclear pores and I am second author (equal second) on this publication (*Genes & Development*, 2014). Additionally to my contribution on this project, I was also involved in an external collaboration leading to an authorship in *Nature Cell Biology* (2016). The authors identified a novel protein called SCAI (suppressor of cancer cell invasion) as a chromatin-associated protein that has a role in several DSB repair pathways in mammalian cells. For this project, I performed experiments using the CRISPR/Cas9 system to induce breaks in pericentric heterochromatin (described above in detail) under control and SCAI knockout conditions. These experiments revealed SCAI's key role in activating DDR in heterochromatin. The corresponding papers are included in the APPENDIX of this manuscript.

Thesis Summary in French

Les dommages de l'ADN sont des événements très fréquents au cours du cycle cellulaire. Ils se produisent à raison de 10^3 à 10^6 lésions moléculaires par cellule et par jour. Ils peuvent être subdivisés en deux catégories principales: les dommages endogènes issus de processus métaboliques cellulaires normaux, et les dommages exogènes causés par des agents externes. Les cassures doubles brins de l'ADN (DSBs), dans lesquelles les deux brins de la double hélice sont coupés, sont particulièrement dangereuses pour la cellule, car elles peuvent conduire à une instabilité génomique, des translocations chromosomiques, des transformations cellulaires et au cancer. Les DSBs activent la voie DDR (DNA Damage Response), une cascade de signalisation qui permet de reconnaître la cassure et d'activer des points de contrôle, ce qui interrompt la progression du cycle cellulaire, laissant le temps à la cellule de réparer les cassures avant de se diviser. Les cellules réparent les DSBs par deux voies principales: la recombinaison homologue (HR) et la jonction d'extrémités non homologues (NHEJ). La HR nécessite la présence d'une séquence identique ou quasi-identique à utiliser comme modèle pour la réparation de la cassure. Elle est activée principalement pendant les phases S et G2, en tirant avantage de l'information codée par la copie homologue qui servira de matrice pour éliminer la DSB sans faute. Dans cette voie, après la reconnaissance de la cassure, les extrémités d'ADN simple brin 3' sortantes sont générées par résection et ensuite liés par la protéine de réplication hétérotrimère A (RPA). Ceci facilite le chargement de RAD51, molécule clé pour l'invasion de brin et la formation de la boucle D et la jonction de Holliday. L'ADN est synthétisé selon le brin homologue et ainsi l'information génétique, lésée par la DSB, est restaurée. NHEJ est-elle considérée comme un mécanisme de réparation plus sujet aux erreurs que HR. En effet, cette voie conduit à la ligature des extrémités libres d'ADN sans la présence d'une matrice non-endommagée. Dans ce cas, la cassure est reconnue par l'hétérodimère Ku80-Ku70, suivie de l'activation d'une cascade de signalisation rapide conduisant à la religation des extrémités lésées. Finalement, HR et NHEJ conduisent à l'arrêt du cycle cellulaire. En cas de dommages persistants, les voies apoptotiques ou de sénescence sont activées.

La réparation de l'ADN se produit dans un contexte de chromatine très structurée. On distingue deux types de chromatines structurellement différentes: l'euchromatine (EC) et l'hétérochromatine (HC), cette dernière étant fortement condensée et limitant les accès à l'ADN. Ainsi, la réparation des DSBs au sein de l'hétérochromatine pourrait être difficile. Il a été montré que des lésions globales ou à particule α entrainent une expansion de l'hétérochromatine et une

relocalisation des cassures à l'extérieur du domaine central de l'hétérochromatine. Plus spécifiquement, chez *Drosophila melanogaster,* les DSBs se déplacent en dehors du domaine de HC pour être réparés par HR, ce qui est finalement accompli au niveau des pores nucléaires. Bien que ces études aient établi les bases pour comprendre comment la réparation de l'ADN se produit dans les régions denses de la chromatine, les mécanismes sous-jacents se produisant dans l'hétérochromatine ne sont pas bien connus. L'objectif de mon doctorat était d'étudier la réparation des DSBs dans l'hétérochromatine de cellules de mammifères.

Pour répondre à cette question, nous avons profité du système CRISPR (Clustered Regularly Interspaced Short Palindromic Repeats) de *S. pyogenes.* Ce système se compose de deux facteurs: Cas9 une endonucléase qui génère des DSBs et un ARN guide (gRNA) conduisant Cas9 à son locus cible. Lors de la liaison à sa cible d'ADN, Cas9 peut induire une DSB trois paires de bases avant la séquence Protospacer Adjacent Motif (PAM), ce qui participe également à la spécificité de sa cible. Dans ce cas, nous avons conçu un système CRISPR / Cas9 dans lequel les DSB peuvent être efficacement et spécifiquement induites dans l'hétérochromatine de fibroblastes de souris NIH3T3. Plus spécifiquement, nous avons conçu un gRNA ciblant les répétitions des satellites majeurs de l'hétérochromatine péricentrique, qui, dans les cellules de souris, correspond aux régions denses au DAPI appelées chromocentres. En utilisant la microscopie haute résolution et la reconstruction 3D, nous constatons qu'en G1, les voies DDR et NHEJ (mais pas HR) sont activées dans le cœur du domaine HC, mis en évidence par le recrutement de Ku80 et plusieurs marqueurs DDR. Cependant en G2, nous constatons que NHEJ et HR sont activées, mais spatialement séparées. Alors que NHEJ se produit exclusivement dans le cœur du domaine HC, HR est limitée en périphérie. En effet, bien que le recrutement de RPA soit observé au niveau du cœur du domaine HC, celui de RAD51 est entièrement périphérique. Ceci indique que la résection de l'extrémité de l'ADN et la recherche de l'homologie sont séparées spatialement et suggère que les extrémités d'ADN réséquées se relocalisent à la périphérie de HC pour effectuer les dernières étapes de HR. De plus, nous avons montré que la relocalisation de la DSB n'implique pas de relaxation du cœur du domaine HC, ou la libération des HP1s, mais nécessite plutôt la résection de la cassure de l'ADN et l'exclusion active de RAD51 du cœur du domaine HC.

Pour étudier si les résultats ci-dessus sont spécifiques à l'hétérochromatine péricentrique, nous avons également utilisé le système CRISPR / Cas9 pour induire des DSB dans l'hétérochromatine centromérique, correspondant aux centromères de fibroblastes de souris NIH3T3. Dans ce cas,

nous avons conçu un gRNA dirigé contre les répétitions des satellites mineures des centromères et nous y avons spécifiquement induit des DSBs. Contrairement aux DSBs induits dans l'hétérochromatine péricentrique, nous avons montré que RAD51 est efficacement recrutée au niveau des lésions centromériques à la fois en G1 et G2, ce qui suggère que HR est active tout au long du cycle cellulaire. D'autre part, Ku80 est recrutée de la même manière que dans l'hétérochromatine péricentrique. Ces résultats ont été publiés le 21 juillet 2016 dans *Molecular Cell*. A partir de ces données, nous avons donné un aperçu de la régulation temporelle et spatiale des voies de réparation des DSBs au sein de l'hétérochromatine dans les cellules de mammifères. Nous avons également montré des différences frappantes dans le mode de réparation entre l'hétérochromatine centromérique et péricentrique.

À la suite de ces données récemment publiées, nous sommes particulièrement intéressés à comprendre la différence de réparation entre les lésions centromériques et pericentromériques. Bien que ces deux structures, typiques de l'hétérochromatine constitutive, soient fortement condensées, elles sont caractérisées par des différences dans la séquence d'ADN, dans les modifications de la chromatine et dans la composition de variants d'histone. Ces différences pourraient avoir un impact sur le résultat de la réparation de l'ADN. Plus précisément, l'hétérochromatine péricentrique est enrichie en H3K9me3 et HP1s qui sont considérés comme les marqueurs clés de l'hétérochromatine constitutive. D'autre part, les nucléosomes de centromères sont enrichis en CENP-A, un variant d’histone H3 (spécifique des centromères) ainsi qu’en H3K36me2 et H3K4me2 qui représentent un environnement de chromatine plus actif. Notre but est d'étudier si cette structure unique de l'hétérochromatine centromérique pourrait permettre le recrutement de RAD51 et donc l'activation de HR tout au long du cycle cellulaire en comparaison avec l'hétérochromatine péricentrique où HR est inhibée en G1. Pour répondre à cette question, nous utilisons deux approches: une approche candidat et une approche non biaisée. Pour l'approche candidat, nous exprimons différentes protéines HR dans les cellules et nous vérifions leur recrutement dans les lésions centromériques induites par Cas9 comparé aux lésions péricentromériques en G1. Notre précédente découverte montrant que RAD51 est recruté en G1 dans les centromères mais pas dans les péricentromères, suggérant une activation différentielle de HR entre ces deux structures, est également soutenue par nos résultats préliminaires puisque d'autres protéines HR sont principalement recrutées aux centromères après l'induction de dommages. De plus, les caractéristiques centromériques uniques semblent affecter positivement la HR en G1 puisque le recrutement de RAD51 est diminué dans les

conditions de knockdown de CENP-A. Des résultats similaires sont obtenus après knockdown de la protéine chaperonne HJURP, spécifique de l'histone CENP-A.

En dehors de l'approche candidat et afin d'identifier de nouveaux facteurs qui permettent l'activité HR dans les centromères en G1, nous avons effectué des expériences de protéomique non biaisées en utilisant la technologie Bio-ID. Dans cette technologie, on utilise une variété de biotine ligase issue de E. coli, BirA *, qui biotinyle les protéines à sa proximité immédiate, en présence de biotine. Ceci permet l'isolement efficace de protéines biotinylées en utilisant des billes couplées à la streptavidine. Ces protéines seront ensuite identifiées par spectrométrie de masse. Pour nos expériences, nous avons créé une lignée cellulaire NIH3T3 qui exprime de manière stable Cas9 fusionné à BirA *. Ce Cas9-BirA * est efficacement ciblé sur les centromères ou les péricentromères selon l'expression de l'ARNg correspondant. Cela induit des DSB et biotinyle les protéines à proximité, contrôlé par le recrutement de différents facteurs DDR et la signalisation de streptavidine respectivement (mis en évidence par immunofluorescence et des analyses de Western blot). Ces protéines biotinylées ont été isolées en utilisant des billes couplées à la streptavidine et identifiées par spectrométrie de masse, révélant quelques candidats intéressants qui pourraient être impliqués dans l'activité de HR dans les centromères en G1. Ce projet mettra en lumière les différences dans la réparation des DSBs entre deux structures hétérochromatiques ayant des caractéristiques différentes, mettant ainsi en évidence comment l'environnement de la chromatine et sa compaction peut affecter l'issue de la réparation.

En dehors de mon projet, j'ai également contribué au projet d'un autre étudiant de doctorat dans le laboratoire, travaillant sur le choix des voies de réparation de l'ADN dans les différents compartiments nucléaires. Afin de tester si la localisation de la cassure affecte le choix de la réparation, nous avons comparé la réparation des DSBs induites à la membrane nucléaire (lamina) ou aux pores nucléaires par opposition à l'intérieur du noyau et nous avons montré que les cassures induites à la lamina ne permettent pas d'activer rapidement la DDR et de réparer par HR contrairement aux deux autres compartiments nucléaires. Ils sont également immobiles, ne se déplaçant pas vers un environnement permettant HR comme les pores ou l'intérieur du noyau, par contre ils sont réparés in situ par une voie très mutagène. Pour ce projet, j'ai réalisé toutes les expériences liées aux pores nucléaires et je suis second co-auteur de cette publication (*Genes & Development*, 2014). J'ai également participé à une collaboration externe menant aboutissant à une publication dans *Nature Cell Biology* (2016). Les auteurs ont identifié une nouvelle protéine appelée SCAI (supressor of cancer cell invasion) comme une protéine associée

à la chromatine qui a un rôle dans plusieurs voies de réparation des DSBs dans les cellules de mammifères. Pour ce projet, j'ai effectué des expériences utilisant le système CRISPR / Cas9 pour induire des cassures dans l'hétérochromatine péricentrique (décrit ci-dessus en détail) sur des cellules knockout pour SCAI comparé au contrôle. Ces expériences ont révélé le rôle-clé de SCAI dans l'activation de DDR dans l'hétérochromatine

1. Introduction

1.1 DNA lesions and genome integrity

Genetic information that is encoded in the nucleotide sequence of DNA defines all biological processes in all living organisms. Thus the maintenance of genome integrity is of key importance for cell survival and proper cell function. Genome integrity is constantly threatened by different damaging agents causing different types of molecular lesions in a rate of 10^3 to 10^6 per cell per day (Lindahl, 1993). DNA damage can be subdivided into two categories: endogenous damage occurring via normal metabolic processes inside cells and exogenous damage caused by external DNA damaging agents (Aguilera and Garcia-Muse, 2013; Hoeijmakers, 2001) (Figure 1.1A).

Representative examples of endogenous damage are the ROS produced by the oxidative respiration process or DNA hydrolysis reactions (like deamination) that lead to base modifications/conversions and consequently to base-pairs mismatches and mutations during replication. An additional challenge for the cells is the slowing or stalling of replication fork progression known as replication stress. When the replication fork cannot restart, it collapses leading to the formation of a DSB (Double Strand Break). Telomeres, as the ends of chromosomes, could resemble a broken part of DNA double-helix that could activate DNA repair pathways (de Lange, 2002). Though specific proteins protect them from being recognized as breaks creating a telomere cap structure, telomere shortening in mammalian cells leads to capping defects (de Lange, 2002). These de-protected telomeres are considered DSBs that can lead to chromosomal rearrangements and they are often used as a system to study DSB repair (Celli and de Lange, 2005; de Lange, 2002; Dimitrova et al., 2008). DNA lesions can also be induced by the cells in a programmed way in order to induce genetic variability in meiosis and in the establishment of immune responses repertoire (Alt et al., 2013; Baudat et al., 2013).

Regarding the exogenous sources of damage, different environmental factors are considered damaging agents. Firstly, the UV component of sunlight is one of the major external DNA damaging agent leading to different photoproducts such as cyclobutane pyrimidine dimers that can alter the structure of DNA and thus inhibit polymerases and arrest replication. Furthermore, IR produced by radioactive decay of naturally radioactive compounds or by radiotherapy causes various types of lesions, including DSBs. Radiomimetic drugs used in cancer chemotherapy have similar effect. Last but not least, tobacco products are well-known genotoxic chemicals inducing different types of lesions that are correlated with different types of cancer.

1.2 Physiological roles of DNA lesions

1.2.1 Meiosis. Meiosis ensures the proper segregation of chromosomes during sexual reproduction in eukaryotes. It has been shown that a programmed induction of DSBs happens at the first meiotic division leading to exchange of genetic material between homologous chromosomes and thus increasing genome diversity (Baudat et al., 2013). Moreover, it is essential for proper chromosome segregation (Baudat et al., 2013). The induction of DSBs is a highly regulated process catalyzed by the SPO11 enzyme that recognizes and cuts specific genomic regions called “recombination hotspots” (Keeney et al., 1997). SPO11-induced DSBs promote HR (HR is described in detail in 1.5.1) pairing of chromosome homologues leading to non-crossover and crossover products that can affect the genetic diversity.

1.2.2 V(D)J recombination. V(D)J recombination is a unique mechanism giving rise to the highly diverse repertoire of immunoglobulins (Igs) and T cell receptors (TCR) produced by B and T cells, respectively (Alt et al., 2013). Igs and TCRs have an N-terminal variable region consisting of the V(variable), D (diversity) and J (Joining) gene segments that are assembled in various combinations, resulting in different amino-acid sequences of the antigen binding regions of Igs and TCRs. This allows for the recognition of antigens nearly from all pathogens. This recombination process is mediated by DSBs induced by the lymphocyte-specific endonucleases RAG1 and RAG2 next to the V, D, J segments (Schatz and Baltimore, 2004). These segments are then fused through the NHEJ repair pathway (Taccioli et al., 1993) (NHEJ is described in detail in 1.5.2).

1.2.3 Class switch recombination and somatic hypermutation. Immunoglobulins produced by B cells during V(D)J recombination are further processed through the mechanism of Class Switch Recombination (CSR) and Somatic Hypermutation (SHM) (Alt et al., 2013). Somatic hypermutation introduces point mutations to the V region exons leading to the production of higher-affinity antibodies (McKean et al., 1984). Apart from the variable region of Igs that is altered through V(D)J recombination and SHM, the constant part of Igs is also modified through CSR to allow for production of different antibody isotypes that can interact with different effector molecules and consequently increase the efficiency of the immune response. Both SMH and CSR are mediated by the AID cytidine deaminase that catalyzes the deamination of cytosine to uracil (Pavri and Nussenzweig, 2011). Since uracil residues are not normally found in DNA, they are rapidly recognized and removed by a uracil-DNA glycosylase, thus creating an abasic site. In the case of SHM, error-prone DNA polymerases are then recruited to fill in the gap and create mutations

(Alt et al., 2013). On the other hand, during CSR, they are further converted to nicks and eventually DSBs that will be joined through NHEJ (Alt et al., 2013).

1.3 Role of DNA lesions in aging and pathology

In order to preserve their genome integrity, cells have developed different repair mechanisms for the different types of DNA lesions (Figure 1.1A). In case they are not properly repaired, DNA lesions can be correlated with ageing and cancer (Figure 1.1B). More specifically, it has been shown that DNA lesions accumulate with age in the nuclear and mitochondrial genome (Sedelnikova et al., 2004), inducing cell senescence and apoptosis that could be partially responsible for ageing (Garinis et al., 2008). Additionally, they are correlated with cancer since they lead to single point mutations, insertions and deletions that alter the expression of oncogenes or tumor-suppressor genes resulting in tumorigenesis (Lengauer et al., 1998). Another causal tumorigenesis factor is chromosomal translocations arisen from DSBs that are aberrantly rejoined and have different outcomes: creation of a chimeric fusion protein with oncogenic potential, fusion of an oncogene to a transcriptionally strong promoter or disruption of a tumor-suppressor gene (Roukos and Misteli, 2014).

Apart from ageing and cancer, DNA lesions are implicated in neurodegenerative disorders (Kulkarni and Wilson, 2008). Since neuronal cells have limited capacity to proliferate in adulthood, DNA damage can accumulate and possibly lead to neuronal dysfunction and degeneration (Kulkarni and Wilson, 2008; Rass et al., 2007). Moreover, neurons exhibit high mitochondrial respiration that creates ROS which can potentially lead to a significant amount of lesions (Weissman et al., 2007). Finally, since programmed DNA lesions are important for meiosis and immune system related processes, defects in their repair can lead to infertility or immune deficiencies (Alt et al., 2013; Matzuk and Lamb, 2008).

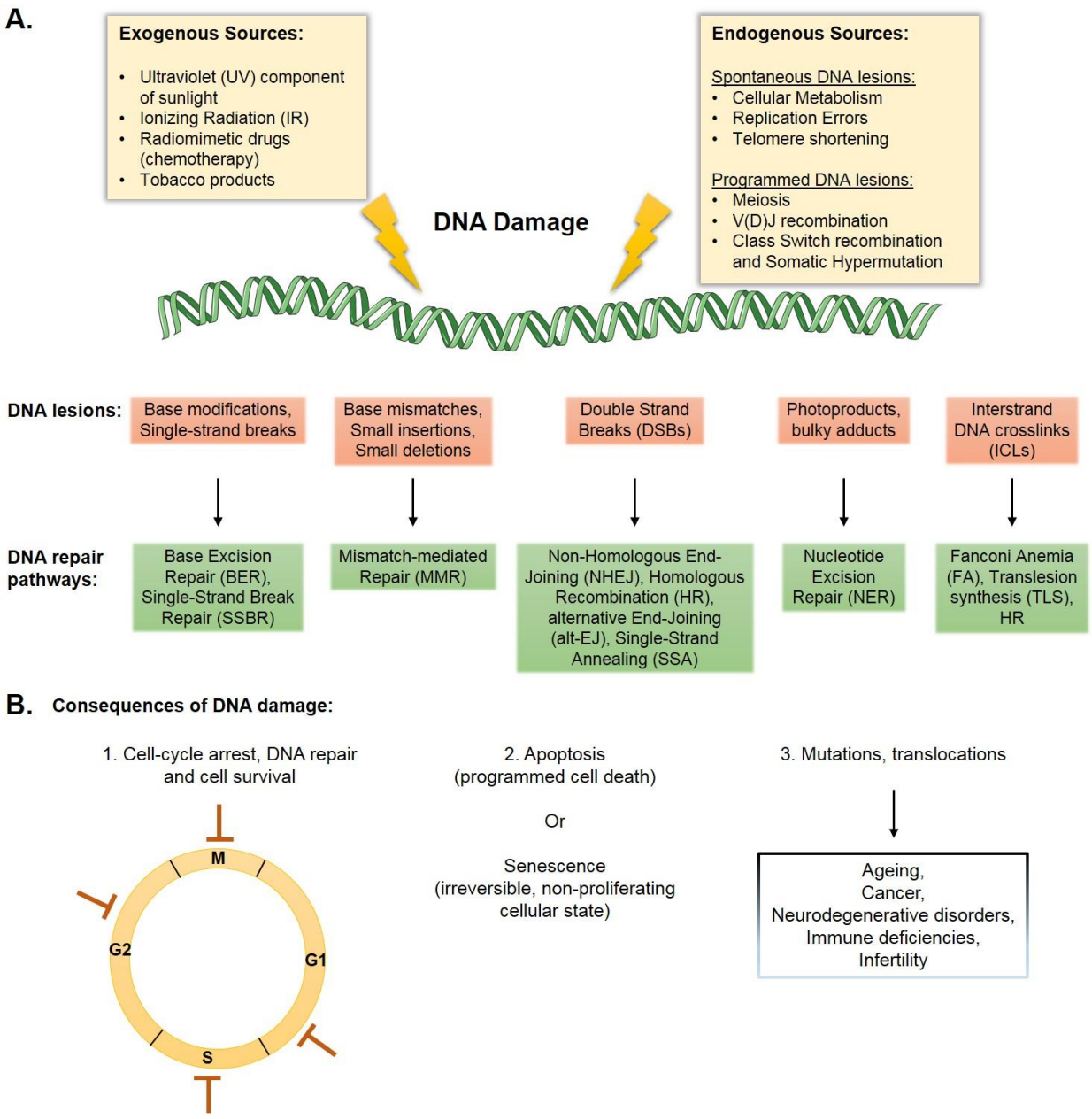

Figure 1.1: DNA lesions created by different damaging agents activate distinct repair pathways and can lead to different outcomes. A. Sources of DNA damage can be exogenous or endogenous. They lead to different types of DNA lesions that are repaired by specific repair pathways. Modified bases and single strand breaks are repaired by Base Excision Repair (BER) and Single-Strand Break Repair (SSBR), respectively. Mismatched-mediated Repair (MMR) is activated upon base mismatches, small deletions or insertions. DSBs are repaired by NHEJ, HR, Alt-EJ and SSA. Nucleotide Excision Repair (NER) is activated upon photoproducts and bulky adducts. Interstrand Crosslinks (ICLs) are repaired by the pathways of Fanconi Anemia (FA), Translesion Synthesis (TLS) and HR. **B.** Induction of damage leads to cell-cycle arrest and repair of the break (1). In case of excessive damage or not repaired breaks, apoptosis or senescence can be activated (2). In case the breaks are not repaired properly they can also lead to genome rearrangements leading to cancer and other pathological conditions (3).

1.4 Double Strand Breaks (DSBs) and the DNA Damage Response (DDR) pathway

Among the different types of DNA lesions described above, DSBs in which both strands of the double helix are severed, are particularly hazardous to the cell because they can lead to genomic instability, chromosomal translocations, cellular transformation and cancer (Jackson and Bartek, 2009). DSBs activate the DNA Damage Response (DDR) pathway, a complex network of processes that allows recognition of the break and activation of checkpoints, which pause cell cycle progression, giving time to the cell to repair the breaks before dividing (Bekker-Jensen and Mailand, 2010; Chapman et al., 2012b) (Figure 1.2). Several DDR factors are recruited at the sites of breaks in a highly ordered and hierarchical way creating the so called Ionizing Radiation-Induced Foci (IRIF) (Bekker-Jensen and Mailand, 2010). The early step of this signaling cascade involves the recognition of DSBs by different sensors (DSB recognition) that will subsequently recruit the Pl3K-like kinases ATM, ATR and DNAPK. These kinases will phosphorylate different DDR mediators (signal transduction) that will allow the amplification of the DDR signal (signal amplification) and regulate cell cycle progression by promoting cell cycle arrest, senescence or apoptosis (DDR outcomes).

1.4.1 DSB recognition.

Different sensors have been implicated in the recognition of DSBs (Figure 1.2A). The Ku70-Ku80 heterodimer rapidly recognizes and localizes at DSBs where it recruits DNAPKcs and initiates repair by NHEJ. On the other hand, the MRN/X complex composed by Mre11, RAD50 and NBS1/XRS2 proteins (MRN in mammalian cells and MRX in yeast) can be directly bound to double-stranded DNA ends through the Mre11 DNA binding domains (D'Amours and Jackson, 2002). Apart from mediating the DNA binding, Mre11 triggers the activation and recruitment of ATM kinase but it also initiates end-resection through its nuclease activity, a major step of HR (D'Amours and Jackson, 2002) (described in detail in 1.5.1). RAD50 that is a member of SMC family of ATPases, can also bind directly to DNA (D'Amours and Jackson, 2002). Its ATPase activity is necessary for DNA binding but also for the stimulation of Mre11 nuclease activity (Alani et al., 1990; Bhaskara et al., 2007). NBS1 interacts directly with Mre11, stabilizes the Mre11/RAD50 complex and is responsible for its localization in the nucleus (D'Amours and Jackson, 2002). Moreover, MDC1 is required for its accumulation at DSBs (Chapman and Jackson, 2008; Lukas et al., 2004; Spycher et al., 2008; Stucki et al., 2005) where it will then promote ATM activation (Falck et al., 2005) along with other mechanisms.

Parylation, a post-translational modification of proteins, has been implicated in DSB recognition (Beck et al., 2014b). It consists of the covalent addition of poly-ADP-ribose on protein substrates

catalyzed by poly-ADP-ribosyl polymerases (PARPs) and removed by poly-ADP-ribose glycohydrolases (PARGs) (Beck et al., 2014b). PARP inhibition renders cells sensitive to DNA damage, showing its role in the repair signaling cascade (Audebert et al., 2004; Boulton et al., 1999; Rulten et al., 2011). In line with these data, it has been shown that PARP1 and PARP3 are rapidly recruited to DSBs (Boehler et al., 2011; Haince et al., 2008; Langelier et al., 2012; Rulten et al., 2011). PARP1 has been shown to promote the recruitment of MRN complex and ATM kinase at the sites of breaks, thus participating in the early DDR signaling (Haince et al., 2007; Haince et al., 2008). Moreover, it was proposed that PARP1 favors HR and alt-EJ both by recruiting Mre11 and thus facilitating end-resection and by minimizing the association of NHEJ complexes at the sites of breaks (Bryant et al., 2009; Hochegger et al., 2006; Paddock et al., 2011; Wang et al., 2006). On the other hand, PARP3 seems to promote NHEJ through its interaction with the APLF histone chaperone to accelerate the XRCC4-DNA ligase IV-mediated ligation (Grundy et al., 2013; Rulten et al., 2011). Moreover, it was shown that PARP3 interacts with Ku heterodimer to protect DNA ends from end resection and thus promoting repair by NHEJ (Beck et al., 2014a). Thus, besides its role in the very first step of DDR, parylation through different PARPs can differentially affect DNA repair.

1.4.2 Signal transduction.

After break recognition, ATM, ATR and DNAPK kinases can be recruited to the sites of damage (Falck et al., 2005) (Figure 1.2A). Although all of them can phosphorylate the histone variant H2AX on S139 (γ-H2AX) in mammalian cells, ATM is the major kinase mediating the megabase spreading of γ-H2AX around the break (Falck et al., 2005; Tomimatsu et al., 2009). Recruitment of ATM at the sites of breaks is mediated by the MRN complex through its direct interaction with NBS1 (Difilippantonio et al., 2005; Lee and Paull, 2004, 2005). Moreover, the signal spreading factor MDC1 directly recognizes ATM-induced γ-H2AX through its C-terminal tandem BRCT repeats and is able to recruit additional ATM molecules at the sites of DSBs, thus creating a positive feedback loop that mediates the signal spreading around the break (Savic et al., 2009; Stucki et al., 2005). Upon damage, ATM that exists in the cells as an inactive homodimer, is activated through auto-phosphorylation on S1981 that leads its dissociation to an active monomer (Bakkenist and Kastan, 2003) that is further modified by different post-translational modifications. These modifications involve its autophosphorylation at different residues (Pellegrini et al., 2006; So et al., 2009) and its acetylation by the TIP60 acetyltransferase that are necessary for its activation (Sun et al., 2009; Sun et al., 2007; Yan et al., 2007). After being activated, ATM directly phosphorylates an extensive range of substrates including Chk2 and p53 that block the cell cycle

in G2/M phase (Matsuoka et al., 2000; Saito et al., 2002). Since Chk2 also phosphorylates directly p53 to block the cell cycle, it is possible that these two kinases work synergistically to ensure p53 activation.

ATR is another kinase that is recruited to DSBs but also to stalled replication forks (Falck et al., 2005). It is recruited at single-stranded DNA (ssDNA) through the interaction of its cofactor ATRIP with RPA (Zou and Elledge, 2003). RPA is a trimeric complex formed by a 70kDa (RPA1), a 32 kDa (RPA2) and a 14kDa (RPA3) subunit that binds ssDNA and protects it from degradation and secondary structures formation. RPA allows the recruitment of ATRIP that then interacts and promotes the recruitment of ATR at the sites of damage (Zou and Elledge, 2003). Similarly to ATM, ATR also needs to be activated upon its recruitment at DSBs. Apart from the RPA-bound ssDNA, the junction of ssDNA and dsDNA is also important for ATR activation. These ssDNA-dsDNA junction are recognized by the Rad17-RCF-5 clamp loader that in turn loads the ring-shaped Rad9-Rad1-Hus1 (9-1-1) clamp (Ellison and Stillman, 2003; Zou et al., 2003). Although in yeast it has been shown that the 9-1-1 (Ddc1-Rad17-Mec3) complex can directly activate Mec1 (yeast homolog of ATR) (Majka et al., 2006), a similar mechanism in vertebrates has not yet been described. Another major activator of ATR in yeast and mammalian cells is TopBP1 (or its yeast orthologue Dpb11) that can stimulate its activity even in the absence of damage (Kumagai et al., 2006; Mordes et al., 2008; Navadgi-Patil and Burgers, 2008). In addition, ETAA1 was recently identified as an RPA-binding factor that stimulates ATR activity independently of TopBP1 in mammalian cells (Bass et al., 2016; Haahr et al., 2016; Lee et al., 2016). ATR activation also requires Mre11 and ATM (Jazayeri et al., 2006; Myers and Cortez, 2006). After its activation, ATR phosphorylates all its interacting factors including Chk1 leading to cell cycle arrest. This phosphorylation is facilitated by the adaptor protein Claspin that interacts with Chk1 in a TopBP1-dependent way upon damage, thus mediating the interaction between Chk1 and ATR (Kumagai and Dunphy, 2003; Liu et al., 2006). After its phosphorylation, Chk1 dissociates from chromatin and phosphorylates its targets blocking the cell cycle progression (Smits et al., 2006).

DNAPK is a Pl3K-like kinase composed of Ku70, Ku80 and DNAPK catalytic subunit proteins (DNAPKcs) that has been shown to play a major role in NHEJ. As it was previously mentioned, working in a cooperative way with ATM, it can also phosphorylate H2AX, promoting the DDR signaling (Caron et al., 2015; Falck et al., 2005; Stiff et al., 2004). Moreover it has been reported that it phosphorylates the RPA2 subunit of RPA upon replication stress and ionizing radiation,

facilitating the S or G2/M cell cycle arrest (Block et al., 2004; Liaw et al., 2011; Liu et al., 2012a; Wang et al., 2001).

1.4.3 Signal amplification.

As previously mentioned, MDC1 is recruited at the sites of breaks through direct recognition of γ-H2AX, where it recruits more MRN-ATM complexes, thus creating a positive feedback loop for DDR signal amplification and spreading around the break (Chapman and Jackson, 2008; Lukas et al., 2004; Spycher et al., 2008; Stucki et al., 2005) (Figure 1.2A). After the exceedingly rapid accumulation of these factors, a second wave of protein accumulation starts at the sites of damage. The RNF8 E3 ubiquitin is recruited to DSBs through recognition of the ATM-induced phosphorylation residues of MDC1, where it subsequently ubiquitinates H2A and H1 histones and promotes recruitment of downstream effectors like 53BP1 and BRCA1 (Huen et al., 2007; Mailand et al., 2007; Thorslund et al., 2015). RNF168 is another E3 ubiquitin ligase recruited at the breaks in an RNF8-dependent manner that induces ubiquitination of H2A histones, thus enhancing 53BP1 and BRCA1 retention at DSBs (Doil et al., 2009; Mattiroli et al., 2012; Pinato et al., 2009).

BRCA1 is recruited to ubiquitinated chromatin regions through its interaction with the BRCA1 A complex (Huen et al., 2010). A central component of this complex is RAP80 that contains two ubiquitin interaction motifs (UIMs) that are directly bound to ubiquitinated histones after damage (Wu et al., 2009). RAP80 forms a complex with Abraxas, BRCC36, BRE and MERIT40 and BRCA1 is loaded on ubiquitinated histones through its interaction with Abraxas (Kim et al., 2007; Wang et al., 2007). BRCA1 recruitment at DSBs is also mediated by its major partner BARD1 through PARP recognition (Li and Yu, 2013). Moreover, ZMYM3 is a chromatin-interacting protein recruited to DSBs that interacts with Abraxas and RAP80, thus regulating BRCA1 recruitment at the sites of damage (Leung et al., 2017). On the other hand, 53BP1 can directly recognize and bind RNF168-induced ubiquitinated H2A histones (Fradet-Turcotte et al., 2013). After its binding (described in detail in 1.7.5), 53BP1 mediates the recruitment of RIF1 and PTIP at the sites of damage, two factors that have a role in the repair pathway choice (Gong et al., 2009; Jowsey et al., 2004; Munoz et al., 2007; Silverman et al., 2004).

1.4.4 DDR outcomes.

Cell cycle arrest is the major outcome of DDR that gives the cell time to repair the break before dividing (Figure 1.2B). As previously mentioned, ATM kinase phosphorylates Chk2 and p53 and ATR phosphorylates Chk1 (Bartek and Lukas, 2003). Chk1 phosphorylates Cdc25 phosphatases

leading to their degradation, thus blocking the dephosphorylation of CDK complexes, a step necessary for cell cycle progression (Bartek and Lukas, 2003). Through targeting Cdc25, cell cycle arrest can occur at G1/S transition, S phase or G2/M transition (Bartek and Lukas, 2003). Similarly Chk2 can induce cell cycle arrest by targeting Cdc25 (Bartek and Lukas, 2003). Additionally, it also phosphorylates and stabilizes p53, blocking the cell cycle progression in G1/S or leading to apoptosis if the break cannot be repaired (d'Adda di Fagagna, 2008). Alternatively, p53 can also induce cellular senescence that is the irreversible condition in which damaged cells remain metabolically active but they do not proliferate (d'Adda di Fagagna, 2008).

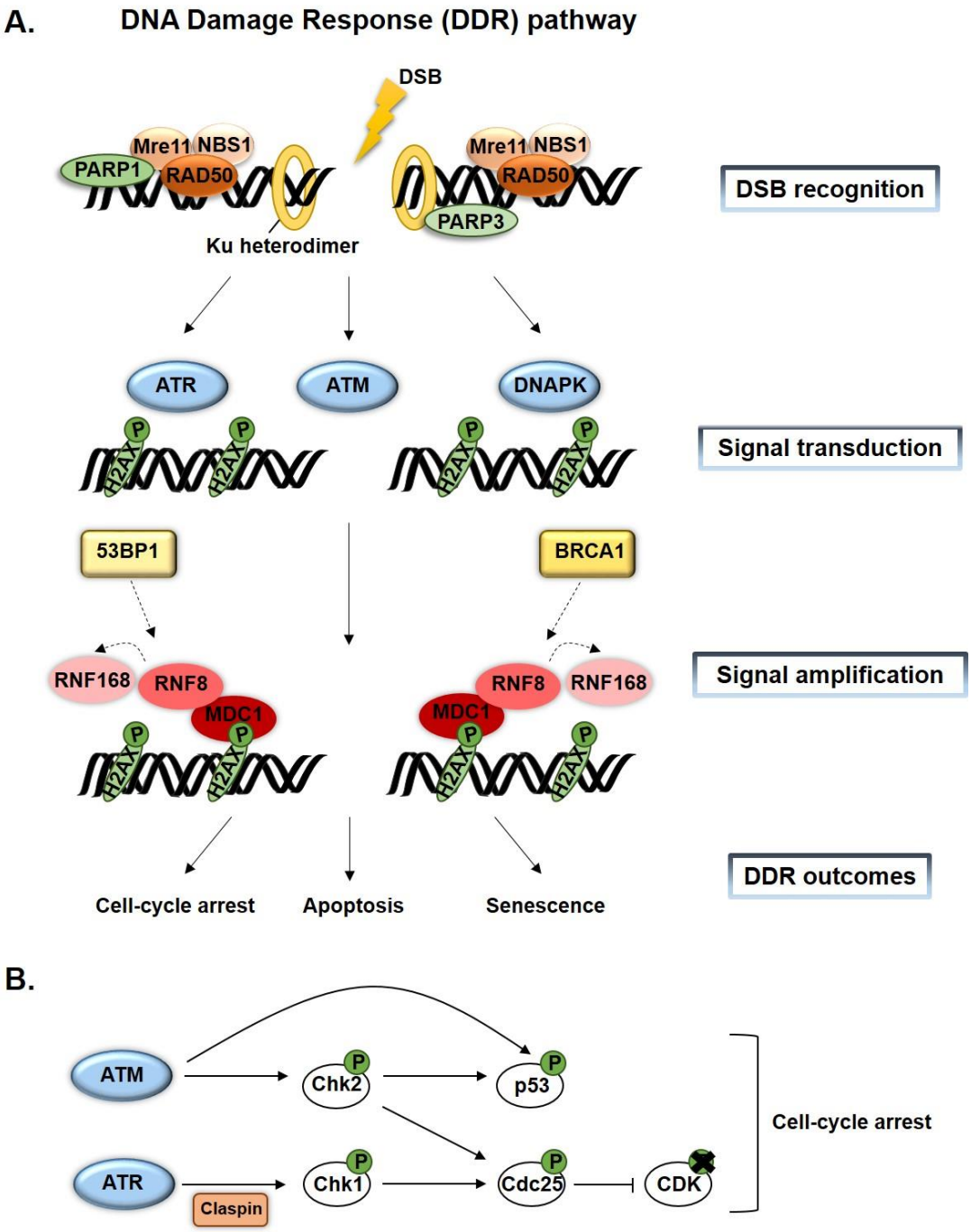

Figure 1.2: DSBs activate the DDR pathway. A. DDR starts with recognition of the break, a process that involves binding of MRN complex or Ku heterodimer facilitated by PARP1 or PARP3, respectively (DSB recognition). The Plk3-like kinases ATM, ATR and DNAPK are subsequently recruited through distinct mechanisms (not depicted in this figure) and phosphorylate downstream effectors as well as the histone variant H2AX (γ-H2AX) (Signal transduction). γ-H2AX is recognized by MDC1 that promotes RNF8 and RNF168 E3 ubiquitin ligases and thus 53BP1 and BRCA1 recruitment (Signal amplification). DDR will ultimately lead to cell-cycle arrest, apoptosis or senescence (DDR outcomes). **B.** Cell-cycle arrest is mediated by ATM and ATR kinases that phosphorylate Chk2 and Chk1, respectively. Chk2 phosphorylates p53 and Cdc25 to block the cell-cycle. Chk1 also blocks the cell cycle progression through phosphorylation of Cdc25. P represents phosphorylation events. All the factors depicted in this figure correspond to mammalian cells.

1.5 Double Strand Break repair pathways

Since DSBs can lead to genomic instability and tumorigenesis, they should be repaired fast and faithfully to avoid such a catastrophic cellular event. This is achieved through DNA repair mechanisms with extreme sensitivity in order to scan large genomes like the mammalian one, spot the DSB and repair it according to its location and the corresponding chromatin structure, the nature of the genomic sequence and the phase of the cell cycle. That is why there are different DSB repair pathways to repair a precise break in space and time (Chapman et al., 2012b). After DDR activation, different mechanisms can be subsequently involved to repair the breaks. The two main DSB repair pathways are Homologous Recombination (HR) and Non-Homologous End-Joining (NHEJ). More highly mutagenic pathways are also involved in DSB repair: alternative End-Joining (alt-EJ), Single Strand Annealing (SSA) and Break-Induced Replication (BIR).

1.5.1 Homologous Recombination (HR)

HR is an evolutionary conserved pathway from yeast to mammals (Jasin et al., 1985; Liang et al., 1998) (Figure 1.5A). It requires the presence of an identical or nearly identical sequence to be used as template for repair and thus it functions mainly in S/G2 phases, taking advantage of the sister chromatid to repair the break in an error-free manner (Jasin and Rothstein, 2013). The defining step of this pathway is the creation of 3' ssDNA that will subsequently invade into a homologous duplex and it will be used as a primer for the template-based repair synthesis. These 3' single-stranded overhangs will be created through a process called resection (Figure 1.4) and they will provide a substrate for RAD51 loading needed for strand invasion and subsequent D-loop and Holliday-Junction (HJ) formation. The D-loop represents the branching point of three different subpathways of HR (Heyer et al., 2010) (Figure 1.3). If a single-ended DSB invades, D-loop is transformed in a full-fledged replication fork and this repair subpathway is called Break-Induced Replication (BIR). This pathway can lead to loss-of-heterozygosity of all genetic information distal to the DSB. On the other hand, if there is a second end of DSB, it anneals with the resected strand of the first end in the Synthesis-Dependent Strand Annealing (SDSA), thus avoiding crossovers. SDSA seems to be the major subpathway in somatic cells. In contrast to this, double HJ formation subpathway leads to crossovers and that thus it is mainly used during meiotic recombination.

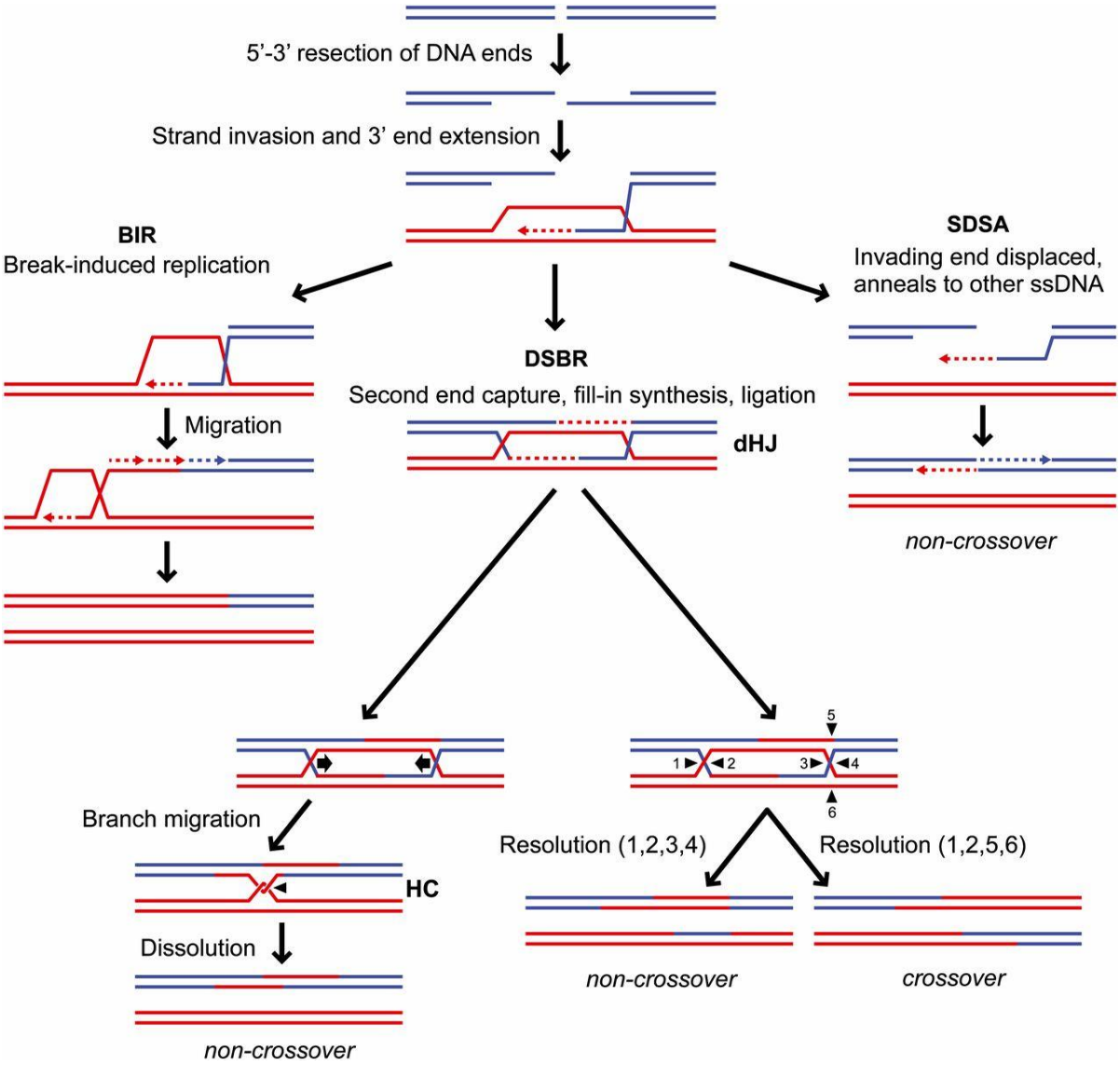

Figure 1.3: Subpathways of HR. The resected DNA ends invade an intact homologous duplex (in red) to start DNA synthesis. If a single-ended DSB invades, D-loop is transformed in a full-fledged replication fork and the complementary strand is synthesized by conservative replication. This repair subpathway is called Break-Induced Replication (BIR). If a double-ended DSB occurs, the 3' ssDNA end will pair with the donor duplex and DNA synthesis will start. Based on the classical double-strand break repair (DSBR) model, this newly synthesized DNA will be ligated to the 5' resected DNA end, creating a dHJ intermediate. The dHJ can be either dissolved by branch migration into a hemicatenane (HC) leading to noncrossover (NCO) products or resolved by endonucleolytic cleavage to produce NCO (positions 1, 2, 3, and 4) or CO (positions 1, 2, 5, and 6) products. In mitotic cells, the invading strand is often displaced after limited synthesis and the nascent complementary strand anneals with the 3′ single-stranded tail of the other end of the DSB and after fill-in synthesis and ligation generate exclusively NCO products (synthesis-dependent strand annealing, SDSA). Adapted from (Symington et al., 2014).

Break recognition and resection. DSBs are recognized by the MRN/X complex that will initiate resection, together with CtIP/Sae2 protein both in mammalian and yeast cells (D'Amours and Jackson, 2002; Huertas et al., 2008; Huertas and Jackson, 2009; Zhang et al., 2007) (Figure 1.5). CtIP is recruited to DSBs through its interaction with Mre11 and it promotes the recruitment of RPA and ATR kinase (Sartori et al., 2007). ATM also participates in end resection by stimulating the nucleolytic activity of CtIP and Mre11 to generate 3'-ssDNA overhangs (Bakr et al., 2015; Geuting et al., 2013; Yamane et al., 2013). After this initial processing of the DNA ends, extensive resection is needed to promote HR (Figure 1.4). Indeed, it has been shown in yeast that Mre11 and Sae2 mediate a short-range processing of DNA ends to form an early resected intermediate that will be rapidly and extensively processed further by Exo1 and Sgs1/DNA2 nucleases (Cannavo and Cejka, 2014; Garcia et al., 2011; Mimitou and Symington, 2008). Similarly in mammalian cells long-range resection involves BLM, DNA2 helicase/nuclease, EXO1, the MRN complex and RPA (Nimonkar et al., 2011). The MRN complex recruits BLM that interacts with DNA2 to resect DNA through their helicase and nuclease activity, respectively (Nimonkar et al., 2011; Sturzenegger et al., 2014). Apart from BLM, DNA2 also interacts with WRN helicase to promote resection (Pinto et al., 2016). BLM, MRN, RPA and the recently identified factor PHF11 also stimulate the activity of EXO1 to resect DNA ends (Gong et al., 2017; Nimonkar et al., 2011). EXD2 in another essential 3'-5' exonuclease that is recruited to DSBs through its interaction with CtIP and cooperates with Mre11 to promote resection (Broderick et al., 2016). Long range resection is also negatively regulated by the helicase HELB that is recruited to resected ends through RPA and inhibits EXO1 and BLM-DNA2 activity in mammalian cells using its 5'-3' ssDNA translocase activity (Tkac et al., 2016).

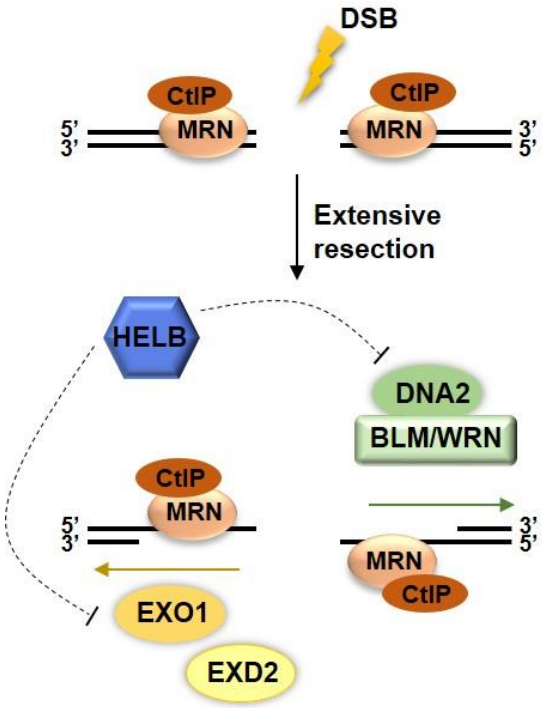

Figure 1.4: Short-range and extensive resection in HR. MRN complex and CtIP are needed for the first short-range processing of the two broken DNA ends. After this limited resection, the DNA ends are extensively processed by EXO1, EXD2 and DNA2 nucleases. DNA2 interacts with BLM or WRN helicases to promote resection. HELB helicase negatively affects resection.

End resection is also facilitated by BRCA1, using its N-terminal Ring domain with E3 ubiquitin ligase activity and its tandem C-terminal BRCT domains that can recognize phosphorylated proteins (Huen et al., 2010). Resection is promoted by binding to phosphorylated CtIP that is subsequently ubiquitinated by BRCA1, thus enhancing its association with damaged chromatin (Yu et al., 2006). The ssDNA ends produced by resection are protected by the heterotrimeric complex of RPA.

RAD51 assembly and strand invasion. RAD51 binds to the resected DNA ends to mediate the next step of HR. RAD51 is homologous to bacterial RecA ATPase and has been involved in HR after damage and during meiosis (Chen et al., 2008b; Shinohara et al., 1992). RPA binding at resected ends prevents the assembly of RAD51 nucleoprotein filaments (San Filippo et al., 2008). This inhibition is alleviated by RAD52 in yeast and BRCA2 in mammalian cells (Carreira and Kowalczykowski, 2011; Lisby et al., 2004; San Filippo et al., 2008; Sugawara et al., 2003). BRCA2 directly binds RAD51 allowing its polymerization and filament formation that will invade the homologous sequence forming a D-loop. The deubiquitinase UCHL3 is phosphorylated by ATM upon damage and it subsequently deubiquitinates RAD51 promoting its interaction with BRCA2 (Luo et al., 2016). It was recently reported that optimal loading of RAD51 on RPA-coated DNA ends depends on the DEK chromatin bound protein (Smith et al., 2017). BRCA1 is also involved

at this step of HR, since it interacts with PALB2, facilitating the loading of BRCA2 at the sites of breaks (Huen et al., 2010). PALB2 localization depends on the presence of MDC1, RNF8, RAP80 and Abraxas upstream of BRCA1 (Zhang et al., 2012). Moreover, PALB2 physically interacts with RNF168 in S/G2 facilitating HR (Luijsterburg et al., 2017). In addition, the recruitment of BRCA1-PALB2-BRCA2 complex at the sites of damage is also dependent on CDK9; depletion of CDK9 leads to failure to form BRCA1 and RAD51 foci at the sites of damage resulting in reduced HR efficiency (Nepomuceno et al., 2017). The RAD54 protein that is subsequently recruited promotes the stabilization of the D-loop but also regulates the transition to DNA synthesis by dissociating RAD51 from DNA (Heyer et al., 2006).

Five RAD51 paralogs sharing 20-30% sequence identity with human RAD51 have been identified (RAD51B, RAD51C, RAD51D, XRCC2 and XRCC3) that are recruited to the breaks together with RAD51 in S/G2 phase of the cell cycle (Rodrigue et al., 2006; Taylor et al., 2015; Thompson and Schild, 2001). XRCC3 depletion was shown to lead to a 25-fold decrease in DSB repair in hamster cells (Pierce et al., 1999) and knockout of all paralogs leads to chromosomal instability, spontaneous chromosomal breaks and reduced growth rates in chicken cells (Takata et al., 2001). This phenotype was partially rescued by RAD51 overexpression, showing that RAD51 paralogs might work as cofactors of RAD51. Moreover, RAD51 foci formation is significantly decreased in the absence of these RAD51 paralogs (Bishop et al., 1998; French et al., 2002; Taylor et al., 2015). RAD51B, RAD51D and XRCC2 deficient mice are embryonic lethal, something that highlights their importance (Deans et al., 2000; Pittman and Schimenti, 2000; Shu et al., 1999). Interestingly, these three RAD51 paralogs were also shown to participate in SSA in *Arabidopsis thaliana* (Serra et al., 2013).

1.5.2 Non-homologous end joining (NHEJ)

NHEJ is an evolutionary conserved repair pathway from prokaryotes to higher eukaryotes (Deriano and Roth, 2013; Shuman and Glickman, 2007) (Figure 1.5B). Though it was firstly shown that mammalian cells can efficiently join unrelated DNA fragments (Wilson et al., 1982), NHEJ factors that could mediate this process were also discovered later in prokaryotes, showing that this pathway is more evolutionarily conserved than initially thought (Aravind and Koonin, 2001; Shuman and Glickman, 2007; Weller et al., 2002). It does not require a homologous template for the repair, although microhomologies of one to six complementary bases can appear at the junctions and help to align the broken ends (Roth and Wilson, 1986). Moreover, NHEJ is active throughout the cell cycle, mainly in G1 (Rothkamm et al., 2003). In order to distinguish it from alternative NHEJ pathways that involve short homology sequences (Biehs et al., 2017; Wang and

Xu, 2017), it has been renamed classical NHEJ (cNHEJ). Except for alt-EJ, it was recently reported that cNHEJ in G1 can be resection-dependent involving CtIP, Mre11 exonuclease, EXD2, Exo1 as well as Artemis nuclease that completes this process (Biehs et al., 2017). Although resection-dependent cNHEJ could be an interesting concept for the induction of genomic instability and potentially translocations, more studies are needed to clarify its biological significance.

Break recognition. In this pathway, break recognition starts by the Ku70-Ku80 molecules forming a symmetric dimer that creates a protein ring around the broken helix of the DNA (Walker et al., 2001). Although this dimer is stably bound on DNA, *in vitro* evidence suggest that it could be displaced from breaks through a K48-linked ubiquitination mechanism (Postow et al., 2008). The involvement of ubiquitination in Ku heterodimer removal from DSBs was also confirmed by *in vivo* data in a more recent study (Brown et al., 2015). Ku has also been shown to limit DSB mobility keeping the two broken ends together; its depletion leads to increased mobility and separation of the two broken ends that can potentially increase the translocations frequency (Roukos et al., 2013; Soutoglou et al., 2007). In line with these data, mouse cells deficient for Ku80 have chromosomal instabilities (Difilippantonio et al., 2000). Combined with p53 depletion, these $Ku80^{-/-}$ cells develop B-cell lymphomas created by the translocation event between IgH and c-Myc loci, supporting the role of Ku80 in suppressing chromosomal rearrangements (Difilippantonio et al., 2000). Moreover, $Ku80^{-/-}$ mice have deficient V(D)J recombination since the Ku70-Ku80 heterodimer binds the RAG1/2-induced DSBs to start NHEJ, and although they are viable, they have growth defects (Nussenzweig et al., 1996; Zhu et al., 1996).

DNAPKcs recruitment. After the formation of the Ku70-Ku80 initial complex, DNAPKcs is recruited at the sites of damage through its interaction with Ku and induces an inward translocation of this dimer by about one helical turn (Dynan and Yoo, 1998; Gottlieb and Jackson, 1993; Yoo and Dynan, 1999). This allows DNAPKcs contact with an approximately 10bp-long DNA region at both termini (Yoo and Dynan, 1999). Its interaction with Ku stimulates its kinase activity which is necessary for the repair process (Singleton et al., 1999). Although DNAPKcs phosphorylates several NHEJ factors (Ku70-Ku80 (Chan et al., 1999), Artemis (Goodarzi et al., 2006; Ma et al., 2005), XRCC4 (Leber et al., 1998), XLF (Yu et al., 2008), DNA ligase IV (Wang et al., 2004)), these phosphorylation events are not required for efficient NHEJ, suggesting that probably there is a functional redundancy among them. This idea is supported by the functional redundancy of XRCC4 and XLF phosphorylation by DNAPKcs that promotes their dissociation

from DNA (Roy et al., 2012). Additionally to its phosphorylation targets, DNAPKcs is autophosphorylated in different sites that can have contradictory role in the regulation of DNA repair (Cui et al., 2005; Neal et al., 2011; Neal and Meek, 2011). Autophosphorylation leads to structural changes that are proposed to affect the ability of DNA end-processing enzymes and ligases to access the DNA ends and promote NHEJ (Dobbs et al., 2010; Neal et al., 2011). Accordingly it was shown that autophosphorylation of DNAPKcs is necessary for end-ligation by removing the physical blockage imposed by the DNAPKcs protein itself (Jiang et al., 2015). Apart from its autophosphorylation, DNAPKcs is also transphosphorylated by ATM, a step necessary for recruitment of the Artemis nuclease (Jiang et al., 2015). Mice depleted for DNAPKcs, though viable, are severely immunodeficient because of impaired V(D)J recombination but in contrast to Ku80, they do not exhibit any growth retardation (Gao et al., 1998; Taccioli et al., 1998). On the other hand, when expressing a catalytically inactive DNAPKcs protein, they show embryonic lethality, hypersensitivity to IR and increased neuronal apoptosis, suggesting that the catalytic activity in auto- and trans-phosphorylation and not the presence itself is important for repair but possibly also for other cellular processes (Jiang et al., 2015).

End processing. Compatible DNA termini that possess a 5' phosphate and a 3' hydroxyl can be directly ligated in contrast to more complex ones that need further processing. Complex DNA ends include chemically modified ends after irradiation-induced damage or hairpin structures like the ones created by the RAG1/2 nucleases. Processing of these ends can be catalyzed by the Artemis nuclease that interacts with DNAPKcs at the sites of breaks and can process complex DNA ends through its endonuclease activity (Ma et al., 2002). Artemis was initially identified as a protein involved in V(D)J recombination since its mutation leads to severe combined immune deficiency (Moshous et al., 2001). It has been reported that processing of DNA ends can also be performed by Ku80 (Roberts et al., 2010). Moreover, the polynucleotide kinase/phosphatase (PNKP) has been implicated in this process as an enzyme that phosphorylates 5'-OH DNA ends and dephosphorylates 3'-P ends, creating the correct chemical groups required for ligation (Chappell et al., 2002). Additionally, it was shown that the NHEJ factor XLF facilitates the gap filling of the broken ends through its interaction with polymerase λ and μ, further promoting their ligation (Akopiants et al., 2009). WRN was also shown to interact with Ku heterodimer and XRCC4 to process the broken DNA ends with its 3' to 5' exonuclease activity (and not its helicase activity) (Cooper et al., 2000; Kusumoto et al., 2008; Perry et al., 2006).

End joining. The XRCC4/DNA Ligase IV/ XLF complex will perform the last step of ligation between the two broken DNA ends. The ability of DNA ligase IV to ligate free DNA ends is stimulated by its interaction with XRCC4 at DSBs (Grawunder et al., 1997; Grawunder et al., 1998; Wilson et al., 1997). XLF (also named Cernunnos) was discovered as a factor mutated in an immunodeficiency syndrome with microcephaly and increased cellular sensitivity to IR and by a yeast-two hybrid screen for proteins that interact with XRCC4 (Ahnesorg et al., 2006; Buck et al., 2006). It shares structural similarities with XRCC4 and though it does not directly interact with DNA ligase IV, it stimulates the ligase activity of the complex (Andres et al., 2007; Riballo et al., 2009). Structural data of XRCC4-XLF complex support a model in which these two molecules bridge the two broken ends facilitating cNHEJ (Andres et al., 2012; Brouwer et al., 2016). PAXX was recently identified as a new NHEJ factor belonging to the XRCC4 superfamily (Ochi et al., 2015). Its depletion has no effect on the cellular sensitivity to radiomimetic drugs and on V(D)J recombination, suggesting its functional redundancy with another NHEJ factor (Liu et al., 2017). Indeed, its functional redundancy with XLF was shown, since it interacts with Ku70 and stimulates the activity of XRCC4/DNA ligase IV complex only under XLF depletion conditions (Liu et al., 2017; Tadi et al., 2016). Moreover, supporting these data, it was also reported that combined depletion of PAXX and XLF can lead to inability to join the RAG-induced DSBs during V(D)J recombination (Lescale et al., 2016).

Although $Ku80^{-/-}$ mice are viable, depletion of XRCC4 or DNA ligase IV leads to embryonic lethality, suggesting that these factors are involved in processes in which Ku is dispensable (Frank et al., 1998; Gao et al., 2000). More specifically, apart from its effect on V(D)J recombination, depletion of DNA ligase IV leads to growth defects and eventually lethality because of extensive apoptotic cell death in the embryonic central nervous system (Barnes et al., 1998; Frank et al., 1998). Similarly, disruption of XRCC4 leads to massive neuronal apoptosis (Gao et al., 2000). Although embryonic lethality caused by XRCC4 depletion is rescued by simultaneous depletion of p53 that blocks neuronal apoptosis, V(D)J recombination and lymphocyte development remains impaired and these mice develop B-cell lymphomas (Gao et al., 2000). As mentioned previously, though XLF depletion does not have any significant phenotype (Liu et al., 2017), combined depletion with PAXX leads to impaired V(D)J recombination (Lescale et al., 2016), showing the redundancy between these two factors. Apart from PAXX, XLF has redundant functional role with two DDR factors, ATM and 53BP1. Although ATM or 53BP1 deficiency has minor effect on V(D)J recombination, combined depletion with XLF almost blocks mouse

lymphocyte development (Liu et al., 2012b; Oksenych et al., 2012; Zha et al., 2011). Similar results were obtained for depletion of DNAPKcs and XLF (Oksenych et al., 2012).

The depletion phenotypes of various NHEJ factors described above show the major role of this pathway not only in the proper development and response of the immune system but also in the maintenance of genomic stability. Representative examples are Ku80 and XRCC4 whose depletion, combined with disruption of p53, leads to increased translocation events leading to B-cell lymphoma formation (Difilippantonio et al., 2000; Gao et al., 2000). Moreover, invasive bladder tumors have been correlated with reduced Ku binding at the sites of breaks and increased error-prone repair involving microhomologies (Bentley et al., 2004; Bentley et al., 2009). Although NHEJ seems to protect genome integrity, Ghezraoui et al. showed that it can also be involved in the formation of chromosomal translocations in human cells (Ghezraoui et al., 2014) but this mechanism needs to be further investigated.

1.5.3 Alternative end-joining (Alt-EJ)

Alt-EJ is considered a backup mechanism in yeast and mammalian cells, being activated when cNHEJ is impaired (Figure 1.5C). In yeast, it has been shown that Ku70 promotes accurate repair and its depletion activates error prone pathways leading to deletions before ligation (Boulton and Jackson, 1996). Moreover, alt-EJ is activated during CSR and V(D)J recombination in cNHEJ-deficient cells and it increases the frequency of translocations when cNHEJ is not functional (Corneo et al., 2007; Yan et al., 2007; Zhu et al., 2002). On the other hand, RAG-mutant cells that are proficient for cNHEJ, activate robustly alt-EJ (Corneo et al., 2007). Additionally, alt-EJ was reported to be activated at the significant frequency when both HR and cNHEJ are also available (Truong et al., 2013). Though cNHEJ factors have been identified in different bacteria, it is worth mentioning that *E.coli* does not have these factors but instead it uses an alternative NHEJ repair pathway characterized by extensive end resection (Chayot et al., 2010). Altogether these data suggest that alt-EJ might have emerged as a distinct pathway with a specific biological function during evolution, apart from being a mechanism used when cNHEJ is not functional (Sfeir and Symington, 2015).

Break recognition and Resection. Different factors have been implicated in alt-EJ but the exact underlying mechanism of this pathway is still unclear (Sinha et al., 2016; Wang and Xu, 2017). The recognition step of the breaks depends on PARP1 that competes with Ku for the binding to the DNA (Audebert et al., 2004; Wang et al., 2006). Consistently, PARP1 was reported to favor

alt-EJ during CSR (Robert et al., 2009). After break recognition, alt-EJ shares the initial step of end resection with HR, though in this case it is significantly limited (Truong et al., 2013). Similarly to HR, the nuclease activity of Mre11 is important to stimulate resection in this repair pathway (Deriano et al., 2009; Ma et al., 2003; Rass et al., 2009; Truong et al., 2013; Xie et al., 2009). The resection activity of CtIP also has an essential role in alt-EJ since its depletion leads to defects of this pathway in CSR of cNHEJ-deficient cells and to significantly less translocations (Boboila et al., 2010; Lee-Theilen et al., 2011; Zhang and Jasin, 2011). On the other hand, BLM/Exo1 in mammalian cells and Sgs1-DNA2/Exo1 in yeast that promote long-range resection seem to suppress alt-EJ, most likely because extended resection will favor HR in contrast to small microhomologies that will promote alt-EJ (Deng et al., 2014; Truong et al., 2013). RPA binding to resected ends was shown to prevent spontaneous annealing between microhomologous sequences in yeast and mammalian cells (Ahrabi et al., 2016; Deng et al., 2014). Data regarding the role of BRCA1 in this pathway are more contradictory. It has been reported in chicken B cells that BRCA1 does not affect alt-EJ (Yun and Hiom, 2009) in contrast to human cells where it works as a suppressor of this pathway as was also shown for BRCA2 and RAD51 (Ahrabi et al., 2016). Moreover, it was shown that BRCA1 and CtIP promote alt-EJ at uncapped telomeres (Badie et al., 2015).

End processing and final joining. Polθ is another player of alt-EJ pathway that catalyzes overhang extension and thus promotes alt-EJ in *Drosophila* and mammalian cells (Chan et al., 2010; Yu and McVey, 2010). In the case of uncapped telomeres and irradiated human cells, it was shown that Polθ is recruited by PARP1 and promotes alt-EJ at the expense of HR (Mateos-Gomez et al., 2015). More specifically, Polθ contains RAD51 binding motifs that mediate the interaction between the two proteins, leading to inhibition of RAD51-mediated recombination (Ceccaldi et al., 2015). Apart from its replication activity, it was also suggested that it promotes DNA synapse formation and strand annealing (Kent et al., 2015). The final ligation step is mediated by the XRCC1-Ligase III complex, although a role of Ligase I has also been described (Boboila et al., 2012; Dutta et al., 2016; Simsek et al., 2011). Though depletion of Ligase I has no effect on the translocation frequency, depletion of Ligase III significantly decreases it. This decrease is further enhanced by simultaneous depletion of Ligase I, suggesting that Ligase III acts as the major ligase of alt-EJ and Ligase I works as a backup (Simsek et al., 2011).

In contrast to NHEJ protective role in genome integrity as described in, alt-EJ has been suggested as the main mechanism leading to translocations in mouse cells. Depletion of CtIP and Ligase I

and III exhibit decreased translocation frequency (Simsek et al., 2011; Zhang and Jasin, 2011). Additionally, genomic analysis of different types of breast cancer and leukemias revealed that they are characterized by microhomologies associated with alt-EJ, further pointing its role in tumorigenesis (Stephens et al., 2009; Zhang and Rowley, 2006).

1.5.4 Single Strand Annealing (SSA)

Apart from HR and alt-EJ, resected DSBs can also be repaired by SSA (Figure 1.5D). SSA differs from HR since it does not need a donor sequence for the repair and thus it does not involve strand invasion and RAD51 activity (Sung, 1997). Instead, it occurs in repeated sequences where it uses resection to reveal and then anneal exposed complementary ends, forming a synapse intermediate (Bhargava et al., 2016). Although the molecular mechanism of this pathway is better described in yeast, homologues of some yeast factors have also been identified in mammalian cells (Bhargava et al., 2016). These factors include CtIP and RPA that participate in end resection of SSA (Bhargava et al., 2016). Annealing of the resected complementary ends is mediated by the RAD52 DNA binding protein (Sugawara et al., 2003; Symington, 2002). Before the ligation step, the synapse intermediate is processed in order to remove the 3' ssDNA ends that are not homologous and to fill in any gaps by polymerases. The cleavage of 3' ssDNA ends is performed by the ERCC1/XLF complex's nucleolytic activity (Motycka et al., 2004). However, the specific polymerases and ligases required for completion of this pathway are not yet known.

SSA is considered a highly mutagenic pathway since it results in deletion rearrangements between homologous repeats corresponding to significant loss of genetic information. Although it is mutagenic, its conservation though evolution raises the question of its functional significance for the cells. Different scenarios could explain why SSA can be favored under certain conditions. For example, it might be important to repair breaks that have undergone extensive resection and they cannot be repaired by HR or alt-EJ. Alternatively, it could be used when the sister chromatid is not yet available for repair by HR. Future studies will shed light on the factors and the cellular context that favors SSA versus other DNA repair pathways, also highlighting the reasons of its conservation through evolution.

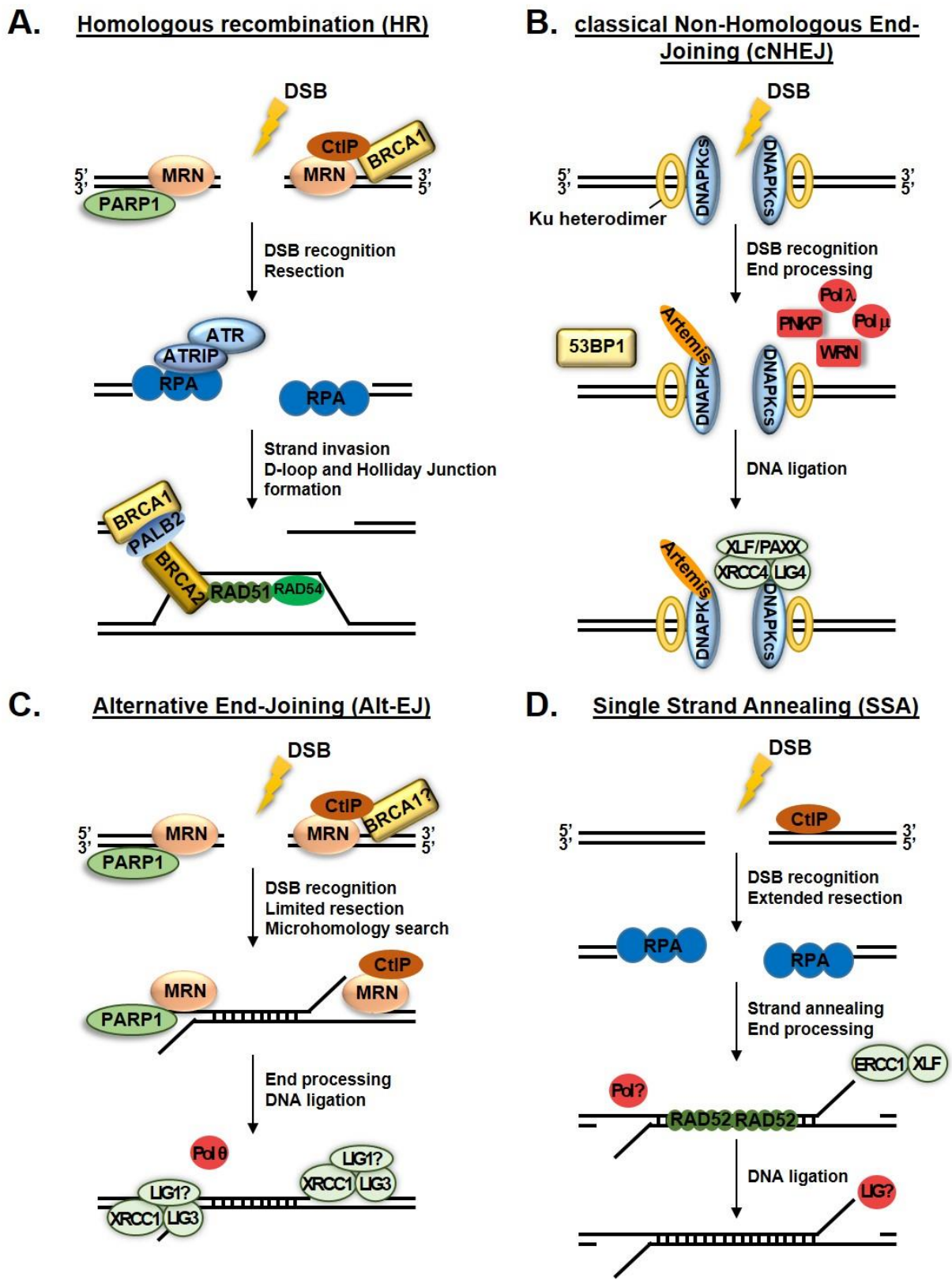
A.
Homologous recombination (HR)
DSB
CtIP
BRCA1
MRN
MRN
PARP1
5'
3'
3'
5'
DSB recognition
Resection
ATR
ATRIP
RPA
RPA
Strand invasion
D-loop and Holliday Junction
formation
BRCA1
PALB2
BRCA2
RAD51
RAD54
B.
classical Non-Homologous End-
Joining (cNHEJ)
DSB
DNAPKcs
DNAPKcs
Ku heterodimer
DSB recognition
End processing
Pol λ
PNKP
Pol μ
WRN
53BP1
Artemis
DNAPKcs
DNAPKcs
DNA ligation
XLF/PAXX
XRCC4
LIG4
Artemis
DNAPKcs
DNAPKcs
C.
Alternative End-Joining (Alt-EJ)
DSB
CtIP
BRCA1?
MRN
MRN
PARP1
DSB recognition
Limited resection
Microhomology search
CtIP
MRN
MRN
PARP1
End processing
DNA ligation
Pol θ
LIG1?
XRCC1
LIG3
LIG1?
XRCC1
LIG3
D.
Single Strand Annealing (SSA)
DSB
CtIP
DSB recognition
Extended resection
RPA
RPA
Strand annealing
End processing
ERCC1
XLF
Pol?
RAD52
RAD52
DNA ligation
LIG?

Figure 1.5: DSBs are repaired by HR, cNHEJ, alt-EJ or SSA. A. HR. Break recognition is mediated by PARP1 and the MRN complex. CtIP is subsequently recruited to initiate resection in parallel with Mre11. Resected ends are protected by RPA that recruits ATR kinase through ATRIP. Strand invasion is then mediated by BRCA1-PALB2-BRCA2 complex that facilitates Rad51 loading. Rad54 is also recruited to stabilize the D-loop. **B.** c**NHEJ.** DSB is recognized by Ku heterodimer that subsequently recruits DNAPKcs. DNA ends are then processed by different factors including Artemis, PNKP, WRN, Polλ and Polμ. Afterwards, XRCC4-LIG4-XLF/PAXX mediates the ligation of the two broken ends. **C. Alt-EJ.** Break recognition is mediated by PARP1 and the MRN complex. CtIP is recruited to initiate resection in parallel with Mre11. Resection is limited and facilities the microhomology search. The ends are then ligated by XRCC1-LIG3 (or LIG1) complex. Polθ is involved in the filling of gaps before ligation. **D. SSA.** Resection proteins like CtIP are involved in the first step of break recognition. Resected ends are bound by RPA and the homologous ssDNA segments are annealed through the activity of Rad52. Then, they are ligated after being processed by the ERCC1-XLF complex.

1.6 Regulation of DNA repair pathway choice

As previously described, DSBs can be repaired mainly by four different pathways. cNHEJ and HR, the two main DSB repair pathways, are differentially activated during the cell cycle whereas alt-EJ is mainly activated when cNHEJ is impaired. On the other hand, SSA is specifically used to repair DSBs in repetitive DNA sequences. In order to maintain genomic stability, the choice among these repair pathways is highly regulated by the cell cycle, the different factors competing to specifically favor a pathway as well as the chromatin structure and the associated proteins. These regulatory mechanisms of DNA repair pathway choice will be described below.

1.6.1 Role of end resection in DNA repair pathway choice

As previously mentioned, end resection is a process involved in three different repair pathways, HR, alt-EJ and SSA. The extent of resection needed for each pathway significantly differs; Alt-EJ requires end processing of a relatively small number of base pairs, whereas commitment to HR and SSA needs extensive resection (Ceccaldi et al., 2016). Mre11 and CtIP catalyze the first step of limited resection and additional helicases and exonucleases mediate the second step of long range resection. Given that end resection is a major step for three repair pathways, it is reasonable that it has a major role in the choice among them. Different factors compete to promote or inhibit resection in a cell-cycle dependent manner and thus having a crucial role in the DNA repair pathway choice.

This competition among the repair pathways already starts from the break recognition by the Ku heterodimer or the MRN complex. In yeast, it has been shown that Mre11 and Sae2/CtIP can start limited resection that is enough to reduce the ability of Ku to bind to DSBs since their depletion leads to increased amounts of Ku bound to DSBs (Zhang et al., 2007). Moreover, depletion of NHEJ factors leads to increased Mre11 recruitment and subsequent end resection (Clerici et al., 2008; Zhang et al., 2007; Zierhut and Diffley, 2008). In line with this, Ku-deficient cells are able to start resection in G1 (Clerici et al., 2008; Zierhut and Diffley, 2008). Interestingly, Ku70 is also downregulated during meiosis where HR is the pathway used to establish genetic variability (Goedecke et al., 1999). Thus, the competition between Ku and Mre11 is well established but future studies are needed to define if it takes place at the binding level or afterwards.

Further regulation of resection occurs through the competition between 53BP1 and BRCA1 (Panier and Boulton, 2014) (Figure 1.6). Although the mechanism for their recruitment shares

some common DDR factors, their localization at DSBs is mutually exclusive as it was revealed using super-resolution microscopy (Chapman et al., 2012a), suggesting that these two factors have distinct functions. Indeed, 53BP1 was shown to negatively regulate resection in G1 (Bothmer et al., 2010). On the other hand, BRCA1 promotes the removal of 53BP1 in S-phase to allow resection; cells depleted for BRCA1 are characterized by impaired resection that allows the inappropriate activation of NHEJ in S phase leading to chromosomal rearrangements (Bunting et al., 2010). These rearrangements combined with the embryonic lethality of $BRCA1^{-/-}$ mice are rescued by depletion of 53BP1, highlighting the role of these two proteins to regulate the transition between NHEJ and HR (Bouwman et al., 2010; Bunting et al., 2012; Bunting et al., 2010; Cao et al., 2009). The differentially regulated recruitment of these factors plays an indirect but also crucial role in the repair pathway choice and it is described in detail in 1.7.5.

53BP1 is phosphorylated by ATM but these phosphorylation sites are not necessary for its localization, suggesting that they mediate interactions with other effector proteins (Bothmer et al., 2011) (Figure 1.5). One such protein is RIF1 that similarly to 53BP1 is required for cNHEJ and is removed from DSBs in S/G2 in a BRCA1- and CtIP-dependent manner (Chapman et al., 2013; Di Virgilio et al., 2013; Escribano-Diaz et al., 2013; Feng et al., 2013; Silverman et al., 2004). More specifically, BRCA1 promotes the dephosphorylation of 53BP1 through the PP4C phosphatase in G2, leading to RIF1 release and thus allowing resection (Isono et al., 2017). An additional regulatory mechanism that facilitates HR in S phase is the ubiquitination of RIF1 by the UHRF1 E3 ubiquitin ligase that is specifically recruited to breaks through BRCA1 and induces its dissociation from 53BP1 (Zhang et al., 2016). In contrast to 53BP1 depletion, loss of RIF1 does not fully rescue the resection deficient phenotype of $BRCA1^{-/-}$ cells (Feng et al., 2013), suggesting that another protein may be involved in the attenuation of HR to favor NHEJ. Indeed, PTIP is another effector protein that recognizes ATM-phosphorylated 53BP1 and its depletion partly restores resection of $BRCA1^{-/-}$ cells (Callen et al., 2013; Gong et al., 2009; Jowsey et al., 2004; Munoz et al., 2007; Yan et al., 2011). Though their role in NHEJ is well reported, the interplay between RIF1 and PTIP binding to 53BP1 needs to be further investigated.

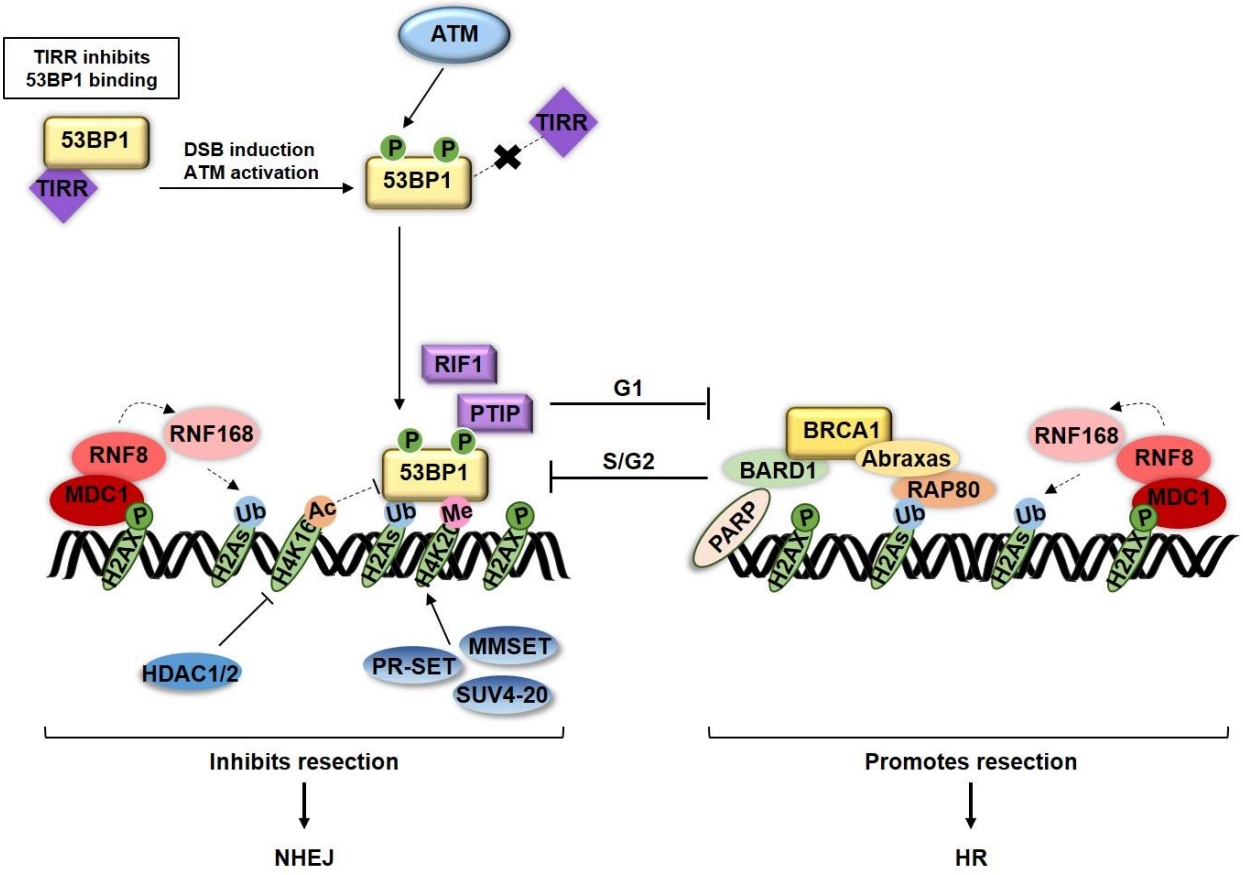

Figure 1.6: 53BP1 and BRCA1 compete to inhibit and promote resection, respectively. 53BP1 is recruited to the sites of damage by recognizing RNF8- and RNF168-ubiquitinated H2A histones as well as H4K20me2 induced by MMSET and the sequential activity of PR-SET and SUV4-20 enzymes. Recognition of H4K20me2 is inhibited by TIRR that interacts with 53BP1 and masks its methyl-binding domain. H4K16Ac also blocks the binding of 53BP1. After DSB induction, ATM phosphorylates 53BP1 disrupting its interaction with TIRR and promoting its interaction with RIF1 and PTIP. Interaction with these factors lead to inhibition of end resection and thus promotion of NHEJ. On the other hand, RAP80 recognizes ubiquitinated H2As and then interacts with Abraxas that also brings BRCA1. Moreover, BRCA1-cofactor BARD1 promotes its recruitment to the breaks through recognition of parylation. BRCA1 works in competition with 53BP1 to promote resection and HR. P, Ub and Me represent phosphorylation, ubiquitination and methylation events, respectively.

As it becomes obvious from the data described above, cells have the ability to switch from 53BP1 and NHEJ in G1 to BRCA1 and resection in S/G2. Cell-cycle regulated phosphorylation of CtIP plays a role in this process. CtIP/Sae2 is phosphorylated by CDK1 (Ser267 in Sae2 and Thr847 in CtIP) to promote efficient end-resection in S phase in yeast and mammals (Huertas et al., 2008; Huertas and Jackson, 2009). Moreover, it is phosphorylated on a distinct residue (Ser327) to promote its recognition by BRCA1 and thus the creation of a CtIP-MRN-BRCA1 complex

specifically in S/G2 to allow resection (Chen et al., 2008a; Greenberg et al., 2006). The finding that RIF1 is not removed from DSBs in a CtIP phospho-mutant, suggests that this CtIP-MRN-BRCA1complex triggers the removal of 53BP1-RIF1 to promote resection (Escribano-Diaz et al., 2013). Furthermore, cell-cycle dependent phosphorylation of BACH1, a cofactor of BRCA1, allows their binding only in S/G2 phase in order to promote resection (Dohrn et al., 2012). Moreover, the BRCA1 A complex that facilitates BRCA1 loading on DSBs is not enriched in G1, further supporting the idea of a cell-cycle regulated recruitment of BRCA1 at the sites of breaks (Hu et al., 2011). Cell-cycle regulated phosphorylation of DNA2 in yeast and EXO1 in mammalian cells seems to promote resection in G2 (Chen et al., 2011; Tomimatsu et al., 2014). More specifically, impairment of EXO1 phosphorylation attenuates resection and increases NHEJ in G2 (Tomimatsu et al., 2014). Moreover, CDK-phosphorylation of NBS1 in S, G2 and M phases of the cell cycle seems to be necessary to promote HR (Falck et al., 2012). In contrast to this study, it was recently reported that the same phosphorylation site of NBS1 is necessary for cNHEJ activation at deprotected telomeres (Rai et al., 2017).

Apart from phosphorylation events, cell cycle stage can affect the pathway choice by other means. More specifically, the interaction between BRCA1 and PALB2-BRCA2 is regulated by the presence of the USP11 de-ubiquitinase that is cell-cycle specific (Orthwein et al., 2015). The BRCA1-interacting region of PALB2 is constitutively ubiquitinated blocking the interaction of these two proteins (Orthwein et al., 2015). In S/G2, USP11 is stabilized and catalyzes the deubiquitination of PALB2 allowing its interaction with BRCA1 (Orthwein et al., 2015). On the other hand, in G1, USP11 is rapidly degraded after damage induction, thus the interaction of PALB2 with BRCA1 remains blocked and HR cannot happen (Orthwein et al., 2015).

1.6.2 Role of RAD51 in homology based repair pathway choice

Once resection has occurred, cNHEJ is inhibited but HR, SSA and alt-EJ can be used to repair DSBs. As described above, RPA binds to resected ends protecting them from degradation and formation of secondary structures, but it also suppresses alt-EJ, thus favoring HR or SSA (Deng et al., 2014). Moreover, it blocks RAD51 loading and this inhibition is alleviated by BRCA2 for mammalian cells and RAD52 for yeast in order to promote the next step of strand-invasion in HR (Carreira and Kowalczykowski, 2011; Esashi et al., 2007; Moynahan et al., 2001; Sugawara et al., 2003; Symington, 2002).

On the other hand, negative regulators of RAD51 loading have also been identified that could favor alt-EJ and SSA that are RAD51-independent repair processes. These factors include the Srs2 yeast helicase and the PARI mammalian helicase that were shown to remove RAD51 nucleofilaments through an active ATP-driven process (Chiolo et al., 2005; Krejci et al., 2003; Moldovan et al., 2012). Depletion of Srs2 was shown to allow undesirable HR and in parallel reduces alt-EJ and SSA, showing that it has a regulatory role in the balance between HR, alt-EJ and SSA (Chiolo et al., 2005; Krejci et al., 2003). The RECQL5 mammalian helicase also limits HR by disrupting RAD51 filaments and thus it promotes synthesis-dependent strand-annealing (SDSA) (Islam et al., 2012). Two more helicases, FANCJ and FBH1 also promote disassembly of RAD51 filaments, possibly having a role in error-prone pathways (Simandlova et al., 2013; Sommers et al., 2009). Additionally, Polθ was shown to block RAD51 loading and thus favor alt-EJ (Mateos-Gomez et al., 2015).

Depletion of RAD51 itself in mammalian cells upregulates RAD52-mediated SSA activity (Bennardo et al., 2008), suggesting that these two pathways compete for the repair of DSBs. A competitive relationship between these two factors has also been reported for heterochromatic DSBs where depletion of RAD52 leads to their increased localization at the periphery of heterochromatin where RAD51 is recruited (Tsouroula et al., 2016). Additionally, it has been shown that increased loads of DSBs exhaust the available amount of 53BP1 that can bind to damaged chromatin, leading to hyper-resection of these breaks; these hyper-resected DSBs are increasingly unable to load RAD51, promoting its complete replacement by RAD52, further highlighting the interplay between HR and SSA repair pathways (Ochs et al., 2016). Though depletion of RAD52 has no effect on cell growth and viability of mammalian cells, it becomes synthetically lethal with deficiency in BRCA1, PALB2 and BRCA2 HR factors, showing that SSA can work as a backup pathway when HR is not available (Lok et al., 2013).

1.7 Double Strand Break repair in the context of highly-structured chromatin

Upon damage induction, chromatin undergoes different structural changes that involve differences in histone composition, post-translational modifications of histones and the respective interactive proteins such as different chromatin remodelers. According to the “Prime, Repair, Restore” model, damaged chromatin first becomes more accessible to enable DNA repair and after repair is accomplished, chromatin organization is restored (Soria et al., 2012). Thus, chromatin structure and the corresponding factors that can alter chromatin landscape can differentially regulate DDR and DSB repair, also participating in the DNA repair pathway choice.

The impact of chromatin on the different steps of DDR and DSB repair pathways is described below.

1.7.1 Hierarchical organization of chromatin

Chromatin is the structure in which DNA is packaged into the cells through different hierarchical folding steps (Bickmore and van Steensel, 2013; Bonev and Cavalli, 2016) (Figure 1.7). Nucleosome, the first step of this folding process, is the fundamental unit of chromatin and it is composed of 147 base pairs of DNA wrapped around an octamer of the four core histones (H3, H4, H2A and H2B)(Luger et al., 1997). Nucleosomes are connected through short DNA segments called linker DNA, which is also bound by the H1 linker family of histones (Hergeth and Schneider, 2015). Thus, the primary structure of chromatin is a linear arrangement of nucleosomes forming an approximately 10nm fiber that is informally called “beads on a string” (Luger et al., 2012). This 10 nm fiber is further folded in a secondary chromatin structure of 30nm fiber (Luger et al., 2012). Although *in vitro* studies with reconstituted chromatin have suggested different models for the folding of this structure, its existence *in vivo* is still debatable (Tremethick, 2007). The next level of chromatin folding emerges from the interaction of *cis* regulatory elements, leading to the formation of chromatin loops (Lieberman-Aiden et al., 2009; Rao et al., 2014). These loops can be parts of the Topologically Associated Domains (TADs) that are megabase-scale domains of chromosomes, in which regions within the same TAD interact with each other more frequently than with regions located in other domains (Dixon et al., 2012; Nora et al., 2012; Sexton et al., 2012). It has also been suggested recently that long-range interactions of different TADs can give rise to interaction compartments but their functional distinction is not well understood (Wang et al., 2016). Coalescence of compartments of the same chromosome forms the so called chromosome territories, corresponding to the specific regions each chromosome occupies in the nucleus (Lichter et al., 1988; Pinkel et al., 1988).

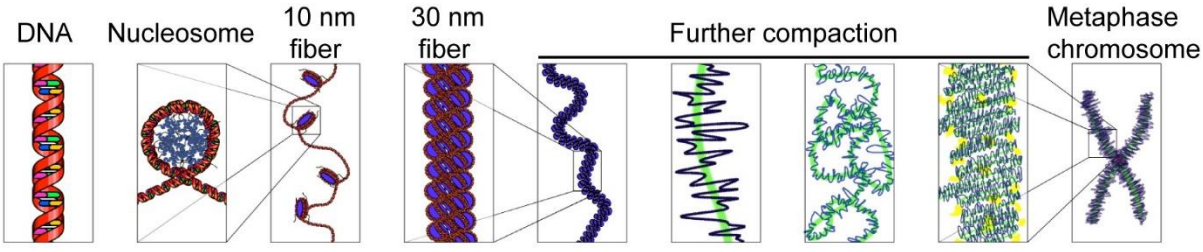

Figure 1.7: Higher order chromatin structure. Different levels of chromatin compaction are depicted. The 10 nm fiber or ‘beads on a string’ represents the first level of eukaryotic DNA compaction, which is further compacted into the 30 nm fiber. The 30 nm fiber gets organized in loops that are further compacted. The highest level of compaction is reached in mitotic chromosomes. Adapted from: https://commons.wikimedia.org/wiki/File:Chromatin_Structures.png.

1.7.2 Regulation of chromatin structure and function

Although chromatin is compacted to fit in the eukaryotic nucleus (as described in 1.7.1), its accessibility is also necessary for different DNA-templated processes such as transcription, replication, repair and recombination. To acquire access to these diverse processes, chromatin structure can undergo very dynamic changes through post-translational modifications (PTMs) of histones, incorporation of histone variants and activity of ATP-dependent chromatin remodelers.

1.7.2.1 Histone post-translational modifications

All core histones consist of two main domains: a globular one that lies within the nucleosomal core and a flexible one corresponding to the N- or C-terminal tails that protrude from the nucleosome core (Luger et al., 1997). Although both histone core domains and histone tails can be modified, only modifications of histone tails will be analyzed below since they are important for the remainder of this manuscript. The last decades, many studies have addressed the question of how these histone tails can be modified and what is their functionality, having identified till now at least 15 different types of modifications and hundreds of different modifiable residues (Huang et al., 2014). Acetylation, phosphorylation and methylation are the best studied small covalent modifications of histones that will be briefly mentioned below (different histone modifications including these 3 are reviewed in (Bannister and Kouzarides, 2011; Kouzarides, 2007)). Acetylation is a highly dynamic modification of histone lysines that is regulated by the opposing action of two families of enzymes, histone acetyltransferases (HATs) and histone deacetylases (HDACs) (Shahbazian and Grunstein, 2007). By neutralizing the positive charge of lysine, acetylation reduces affinity of histones for DNA and diminishes nucleosome-nucleosome interactions thus creating a more “open” chromatin state (Shahbazian and Grunstein, 2007). Another histone modification that affects chromatin structure is phosphorylation that adds a significant negative charge on serines, threonines and tyrosines (Rossetto et al., 2012). This modification is regulated by kinases and phosphatases that add and remove a phosphate group from the histones tails, respectively (Rossetto et al., 2012). Methylation of lysines and arginines of histones, though it does not change their charge, also has a major impact on chromatin structure being correlated with different levels of compaction and distinct DNA regulatory elements such as enhancer and promoters (Greer and Shi, 2012). This modification increases the level of complexity since lysines can be mono-, di- or tri-methylated, whereas arginines may be mono- or di-methylated (Greer and Shi, 2012). Different methyltransferases perform these different modifications that can be removed by specific histone demethylases (Greer and Shi, 2012). All histone modifications have a dual functional role establishing different chromatin

environments and serving as binding platforms for different factors that mediate specific DNA processes. The correlation of specific modifications recognized by specific proteins for different processes led to the “histone code” hypothesis, which postulated that different combinations of histone marks can serve as a code that leads to distinct biological outcomes (Jenuwein and Allis, 2001).

1.7.2.2 Histone variants

Histone variants are paralogues of the so called “canonical” core histones (H3, H2A and H2B; H4 does not have identified variants in higher eukaryotes), with distinct expression and distribution pattern that affects the structural and functional properties of chromatin (Buschbeck and Hake, 2017; Talbert and Henikoff, 2017) (Figure 1.8). Though the canonical histones are incorporated in the nucleosomes during replication, histone variants deposition can happen throughout the cell cycle, something that is directly correlated with the timing of their transcription. Canonical histones are encoded by multiple genes that are mainly organized into clusters and they are expressed in high and equal levels during S-phase of the cell cycle, allowing efficient chromatin folding (Albig et al., 1997). On the other hand, histone variants are mainly encoded by a single gene that is not part of the canonical histone clusters and thus can be expressed and incorporated in the nucleosomes in a variant-specific way (Buschbeck and Hake, 2017). Both canonical and variant histone proteins, after they are expressed, they are properly folded and deposited into chromatin through the action of different histone chaperones (Gurard-Levin et al., 2014; Hammond et al., 2017). Histone variants and histone chaperones (through incorporation of different histones) can alter chromatin dynamics that subsequently affects different DNA processes.

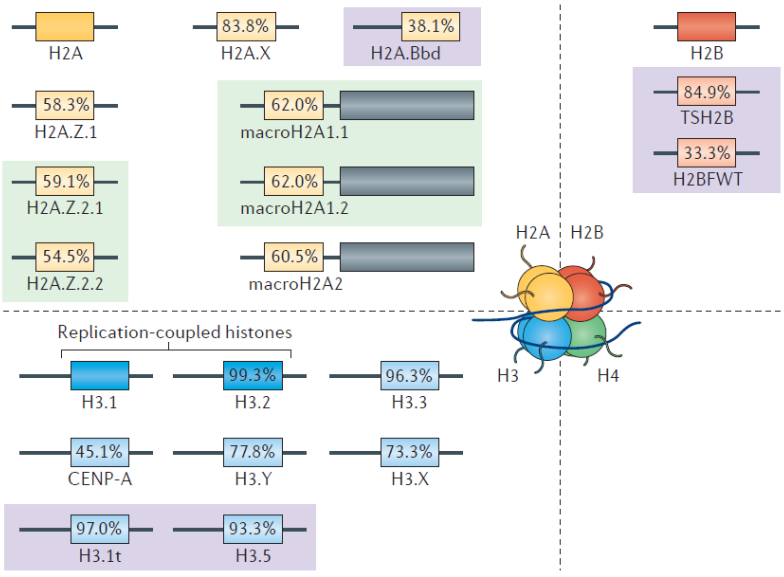

Figure 1.8: Histone variants. The human variants of each histone are depicted in this picture; eight variants of H2A, six variants of H3, two variants of H2B and no variants for H4 since they have not been discovered in higher eukaryotes. Testis-specific histone variants are highlighted by purple boxes and alternative splice isoforms by light green boxes. Percentages indicate total amino acid sequence conservation (% sequence identity) of the variants relative to their replication-coupled counterparts. Adapted from (Buschbeck and Hake, 2017)

1.7.2.3 ATP-dependent chromatin remodelers

Chromatin remodelers are ATP-driven molecular machines that have a major role in the dynamic nature of chromatin since they can alter its structure by different ways (Clapier and Cairns, 2009; Zhou et al., 2016). More specifically, their main functions is to control the consistent spacing of nucleosomes (chromatin organization), to move or eject nucleosomes to facilitate DNA access (chromatin access) and to insert histone variants to specific chromatin regions (chromatin restructuring) (Clapier and Cairns, 2009). Four families of chromatin remodelers have been identified, SWI/SNF, ISWI, CHD and INO80, consisting of unique domains defining their target specificity and a conserved ATPase domain, which catalyzes ATP hydrolysis to alter histone-DNA contacts (Clapier and Cairns, 2009). These family remodelers differ in their composition of different subunits and have distinct roles in various cellular processes like replication, transcription, repair and recombination (Clapier and Cairns, 2009).

1.7.3 Global chromatin environments: Euchromatin and Heterochromatin

Genomic localization of histone modifications, histone variants, chromatin remodelers and their interacting proteins give rise to two geographically distinct chromatin environments, euchromatin and heterochromatin (Fraser and Bickmore, 2007; Van Bortle and Corces, 2012) (Figure 1.9). Euchromatin has an open conformation and has been mainly associated with active transcription in contrast to heterochromatin that is a highly compacted, poorly transcribed structure (Fraser and Bickmore, 2007). Different modifications have been associated with euchromatin, the majority of them being related to transcription. For example, H3K4me1 is enriched at active transcriptional enhancers, H3K4me3 marks the transcriptional start site (TSS) of active genes and H3K36me3 is highly enriched throughout the whole transcribed regions (Barski et al., 2007; Hon et al., 2009). Moreover, euchromatin has high levels of acetylated histones that guarantee a more relaxed chromatin environment.

On the other hand, heterochromatin is a more compact structure with hypoacetylated histones that can be distinguished into facultative and constitutive heterochromatin. Facultative heterochromatin is interchangeable, representing euchromatic gene-rich domains that can be heterochromatinized when specific gene expression is not needed, as in different developmental stages or during differentiation process (Trojer and Reinberg, 2007). The main histone modification of facultative heterochromatin is H3K27me that can be induced, recognized and maintained by Polycomb Group (PcG) proteins (Trojer and Reinberg, 2007). On the other hand, constitutive heterochromatin is characterized by highly repetitive sequences and the histone

modification H3K9me3 that is directly recognized by HP1 (Bannister et al., 2001; Lachner et al., 2001; Maison and Almouzni, 2004). Mammalian cells have 3 isoforms, HP1α, HP1β and HP1γ that could increase the level of complexity in comparison with *D. melanogaster* that has only HP1a and *S. pombe* that has its homologue Swi6 (Maison and Almouzni, 2004). Moreover, there are other proteins ensuring the compacted nature of the heterochromatic domain. In the case of pericentric heterochromatin that is a typical example of constitutive heterochromatin, these proteins are the methyltransferases Suv3-9 and Suv4-20 catalyzing H3K9me3 and H4K20me2/me3 respectively as well as the co-repressor KAP1, interacting with SETDB1 (histone methyltransferase), HDAC1 and HDAC2 (histone deacetylases) and CHD3/Mi-2a (CHD nucleosome remodeling factor) (Maison and Almouzni, 2004). On the other hand, centromeric heterochromatin that is also an example of constitutive heterochromatin, has unique characteristics such as the specific H3 histone variant, CENP-A, high histone acetylation as well as H3K4me2 and H3K36me2 (McKinley and Cheeseman, 2016; Saksouk et al., 2015) (The main differences between pericentric and centromeric heterochromatin are summarized in Figure 3.1C).

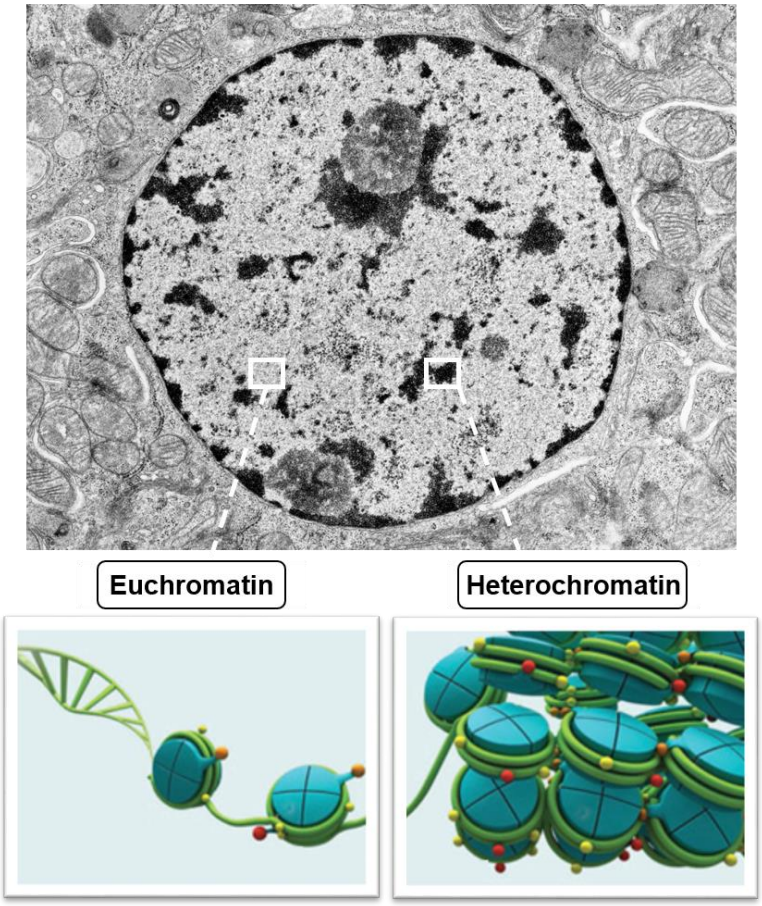

Figure 1.9: Global chromatin environments: Euchromatin and Heterochromatin. The highly condensed nature of heterochromatin compared to euchromatin allows for their visual distinction using transmission electron microscopy (TEM) as shown in this TEM picture of a human nucleus (TEM picture adapted from Yale University: http://medcell.med.yale.edu/histology/cell_lab/euchromatin_and_heterochromatin.php. Cartoons of chromatin adapted from Genetic Engineering & Biotechnology news: http://www.genengnews.com/gen-articles/pcr-assay-for-chromatin accessibility/3685?page=1).

1.7.4 Nuclear compartments

Apart from the highly-ordered folding of chromatin and the creation of distinct chromatin environments as described above, the next level of nuclear organization consists of the compartmentalization of nucleus into distinct substructures (Dundr and Misteli, 2001) (Figure 1.10). These nuclear compartments are not delimited by membranes but they are characterized by a specific set of proteins determining their unique biological function. One such compartment is the nuclear envelope consisting of an inner and an outer nuclear membrane that are fused together in the nuclear pores. Nuclear pores are large transmembrane complexes of about 30 different proteins called nucleoporins (NUPs) and their main function is to regulate the transportation of molecules between the nucleus and the cytoplasm (Beck and Hurt, 2017). Inside the nuclear envelope, there is the nuclear lamina that has a structural role maintaining the nuclear shape but it also participates in the anchoring of chromatin to the nuclear envelope (van Steensel and Belmont, 2017). The most prominent substructure in the nucleus is the nucleolus, which is the site of rRNA synthesis, processing and ribosomal assembly. Other nuclear compartments (also referred as nuclear bodies) have been identified and linked to different cellular processes like mRNA splicing and further processing (Cajal bodies, Cleavage bodies, Nuclear speckles), protein degradation (Clastosomes), heat shock response (Nuclear Stress bodies) and transcription (OPT domains, PML bodies).

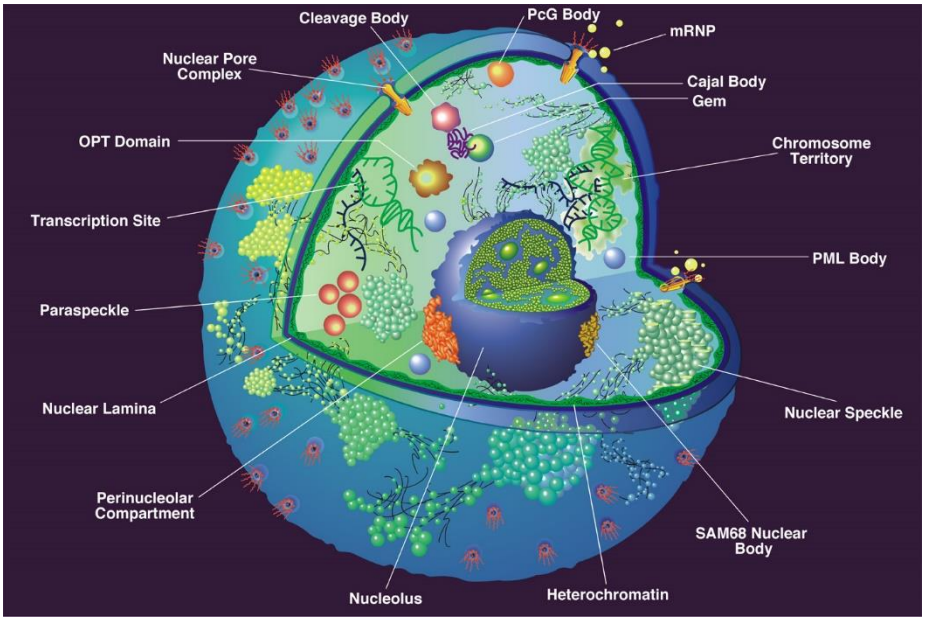

Figure 1.10: Nuclear compartments. The nucleus is organized into different substructures that are not delimited by membranes but they are characterized by a specific set of proteins determining their unique biological function. These substructures are depicted in this picture. Adapted from (Spector, 2001).

1.7.5 Histone post-translational modifications in DDR and DSB repair

1.7.5.1 Histone phosphorylation.

The hallmark of DDR is the phosphorylation of histone variant H2AX on Ser139 (γ-H2AX) in mammalian cells, a modification found in megabase chromatin domains around the lesion (Rogakou et al., 1999; Rogakou et al., 1998). As previously mentioned, this phosphorylation can be induced by the ATM, ATR and DNAPK kinases but only ATM promotes γ-H2AX at maximal distance around DSBs (Savic et al., 2009). Loss of γ-H2AX increases genomic instability and susceptibility to cancer, showing its major role in genome maintenance and cell survival (Celeste et al., 2003a). More specifically, γ-H2AX is not required for the initial recruitment of the repair factors but it is necessary for their retention and thus the formation of IRIF in the nucleus (Celeste et al., 2003b). H2AX is also constitutively phosphorylated on Tyr142 by the WSTF kinase domain preventing MDC1 recruitment at the breaks and instead enhancing recruitment of pro-apoptotic factors (Cook et al., 2009; Xiao et al., 2009). After damage induction, Tyr142p of H2AX is removed by the tyrosine phosphatase EYA1 and γ-H2AX is increased favoring the interaction with MDC1 and thus the repair versus apoptotic signals, revealing a regulatory mechanism for DDR activation (Cook et al., 2009; Xiao et al., 2009). Apart from H2AX, H2B was also reported to be phosphorylated on Ser14 after DSB induction but its functional role remains unclear (Fernandez-Capetillo et al., 2004).

1.7.5.2 Histone acetylation.

Histone acetylation has been extensively correlated with DNA damage and repair pathway choice (Price and D'Andrea, 2013). In yeast, it was reported that H4 is acetylated (K5, K8, K12, K16) at the sites of breaks by ESA1 (yeast homologue of TIP60), the catalytic subunit of the NuA4 histone acetyltransferase complex and these acetylation events promote NHEJ (Bird et al., 2002). Similar results were obtained in human cells where H3 and H4 were acetylated upon damage by the homologous histone acetyltransferases CBP and p300, promoting chromatin relaxation and NHEJ (Ogiwara et al., 2011). On the other hand, it was also shown that NuA4 complex binds to DSBs *in vivo* in mammalian cells and acetylates H4, facilitating HR by induction of chromatin relaxation (Murr et al., 2006). Acetylation of H4 at lysine 16 (H4K16Ac) is one of the most studied histone modifications having a key role in the repair pathway choice. H4K16 is acetylated by the MOF acetyltransferase and it is necessary for γ-H2AX foci formation (Sharma et al., 2010) and affects the recruitment of MDC1, 53BP1 and BRCA1 at the breaks (Li et al., 2010). H4K16Ac antagonizes 53BP1 binding and its induction either by MOF or TIP60 promotes 53BP1 release from the sites of DSBs, thus favoring HR in S/G2 (Clarke et al., 2017; Gupta et al., 2014; Hsiao

and Mizzen, 2013; Tang et al., 2013). In line with these data, H4K16 hypoacetylation induced by HDAC1 and HDAC2 at the sites of damage promotes NHEJ (Miller et al., 2010).

Apart from H4, acetylation of histone H3 can be altered after damage induction. Different residues of H3 (K9, K14, K18, K23) are acetylated by the GCN5 acetyltransferase, facilitating the recruitment of SWI/SNF complex and the spreading of γ-H2AX (Lee et al., 2010). H3K18 is also acetylated by the p300/CBP acetyltransferases, facilitating the recruitment of SWI/SNF complex and NHEJ factors (Ogiwara et al., 2011). Regulation of the extent of H3K18Ac by the SIRT7 deacetylase has a key role in NHEJ (Vazquez et al., 2016). H3K14Ac is also induced after IR treatment in a way dependent on the nucleosome binding protein HMGN1, a necessary step for ATM activation at the sites of breaks (Kim et al., 2009). Results for H3K56Ac after damage induction are more controversial; it has been reported that H3K56Ac is reduced after damage induction in human cells promoting NHEJ (Miller et al., 2010; Tjeertes et al., 2009). These results are in conflict with other studies reporting H3K56 induced acetylation after damage induction in *Drosophila* and human cells (Das et al., 2009; Vempati et al., 2010). H3K36 is also acetylated by GCN5 at DSBs in G2, increasing chromatin accessibility and promoting resection and HR in yeast (Pai et al., 2014).

H2A, another core histone, was also suggested as a potential regulator of repair pathway choice since H2AK15Ac induced by TIP60 at the sites of breaks can compete with H2AK15Ub that is necessary for 53BP1 binding, affecting negatively NHEJ (Jacquet et al., 2016). Apart from core histones, the histone variant H2AX is also acetylated by TIP60, a step that is necessary for its further ubiquitination by UBC13 and release from chromatin after DSB formation, an event that is independent of γ-H2AX formation (Ikura et al., 2007). On the other hand, H2AX is also constitutively acetylated at K36, independently of γ-H2AX and this acetylation is required for survival after ionizing radiation (Jiang et al., 2010). To conclude, besides its role in induced chromatin relaxation after damage induction, histone acetylation can also impact on the repair pathway choice by interacting with representative factors from each pathway.

1.7.5.3 Histone methylation.

Methylation of various histone residues impacts differentially on DDR and DNA repair pathway choice. It has been shown that 53BP1 accumulates at DSBs via the recognition of H4K20me2 by its Tudor domain, a mechanism conserved from yeast to mammals (Botuyan et al., 2006; Sanders et al., 2004) (Figure 1.5). More specifically, H4K20me2 increases locally at the sites of breaks

either directly by the MMSET methyltransferase (Pei et al., 2011) or by the concerted action of PR-Set and SUV4-20 that induce sequentially H4K20me1 and H4K20me2 respectively (Tuzon et al., 2014). Recognition of H4K20me2 by 53BP1 is inhibited by the TIRR protein that binds its Tudor domain and masks its H4K20me2 binding motif (Drane et al., 2017). Upon DNA damage, this inhibition is alleviated through the phosphorylation of 53BP1 by ATM and consequent recruitment of RIF1 (Drane et al., 2017). Moreover, 53BP1 accumulation at IR-induced DSBs depends on H3K79me2 catalyzed by the DOT1L methyltransferase when H4K20me2 levels are low (Huyen et al., 2004; Wakeman et al., 2012). Another modification that plays a role in DDR is the heterochromatic marker H3K9me3. H3K9me3 is recognized the TIP60 acetyltransferase that will in turn activate its acetyltransferase activity that is necessary to acetylate and thus activate ATM kinase (Sun et al., 2009; Sun et al., 2007). It was also shown that H3K9me3 is induced in regions adjacent to DSBs through SUV39h1/KAP1/HP1 complex that is recruited around the lesions, creating a transient repressive chromatin state that may facilitate further steps of the repair process (Ayrapetov et al., 2014). On the other hand, H3K4me3 that is correlated with open chromatin environment, has an essential role in targeting and stimulating the activity of RAG complex involved in V(D)J recombination (Grundy et al., 2010; Shimazaki et al., 2009). Moreover, it has been reported that it is induced at DSBs in yeast and plays a role in DNA repair through NHEJ (Faucher and Wellinger, 2010).

Another histone methylation that is well studied for its role in DNA repair pathway choice is H3K36me3, induced by the SETD2 methyltransferase (Set2 in yeast) (Aymard et al., 2014; Carvalho et al., 2014; Jha and Strahl, 2014; Pai et al., 2014; Pfister et al., 2014). Loss of H3K36me3/Set2 results in a more open chromatin configuration and inappropriate resection during G1 in yeast, supporting the idea that this modification creates a less accessible environment for resection and thus promotes NHEJ in G1 (Jha and Strahl, 2014; Pai et al., 2014). In line with this observation, it was demonstrated that H3K36me2 is induced by the repair protein Metnase (it has a SET histone methyltransferase domain) after IR and enhances repair by NHEJ in human cells (Fnu et al., 2011). On the other hand, data in human cells support that H3K36me3/SETD2 is required for HR facilitating CtIP recruitment, subsequent resection and RAD51 presynaptic filament formation (Carvalho et al., 2014; Pfister et al., 2014). Additionally, it was shown that transcriptionally active loci with H3K36me3 are selectively repaired by HR, a process dependent on SETD2 and LEDGF that is a factor which facilitates resection (Aymard et al., 2014; Daugaard et al., 2012). Taken together, histone methylation seems to have a dual role in the repair: it contributes to the formation of a more repressive environment necessary for DDR

activation and it is actively implicated in the repair pathway choice, as revealed mainly by the H3K36me2/3 data. Considering that histone acetylation is also induced after damage, combined data from the above studies suggest a model in which repressive methylation events might happen at the very early stages of DDR to initiate its activation that are then succeeded by chromatin relaxation through histone acetylation in order to facilitate the recruitment or different repair factors.

1.7.5.4 Histone ubiquitination.

The previously described histone modifications result in small molecular changes compared to ubiquitination that represents a larger covalent modification. Ubiquitin is a 76-aminoacid polypeptide attached to histone lysines via the sequential action of E1-activating, E2-conjugating and E3-ligating enzyme. The DSB signaling response involves different ubiquitination events performed by various E3 ubiquitin ligases (Smeenk and Mailand, 2016). Among them, RNF8 initiates the ubiquitination signaling cascade by interacting with the E2 ubiquitin-conjugating enzyme UBC13 and subsequently adding K36-linked Ub chains to H2A and H1 histones at the sites of breaks (Huen et al., 2007; Kolas et al., 2007; Mailand et al., 2007; Thorslund et al., 2015). The interaction between these two proteins in mediated by another E3 ubiquitin ligase named HERC2 that is necessary to promote RNF8 ubiquitination activity (Bekker-Jensen et al., 2010). These ubiquitination events serve as a docking signal for another E3 ubiquitin ligase, RNF168 that will in turn ubiquitinate the H2A histones at K13 and K15 (H2A/H2AX K13Ub and K15Ub) (Doil et al., 2009; Gatti et al., 2012; Leung et al., 2014; Mattiroli et al., 2012; Pinato et al., 2009; Stewart et al., 2009). H2A K15Ub induced by RNF168 is recognized by 53BP1 and it is necessary for its accumulation at DSBs (Fradet-Turcotte et al., 2013; Wilson et al., 2016). Moreover, various deubiquitinating enzymes (DUBs) have also been implicated in the removal of the Ub chains from H2A histones at the sites of DSBs (Mosbech et al., 2013; Nicassio et al., 2007; Shanbhag et al., 2010; Sharma et al., 2014; Typas et al., 2015). Among them, it has been suggested that USP26 and USP37 have a role in HR by preventing the excessive spreading of RAP80-BRCA1 and promoting the interaction of PALB2-BRCA1 (Typas et al., 2015). Since RNF168-induced H2A ubiquitination is necessary for 53BP1 and BRCA1 recruitment at DSBs, it becomes obvious that it can have a role in the repair pathway choice, also supported by the DUBs data. RNF168 was also reported to promote K27-linked ubiquitylation of H2A/H2AX *in vitro* and *in vivo* and this modification is essential for the assembly of DDR foci (Gatti et al., 2015).

Apart from RNF8 and RNF168, subunits of the Polycomb repressive complex 1 are recruited to DSBs and ubiquitinate H2A/H2AX at K119 (Ginjala et al., 2011; Ismail et al., 2010; Leung et al., 2014; Pan et al., 2011). More specifically, BMI1/RING2 is recruited at the sites of breaks and induces H2A K119Ub (Ginjala et al., 2011; Ismail et al., 2010). Loss of BMI1 leads to reduced recruitment of different DDR factors and impaired HR (Ginjala et al., 2011). It has also been reported that H2AX is ubiquitinated on K119/ K120 by RNF2-BMI1 and loss of H2AX K120Ub leads to impaired recruitment of ATM (Pan et al., 2011). BRCA1-BARD1 complex that creates a heterodimeric E3 ubiquitin ligase can also ubiquitinate H2A on K127/K129 that could also have a potential role on DDR, thought the mechanism is not known (Densham et al., 2016; Kalb et al., 2014). Except for H2A, H2B is also ubiquitinated on K120 by RNF20-RNF40 complex after DSB induction, promoting the accumulation of NHEJ and HR factors (Moyal et al., 2011; Nakamura et al., 2011). Furthermore, BBAP E3 ligase ubiquitinates H4 on K91 that is required for H4K20me1 and the H4K20me2 induction that is major for 53BP1 recruitment at DSBs (Yan et al., 2009).

1.7.6 Histone variants in DDR and DSB repair

Different histone variants are involved in DDR activation and DSB repair (Polo, 2015; Soria et al., 2012). H2AX is the best studied histone variant since its phosphorylated form is the main marker of DDR that can also undergo further modifications in this context. Apart from H2AX, H2AZ is transiently recruited to DSBs and promotes genomic stability in yeast and mammalian cells (Gursoy-Yuzugullu et al., 2015; Papamichos-Chronakis et al., 2006; Papamichos-Chronakis et al., 2011; Xu et al., 2012b). More specifically, it has been reported that H2AZ rapidly accumulates at DSBs of human cells but soon afterwards is removed by the histone chaperone ANP32e (Gursoy-Yuzugullu et al., 2015; Xu et al., 2012b). Its removal from the sites of breaks is necessary for induction of H4 acetylation that will create a more open chromatin structure as well as for HR promotion in contrast to its accumulation that will eventually favor Ku70/Ku80 binding and thus NHEJ (Gursoy-Yuzugullu et al., 2015; Xu et al., 2012b). Although the above-mentioned studies have reported the accumulation of H2AZ at the sites of breaks, it is worth mentioning that Taty-Taty et al. did not observe a similar recruitment (Taty-Taty et al., 2014). MacroH2A is another H2A variant with 2 splicing forms, macroH2A1.1 and macroH2A1.2 that have been implicated in DSB repair. Although only macroH2A1.1 can recognize PARylated chromatin, they are both recruited transiently at DSBs inducing chromatin compaction (Khurana et al., 2014; Mehrotra et al., 2011; Timinszky et al., 2009; Xu et al., 2012a). After DSB induction, they are both transiently depleted from the sites of breaks to allow chromatin relaxation, but they re-accumulate rapidly creating a repressive chromatin environment through interaction with the histone

methyltransferase PRDM2 that induces H3K9me2 (Khurana et al., 2014). This chromatin environment promotes BRCA1 retention at the sites of breaks favoring end resection and thus HR.

On the other hand, an H3 histone variant, H3.3 is incorporated at DSBs through the action of CHD2 chromatin remodeler and favors NHEJ (Luijsterburg et al., 2016). It was also reported that the centromere specific H3 histone variant, CENP-A is recruited at the sites of DSBs (Zeitlin et al., 2009) and its specific chaperone HJURP is involved in HR (Kato et al., 2007), but their functional role in the repair process is not defined. On the other hand, data from Helfricht et al. did not confirm CENP-A recruitment at the sites of DNA lesions (Helfricht et al., 2013). To conclude, it becomes obvious that apart from H2AX, other histone variants also have a significant role in genomic stability, favoring different repair pathways. Although the focus of this introduction is on DSBs, it is worth mentioning that local histone exchange has been reported at sites of UV-induced lesions where the H3 histone variants H3.1 and H3.3 are deposited *de novo*, underlying the importance of chromatin landscape changes at the sites of DNA damage (Adam et al., 2013; Dinant et al., 2013; Polo et al., 2006).

1.7.7 Chromatin remodelers in DDR and DSB repair

1.7.7.1 SWI/SNF family remodelers.

The SWI/SNF family remodelers have been extensively correlated with DNA damage mainly by inducing chromatin relaxation at the sites of breaks and thus having a major role in DDR activation and DSB repair, conserved from yeast to mammals (Papamichos-Chronakis and Peterson, 2013). In yeast, it has been shown that the two members of this family remodelers, SWI/SNF and RSC complexes are recruited to DSBs mainly in S/G2 phases of the cell cycle, ejecting nucleosomes from the sites of breaks and thus promoting DDR activation (Bennett et al., 2013; Liang et al., 2007; Shim et al., 2007). SWI/SNF recruitment at DSBs depends on the acetyltransferase activity of NuA4 complex and GCN5 acetyltransferase, suggesting a potential role of histone acetylation in this process (Bennett and Peterson, 2015). Both complexes seem to have a role in HR, since SWI/SNF is necessary and recruited at the early steps of the pathway, in contrast to RSC that is important for the first and late steps of HR since it is also recruited after strand invasion (Chai et al., 2005; Kent et al., 2007). It is also suggested that RSC participates at the loading of cohesion to facilitate HR using the sister chromatid (Oum et al., 2011). In line with these data, SWI/SNF has been reported to facilitate the strand invasion step of HR in yeast heterochromatin-like domains (Sinha et al., 2009). Another SWI/SNF- like remodeler, Fun30 is recruited to DSBs where

it promotes extensive Exo1 and CtIP-driven resection by inhibiting Rad9 checkpoint adaptor protein (Chen et al., 2012; Costelloe et al., 2012; Eapen et al., 2012). Similar results for its role in resection were obtained for the mammalian homologue of Fun30, SMARCAD1 (Costelloe et al., 2012). Fun30 is loaded on DSBs through its interaction with Dpb11 that is cell-cycle regulated happening only in S-M phase and not in G1, restricting its ability to enhance resection outside G1 (Bantele et al., 2017). Artificial tethering of Fun30 at the sites of breaks can induce long range resection in G1, bypassing its cell-cycle regulated loading (Bantele et al., 2017).

In mammalian cells, knockdown of the catalytic subunits BRM and BRG1 results in defect in γ-H2AX induction and IRIF formation, suggesting the role of this complex in genomic stability (Lee et al., 2010; Park et al., 2006). BRG1 is recruited to DSBs where it is phosphorylated by ATM kinase, increasing its affinity for binding at γ-H2AX nucleosomes as well as to H3 acetylated histones (Kwon et al., 2015; Lee et al., 2010). Upon its binding, it further increases H3 acetylation by recruiting the GCN5 acetyltransferase, thus creating a very accessible chromatin environment for DDR and DNA repair factors (Lee et al., 2010). BRM recruitment is also dependent on the acetyltransferases CBP/p300 and promotes Ku binding and thus NHEJ (Ogiwara et al., 2011). Apart from BRM and BRG1, two other subunits of this remodeler, BAF170 and BAF155 interact with BRIT1 that is a factor recruited at DSBs at the early steps of DDR (Rai et al., 2006), suggesting a possible mechanism for their regulated recruitment at DSBs (Peng et al., 2009).

1.7.7.2 ISWI family remodelers.

Different subunits of the ISWI chromatin remodeling complexes are recruited to DSBs, changing chromatin structure and subsequently affecting DDR activation and repair (Aydin et al., 2014). SNF2H that is the catalytic subunit of different complexes from this family remodelers is recruited to DSBs in a PARP-1 dependent manner where it promotes the accumulation of RNF168 and thus affects DDR activation and repair (Smeenk et al., 2013). It has been reported that NuMA is required for its accumulation at the sites of breaks and knockdown of these two factors results in defective Ub formation, impaired recruitment of CtIP, BRCA1 and RAD51, suggesting their role in HR (Vidi et al., 2014). In line with these data regarding its role in HR, SNF2H recruitment depends on RNF20 that induces H2BK120Ub at the sites of breaks and knockdown of these factors leads to impaired resection, BRCA1 and RAD51 recruitment (Nakamura et al., 2011). Moreover, the deacetylase SIRT6 enhances its binding to DSBs by deacetylation of H3K56 where then SNF2H induces chromatin relaxation and allows for efficient signaling at DSBs (Toiber et al., 2013). Another way this interaction of SIRT6/SNF2H promotes DDR signaling is by enhancing

the stability of H2AX (Atsumi et al., 2015). SIRT6/SNF2H blocks the E3 Ub ligase HUWE1 that degrades H2AX under normal cellular condition, specifically at the sites of DSBs, thus allowing for efficient induction of γ-H2AX (Atsumi et al., 2015).

Together with SNF2H, its binding factor ACF1 is also recruited to DSBs where it is involved in both NHEJ and HR (Lan et al., 2010). It has also been shown that both factors are recruited to heterochromatic DSBs where they induce further chromatin relaxation after the disruption of KAP1-CHD3 interaction (Klement et al., 2014). Apart from ACF1, SNF2H associates with WSTF and RSF1 to form WICH and RSF remodelers (Clapier and Cairns, 2009). WSTF role in DDR was discussed in 1.7.5.1. RSF1 has been correlated with DSBs since its overexpression leads to induction of DSBs and genomic instability through an unknown mechanism (Sheu et al., 2010). Moreover, it was shown that it is recruited to DSBs where it promotes HR by recruiting RPA and RAD51 (Min et al., 2014). Additionally, it is recruited to IR-induced breaks where it induces the recruitment of CENP-S and CENP-X centromeric proteins as well as the interstrand crosslink repair proteins FANCD2 and FANCI (Pessina and Lowndes, 2014). The sequential recruitment of these proteins seems to be important for DNA repair but the exact molecular mechanism for their action was not defined (Pessina and Lowndes, 2014). More data about the functional role of CENP-S and CENP-X came from a second study where it was reported that these two centromeric proteins are recruited to DSBs through RSF1 and they promote the assembly of NHEJ factor XRCC4 (Helfricht et al., 2013). Although their loading did not affect HR, RSF1 was found to promote HR through a different but not defined mechanism (Helfricht et al., 2013).

1.7.7.3 CHD family remodelers.

Different CHD remodelers have been implicated in DDR (Stanley et al., 2013). The mammalian NuRD complex has been extensively reported to affect DDR signaling since different subunits of it are recruited to DSBs (Chou et al., 2010; Goodarzi et al., 2011; Klement et al., 2014; Larsen et al., 2010; Miller et al., 2010; Polo et al., 2010; Smeenk et al., 2010). CHD4, the catalytic subunit of NuRD and the non-catalytic subunit MTA1 accumulate at DSBs in a PARP-dependent manner, where they stimulate the ubiquitination activity of RNF8 and subsequent recruitment of RNF168 and BRCA1 (Chou et al., 2010; Larsen et al., 2010; Polo et al., 2010; Smeenk et al., 2010). Moreover, two other subunits of this complex, the histone deacetylases HDAC1 and HDAC2 are recruited fast at DSBs where they promote NHEJ (Miller et al., 2010). NuRD complex, being involved in the maintenance of heterochromatin, it has also been related to heterochromatic DSB

where it was shown that CHD3, its alternative catalytic subunit, is released from chromatin after DSB induction (Goodarzi et al., 2011; Klement et al., 2014).

CHD2 that is another member of these remodelers has been implicated in DDR since its loss leads to persistent γ-H2AX levels (Nagarajan et al., 2009). More specifically, it was shown to be recruited at the sites of damage through its interaction with PARP1 both in G1 and S/G2 phases of cell cycle, where it promotes NHEJ through local chromatin remodeling that involves histone H3.3 incorporation (Luijsterburg et al., 2016). A CHD1-like protein named ALC1 was also reported to be rapidly recruited to DSBs, where it interacts with PARP1, DNAPK and Ku80 (Ahel et al., 2009; Gottschalk et al., 2009).

1.7.7.4 INO80 family remodelers.

The INO80 chromatin remodelers have been extensively implicated in DDR and DSB repair from yeast to mammals (Papamichos-Chronakis and Peterson, 2013). In yeast, there are two complexes of this family, INO80 and SWR1 that are both recruited to DSBs in a γ-H2AX dependent way (Papamichos-Chronakis et al., 2006). It was shown that INO80 exchanges H2AZ nucleosomes with H2A/H2B globally in chromatin and its depletion leads to genomic instability, supporting its role in DNA damage signaling (Papamichos-Chronakis et al., 2011). Moreover, INO80, but not SWR1, is required for the eviction of H2AZ and γ-H2AX from the sites of breaks, thus facilitating Mre11 binding, resection and HR (Morrison et al., 2004; Tsukuda et al., 2009; van Attikum et al., 2007; van Attikum et al., 2004). Similar results for its role in HR were obtained in *Arabidopsis thaliana* (Fritsch et al., 2004). Additionally, it has been shown that INO80 increases the mobility of a non-damaged locus, leading to spontaneous gene conversion, suggesting the potential role of this factor in homologous-directed repair (Neumann et al., 2012). On the other hand, SWR1 facilitates Ku recruitment and thus NHEJ (van Attikum et al., 2007). The distinct role of these two complexes in DNA repair is also highlighted by their impact on localization and repair of irreparable DSBs that move to the nuclear periphery (Horigome et al., 2014). More specifically, H2AZ is incorporated by SWR1 at the sites of breaks, a necessary step for their shift to the nuclear periphery, both at the pores and the inner nuclear membrane (Horigome et al., 2014). On the other hand, INO80 is selectively required for association of the breaks with the inner membrane protein Mps3 that is a recombination-repressive environment in contrast to nuclear pores (Horigome et al., 2014).

The mammalian INO80 complex is also recruited to DSBs but in contrast to yeast data in a γ-H2AX independent manner (Kashiwaba et al., 2010). It has been shown that is necessary for end resection and thus HR (Gospodinov et al., 2011; Wu et al., 2007). On the other hand, it is also recruited to I-PpoI-induced DSBs in an ATM dependent way where it disassembles chromatin to promote NHEJ (Li and Tyler, 2016). Moreover, it was reported that it can indirectly affect the repair process since it upregulates RAD54B and XRCC3 expression; over-expression of these two factors rescued the repair defect observed in INO80-deficient cells (Park et al., 2010). Apart from INO80, Tip60 belongs to this family of remodelers. p400, the catalytic subunit of this complex, is recruited to DSBs where it destabilizes the nucleosomes promoting RNF8 ubiquitination, BRCA1 and 53BP1 binding (Xu et al., 2010). In contrast to this study, p400 was reported not to affect DDR activation but its depletion led to HR defects since it interacts and thus promotes RAD51 loading (Courilleau et al., 2012). Since resection happens normally but RAD51 recruitment is impaired under p400 knockdown conditions, its depletion leads to increased levels of alt-NHEJ (Taty-Taty et al., 2016). Another subunit of Tip60, RUVBL1 was also found to be methylated by the arginine methyltransferase PRMT5 at the sites of damage, promoting H4K16Ac induced by Tip60, and leading to release of 53BP1 and thus promotion of HR (Clarke et al., 2017). The release of 53BP1 that favors HR is also facilitated by another recently identified subunit of this complex called MBTD1 (Jacquet et al., 2016).

1.8 Double Strand Break repair in heterochromatin

As previously described, heterochromatin is a highly compacted structure, characterized by highly repetitive sequences and a complex protein network (Maison and Almouzni, 2004). This compaction could be a barrier for the repair process, preventing the repair machinery to recognize and reach the break. Supporting this hypothesis, it was reported that γ-H2AX is preferentially localized in euchromatin compared to heterochromatin of retina rod cells suggesting that euchromatin is damage-prone whereas heterochromatin blocks damage events (Lafon-Hughes et al., 2013). Moreover, transmission electron microscopy experiments to detect gold-labeled pKu70 and pDNA-PKs within the nuclear ultrastructure showed that DNA lesions in euchromatin are promptly sensed and rejoined in contrast to heterochromatic breaks where DSB processing seems to be delayed (Lorat et al., 2012; Lorat et al., 2016) Thus, the nature of heterochromatin renders heterochromatic DSB repair a challenge that cells need to overcome in order to preserve their genome integrity. For that reason, cells have developed different mechanisms to alleviate the high degree of heterochromatin compaction.

To this direction, many studies have shown the need for chromatin relaxation as the first necessary step for the repair of heterochromatic DSBs (Figure 1.11). ATM kinase has a key role in this process, since its inhibition leads to persistent breaks within heterochromatin but it has no effect on euchromatic DSBs (Goodarzi et al., 2008). Furthermore, inhibition of ATM in parallel with KAP1 or HP1 knockdown rescues this phenotype, supporting that ATM's role in heterochromatic DSB repair is to induce chromatin relaxation, possibly through different pathways (Goodarzi et al., 2008). It has been shown that KAP1 is phosphorylated by ATM (Ziv et al., 2006), interrupting its interaction with CHD3 and thus allowing chromatin to have a more open configuration (Goodarzi et al., 2011). Murine rod photoreceptors that fail to accumulate ATM at heterochromatic DSBs and exhibit low levels of KAP1 and phospho-KAP1 are incapable of repairing heterochromatic lesions, further strengthening the major role of ATM and KAP1 in this process (Frohns et al., 2014). Localization of activated ATM specifically at the heterochromatic breaks and subsequent robust and local KAP1 phosphorylation requires 53BP1 (Noon et al., 2010). Depletion of 53BP1 causes a defect in heterochromatic DSB repair that can be relieved by KAP1 or HP1 depletion (Kakarougkas et al., 2013). It was recently discovered the poorly characterized protein SCAI as a mediator of 53BP1-dependent DSB repair in heterochromatin (Hansen et al., 2016). These data strongly support the role of ATM and 53BP1 in chromatin relaxation as a first key step of DSB repair in heterochromatin. It was also proposed that after its initial role in chromatin relaxation, ATM is released from heterochromatic DSBs in G2 to facilitate the reconstitution of chromatin state that will subsequently promote HR (Geuting et al., 2013).

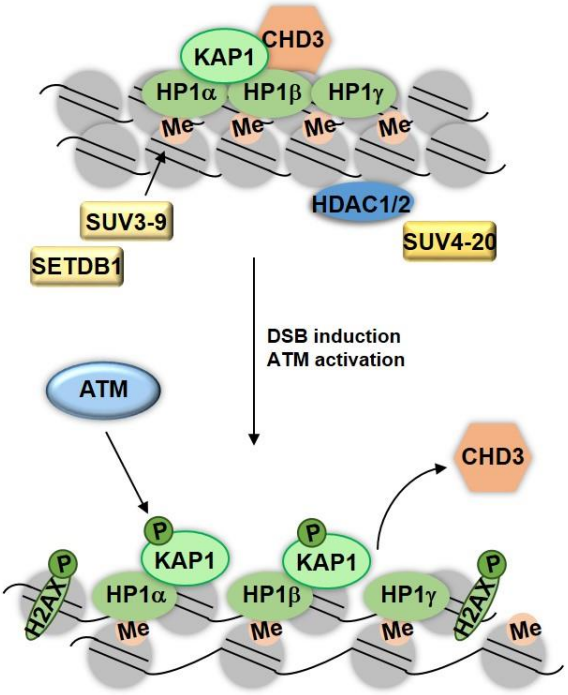

Figure 1.11: DSBs in heterochromatin. KAP1-rich heterochromatic domains prevent efficient DSB repair. Upon DSB induction, ATM becomes activated and phosphorylates KAP1, disrupting its interaction with CHD3. Release of CHD3 leads to chromatin relaxation and allows the repair to happen. P and M represent phosphorylation and methylation events, respectively.

Apart from chromatin relaxation, cells have developed more mechanisms in order to repair efficiently and faithfully DSBs in the refractory environment of heterochromatin. More specifically, in *D. melanogaster* cultured cells, DSBs can be formed within the heterochromatic domain after damage induction by γ-irradiation, but they soon relocate to the periphery of the structure where RAD51 is recruited to be repaired by HR (Chiolo et al., 2011). HR will be ultimately accomplished at the nuclear pores through a SUMO-regulated pathway (Ryu et al., 2016; Ryu et al., 2015). In this case, chromatin compaction is refractory to RAD51 entrance and thus DSBs relocation outside of this structure is necessary for their repair (Chiolo et al., 2011). In this study, heterochromatin expansion is also reported as a prerequisite for DSB relocation, a process dependent on resection and ATR activity (Chiolo et al., 2011). Similar movement of a single heterochromatic I-SceI induced DSB also occurs *in vivo in Drosophila* (Janssen et al., 2016). Furthermore, relocation of the breaks at the periphery of heterochromatin was also observed in mouse fibroblasts after damage induction with heavy ion irradiation as revealed by γ-H2AX distribution (Jakob et al., 2011). This peripheral localization of DSBs in heterochromatin was also recently reported in mouse fibroblasts after Cas9-induced breaks in constitutive heterochromatin (Tsouroula et al., 2016). Contrary to previous data, the localization of DSBs is cell-cycle specific and is directly correlated with the repair pathway choice; in G1, breaks are positionally stable and are repaired by NHEJ within heterochromatin in contrast to G2 that breaks are mobile and they relocate to the periphery of the domain where RAD51 is recruited to be repaired by HR (Tsouroula et al., 2016). Additionally, chromatin compaction does not block RAD51 entrance in heterochromatin, which is a main difference between mammalian and *Drosophila* cells (Tsouroula et al., 2016). Cas9-induced breaks in the heterochromatic structures of centromeres also trigger the peripheral localization of DSBs both in G1 and G2 where RAD51 is recruited (Tsouroula et al., 2016). From the previously described data, it becomes obvious that relocation of the break is one strategy to cope with heterochromatic DSB repair. On the other hand, it has also been reported that DSBs induced at the nuclear lamina are less mobile and they do not migrate to a more permissive environment for their repair (Lemaitre et al., 2014). Although, DDR activation is delayed and HR is defective in the chromatin environment of nuclear lamina, these DNA lesions are immobile and are repaired by alt-EJ pathway (Lemaitre et al., 2014).

DSB repair in heterochromatin has two different aspects; apart from the mechanisms that cells have developed to overcome the high level of compaction of heterochromatin, heterochromatic proteins have also been implicated in DSB repair but their role is controversial. HP1α has been shown to be rapidly and transiently recruited at laser-induced damaged sites of mammalian cells

through p150CAF-1 (the largest subunit of CAF-1), within both euchromatin and heterochromatin (Baldeyron et al., 2011). Further supporting its role in repair, depletion of HP1α leads to impaired accumulation of 53BP1 and RAD51 at the sites of damage (Baldeyron et al., 2011). In the case of HP1β, it has been shown that it is released from heterochromatin within 5 min after irradiation-induced damage and it is progressively restored (Ayoub et al., 2008). Its release is triggered by the phosphorylation of Thr51 of the HP1β chromodomain (CD) domain by CK2 kinase and this phosphorylation event seems to be essential for γ-H2AX foci formation at IR-damaged sites (Ayoub et al., 2008). In contrast to these data, Luijsterburg et al. (2009) showed that all HP1 proteins are recruited to DSBs after irradiation and this recruitment depends only on their chromo-shadow domain (CSD) and not the CD domain (Luijsterburg et al., 2009). Further support for this recruitment model of HP1s comes from quantitative FRAP and FLIP studies showing that HP1s are recruited to damaged regions both in euchromatin and heterochromatin within few minutes after damage (Zarebski et al., 2009). In agreement with these data, it was also showed recently the recruitment of all HP1 proteins as well as of KAP1 at the sites of DSBs in pericentric heterochromatin in G2 phase of cell cycle (Tsouroula et al., 2016). Supporting the active role of these proteins in repair, RAD51 recruitment was significantly impaired upon simultaneous knockdown of HP1s or KAP1 (Tsouroula et al., 2016). It has also been reported that KAP1 is necessary for heterochromatic DSB commitment to HR in G2 (Geuting et al., 2013). As previously mentioned, other proteins related to heterochromatin (HDAC1, HDAC2, CHD4, MTA1, subunits of the Polycomb repressive complex 1) are also recruited to DSBs affecting DDR and DSB repair (Chou et al., 2010; Ginjala et al., 2011; Ismail et al., 2010; Larsen et al., 2010; Leung et al., 2014; Miller et al., 2010; Polo et al., 2010; Smeenk et al., 2010).

As it becomes obvious from the above-mentioned studies, heterochromatin can be a refractory environment for DSB induction and repair. Chromatin relaxation seems to be one of the first important steps, making chromatin accessible to repair factors and allowing break recognition and processing. To achieve chromatin relaxation, HP1s and KAP1 are released from chromatin at the very early time points after damage induction, but they can be recruited again at later time points having an active role in the repair process. In order to avoid unscheduled recombination events within the highly repetitive heterochromatin, heterochromatic breaks relocate outside of this domain to be repaired by HR as it was shown in *D. melanogaster* (Chiolo et al., 2011; Ryu et al., 2015) and mouse fibroblasts (Jakob et al., 2011; Tsouroula et al., 2016) or they are immobile and they are repaired by alt-EJ as it is shown in human cells (Lemaitre et al., 2014). Although avoiding recombination events within heterochromatin seems to be a conserved mechanism

among different species, future studies are needed to shed more light on the distinct molecular mechanisms used to achieve this goal.

1.9 DSB mobility and repair pathway choice in the compartmentalized nucleus

In addition to highly ordered chromatin structure, the eukaryotic nucleus contains many functionally distinct subnuclear compartments (Spector, 2006) that could also affect the DNA repair outcome. In the last decade, many studies have addressed the issue of whether DNA repair is compartmentalized and whether DSBs acquire mobility towards specific nuclear compartments in order to be efficiently and faithfully repaired (Dion and Gasser, 2013; Lemaitre and Soutoglou, 2014; Mine-Hattab and Rothstein, 2013; Misteli and Soutoglou, 2009).

Different model organisms and different methods for DSB induction have been used to address this question. Many studies have been performed in *S. cerevisiae*, supporting mainly the idea of increased chromatin mobility after damage (Figure 1.12A). It has been shown that Rad52 foci can act as centers of DNA repair within the nucleus, capable of simultaneously recruiting more than one DSB (Lisby et al., 2003). In line with these data, live cell imaging experiments and Mean Squared Displacement (MSD) measurements indicated that a damaged locus has increased mobility in comparison with the non-damaged and this enhanced mobility requires Rad51, Rad54, Mec1 and Rad9 activity (Dion et al., 2012). A global increase of chromatin mobility can also be noticed but only above a certain threshold of damage and this is dependent on Mec1, the checkpoint kinase Rad53 and the chromatin remodeler INO80 (Seeber et al., 2013). Similar results were obtained studying two homologous loci, that occupy largely separated regions in yeast nucleus where the cut and the uncut chromosome had increased mobility, colocalizing ten times more often after the break induction (Mine-Hattab and Rothstein, 2012). These studies support a homology search machinery model, where not only the damaged but also the undamaged locus has increased mobility after break induction, facilitating the search for a homologous sequence that will allow its repair by HR in yeast nucleus.

Apart from the homology search to perform HR, DSB mobility in yeast has been correlated with movement to different nuclear compartments that promote different repair pathways. It has been reported that irreparable DSBs and telomeres relocate to the nuclear periphery, either at the inner nuclear membrane through interaction with the integral membrane protein Mps3 (Kalocsay et al., 2009; Oza et al., 2009; Schober et al., 2009) or at the nuclear pores through interaction with the nucleoporin Nup84 (Kalocsay et al., 2009; Khadaroo et al., 2009; Nagai et al., 2008; Therizols et

al., 2006). The relocation to the inner nuclear membrane has been related with decreased recombination rate and it seems to be necessary for genome stability since loss of Mps3 leads to gross chromosomal rearrangements (Oza et al., 2009; Schober et al., 2009). On the other hand, nuclear pores represent a more permissive environment for DSB repair and recombination events (Nagai et al., 2008; Therizols et al., 2006). These distinct relocalization events might be interconnected as suggested by eroded telomeres that delocalize from the inner nuclear membrane to the nuclear pores in case their repair is inefficient (Khadaroo et al., 2009; Su et al., 2015). Distinct mechanisms mediate this relocation of persistent DSBs to the nuclear membrane or to the pores, with SWR-C chromatin remodeler being necessary for both throughout the cell cycle, though INO80 only for the relocation to the nuclear membrane outside G1 (Horigome et al., 2014). Thus, according to the above data, the inner nuclear membrane can be a restrictive environment for recombination events in comparison with the permissive nuclear pores, possibly prompting breaks relocation to the pores in case their repair in inefficient at the nuclear membrane.

In agreement with these yeast data, heterochromatic DSBs in *D. melanogaster* move outside of this structure and they relocate to the nuclear pores in order to be repaired by HR (Chiolo et al., 2011; Ryu et al., 2015) (Figure 1.12B). Similar results are obtained for the damaged repetitive ribosomal locus which delocalizes outside of the nucleolus domain to be repaired by HR in yeast and in human cells (Harding et al., 2015; Torres-Rosell et al., 2007; van Sluis and McStay, 2015; Warmerdam et al., 2016) (Figure 1.12A and 1.12C). In yeast, nucleolar integrity and cohesion restricts further mobility of these breaks (Dion et al., 2013), a mechanism that probably does not allow them to migrate to the pores. Moreover, DSBs induced in centromeres and pericentromeres of mouse cells also relocate to the periphery of the heterochromatin to be repaired by HR, but no movement to the nuclear pores was observed in this case (Jakob et al., 2011; Tsouroula et al., 2016) (Figure 1.12C). In addition, in human cells where DSBs at the nuclear periphery fail to activate HR, they do not relocate to the pores that could be a more permissive environment for HR, but instead they are immobile and they are repaired *in situ* by alt-EJ (Lemaitre et al., 2014) (Figure 1.12C). Thus, it becomes obvious that HR inhibition within heterochromatin is an evolutionary conserved mechanism that can be achieved indirectly through DSB mobility like in *D. melanogaster*, yeast and mouse cells or directly like in human cells. The different chromatin structure and protein composition of the heterochromatic domains studied in each case could explain the diverse ways followed by the cells to avoid recombination within repetitive sequences.

In mammalian cells the results of similar studies regarding DSB mobility are more controversial (Figure 1.12C). In HeLa cells, DSBs induced with α-particles can be clustered progressively during time, a process that seems to be cell-cycle specific since it is mainly reported for cells in G1 (Aten et al., 2004). In agreement with these data, it was recently shown that AsiSI-induced DSBs exhibit increased clustering ability in G1 (Aymard et al., 2017; Caron et al., 2015). These DSBs correspond to transcriptionally active genes that are HR-prone (Aymard et al., 2014) and their clustering is an active process dependent on ATM activity, actin organization and cytoskeleton LINC complex (Aymard et al., 2017). Additionally, chromatin domains containing DSBs induced by γ-irradiation or etoposide treatment are more mobile than intact chromatin and are capable of roaming a more than twofold larger area of the nucleus (Krawczyk et al., 2012). Diametrically opposed to this observation, it was shown that UV-laser and irradiation-induced DSBs are quite immobile in mammalian cells (Becker et al., 2014; Kruhlak et al., 2006). Favoring this idea, Soutoglou et al. (2007) proved that the two ends of a break are positionally stable and unable to roam the cell nucleus, as revealed with the *LacO/LacR* system and live-cell imaging (Soutoglou et al., 2007). More specifically, the immobility of the two broken ends seems to be mediated by an active mechanism where NHEJ is involved through Ku70-Ku80 or XRCC4-XLF complex that can bridge and hold together the two broken DNA ends (Brouwer et al., 2016; Soutoglou et al., 2007). In agreement with the Soutoglou et al. (2007), DSBs induced by FokI endonuclease fused to LacR (*LacO/LacR* system) do not exhibit increased mobility in human cells (Cho et al., 2014). Furthermore, DSBs induced with heavy ions exhibit movement very close to the Brownian one and in very rare cases a higher MSD value, indicating possibly a migration process (Jakob et al., 2009). Thus, mammalian DSBs seem to be less mobile than in yeast and they are not able to search the whole nucleus for a homologous sequence as a repair template. This is strongly supported by the data of Roukos et al. (2013) where they showed that only these DSBs that will pair are more mobile and they can rarely lead to translocations, happening mainly between proximal DSBs (Roukos et al., 2013). In the same direction, it was also reported that recombination events will happen preferentially between proximal DSBs in yeast (Agmon et al., 2013; Renkawitz et al., 2013).

Another aspect of DSB mobility and repair pathway choice comes from the study of telomeres under damage conditions. Based on time-lapse microscopy data, unprotected telomeres that activate the DDR pathway have increased mobility and they can sample larger territories within the nucleus, a phenomenon dependent on 53BP1 presence (Dimitrova et al., 2008). These unprotected telomeres will be repaired by NHEJ (Dimitrova et al., 2008). Moreover, tracking of

telomere dynamics in live cells by CRISPR/Cas9 system revealed their confined diffusion that can be increased after disrupting the telomere shelterin complex, according to the MSD measurements (Chen et al., 2013). In a recent study focusing on the mechanism of Alternative Lengthening of Telomeres (ALT), a hallmark of certain cancer types, it is shown that ALT telomeres exhibit a directional movement towards RAD51 molecules where they are clustered with different chromosomal termini in order to be repaired by HR (Cho et al., 2014). This homology directed telomere synthesis could resemble the suggested homology search machinery model in yeast.

In conclusion, DSB mobility and repair pathway choice has become the key question of many studies, having contradictory results and consequently supporting different models about DSBs movement and its functionality to the repair process. Yeast DSBs show increased mobility, searching the whole nucleus for a homologous sequence as a template for their repair. This movement that corresponds to 1μm yeast nucleus size could only represent a restricted movement in the mammalian nucleus, which is ten times larger. On the other hand, data in human cells show that DSBs mobility is actively inhibited, preventing possibly translocations formation. Nevertheless, DSBs repositioning and mobility is also observed in heterochromatin of mouse and *Drosophila* cells being correlated with the repair pathway choice. This movement does not correspond to the large-scale movement observed in yeast. Overall in these studies, different model organisms and cells lines are used, under diverse growth conditions. Moreover, DNA damage is induced by different means and breaks are followed by variable methods. Thus, these conflicting data can be reconciled taking into consideration these differences, supporting a distinct role of each study to this debatable issue.

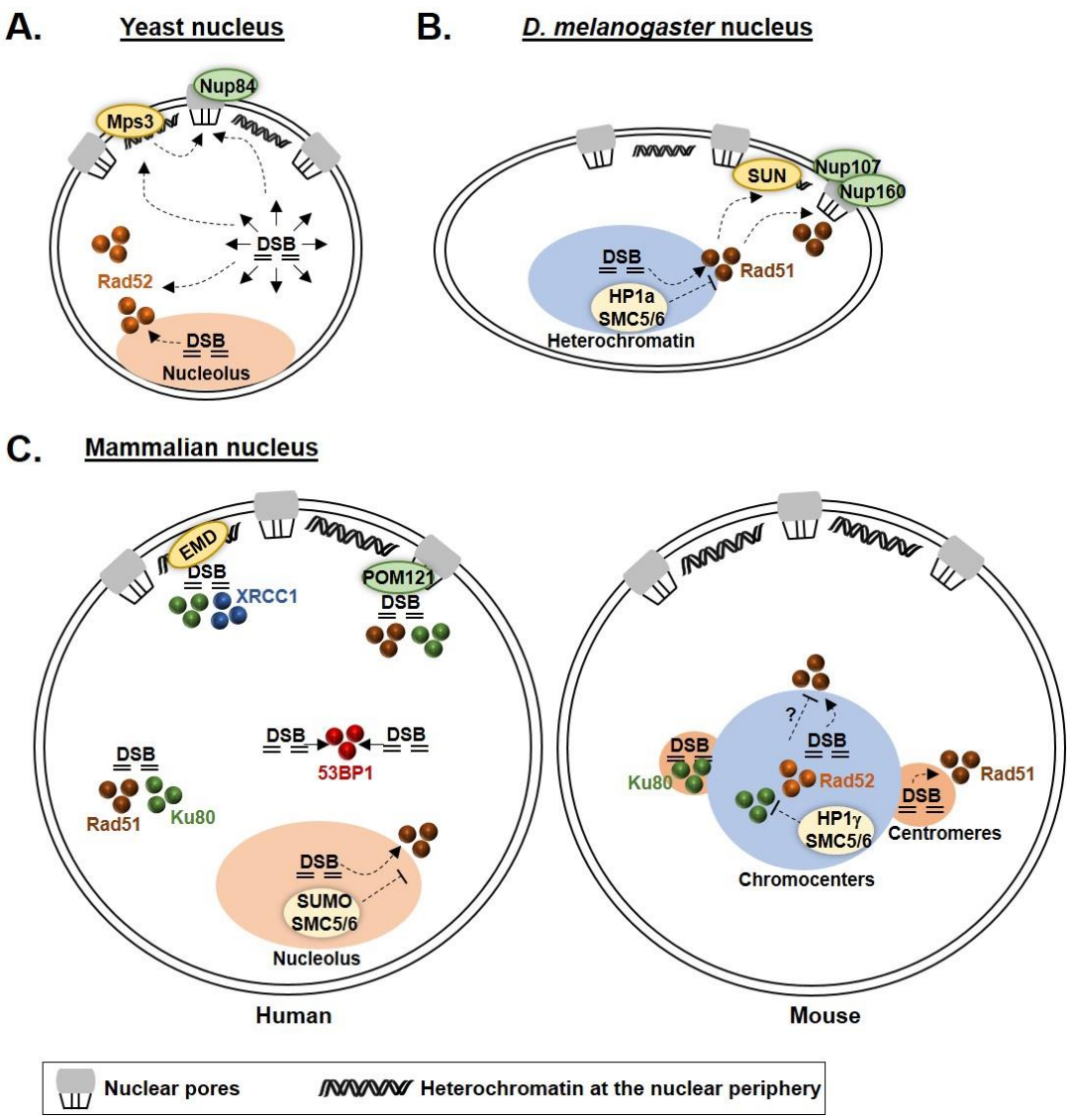

Figure 1.12: DSB mobility and repair pathway choice. A. In yeast, DSBs exhibit increased mobility in comparison with undamaged loci, suggesting that they roam the whole nucleus to find homologous template for their repair. Several DSBs can be recruited at Rad52 repair centers. Irreparable DSBs migrate to the nuclear periphery (Mps3) or at the nuclear pores (Nup84) to be repaired. Since nuclear periphery is a suppressive environment for homologous-mediated repaired, they can further move to a more permissive environment like the pores. Nucleolar DSBs relocate outside of nucleolus to be repaired by HR. **B.** In *D.melanogaster*, heterochromatic DSBs move to the periphery to be repaired by HR that is finally accomplished at the nuclear pores. RAD51 is restricted from the inner part of the heterochromatic domain through HP1a and SMC5/6 complex. **C.** In human cells, DSBs are quite immobile and they are repaired individually by HR (RAD51) or NHEJ (Ku80) when they are induced in the interior of the nucleus. When they are not repaired, they can cluster together in G1 (53BP1). Breaks induced at the nuclear lamina do not migrate to a more permissive environment for their repair but instead they are repaired *in situ* by alt-EJ (XRCC1). DSBs induced at the pores are repaired by HR or NHEJ. Breaks in the nucleolus move to the periphery to be repaired by HR. In mouse cells, DSBs induced within chromocenters migrate to the periphery of these domains to be repaired by HR in G2. In G1 they are repaired *in situ* by NHEJ and SSA (Rad52). On the other hand, centromeric lesions activate NHEJ and HR both in G1 and G2. Not drawn to scale. (Dashed arrows: migration process)

2. Aim of Study

DNA repair occurs in the context of highly structured chromatin. As previously described, heterochromatin, being highly condensed and restricting DNA transactions, renders DSB repair a challenging process for the cells. It has been shown that global and α-particle induced DNA damage results in heterochromatin expansion and relocation of the breaks outside of the heterochromatin core domain. More specifically, in *Drosophila melanogaster* DSBs move outside of the heterochromatic domain in order to be repaired by HR that is finally completed at the nuclear pores. Although these studies have set the basis for understanding how DNA repair proceeds in chromatin dense regions, the underlying mechanisms of DNA repair of heterochromatic breaks are not well understood.

The goal of my PhD was to investigate DSB repair within heterochromatin in mammalian cells. Although HR was identified as the major repair pathway activated after DSB induction in heterochromatin of Drosophila cells, our aim was to verify if this is also the case in mammalian cells or more repair pathways could be activated upon damage induction. Moreover, we wanted to determine if the repair of mammalian heterochromatic DSBs involves chromatin relaxation and break mobility and how this is correlated with the different phases of the cell cycle. An additional aim was to study the repair of different heterochromatic structures in mammalian cells in order to discover if there is a general mechanism for DSB repair in heterochromatin or it is specific for each structure.

To address these questions, we took advantage of the CRISPR system from *S. pyogenes* that consists of two components: Cas9, an endonuclease that generates DSBs and a guide RNA (gRNA) driving it to its target locus. Upon binding to its DNA target, Cas9 can induce one DSB three base pairs before the Protospacer Adjacent Motif (PAM) sequence, another determinant factor for its target specificity. In this case, we engineered a CRISPR/Cas9 system in which DSBs can be efficiently and specifically induced at heterochromatin of NIH3T3 mouse fibroblasts. More specifically, we have designed a gRNA targeting major satellite repeats of pericentric heterochromatin, which in mouse cells corresponds to the DAPI-dense regions known as chromocenters. In parallel, we also designed a gRNA targeting minor satellite repeats of centromeric heterochromatin. Both systems give us the opportunity to address all the above-mentioned questions studying the repair of different heterochromatic structures in mammalian cells.

3. Results

3.1 Temporal and spatial uncoupling of DNA Double Strand Break Repair pathways within mammalian heterochromatin

To address the question of DSB repair in heterochromatin, we took advantage of the CRISPR system from *S. pyogenes* that consists of two components: Cas9, an endonuclease that generates DSBs and a guide RNA (gRNA) driving it to its target locus (Cong et al., 2013). Upon binding to its DNA target, Cas9 can induce one DSB three base pairs before the Protospacer Adjacent Motif (PAM) sequence, another determinant factor for its target specificity (Cong et al., 2013). In this case, we engineered a CRISPR/Cas9 system in which DSBs can be efficiently and specifically induced in heterochromatin of NIH3T3 mouse fibroblasts. More specifically, we have designed a gRNA targeting major satellite repeats of pericentric heterochromatin, which in mouse cells corresponds to the DAPI-dense regions known as chromocenters (Figure 3.1A and 3.1B).

Using high-resolution imaging and 3D reconstruction we find that in G1, both DDR and NHEJ (but not HR) are activated within the heterochromatic core domain, exemplified by the recruitment of Ku80 and several DDR markers. In G2, however, we find that both NHEJ and HR are activated. Nevertheless, contrary to NHEJ (occurring exclusively at the core), HR activity is spatially restricted. While RPA recruitment is observed at the core HC domain, RAD51 is entirely peripheral. This indicates that DNA-end resection and the search for homology are spatially separated and suggests that resected DNA ends relocate to the HC periphery to perform the late steps of HR. Mechanistically, we show that DSB relocation does not involve relaxation of the core HC structure, or the release of HP1s, but rather requires DNA end-resection and the active exclusion of RAD51 from the core HC domain.

To investigate whether the above results are specific to pericentric heterochromatin, we also used the CRISPR/Cas9 system to induce DSBs in centromeric heterochromatin, corresponding to centromeres of NIH3T3 mouse fibroblasts. In this case, we designed a gRNA against centromeric minor satellite repeats and we induced specifically DSBs in centromeres (Figure 3.1A and 3.1B). In contrast to DSBs induced in pericentric heterochromatin, we showed that RAD51 is efficiently recruited at centromeric lesions both in G1 and G2, suggesting that in this case HR is active throughout the cell cycle. On the other hand, Ku80 is recruited in the same way as in pericentric heterochromatin. These results were published on the July 21st 2016 issue of *Molecular Cell*. Based on these data, we have provided insight into the temporal and spatial regulation of DSB

repair pathways within heterochromatin in mammalian cells and we have shown striking differences in the mode of repair between centromeric and pericentric heterochromatin.

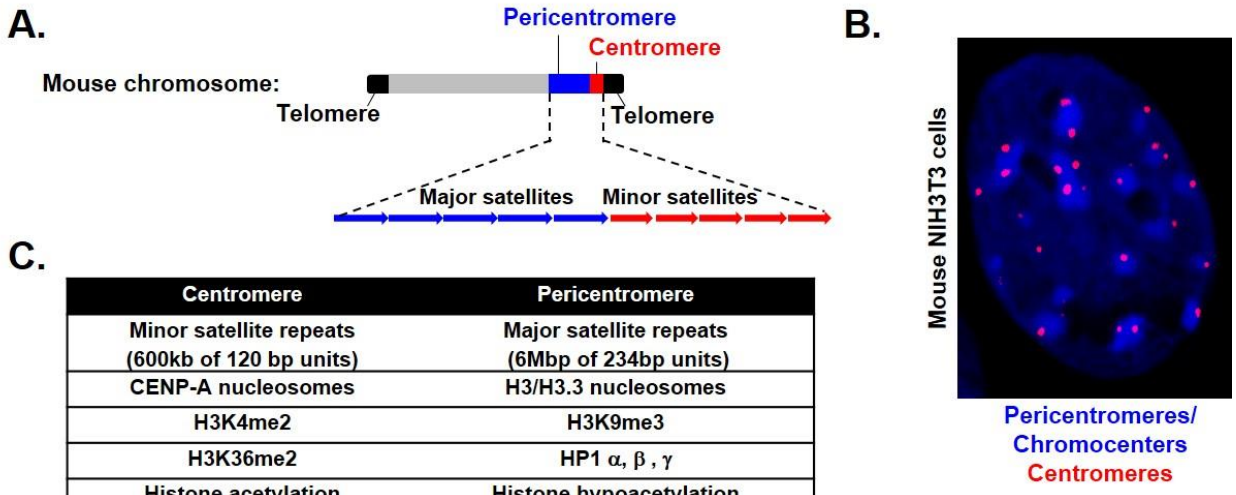

C.

Centromere	Pericentromere
Minor satellite repeats (600kb of 120 bp units)	Major satellite repeats (6Mbp of 234bp units)
CENP-A nucleosomes	H3/H3.3 nucleosomes
H3K4me2	H3K9me3
H3K36me2	HP1 α, β , γ
Histone acetylation	Histone hypoacetylation
	H4K20me2/3
	H3K27me1, H3K64me3

Figure 3.1: Structure of mouse chromosomes and individual characteristics of centromeres and pericentromeres. A. Mouse chromosomes are acrocentric. Centromeric DNA sequence composed of minor satellite repeats is positioned next to pericentric major satellite repeats. **B.** Immunofluorescence (IF) confocal analysis of mouse NIH3T3 cells stained with DAPI (blue -Pericentromeres/Chromocenters) and an antibody specific for CENP-A (red - centromeres). **C.** Differences in the chromatin nature of centromeres and pericentromeres.

Article

Molecular Cell

Temporal and Spatial Uncoupling of DNA Double Strand Break Repair Pathways within Mammalian Heterochromatin

Graphical Abstract

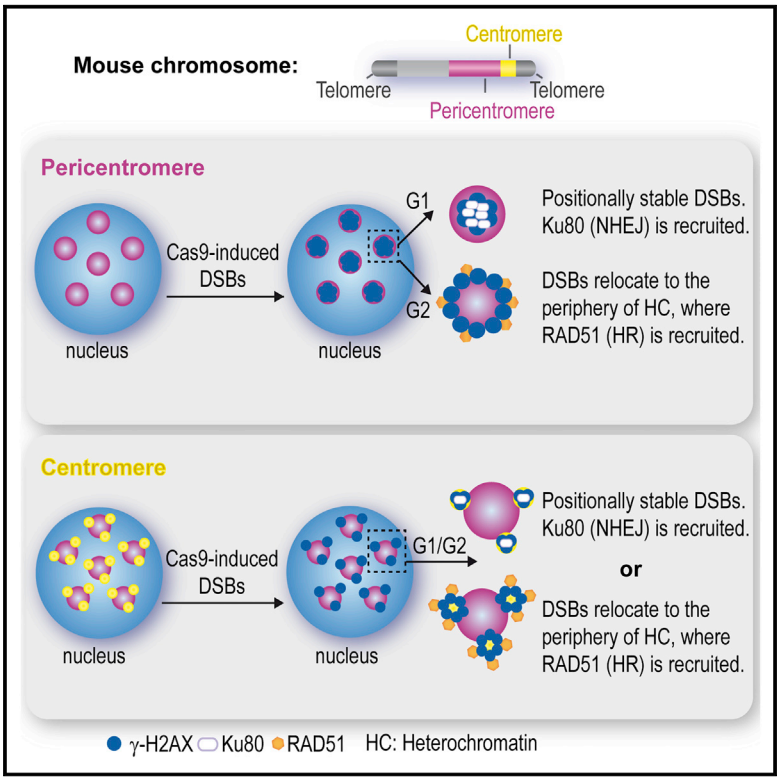

Highlights

- DSBs at pericentric heterochromatin in G1 are positionally stable and recruit Ku80
- DSBs in S/G2 relocate to the periphery of heterochromatin to be bound by RAD51
- DSB relocation requires end resection and RAD51 exclusion from the core
- DSB repair at centromeric and pericentric heterochromatin is strikingly different

Authors

Katerina Tsouroula, Audrey Furst, Melanie Rogier, ..., Alexia Ferrand, Bernardo Reina-San-Martin, Evi Soutoglou

Correspondence

reinab@igbmc.fr (B.R.-S.-M.), evisou@igbmc.fr (E.S.)

In Brief

Tsouroula et al. show that DSBs arising at pericentric heterochromatin in G1 can activate NHEJ at the core. In S/G2, DSBs activate NHEJ, SSA, or HR, with the latter being preferential and spatially restricted to the periphery of heterochromatin. Centromeric DSBs are peripheral and activate NHEJ and HR, independently of the cell cycle.

Tsouroula et al., 2016, Molecular Cell 63, 293–305
July 21, 2016 © 2016 Elsevier Inc.
http://dx.doi.org/10.1016/j.molcel.2016.06.002

Molecular Cell
Article

Temporal and Spatial Uncoupling of DNA Double Strand Break Repair Pathways within Mammalian Heterochromatin

Katerina Tsouroula,[1,2,3,4] Audrey Furst,[1,2,3,4] Melanie Rogier,[1,2,3,4] Vincent Heyer,[1,2,3,4] Anne Maglott-Roth,[1,2,3,4] Alexia Ferrand,[5] Bernardo Reina-San-Martin,[1,2,3,4,6,*] and Evi Soutoglou[1,2,3,4,6,*]
[1]Institut de Génétique et de Biologie Moléculaire et Cellulaire, 67404 Illkirch, France
[2]Institut National de la Santé et de la Recherche Médicale, U964, 67404 Illkirch, France
[3]Centre National de Recherche Scientifique, UMR7104, 67404 Illkirch, France
[4]Université de Strasbourg, 67081 Strasbourg, France
[5]Biozentrum, University of Basel, Klingelbergstrasse 50/70, 4056 Basel, Switzerland
[6]Co-senior author
*Correspondence: reinab@igbmc.fr (B.R.-S.-M.), evisou@igbmc.fr (E.S.)
http://dx.doi.org/10.1016/j.molcel.2016.06.002

SUMMARY

Repetitive DNA is packaged into heterochromatin to maintain its integrity. We use CRISPR/Cas9 to induce DSBs in different mammalian heterochromatin structures. We demonstrate that in pericentric heterochromatin, DSBs are positionally stable in G1 and recruit NHEJ factors. In S/G2, DSBs are resected and relocate to the periphery of heterochromatin, where they are retained by RAD51. This is independent of chromatin relaxation but requires end resection and RAD51 exclusion from the core. DSBs that fail to relocate are engaged by NHEJ or SSA proteins. We propose that the spatial disconnection between end resection and RAD51 binding prevents the activation of mutagenic pathways and illegitimate recombination. Interestingly, in centromeric heterochromatin, DSBs recruit both NHEJ and HR proteins throughout the cell cycle. Our results highlight striking differences in the recruitment of DNA repair factors between pericentric and centromeric heterochromatin and suggest a model in which the commitment to specific DNA repair pathways regulates DSB position.

INTRODUCTION

DNA double-strand breaks (DSBs) are at the origin of genome instability, chromosomal translocations, and cancer (Mills et al., 2003). DSBs are repaired by two main pathways, homologous recombination (HR) that takes place in S/G2, when sister chromatids are present, and non-homologous end joining (NHEJ) that is active throughout the cell cycle (Ciccia and Elledge, 2010). In addition to these, other DNA repair pathways have been described: alternative end joining (AEJ) (Decottignies, 2013) and single-strand annealing (SSA) (Hartlerode and Scully, 2009). These are highly mutagenic and are activated when the main pathways are perturbed. AEJ is involved in the formation of chromosomal translocations in mouse cells (Brunet et al., 2009) and SSA in genomic instability associated with repetitive sequences (Stark et al., 2004). Moreover, excessive use of a main pathway (i.e., uncontrolled recombination), especially between repetitive sequences, can be deleterious for genomic integrity (Guirouilh-Barbat et al., 2014). Chromatin and its compaction state also participate in the regulation of the balance between different DNA repair pathways to suppress mutagenic events and limit their oncogenic potential. Recent findings reveal that the mutation rate at repressive chromatin is higher than in euchromatin and suggest that these environments have impaired repair kinetics or use mutagenic pathways for DNA repair (Roberts and Gordenin, 2014).

Heterochromatin is enriched with deacetylated histones and trimethylated histone H3 on lysine 9 (H3K9me3), as well as non-histone repressive proteins such as KAP1 and the heterochromatin protein 1 (HP1), which bind H3K9me3 (Almouzni and Probst, 2011). It was proposed that heterochromatin needs to decondense to allow efficient DNA repair (Goodarzi et al., 2008; Noon et al., 2010). The mechanisms by which chromatin decompaction occurs after DSB induction appear to involve either the activity of the ataxia telangiectasia mutated (ATM) kinase that phosphorylates KAP1 (Goodarzi et al., 2008; Noon et al., 2010; Ziv et al., 2006) or the release of the heterochromatin protein HP1β (Ayoub et al., 2008).

In *Drosophila*, heterochromatic DSBs initially relocate to the periphery of the heterochromatin domains (Chiolo et al., 2011) and later to the nuclear pore (Ryu et al., 2015). Relocation to the periphery of heterochromatin was also observed in mammalian cells in response to linear ion tracks (Jakob et al., 2011). It was proposed that relocation is a mechanism to avoid recombination between repetitive sequences. Indeed, RAD51 was shown to be recruited only after DSB relocation and was mutually exclusive with HP1α (Chiolo et al., 2011). Interestingly, this relocation requires the activity of ATR kinase and functional DNA end resection (Chiolo et al., 2011).

Here we have established a system using the clustered regularly interspaced short palindromic repeats (CRISPR)/Cas9

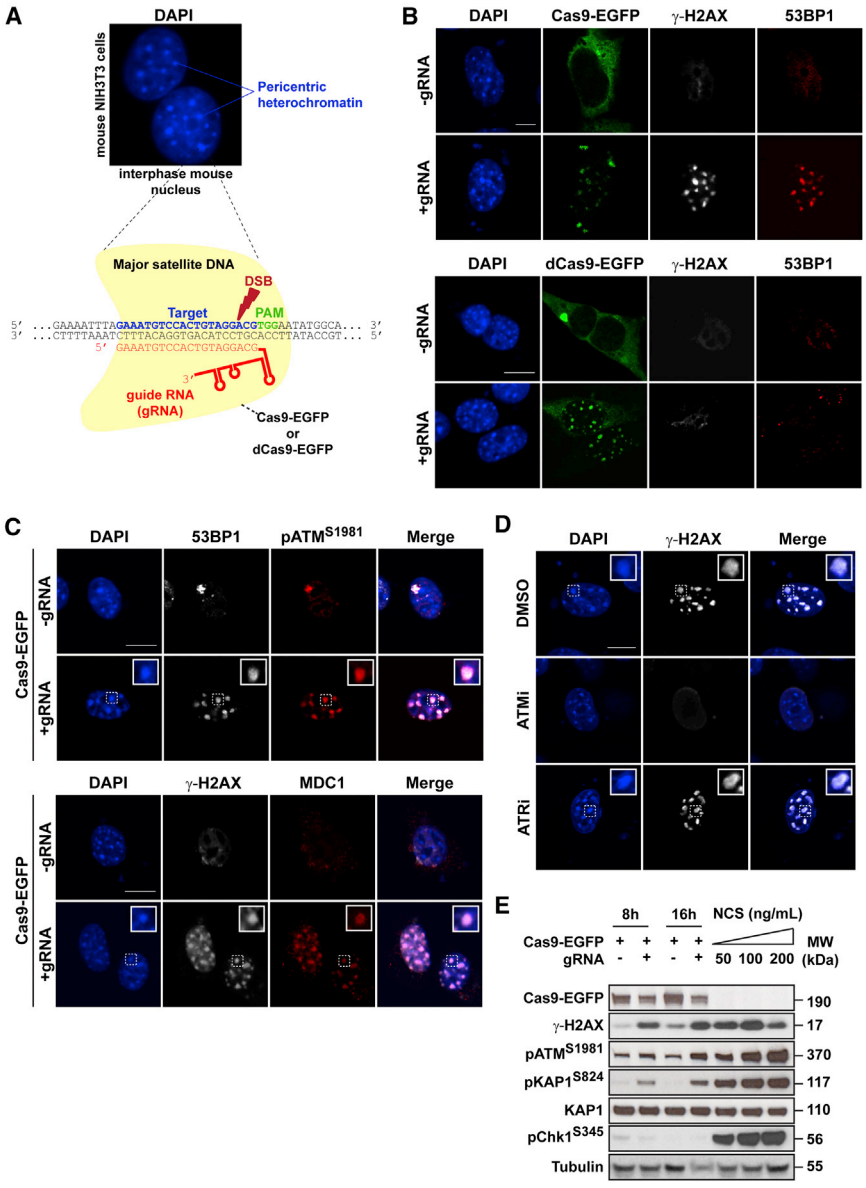

Figure 1. Cas9-Specific Induction of DSBs at Pericentric Heterochromatin

(A) Expression of Cas9-EGFP with a major satellite-specific gRNA in mouse NIH 3T3 cells generates DSBs in pericentric heterochromatin (DAPI-dense regions).

(B) Immunofluorescence (IF) confocal analysis of cells expressing Cas9-EGFP or dCas9-EGFP ± gRNA and stained with DAPI and antibodies specific for γ-H2AX and 53BP1.

(C) IF confocal analysis of cells expressing Cas9-EGFP ± gRNA and stained with DAPI and antibodies specific for 53BP1 and pATM^{S1981} (top) or γ-H2AX and MDC1 (bottom).

(D) IF confocal analysis of cells expressing Cas9-EGFP+gRNA after treatment with ATM (ATMi) or ATR (ATRi) inhibitor or vehicle (DMSO) and stained with DAPI and a γ-H2AX-specific antibody.

(E) Western blot analysis for Cas9-EGFP (EGFP), γ-H2AX, pATM^{S1981}, pKAP1^{S824}, KAP1, pChk1^{S345} and tubulin in protein extracts prepared from cells expressing Cas9-EGFP ± gRNA 8 or 16 hr post-transfection. As a comparison, NIH 3T3 cells were treated with increasing concentrations of NCS. Theoretical molecular weights are indicated.

For confocal images, scale bars represent 10 μm. See also Figure S1.

technology to induce DSBs in specific heterochromatin structures in mammalian cells. We provide insight into the temporal and spatial regulation of DNA repair pathways activated in response to DSBs. Our data also highlight striking differences in the mode of repair between centromeric and pericentric heterochromatin and reveal that the DNA repair pathway regulates the position of the breaks within heterochromatin.

RESULTS

Cas9-Specific Induction of DSBs at Pericentric Heterochromatin and Robust ATM-Dependent DNA Damage Response Activation

To investigate how DSBs occurring within constitutive heterochromatin are repaired, we used the CRISPR/Cas9 technology (Hsu et al., 2014) to engineer a cellular system in which DSBs can be efficiently and specifically induced at heterochromatin (Figure 1A). We designed four different guide RNAs (gRNAs) targeting major satellite repeats of pericentric heterochromatin (Figure 1A; see also Supplemental Information for gRNAs), which in mouse cells correspond to the DAPI-dense regions of the chromocenters, and individually expressed them in mouse NIH 3T3 cells together with the Cas9 nuclease fused to EGFP (Cas9-EGFP). Although Cas9-EGFP is mainly cytoplasmic in the absence of a gRNA (Figure 1B), when coexpressed with any of the four different gRNAs, Cas9-EGFP forms nuclear foci that co-localize with DAPI-dense regions (Figures 1B and S1A). Importantly, Cas9-EGFP recruitment to heterochromatin results in the efficient and robust generation of DSBs, as determined by the appearance of DNA repair foci containing γ-H2AX and 53BP1 (Figures 1B and S1A; we used gRNA #3 for the remainder of the paper). DSB formation is Cas9 dependent as the catalytically inactive Cas9 (dCas9-EGFP) accumulates at DAPI-dense regions but fails to induce γ-H2AX or 53BP1 foci (Figure 1B).

Furthermore, DSBs induced by Cas9-EGFP in heterochromatin efficiently activate the DNA damage response (DDR), as mediator of DNA damage checkpoint 1 (MDC1) and the phosphorylated form of ATM (pATM^{S1981}) are robustly recruited to chromocenters in a gRNA-specific manner (Figure 1C). DDR activation is ATM but not ATR dependent, as only ATM inhibition abrogates γ-H2AX foci formation (Figure 1D) and leads to a

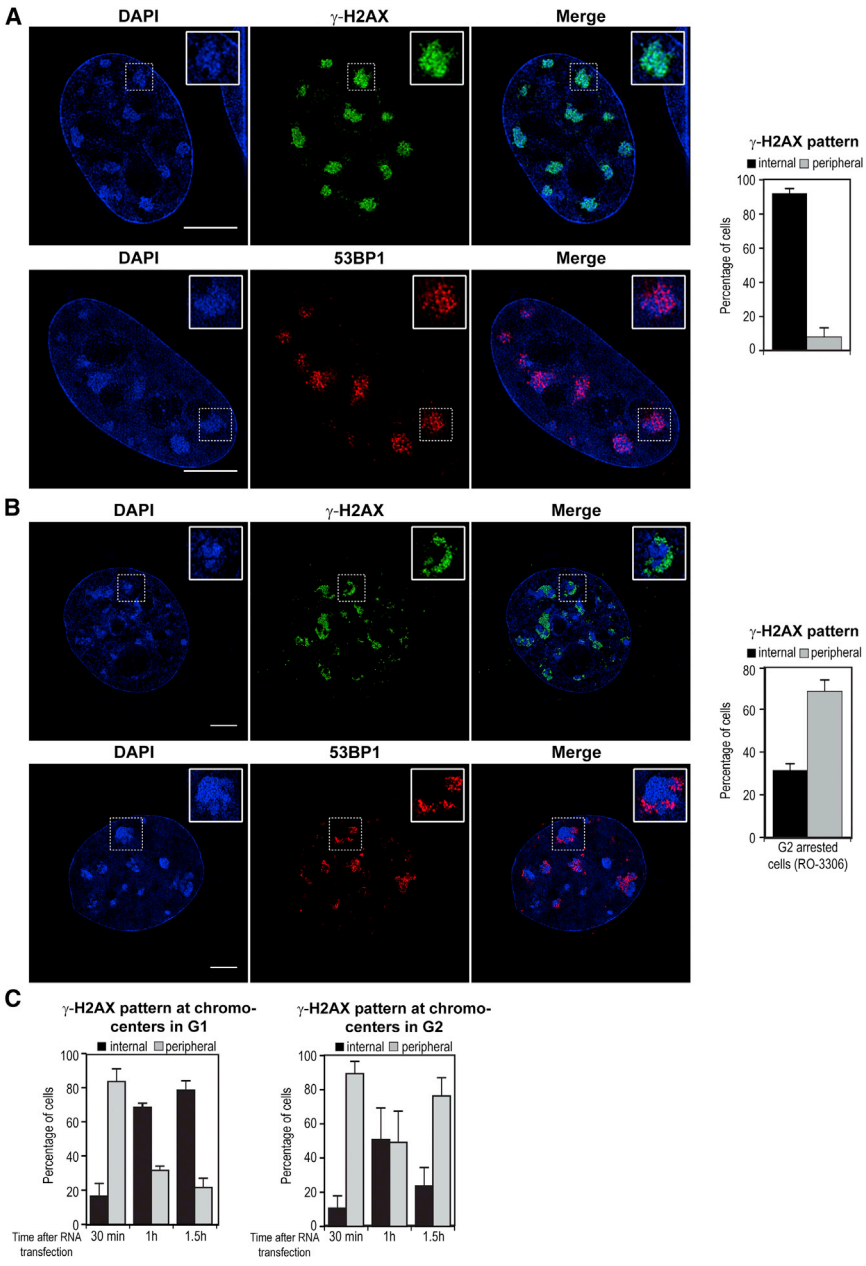

Figure 2. Cell-Cycle-Specific Regulation of DSB Localization in Pericentric Heterochromatin

(A) Super-resolution imaging of cells expressing Cas9-EGFP+gRNA and stained with DAPI and antibodies specific for γ-H2AX (top; Movie S1) or 53BP1 (bottom; Movie S2). Quantification is shown on the right.

(B) Super-resolution imaging analysis of G2 (RO-3306-treated) cells expressing Cas9-EGFP+gRNA and stained with DAPI and antibodies specific for γ-H2AX (top; Movie S3) or 53BP1 (bottom; Movie S4). Quantification is shown on the right.

(C) Quantification of γ-H2AX pattern in G1 (EdU^-/$H3S10p^-$) and G2 (RO-3306-treated, EdU^-/$H3S10p^+$) cells stably expressing Cas9 and transfected with in vitro transcribed major satellite-specific gRNA for the indicated time points and stained with DAPI and antibody specific for γ-H2AX.

For super-resolution images, scale bars represent 5 μm. Values represent mean ± SD of three independent experiments with n = 50 cells. See also Figures S2 and S3.

substantial reduction of the phosphorylation of H2AX, ATM, and KAP1 (Figures S1B and S1C). We also detected a contribution of $DNAPK_{CS}$, as the co-inhibition of $DNAPK_{CS}$ and ATM further reduced the γ-H2AX signal (Figure S1D). The amount of DSBs induced by Cas9-EGFP, as determined by western blot for γ-H2AX, $pATM^{S1981}$, and $pKAP1^{S824}$, is equivalent to treating cells with commonly used doses of neocarzinostatin (NCS; Figure 1E). Furthermore, Cas9-EGFP-induced DSBs do not result in the phosphorylation of Chk1 (Figure 1E), supporting the observation that in this system, DSB signaling is ATR independent (Figures 1D and S1C).

To visualize the accumulation of DDR proteins throughout pericentric heterochromatin with higher resolution, we performed 3D structured illumination microscopy (SIM) experiments (Figure 2A). This analysis revealed a diffused γ-H2AX pattern but discrete 53BP1 foci within the chromocenters (Figure 2A). We estimate that Cas9-EGFP expression induces on average 48 ± 17 foci per chromocenter (Figures S2A and S2B). Although 3D SIM resolves individual 53BP1 foci, the resolution limit of this technique does not allow us to reliably determine whether each focus corresponds to a single DSB or to clusters of closely spaced DSBs.

To determine whether Cas9-induced DSBs can be repaired, we expressed Cas9-EGFP fused to an auxin-dependent degron (Nishimura et al., 2009) (Figure S2C). We found that following Cas9-EGFP degradation, the signal of γ-H2AX and other DDR markers is significantly reduced over time (Figure S2C), indicating that these DSBs can be efficiently repaired.

We conclude that targeting Cas9-EGFP using major satellite-specific gRNAs allows us to visualize heterochromatin in living cells and that it results in the robust generation of DSBs, which activate the DDR and can be efficiently repaired.

Cell Cycle-Specific Regulation of DSB Localization in Pericentric Heterochromatin

In response to DSBs induced by γ-irradiation in *Drosophila* heterochromatin, the DDR is initially activated within the core domain but is rapidly excluded, as the lesions relocate toward euchromatic regions at the periphery of the domain (Chiolo

et al., 2011). Moreover, these breaks relocate to the nuclear pore to continue HR (Ryu et al., 2015). Nevertheless, our analysis shows that in mouse cells, the DDR induced by Cas9 in pericentric heterochromatin is activated at the core of the domain in the majority of the cells (Figures 1B–1D), resulting in a γ-H2AX staining spanning the entire heterochromatin core domain (Figure 2A; Movie S1).

To investigate the origin of the discrepancy between *Drosophila* and mouse cells, we assessed the cell-cycle status of the cells expressing Cas9-EGFP by flow cytometry (Figure S2D). We find that 90% of transfected cells that express Cas9-EGFP reside in G1 (Figure S2D), suggesting that DDR localization is cell-cycle dependent and that DSBs occurring in heterochromatin in G1 are positionally stable. As the vast majority of the Cas9-expressing cells reside in G1, we will consider these cells as being in G1 for the remainder of the paper unless otherwise specified. To determine whether DSBs occurring in different stages of the cell cycle behave differently, we expressed Cas9-EGFP+gRNA in cells arrested in G2 by RO-3306 (Figure S2E) and analyzed the γ-H2AX and 53BP1 pattern (Figure 2B). We find that in the majority of cells arrested in G2 (60%–70%), γ-H2AX and 53BP1 are excluded from the core, suggesting that the lesions relocate to the periphery of the domain (Figure 2B; Movies S3 and S4). These results were confirmed by arresting cells in G2 and co-staining with an H3S10p-specifc antibody, which labels cells in G2 (Figures S2F–S2I). Indeed, H3S10p signal at the core of the domain inversely correlated with γ-H2AX intensity (Figures S2G–S2I). To explore in more detail the γ-H2AX distribution throughout the cell cycle, we blocked cells in G1/S and released them to enter S and G2 (Figures S2J and S2K). In G1/S cells, the γ-H2AX signal is preferentially at the core of the domain (internal), whereas it is peripheral in S and G2 cells (Figure S2K).

To get insight into the kinetics of DSB relocalization and to exclude the possibility that Cas9-EGFP induces lesions exclusively at the periphery, we assessed the γ-H2AX pattern in cells stably expressing Cas9-EGFP in G1 and arrested in G2 at different time points after transfection of in vitro transcribed major satellite-specific gRNA (Figure 2C). We find that the γ-H2AX signal is rapidly (30 min) induced at the periphery of the domain and that it spreads to the core, regardless of the cell-cycle stage (Figures 2C and S2L). Although the γ-H2AX signal remains at the core in G1, it is rapidly relocated to the periphery in G2 (Figure 2C), a process that is independent of the catalytic activity of ATM or ATR (Figures S3A and S3B). Contrary to cells in G1 (Figure S1) and consistent with the literature, we find that activation of the DDR in G2 is both ATM and ATR dependent (Figures S3A, S3C, and S3D).

We conclude that DSBs arising in G1 remain within the core, while the majority of those arising in S or G2 relocate to the periphery. These results reveal a mammalian-specific, cell cycle-dependent regulation of DSB localization in pericentric heterochromatin.

The Recruitment of NHEJ and HR Factors to Heterochromatic Structures Is Spatially and Temporally Regulated

To study the main DNA repair mechanisms that are activated in pericentric heterochromatin and their relation with the break distribution in G1 and G2, we assessed the recruitment of DNA repair factors representative of NHEJ (Ku80) and HR (RAD51; Figure 3). Although repetitive DNA sequences can be potential substrates for HR, RAD51 is not recruited in G1 (Figure 3A). On the other hand, RAD51 is recruited in the vast majority of the cells in G2 exclusively at the periphery of the heterochromatin domain, where it co-localizes with γ-H2AX (Figures 3A and S4A; Movie S5). On the other hand, Ku80 can access the core domain in both stages of the cell cycle, with more cells having detectable Ku80 at the chromocenters in G1 than in G2 (Figure 3B).

DSBs induced at the human nucleolus sequences activate HR and DNA synthesis throughout the cell cycle (van Sluis and McStay, 2015). To investigate whether the G2-specific recruitment of HR proteins at pericentric heterochromatin is unique, we induced DSBs in centromeric heterochromatin. We expressed Cas9-EGFP + 4 different gRNAs specific for the centromeric minor satellite repeats (Figure S4B; see also Supplemental Information for gRNAs). DSBs were efficiently induced, exemplified by γ-H2AX and 53BP1 co-localization with the CREST antibody that labels centromeric heterochromatin (Figure S4B; we used gRNA #2 for the remainder of the paper). Surprisingly, and in contrast to DSBs induced in pericentric heterochromatin, RAD51 is efficiently recruited at centromeric lesions both in G1 and G2, suggesting that HR is active throughout the cell cycle as it was shown for the nucleolus (Torres-Rosell et al., 2007; van Sluis and McStay, 2015). Interestingly, super-resolution microscopy revealed that RAD51 does not co-localize with the centromere (Figure S4C; Movies S6 and S7) and is excluded from the heterochromatic domain as in pericentric heterochromatin (Figures 3A and S4A). Moreover, the γ-H2AX pattern is entirely peripheral and reveals that centromeric lesions relocate toward euchromatin in both stages of the cell cycle following recruitment of RAD51 (Figure S4C; Movies S6 and S7). Ku80, on the other hand, is recruited in the same fashion as in pericentric heterochromatin (Figure 3D). Therefore, contrary to pericentric heterochromatin, DSBs arising in centromeric heterochromatin can recruit NHEJ and HR factors throughout the cell cycle.

To investigate the basis of the difference in RAD51 loading to pericentric or centromeric heterochromatin, we tested the recruitment of RPA as indicative of end resection and a prerequisite for RAD51 loading (Ciccia and Elledge, 2010). As expected, RPA was recruited at centromeric lesions both in G1 and G2 in contrast to pericentromeric heterochromatin, where it was only recruited in G2, following RAD51 recruitment (Figure S4D).

To explore the regulation of end resection in the centromeric and pericentromeric lesions in G1 and G2, we depleted factors that are known to inhibit resection, such as Ku80, RIF1, and 53BP1 (Figure S4E). Depletion of 53BP1, but not of Ku80 or RIF1, significantly increases RAD51 recruitment in G1 in pericentric heterochromatin (Figure S4F). Moreover, 53BP1 depletion increases further RAD51 loading to centromeres in G1 and in G2. Significant increase in RAD51 recruitment to centromeres in G1 is also observed upon Ku80 depletion (Figure S4G). Therefore, end resection that is inhibited in pericentric heterochromatin in G1 is only partially blocked at centromeres, revealing a differential regulation of HR between the two structures.

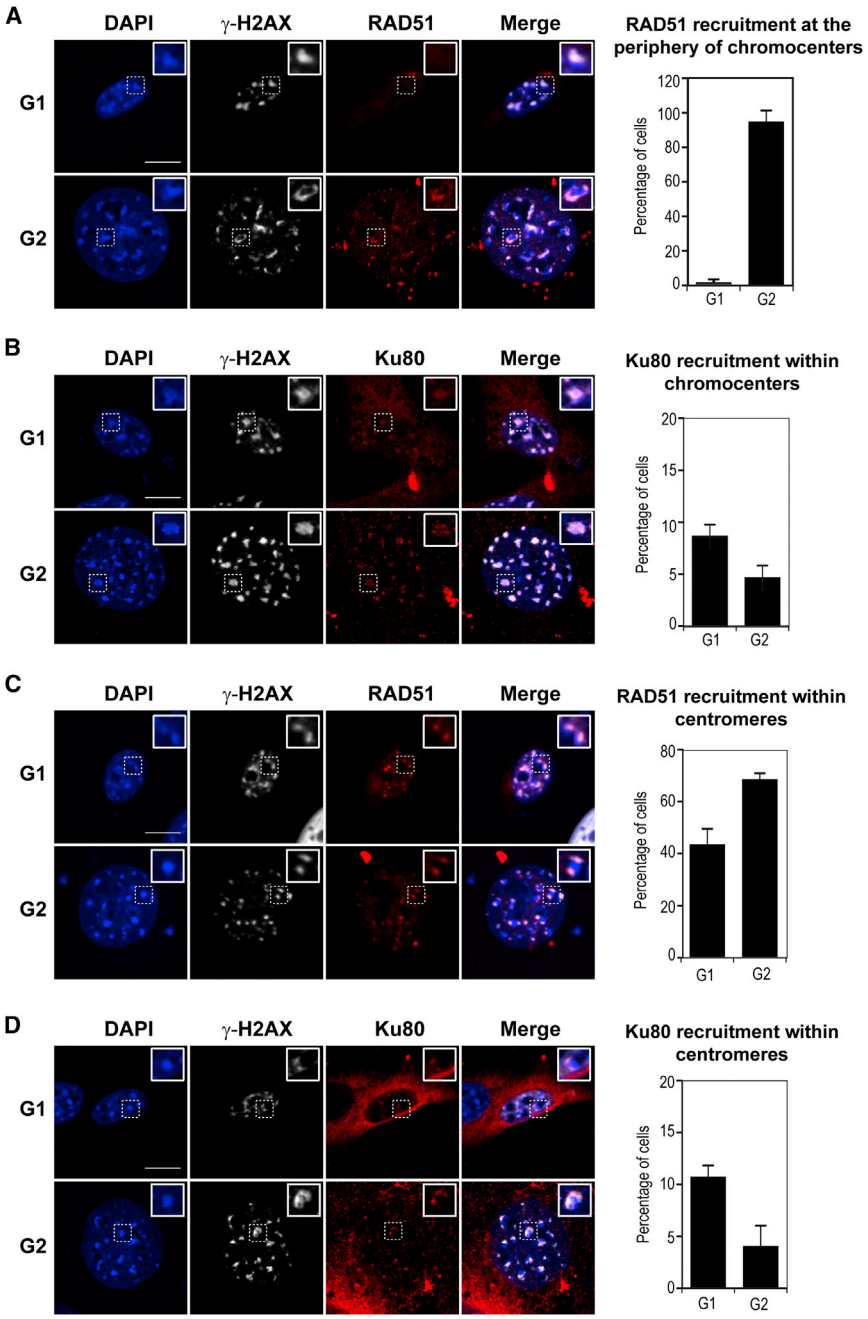

Figure 3. Spatial and Temporal Separation of NHEJ and HR Factor Recruitment in Heterochromatic Structures

(A and B) IF confocal analysis of cells expressing Cas9-EGFP+gRNA specific for major satellite DNA repeats in G1 and G2 and stained with DAPI and antibodies specific for (A) γ-H2AX and RAD51 or (B) γ-H2AX and Ku80. Quantification is shown on the right.

(C and D) IF confocal analysis of cells expressing Cas9-EGFP+gRNA specific for minor satellite DNA repeats in G1 and G2, stained with DAPI and antibodies specific for (C) γ-H2AX and RAD51 or (D) γ-H2AX and Ku80. Quantification of RAD51 or Ku80 recruitment is shown on the right.

Scale bars represent 10 μm. Values represent mean ± SD of three independent experiments with n = 50 cells. See also Figures S4 and S5.

To determine whether the presence of the sister chromatid is required for RAD51 recruitment in pericentric heterochromatin, we induced DSBs in cells arrested in G1/S, S or G2. Although RAD51 loading is concomitant with EdU incorporation (Figures S5A, S5B, and S5D), at the centromeric heterochromatin, it is independent of the cell cycle (Figures S5A, S5C, and S5D). This suggests that replication is a pre-requisite for RAD51 loading only at pericentric heterochromatin.

We conclude that the recruitment and localization of Ku80 in response to Cas9-induced DSBs is influenced neither by the sequence nor by the nature of the heterochromatic structure, that it occurs throughout the cell cycle, and that compacted repetitive sequences are accessible. Contrary to Ku80, recruitment of RAD51 is sensitive to the heterochromatin environment. Although RAD51 is always excluded from the core domain, at centromeres it does not require DNA replication, whereas at pericentric heterochromatin it is exclusively post-replicative.

Cas9-Induced DSBs Trigger Chromatin Expansion Independently of the Release of HP1s or Associated Post-translational Modifications

Chromatin undergoes rapid local and global decondensation in response to DSBs, a process that has been proposed to facilitate genome surveillance by enhancing access of DDR proteins to the sites of damage (Misteli and Soutoglou, 2009). To assess the nature and extent of chromatin alterations occurring after DNA damage in heterochromatin, we measured the average intensity of different heterochromatin-related proteins (HP1α, HP1β, HP1γ, KAP1) or post-translational modifications (γ-H2AX, pKAP1^{S824} and H3K9me3) as well as the average area of chromocenters (DAPI-dense regions) in the presence or absence of Cas9-induced DSBs in G1 and G2 (Figure 4A). As expected, the intensity of γ-H2AX and pKAP1^{S824} at the chromocenters increased after DNA damage, in both G1 and G2 (Figures 4B and 4C). Consistent with previous reports (Chiolo et al., 2011), an expansion of heterochromatin is observed throughout the cell cycle (Figure 4D). Surprisingly, chromatin relaxation is accompanied neither by the eviction of HP1α, β, or γ (Figures 4E–4G) nor by the reduction in the repressive mark H3K9me3

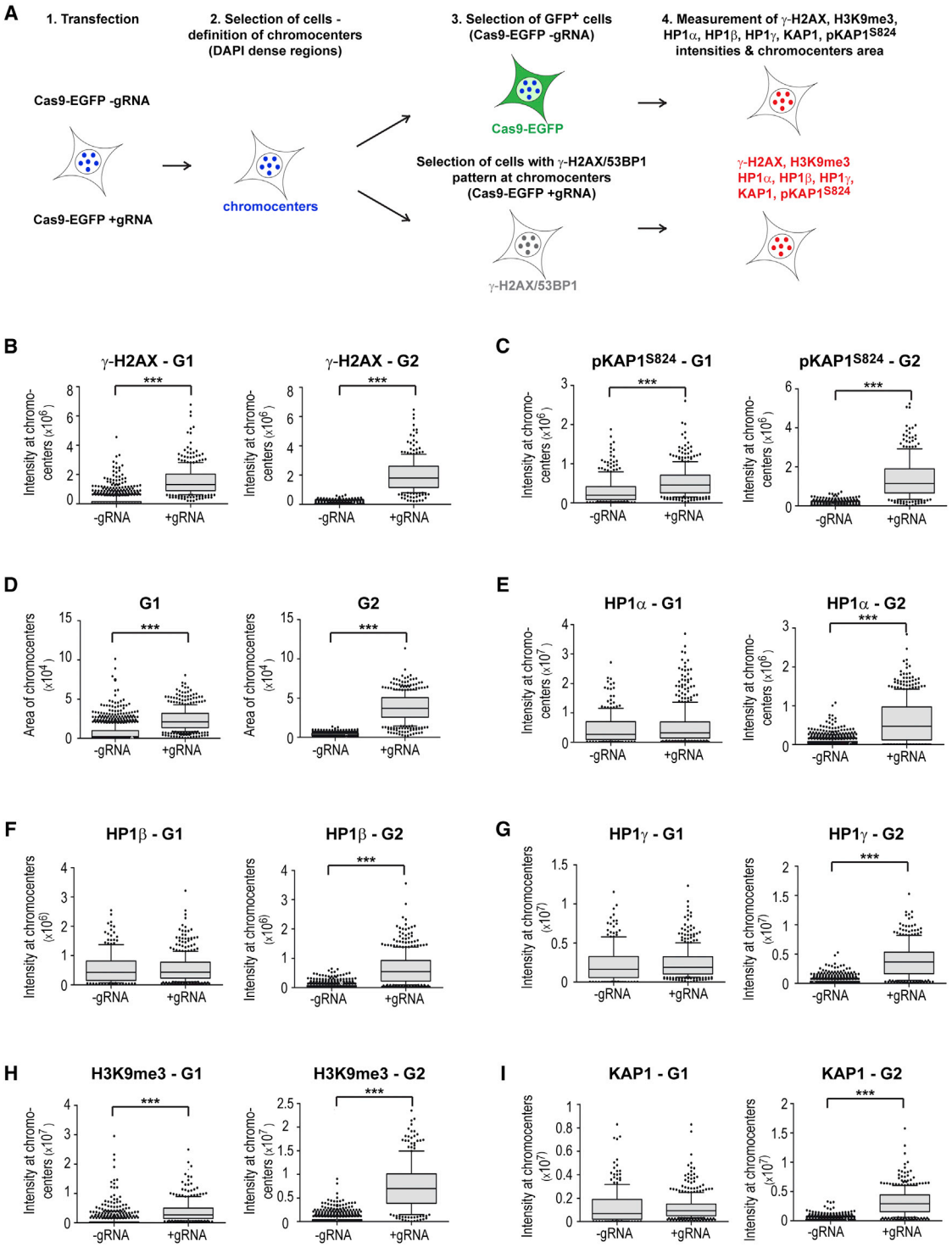

Figure 4. Cas9-Induced DSBs Induce Chromatin Expansion Independently of the Release of HP1s or Associated Modifications

(A–I) Schematic representation of the high-throughput analysis (see Supplemental Experimental Procedures) to measure the intensity of γ-H2AX (B), pKAP1^{S824} (C), HP1α (E), HP1β (F), HP1γ (G), H3K9me3 (H), and KAP1 (I) and the chromocenter (DAPI-dense) area (D). For all plots, individual cell values are represented as box-and-whisker plots (median and quartiles with outliers representing 1% of the population) of two independent experiments with n > 300 cells for G1 and n > 350 cells for G2 (RO-3306 treated cells).

(Figure 4H). On the contrary, the intensity of H3K9me3 increased upon DNA damage (Figure 4H). The HP1 proteins together with KAP1 exert different behavior in G1 and G2. Although the intensity of HP1 (α, β, and γ) does not change in G1, it does follow the increase of H3K9me3 in G2 (Figures 4E–4H). A similar behavior was observed for KAP1 (Figures 4I). Therefore, chromatin expansion triggered by DSBs in heterochromatin is mediated neither by the release of HP1s/KAP1 nor by the reduction in heterochromatin-associated repressive marks.

Compacted Chromatin Is Not Refractory to the Recruitment of DNA Repair Factors

Chromatin expansion and the concomitant eviction of heterochromatin-associated proteins drives DSB relocation toward euchromatic regions to be repaired by HR in *Drosophila* cells (Chiolo et al., 2011). To test whether compacted chromatin is refractory to the recruitment of RAD51 at the core heterochromatin domain and to determine whether the lesions relocate to open chromatin environments, we forced chromatin relaxation at pericentric heterochromatin and assessed the γ-H2AX and RAD51 pattern (Figure 5). We first treated the cells with the histone deacetylase inhibitor Trichostatin A (TSA), which induces robust chromatin relaxation (Lemaître et al., 2014). As previously reported, TSA treatment leads to hyperacetylation of H4 and triggers the release of HP1s from pericentric heterochromatin (Figure S6A). Nevertheless, TSA treatment did not alter the pattern of γ-H2AX or RAD51 recruitment in G1 or G2 (Figures 5A and 5B). Similarly, tethering the transcriptional activator VP64 to pericentric heterochromatin through the expression of Cas9-VP64, which induced transcription of the major satellite repeats (Figure S6B), had no significant effect neither on the γ-H2AX pattern nor in the exclusion of RAD51 from the core domain (Figures 5A and 5B). To consolidate these findings, we used small interfering RNAs (siRNAs) to deplete KAP1, HP1α, β, and γ or the three HP1s together and examined the γ-H2AX and RAD51 patterns in control and siRNA-depleted cells (Figure 5A and 5B). KAP1 and HP1 depletion did not lead to recruitment of RAD51 inside the core domain or to changes in the location of the lesions (Figures 5A and 5B). Interestingly, as previously described (Baldeyron et al., 2011; Lee et al., 2013; Soria and Almouzni, 2013), depletion of HP1 leads to a decrease in the percentage of cells that exert RAD51 recruitment at DSBs in G2, without affecting its spatial distribution (Figure 5B, right). Similar results were obtained upon KAP1 depletion (Figure 5B). Importantly, the individual siRNAs used to knockdown *KAP1* and *HP1s* are specific and did not affect RAD51 protein levels (Figure S6C). Moreover, HP1 depletion did not affect cell-cycle profiles of G1- and G2-arrested cells (Figure S6D).

In *Drosophila*, the SMC5/6 complex is enriched in heterochromatin, and it is required to exclude RAD51 from the heterochromatin domain (Chiolo et al., 2011). To explore the possibility of SMC5/6 involvement in the exclusion of RAD51 from the mammalian heterochromatin, we depleted SMC5, SMC6, or both using siRNAs (Figure S6E). Whereas depletion of SMC5 or SMC6 had no effect on the γ-H2AX pattern (Figure S6F), the combined depletion of both had a minor but significant decrease in the peripheral γ-H2AX pattern in G2 cells (Figure S6G). It did not influence, however, the spatial distribution of RAD51 (Figure S6H), suggesting that an additional mechanism enforces the peripheral localization of RAD51.

We next examined whether chromatin compaction or heterochromatin proteins affect the recruitment of Ku80 in all the above-described conditions in G1 and G2 cells (Figures 5C and S6I). Although we find that the chromatin environment does not influence the access of Ku80 to DSBs within the core, depletion of HP1γ decreased the recruitment of Ku80 (Figure 5C), suggesting that this isoform may play a role in NHEJ. Furthermore, SMC5/6 depletion increased the recruitment of Ku80 in G1 (Figure S6I), suggesting an inhibitory role of the SMC5/6 complex for the binding of Ku80 to DNA ends.

We conclude that the presence of heterochromatin compaction building factors does not render heterochromatin refractory to the recruitment of DNA repair proteins and that it does not influence the spatial distribution of DSBs arising within the domain.

DSB Relocation at the Periphery of the Heterochromatin Domain Is Dependent on DNA End Resection

To exclude the possibility that the peripheral RAD51 loading occurs because end resection is active only at the periphery, we assessed the spatial distribution of RPA at the chromocenters (Figure 6A). We find that RPA is loaded at the core domain (Figure 6A), suggesting that although resection can occur within the core, RAD51 loading occurs only at the periphery. Because resection is the initiating step of HR, we investigated whether it is the driving force of DSB relocalization. We blocked end resection by three different means. We first inhibited MRE11 activity using Mirin (Dupré et al., 2008). We find that Mirin reduces the number of cells with peripheral γ-H2AX pattern and increases those with an internal pattern (Figure 6B). Consistent with this, depletion of CtIP leads to a reversal of the internal/peripheral γ-H2AX pattern (Figure 6C). To further prove that resection is involved in the process, we overexpressed the bacterial ortholog of Ku80 (GAM) fused to emerald GFP (EmGFP). GAM-EmGFP binds to DNA ends and inhibits end resection (Shee et al., 2013). Indeed, expression of GAM-EmGFP is sufficient to reduce the proportion of cells with peripheral γ-H2AX pattern (Figure 6D). The efficiency of Mirin and GAM-EmGFP overexpression in inhibiting resection was verified by the reduction in the recruitment of RAD51 (Figures S7A and S7B). The efficiency of CtIP depletion by siRNA was determined by RT-PCR and western blot (Figure S7C and S7D).

To further investigate the involvement of end resection in the spatial distribution of DSBs in heterochromatin, we tethered CtIP to the chromocenters by expressing Cas9 fused to CtIP. CtIP tethering increased the peripheral γ-H2AX pattern (Figures 6E and S7E). Surprisingly, CtIP tethering is sufficient to boost RAD51 binding to DSBs in G1 (Figure S7F) and to enhance the peripheral γ-H2AX pattern in G1 (Figure S7G).

These results suggest that DNA end resection is a prerequisite for DSBs relocation toward the periphery of heterochromatin.

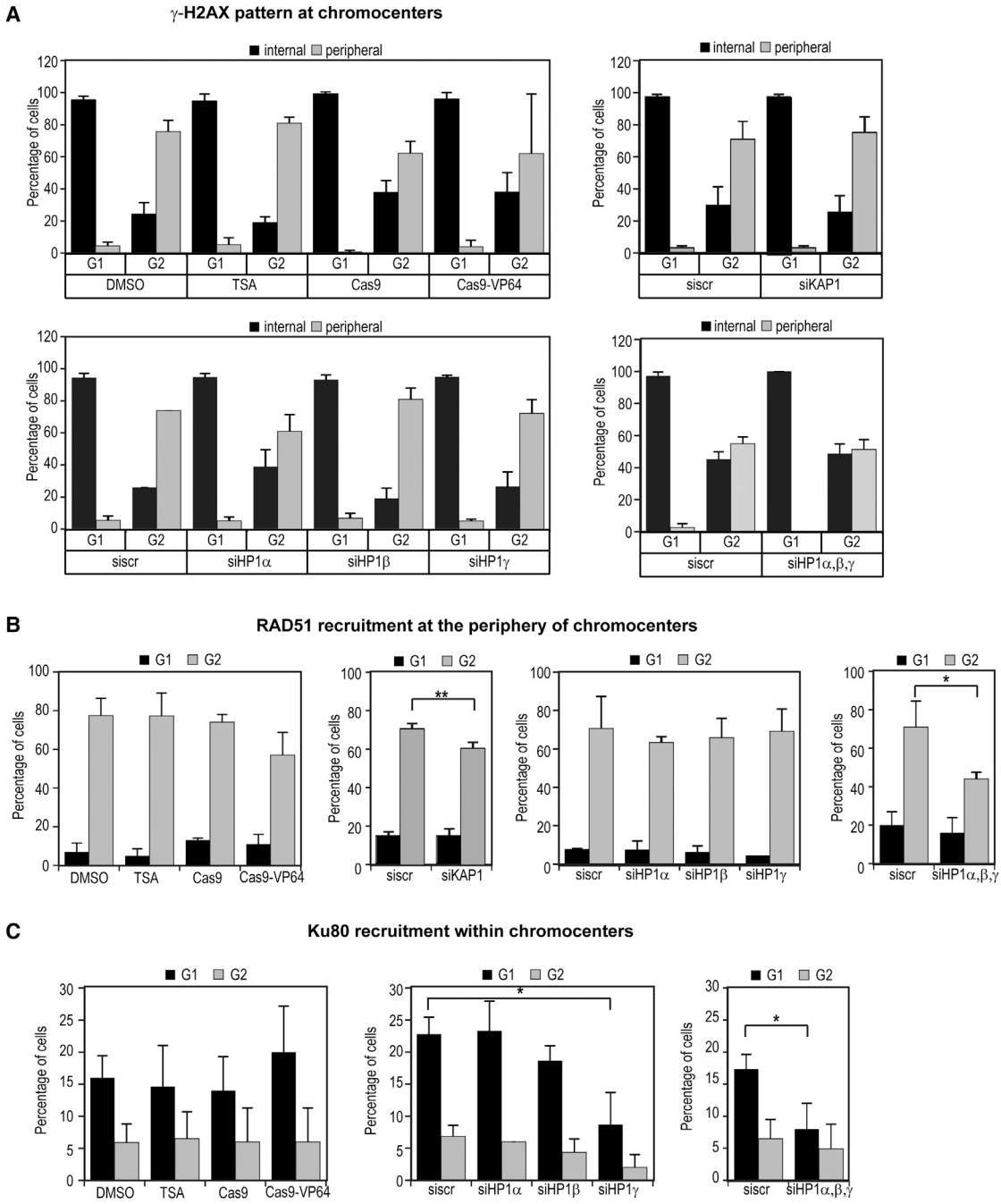

Figure 5. Compacted Chromatin Is Not Refractory to the Recruitment of RAD51

(A–C) Quantification of γ-H2AX pattern (A), RAD51 (B), or Ku80 (C) in G1 and G2 cells expressing Cas9-EGFP+gRNA and treated with DMSO or TSA, expressing Cas9-EGFP+gRNA or Cas9-EGFP-VP64+gRNA or depleted for KAP1, HP1α, HP1β, and HP1γ. Values represent mean ± SD of three independent experiments with n = 50 cells. See also Figure S6.

The RAD51/BRCA2 Complex Stabilizes DSBs at the Periphery of Heterochromatin

Inhibition of resection changes the distribution of γ-H2AX upon DSB induction in G2 (Figure 6). However, lack of DSB movement or internal γ-H2AX pattern is not sufficient to drive the recruitment of RAD51 to the core domain, suggesting an exclusion mechanism that might involve DSB stabilization at the periphery. To investigate the role of RAD51 in DSB relocalization, we depleted BRCA2 (Figure S7H) to inhibit RAD51 loading to resected DNA. As expected, BRCA2 depletion resulted in a dramatic decrease of RAD51 loading to the periphery of the chromocenters in G2 (Figure 7A). Interestingly, the majority of

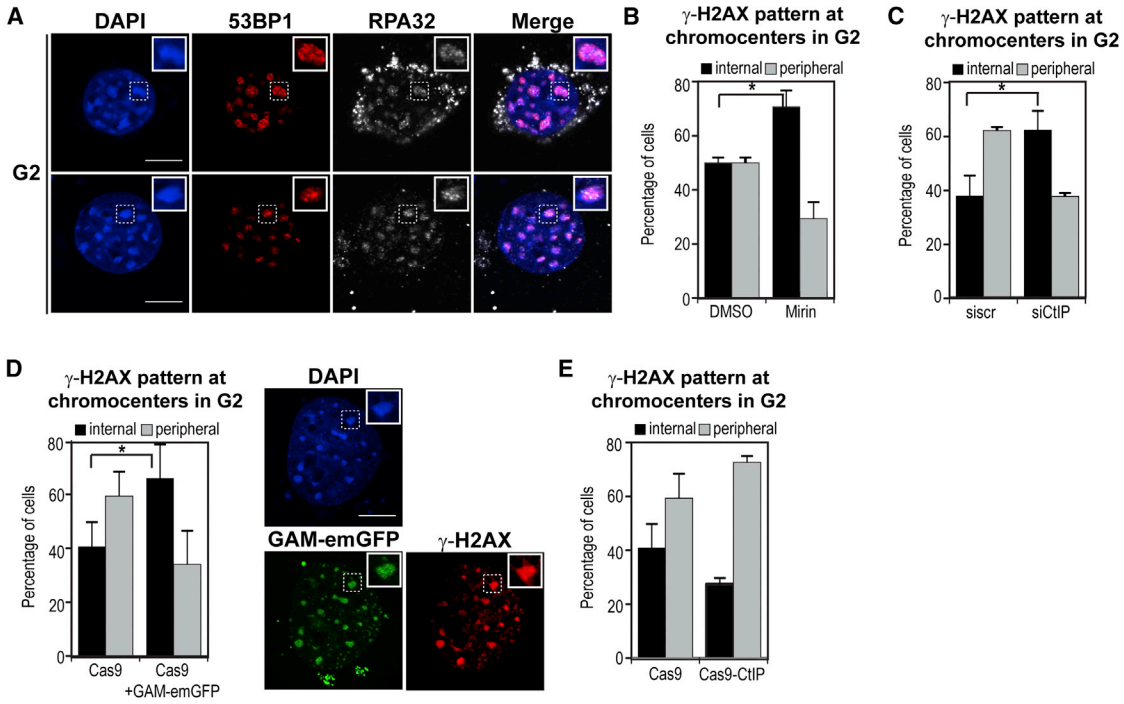

Figure 6. DSB Relocation at the Periphery of the Heterochromatin Domain Is Dependent on DNA End Resection

(A) IF confocal analysis of G2 cells expressing Cas9-EGFP+gRNA stained with DAPI and antibodies specific for 53BP1 and RPA32.

(B–E) Quantification of γ-H2AX pattern in G2 cells expressing Cas9-EGFP+gRNA after treatment with DMSO or Mirin inhibitor (B), *CtIP* knockdown (C), GAM-EmGFP expression (D), or Cas9-CtIP expression (E). (D) IF confocal analysis of G2 cells expressing Cas9-mCherry+gRNA + GAM-EmGFP stained with DAPI and a γ-H2AX-specific antibody is shown.

Scale bars represent 10 μm. Values represent mean ± SD of three independent experiments with n = 50 cells. See also Figures S7A–S7G.

BRCA2-depleted cells displayed an internal instead of a peripheral γ-H2AX pattern (Figure 7B). This suggests that if resected DNA ends are not engaged by factors that promote homology search, they are not stabilized at the periphery. To further investigate the requirement of RAD51 for DSB relocalization, we forced RAD51 to enter the core domain by expressing Cas9 fused to RAD51 (Figure 7D). We find that tethering of RAD51 to the chromocenters inhibits DSB relocalization to the periphery of the structure, highlighting the importance of the exclusion of RAD51 from the core domain in the process (Figure 7C). To get further insight into the involvement of the RAD51/BRCA2 complex in the stabilization of DSBs at the periphery, we fused Cas9 to the BRC3 domain of BRCA2, which tightly binds RAD51 (Reuter et al., 2014), and tethered it to pericentric heterochromatin (Figure 7D). We find that BRC3 tethering is sufficient to bypass the RAD51 exclusion from heterochromatin and that Rad51 accumulates at the core (Figures 7C, S7G, and S7I). Furthermore, BRC3 tethering inhibits DSB relocalization to the periphery, as determined by the γ-H2AX pattern (Figure 7C). This was specific, as tethering of a BRC3 deletion mutant, which does not bind RAD51, failed to do so (Figure 7C).

We conclude that the RAD51/BRCA2 complex is necessary and sufficient to trap DSBs at the periphery of heterochromatin.

DSBs that Fail to Relocate to the Periphery of Heterochromatin Are Engaged by the SSA Factor RAD52

We have shown that the majority of DSBs occurring in G2 relocate to the periphery of heterochromatin where RAD51 is loaded. Nevertheless, there is a fraction of cells that, although RAD51 is recruited at the periphery, display a γ-H2AX staining throughout the structure (Figure 2B), suggesting that in these cells, not all DSBs have relocated to the periphery. To study whether other DNA repair factors can access the heterochromatin core, we assessed the recruitment of RAD52, which is involved in SSA, a DNA repair pathway activated in response to DSBs arising at repetitive sequences (Hartlerode and Scully, 2009). We find that RAD52 is recruited to Cas9-induced DSBs mainly in G2 and in small percentage of cells in G1 (Figures 7E and 7F). The recruitment of RAD52 is apparent both at the core and at the periphery in both stages of the cell cycle, and the percentage of cells with RAD52 at the core correlates with the number of cells that display an internal pattern of γ-H2AX in G2 (Figure 2B), suggesting that although the majority of lesions relocate to the periphery, resected breaks that fail to relocate recruit RAD52. To test the involvement of RAD52 (Figure S7K) in DSB relocation, we assessed the effect of its depletion on γ-H2AX pattern (Figure 7G). We find that depletion of RAD52 leads to increased peripheral γ-H2AX pattern (Figure 7G), suggesting that RAD52 is capable of retaining DSBs within the heterochromatic core. Interestingly,

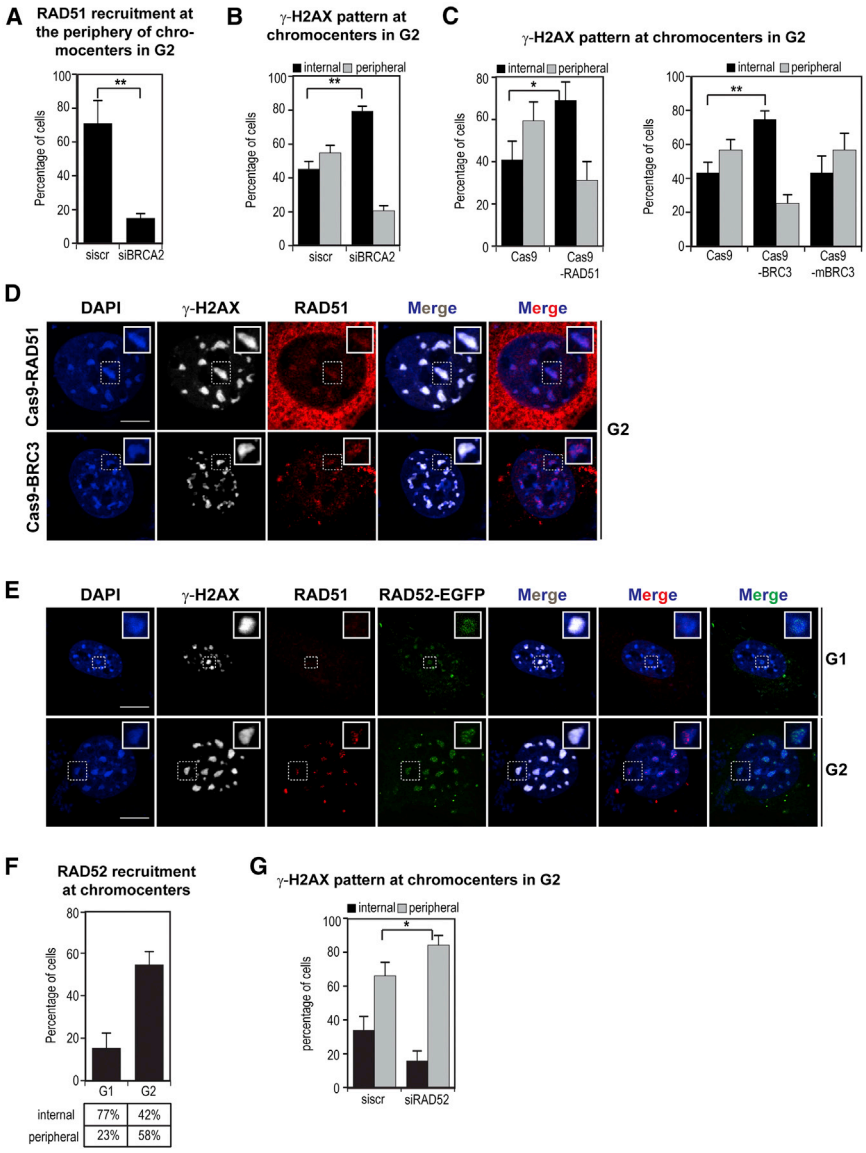

Figure 7. The RAD51/BRCA2 Complex Stabilizes DSBs at the Periphery of Heterochromatin

(A and B) Quantification of RAD51 recruitment (A) and γ-H2AX pattern (B) in G2 cells expressing Cas9-EGFP+gRNA under *BRCA2* knockdown conditions.

(C) Quantification of γ-H2AX pattern in G2 cells expressing Cas9-RAD51 (left) or Cas9-BRC3 or Cas9-mBRC3 (right).

(D) IF confocal analysis of G2 cells expressing Cas9-RAD51 or Cas9-BRC3+gRNA stained with DAPI and specific antibodies for γ-H2AX and RAD51.

(E) IF confocal analysis of G1 and G2 cells expressing Cas9-mCherry + gRNA + RAD52-EGFP stained with DAPI and specific antibodies for γ-H2AX and RAD51.

(F) Quantification of RAD52 recruitment and pattern in G1 and G2 expressing Cas9-mCherry + gRNA + RAD52-EGFP.

(G) Quantification of γ-H2AX pattern in G2 cells expressing Cas9-EGFP + gRNA under *RAD52* knockdown conditions.

Scale bars represent 10 μm. Values represent mean ± SD of three independent experiments with n = 50 cells. See also Figures S7H–S7M.

depletion of RAD52 did not change RAD51 recruitment and vice versa (Figures S7I–S7M), suggesting that if there is a balance between HR and SSA, this occurs prior to the recruitment of these proteins.

Our results are consistent with a model in which the spatial disconnection between DNA end resection and homology search and the exclusion of Rad51 from the core prevent the activation of mutagenic pathways and illegitimate recombination.

DISCUSSION

Repetitive DNA is often packaged into heterochromatin structures in order to prevent illegitimate recombination events and maintain genomic stability. Although heterochromatin integrity is fundamental for faithful mitotic progression, repairing DSBs within this structure represents a challenge that cells need to overcome. Despite great interest and recent progress in the field, little is known about the underlying mechanisms of repairing DSBs in heterochromatin in mammalian cells. Here we have developed a unique system that allows us to simultaneously visualize different heterochromatin structures and to homogeneously and efficiently generate DSBs.

We find that different heterochromatin environments can activate different DNA repair pathways in a unique and characteristic fashion. Although the NHEJ protein Ku80 is recruited throughout the cell cycle both in centromeric and pericentric heterochromatin, end resection and the recruitment of RAD51 is heterochromatin domain specific. At centromeric DSBs, RPA and RAD51 are recruited throughout the cell cycle. Their recruitment is enhanced in G2 and does not require DNA replication. In pericentric heterochromatin, however, RAD51 recruitment occurs exclusively at post-replicative chromatin at the periphery of the heterochromatin domain.

These findings suggest that although both structures are condensed, their unique chromatin modifications, DNA sequence, and histone variant composition might influence the outcome of DNA repair. Indeed, pericentric heterochromatin is enriched in H3K9me3 and HP1s. The centromere core consists of clusters of H3 variant CENP-A and H3 nucleosomes (Chan and Wong, 2012). The H3 nucleosomes are enriched for H3K4me2 and H3K36 methylation and H3 acetylation, marks of active chromatin, and no H3K9me3 could be detected at the centromere core domain (Chan and Wong, 2012). Recently, it was shown that active chromatin marks and especially

H3K36me3 promote DNA end resection and HR by recruiting CtIP through LEDGF, a chromatin binding protein that binds H3K36me3 (Aymard et al., 2014; Daugaard et al., 2012). On the other hand, breaks induced in inactive genes that are not associated with H3K36me3 recruit NHEJ factors (Aymard et al., 2014; Pfister et al., 2014). It is therefore possible that the active chromatin marks present only at the centromere are permissive to resection in G1. Recent data revealed that repair by HR in G1 is inhibited by the suppression of end resection coupled to PALB2 ubiquitination that prevents the assembly of the BRCA1/PALB2/BRCA2 complex (Orthwein et al., 2015). Interestingly, the majority of the resected DSBs in centromeric heterochromatin recruit RAD51 in G1, suggesting that this mechanism is not active in this particular structure. How this mechanism is bypassed is unknown. Nevertheless, it is possible that the deubiquitylase USP11, which counteracts the PALB2 ubiquitination and is normally degraded in G1 upon IR, is locally protected from degradation. Moreover, breaks at Lamin-associated domains that are also heterochromatic fail to activate HR, further suggesting that individual heterochromatin domains are differentially repaired (Lemaître et al., 2014).

As centromeres from different chromosomes are spatially separated within the nucleus and do not cluster together, we think that the risk of chromosomal translocations is minimal and speculate that this could account for the licensing of HR to occur throughout the cell cycle.

We show that Ku80 can access the heterochromatin core in spite of its high level of compaction. This is further strengthened by the fact that chromatin decondensation by TSA, HP1 depletion, or VP64 tethering does not enhance the recruitment of Ku80 at DSBs induced by Cas9 at the chromocenters. This is consistent with studies showing that heterochromatin is not refractory to the diffusion of large proteins (Bancaud et al., 2009). In contrast, depletion of HP1γ leads to a decrease in the percentage of cells with Ku80 at DSBs in pericentric heterochromatin, suggesting that in the absence of HP1γ, end resection is not restricted by Ku80 binding. This could explain previous findings showing that HP1γ inhibits end resection (Kalousi et al., 2015).

Our results also suggest that DSB relocalization in heterochromatin depends on the DNA repair pathway choice. In pericentric heterochromatin, DSBs relocate to the periphery in G2 where HR factors are recruited. At centromeres, RAD51 loading is also occurring in G1, and relocation and exclusion of RAD51 are apparent throughout the cell cycle. Our findings also show that in contrast to what was observed in *Drosophila* (Chiolo et al., 2011; Ryu et al., 2015), the compacted state of heterochromatin is not refractory to RAD51 and that chromatin relaxation does not lead to increased access of RAD51 to the core. Moreover, although DSBs at pericentric and centromeric heterochromatin lead to global expansion of the domain, it is not the cause of DSB relocation. This is in agreement with data in mouse embryonic fibroblasts showing that DSB relocation induced by linear ion track at heterochromatin does not depend on ATM, a factor proposed to promote DSB-induced relaxation of the domain (Goodarzi et al., 2008; Jakob et al., 2011). Therefore, in mammalian cells DSB relocation and heterochromatin expansion are functionally unlinked.

Interestingly, the chromatin expansion observed at the chromocenters is not a consequence of the eviction of heterochromatin proteins or repressive marks. In contrast, we find that H3K9me3 intensity increases both in G1 and G2 and that HP1s together with KAP1 binding are increased in G2. Although we cannot exclude the possibility that Cas9-induced DSBs arrest the cells early in G2, leading to the absence of their eviction before mitosis (Goodarzi et al., 2009) and their apparent accumulation, these experiments have been performed in late G2 arrested cells using RO-3306. Nevertheless, these results are in agreement with previous studies showing a local increase of H3K9me3 in chromatin surrounding a single DSB (Ayrapetov et al., 2014), and others showing recruitment of HP1s and KAP1 at lesions and their particular role in HR (Baldeyron et al., 2011; Lee et al., 2013; Soria and Almouzni, 2013). Moreover, consistent with a positive role for HP1s in HR, depletion of all three isoforms diminished the recruitment of RAD51 at DSBs in heterochromatin. One potential explanation for the increase in HP1s that we observe at the chromocenters after DSB induction could be a tilt in the balance in their turnover. If HP1 binding is enhanced, possibly through dual binding of the chromodomain to H3K9me3 and the chromoshadow domain to DSBs (Luijsterburg et al., 2009), it is then possible that HP1s are further stabilized at the chromocenters, resulting in a net increase of their signal.

In pericentric heterochromatin in G2, the spatial distribution of the DSBs depends on two factors: DNA end resection and active exclusion of RAD51 from the heterochromatin core. Resection was shown to be key in regulating the mobility of breaks in yeast in the process of homology search as well as in relocation of DSBs induced in nucleolar DNA sequences to the periphery of the nucleolus (Torres-Rosell et al., 2007). Resection and check-point activation is essential for the break relocation in *Drosophila* (Chiolo et al., 2011). All these data support the notion that resected DNA ends are able to diffuse and move freely within heterochromatin. On the other hand, the peripheral localization is not only the consequence of DSB mobility but implicates a stabilization mechanism that involves the active exclusion of the RAD51/BRCA2 complex from the core domain. Although the exclusion mechanism is not entirely clear, our results demonstrate that despite the fact that RAD51 has the potential to access the core domain, it is retained at the periphery, possibly through its constitutive interaction with BRCA2 (Reuter et al., 2014). In *Drosophila* cells, however, RAD51 exclusion from heterochromatin does not lead to DSB stabilization at the periphery of the structure, as DSBs further relocate to the nuclear pore to complete HR (Ryu et al., 2015). Hence, the RAD51/BRCA2 strand invasion-promoting complex plays an unprecedented role in the spatial distribution of DSBs in mammalian heterochromatin. This is reminiscent of DNA replication at chromocenters, which also takes place at the periphery (Guenatri et al., 2004), and suggests that pathways that involve DNA synthesis need to be excluded from the core domain.

The spatial uncoupling of DNA repair pathways has several implications. The fact that RAD51 is excluded from the core domain could serve as a mechanism to prevent the activation of HR in order to avoid illegitimate recombination between repetitive sequences. Additionally, our results suggest that breaks that fail

to relocate to the periphery trigger in situ recruitment of DNA repair factors (RAD52) representative of mutagenic pathways such as SSA. We speculate that the activation of SSA at the core could be a safeguard mechanism to ensure that resected DSBs, which fail to localize to the periphery to be repaired by HR, are still repaired. Therefore, relocation might be essential to avoid error-prone DNA repair and enforce high-fidelity repair. Moreover, given the fact that the pericentric domains of several chromosomes are clustered, DSB relocation could prevent HR between different chromosomes, hence preventing chromosomal translocations.

EXPERIMENTAL PROCEDURES

Cell Culture

NIH 3T3 mouse fibroblasts were maintained in DMEM with high glucose supplemented with 10% newborn calf serum and gentamycin (40 μg/ml). For cell treatments, see Supplemental Experimental Procedures. NIH 3T3 cells stably expressing Cas9-EGFP were generated by infection of cells with the pR-18 retroviral vector (see Supplemental Experimental Procedures) followed by puromycin selection for 10 days.

Transfection and siRNA Knockdown

Transient transfections were done with Lipofectamine 2000 (Invitrogen Life Technologies) or Lipofectamine RNAiMAX (Life Technologies) for plasmids or siRNAs and in vitro transcribed major satellite repeats RNA, respectively, and following manufacturer's instructions (see Supplemental Information for siRNAs). Knockdown efficiency was analyzed by western blot and/or RT-qPCR. All microscopy and western blot experiments were performed 72 hr post-knockdown and 8 hr post-transfection, unless otherwise indicated. For statistical analysis of all experiments, t tests were performed: *$p < 0.05$, **$p < 0.01$, and ***$p < 0.001$.

Real-Time qPCR

RNA and cDNA were prepared using standard techniques. qPCR was performed in triplicate using SyberGreen (Qiagen) and a LightCycler 480 (Roche) as previously described (Pankotai et al., 2012). Transcript quantities were calculated relative to standard curves and normalized to HPRT or GAPDH mRNA (see Supplemental Information for primers).

Western Blot Analysis

Proteins were fractionated by SDS-PAGE and transferred to Protran Nitrocellulose membranes (Sigma Aldrich) and blotted with antibodies listed in the Supplemental Information.

Immunofluorescence and Confocal and Super-resolution Microscopy

Cells were cultured on coverslips and pre-extracted in 0.1% Triton/1X PBS for 30 s prior fixation in 4% paraformaldehyde/1X PBS for 10 min on ice. After a second fixation step in 4% paraformaldehyde/1X PBS for 10 min at room temperature, cells were permeabilized in 0.5% Triton/1X PBS for 10 min, blocked in 5% BSA/1X PBS-0.1% Tween for 45 min and incubated with primary antibody for 1 hr (see Supplemental Information for antibodies) and secondary antibody for 1 hr. Cells were counterstained with DAPI (1 mg/ml) and mounted on slides. For EdU incorporation, the Click-iT EdU Alexa Fluor 488 Imaging Kit was used. Cells were observed on a confocal laser scanning microscope (TCS SP8; Leica) using a 63× objective or on an OMX BLAZE 3D-structured illumination, super-resolution microscope.

SUPPLEMENTAL INFORMATION

Supplemental Information includes Supplemental Experimental Procedures, seven figures, and seven movies and can be found with this article online at http://dx.doi.org/10.1016/j.molcel.2016.06.002.

AUTHOR CONTRIBUTIONS

E.S., B.R.S.M., and K.T. designed experiments and wrote the paper. K.T, A. Furst, M.R., V.H., A.M.-R., and A. Ferrand conducted experiments. K.T., A.M.-R., and A.L.-F. analyzed data.

ACKNOWLEDGMENTS

We thank the B.R.-S.-M. and E.S. laboratories for discussions; P. Huertas, T. Misteli, F. Zhang, and M. Tarsounas for providing cDNA constructs; J. Lukas, C. Lukas, D. Durocher, and A. Nussenzweig for comments on the manuscript; B. Gurchenkov, P. Kessler, and M. Koch from the Imaging center of IGBMC for advice on microscopy; N. Ehrenfeuchter from the Biozentrum Imaging facility for help with the analysis of the super-resolution images; C. Ebel for assistance with cell sorting; B. Heller for cell culture; and S. Bour for help with the graphical abstract. K.T. was supported by aDDRess, a Marie Curie Initial Training Network funded by the European Commission 7th Framework Programme (Grant Agreement 316390). This study was supported by the following grants: Fondation ARC (to B.R.-S.-M. and E.S.), Institut National du Cancer (to B.R.-S.-M. and E.S.), EMBO YIP (to E.S.), La Ligue Contre le Cancer (to E.S.), and ANR-10-LABX-0030-INRT, a French state fund managed by Agence Nationale de la Recherche under the program Investissements d'Avenir, labeled ANR-10-IDEX-0002-02.

Received: March 25, 2016
Revised: May 11, 2016
Accepted: May 31, 2016
Published: July 7, 2016

REFERENCES

Almouzni, G., and Probst, A.V. (2011). Heterochromatin maintenance and establishment: lessons from the mouse pericentromere. Nucleus *2*, 332–338.

Aymard, F., Bugler, B., Schmidt, C.K., Guillou, E., Caron, P., Briois, S., Iacovoni, J.S., Daburon, V., Miller, K.M., Jackson, S.P., and Legube, G. (2014). Transcriptionally active chromatin recruits homologous recombination at DNA double-strand breaks. Nat. Struct. Mol. Biol. *21*, 366–374.

Ayoub, N., Jeyasekharan, A.D., Bernal, J.A., and Venkitaraman, A.R. (2008). HP1-beta mobilization promotes chromatin changes that initiate the DNA damage response. Nature *453*, 682–686.

Ayrapetov, M.K., Gursoy-Yuzugullu, O., Xu, C., Xu, Y., and Price, B.D. (2014). DNA double-strand breaks promote methylation of histone H3 on lysine 9 and transient formation of repressive chromatin. Proc. Natl. Acad. Sci. U S A *111*, 9169–9174.

Baldeyron, C., Soria, G., Roche, D., Cook, A.J.L., and Almouzni, G. (2011). HP1alpha recruitment to DNA damage by p150CAF-1 promotes homologous recombination repair. J. Cell Biol. *193*, 81–95.

Bancaud, A., Huet, S., Daigle, N., Mozziconacci, J., Beaudouin, J., and Ellenberg, J. (2009). Molecular crowding affects diffusion and binding of nuclear proteins in heterochromatin and reveals the fractal organization of chromatin. EMBO J. *28*, 3785–3798.

Brunet, E., Simsek, D., Tomishima, M., DeKelver, R., Choi, V.M., Gregory, P., Urnov, F., Weinstock, D.M., and Jasin, M. (2009). Chromosomal translocations induced at specified loci in human stem cells. Proc. Natl. Acad. Sci. U S A *106*, 10620–10625.

Chan, F.L., and Wong, L.H. (2012). Transcription in the maintenance of centromere chromatin identity. Nucleic Acids Res. *40*, 11178–11188.

Chiolo, I., Minoda, A., Colmenares, S.U., Polyzos, A., Costes, S.V., and Karpen, G.H. (2011). Double-strand breaks in heterochromatin move outside of a dynamic HP1a domain to complete recombinational repair. Cell *144*, 732–744.

Ciccia, A., and Elledge, S.J. (2010). The DNA damage response: making it safe to play with knives. Mol. Cell *40*, 179–204.

Daugaard, M., Baude, A., Fugger, K., Povlsen, L.K., Beck, H., Sørensen, C.S., Petersen, N.H., Sorensen, P.H., Lukas, C., Bartek, J., et al. (2012). LEDGF

(p75) promotes DNA-end resection and homologous recombination. Nat. Struct. Mol. Biol. *19*, 803–810.

Decottignies, A. (2013). Alternative end-joining mechanisms: a historical perspective. Front. Genet. *4*, 48.

Dupré, A., Boyer-Chatenet, L., Sattler, R.M., Modi, A.P., Lee, J.H., Nicolette, M.L., Kopelovich, L., Jasin, M., Baer, R., Paull, T.T., and Gautier, J. (2008). A forward chemical genetic screen reveals an inhibitor of the Mre11-Rad50-Nbs1 complex. Nat. Chem. Biol. *4*, 119–125.

Goodarzi, A.A., Noon, A.T., Deckbar, D., Ziv, Y., Shiloh, Y., Löbrich, M., and Jeggo, P.A. (2008). ATM signaling facilitates repair of DNA double-strand breaks associated with heterochromatin. Mol. Cell *31*, 167–177.

Goodarzi, A.A., Noon, A.T., and Jeggo, P.A. (2009). The impact of heterochromatin on DSB repair. Biochem. Soc. Trans. *37*, 569–576.

Guenatri, M., Bailly, D., Maison, C., and Almouzni, G. (2004). Mouse centric and pericentric satellite repeats form distinct functional heterochromatin. J. Cell Biol. *166*, 493–505.

Guirouilh-Barbat, J., Lambert, S., Bertrand, P., and Lopez, B.S. (2014). Is homologous recombination really an error-free process? Front. Genet. *5*, 175.

Hartlerode, A.J., and Scully, R. (2009). Mechanisms of double-strand break repair in somatic mammalian cells. Biochem. J. *423*, 157–168.

Hsu, P.D., Lander, E.S., and Zhang, F. (2014). Development and applications of CRISPR-Cas9 for genome engineering. Cell *157*, 1262–1278.

Jakob, B., Splinter, J., Conrad, S., Voss, K.O., Zink, D., Durante, M., Löbrich, M., and Taucher-Scholz, G. (2011). DNA double-strand breaks in heterochromatin elicit fast repair protein recruitment, histone H2AX phosphorylation and relocation to euchromatin. Nucleic Acids Res. *39*, 6489–6499.

Kalousi, A., Hoffbeck, A.S., Selemenakis, P.N., Pinder, J., Savage, K.I., Khanna, K.K., Brino, L., Dellaire, G., Gorgoulis, V.G., and Soutoglou, E. (2015). The nuclear oncogene SET controls DNA repair by KAP1 and HP1 retention to chromatin. Cell Rep. *11*, 149–163.

Lee, Y.-H., Kuo, C.-Y., Stark, J.M., Shih, H.-M., and Ann, D.K. (2013). HP1 promotes tumor suppressor BRCA1 functions during the DNA damage response. Nucleic Acids Res. *41*, 5784–5798.

Lemaître, C., Grabarz, A., Tsouroula, K., Andronov, L., Furst, A., Pankotai, T., Heyer, V., Rogier, M., Attwood, K.M., Kessler, P., et al. (2014). Nuclear position dictates DNA repair pathway choice. Genes Dev. *28*, 2450–2463.

Luijsterburg, M.S., Dinant, C., Lans, H., Stap, J., Wiernasz, E., Lagerwerf, S., Warmerdam, D.O., Lindh, M., Brink, M.C., Dobrucki, J.W., et al. (2009). Heterochromatin protein 1 is recruited to various types of DNA damage. J. Cell Biol. *185*, 577–586.

Mills, K.D., Ferguson, D.O., and Alt, F.W. (2003). The role of DNA breaks in genomic instability and tumorigenesis. Immunol. Rev. *194*, 77–95.

Misteli, T., and Soutoglou, E. (2009). The emerging role of nuclear architecture in DNA repair and genome maintenance. Nat. Rev. Mol. Cell Biol. *10*, 243–254.

Nishimura, K., Fukagawa, T., Takisawa, H., Kakimoto, T., and Kanemaki, M. (2009). An auxin-based degron system for the rapid depletion of proteins in nonplant cells. Nat. Methods *6*, 917–922.

Noon, A.T., Shibata, A., Rief, N., Löbrich, M., Stewart, G.S., Jeggo, P.A., and Goodarzi, A.A. (2010). 53BP1-dependent robust localized KAP-1 phosphorylation is essential for heterochromatic DNA double-strand break repair. Nat. Cell Biol. *12*, 177–184.

Orthwein, A., Noordermeer, S.M., Wilson, M.D., Landry, S., Enchev, R.I., Sherker, A., Munro, M., Pinder, J., Salsman, J., Dellaire, G., et al. (2015). A mechanism for the suppression of homologous recombination in G1 cells. Nature *528*, 422–426.

Pankotai, T., Bonhomme, C., Chen, D., and Soutoglou, E. (2012). DNAPKcs-dependent arrest of RNA polymerase II transcription in the presence of DNA breaks. Nat. Struct. Mol. Biol. *19*, 276–282.

Pfister, S.X., Ahrabi, S., Zalmas, L.P., Sarkar, S., Aymard, F., Bachrati, C.Z., Helleday, T., Legube, G., La Thangue, N.B., Porter, A.C., and Humphrey, T.C. (2014). SETD2-dependent histone H3K36 trimethylation is required for homologous recombination repair and genome stability. Cell Rep. *7*, 2006–2018.

Reuter, M., Zelensky, A., Smal, I., Meijering, E., van Cappellen, W.A., de Gruiter, H.M., van Belle, G.J., van Royen, M.E., Houtsmuller, A.B., Essers, J., et al. (2014). BRCA2 diffuses as oligomeric clusters with RAD51 and changes mobility after DNA damage in live cells. J. Cell Biol. *207*, 599–613.

Roberts, S.A., and Gordenin, D.A. (2014). Hypermutation in human cancer genomes: footprints and mechanisms. Nat. Rev. Cancer *14*, 786–800.

Ryu, T., Spatola, B., Delabaere, L., Bowlin, K., Hopp, H., Kunitake, R., Karpen, G.H., and Chiolo, I. (2015). Heterochromatic breaks move to the nuclear periphery to continue recombinational repair. Nat. Cell Biol. *17*, 1401–1411.

Shee, C., Cox, B.D., Gu, F., Luengas, E.M., Joshi, M.C., Chiu, L.Y., Magnan, D., Halliday, J.A., Frisch, R.L., Gibson, J.L., et al. (2013). Engineered proteins detect spontaneous DNA breakage in human and bacterial cells. eLife *2*, e01222.

Soria, G., and Almouzni, G. (2013). Differential contribution of HP1 proteins to DNA end resection and homology-directed repair. Cell Cycle *12*, 422–429.

Stark, J.M., Pierce, A.J., Oh, J., Pastink, A., and Jasin, M. (2004). Genetic steps of mammalian homologous repair with distinct mutagenic consequences. Mol. Cell. Biol. *24*, 9305–9316.

Torres-Rosell, J., Sunjevaric, I., De Piccoli, G., Sacher, M., Eckert-Boulet, N., Reid, R., Jentsch, S., Rothstein, R., Aragón, L., and Lisby, M. (2007). The Smc5-Smc6 complex and SUMO modification of Rad52 regulates recombinational repair at the ribosomal gene locus. Nat. Cell Biol. *9*, 923–931.

van Sluis, M., and McStay, B. (2015). A localized nucleolar DNA damage response facilitates recruitment of the homology-directed repair machinery independent of cell cycle stage. Genes Dev. *29*, 1151–1163.

Ziv, Y., Bielopolski, D., Galanty, Y., Lukas, C., Taya, Y., Schultz, D.C., Lukas, J., Bekker-Jensen, S., Bartek, J., and Shiloh, Y. (2006). Chromatin relaxation in response to DNA double-strand breaks is modulated by a novel ATM- and KAP-1 dependent pathway. Nat. Cell Biol. *8*, 870–876.

Molecular Cell, Volume *63*

Supplemental Information

Temporal and Spatial Uncoupling of DNA Double Strand Break Repair Pathways within Mammalian Heterochromatin

Katerina Tsouroula, Audrey Furst, Melanie Rogier, Vincent Heyer, Anne Maglott-Roth, Alexia Ferrand, Bernardo Reina-San-Martin, and Evi Soutoglou

Figure S1 (Related to Figure 1).

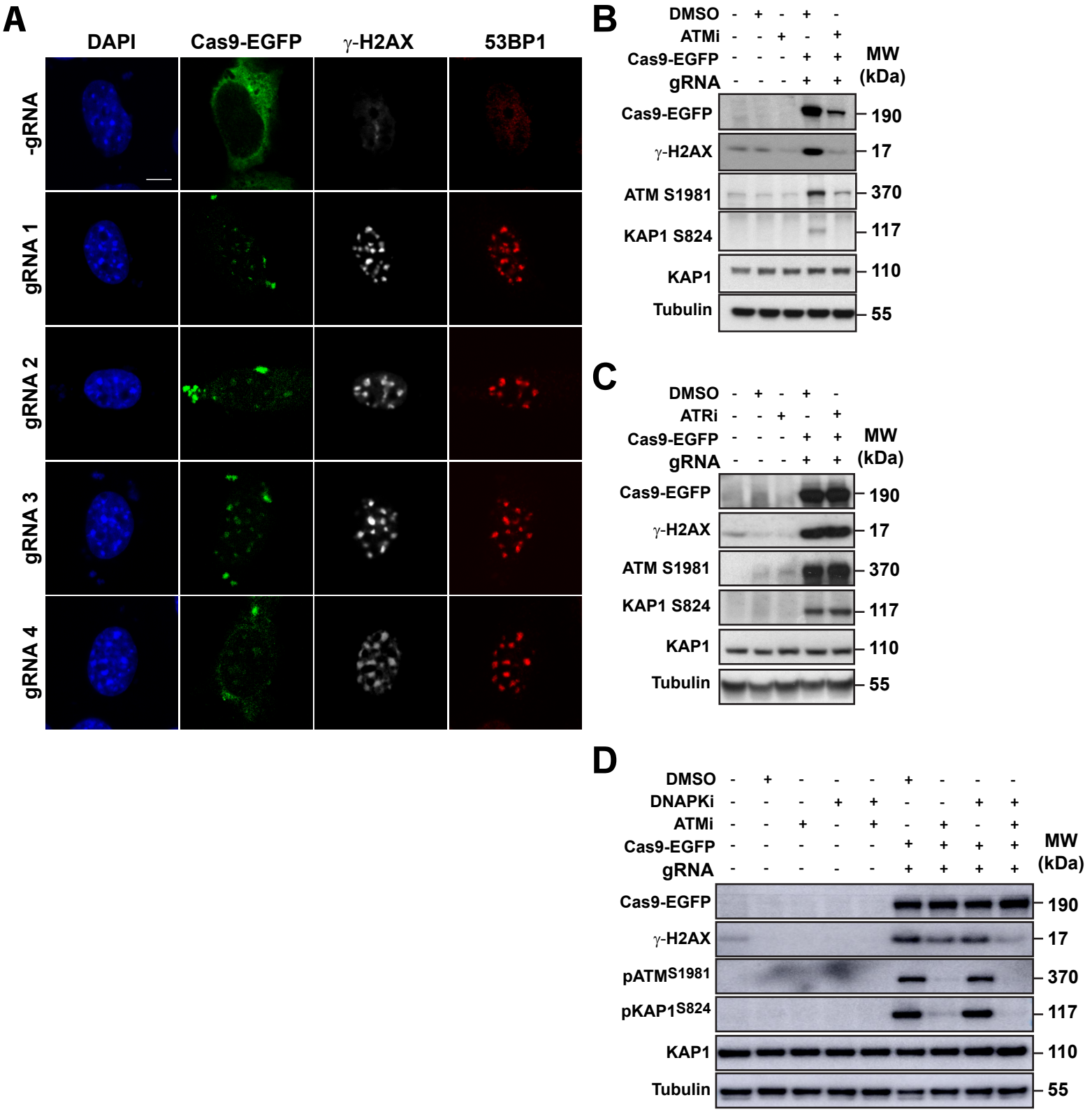

Figure S2 (Related to Figure 2).

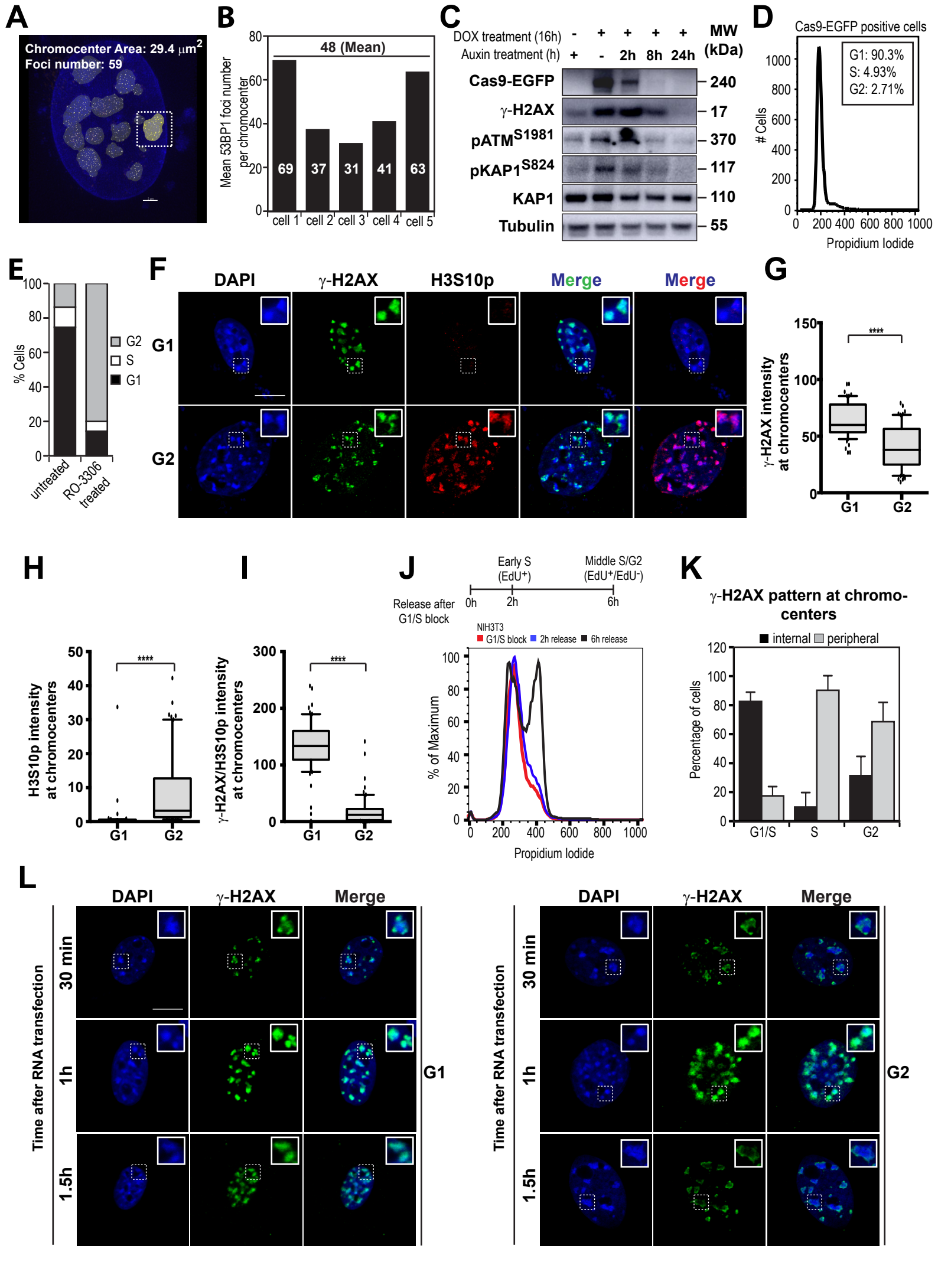

Figure S3 (Related to Figure 2).

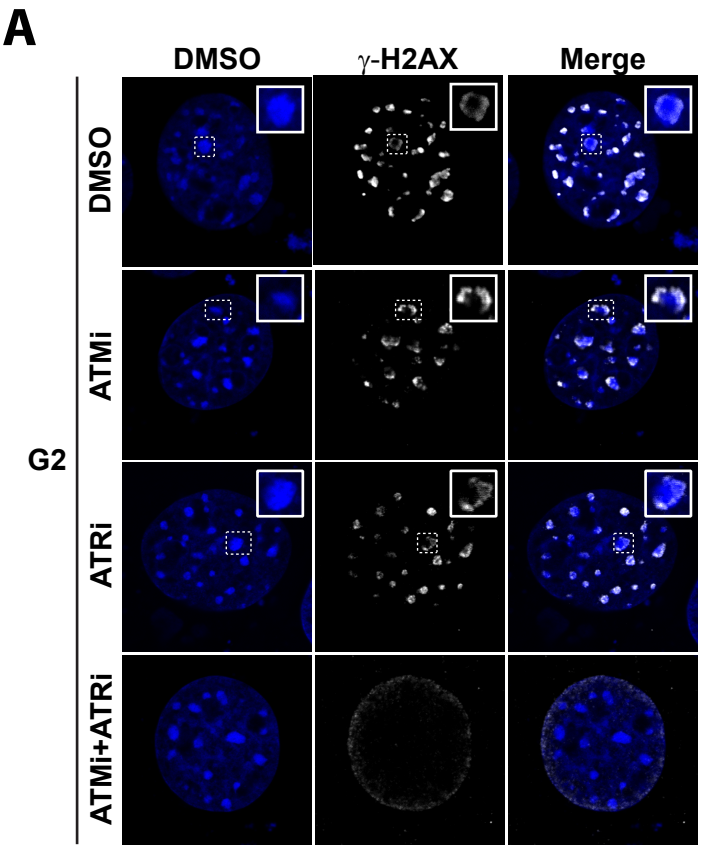

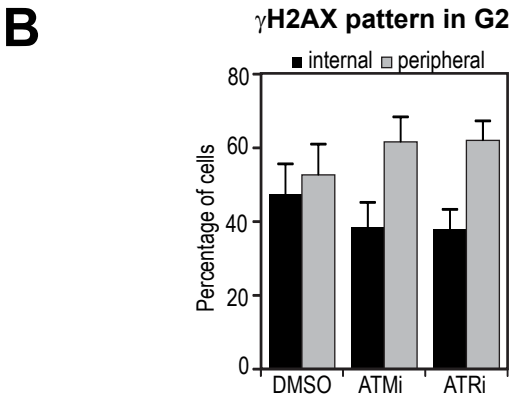

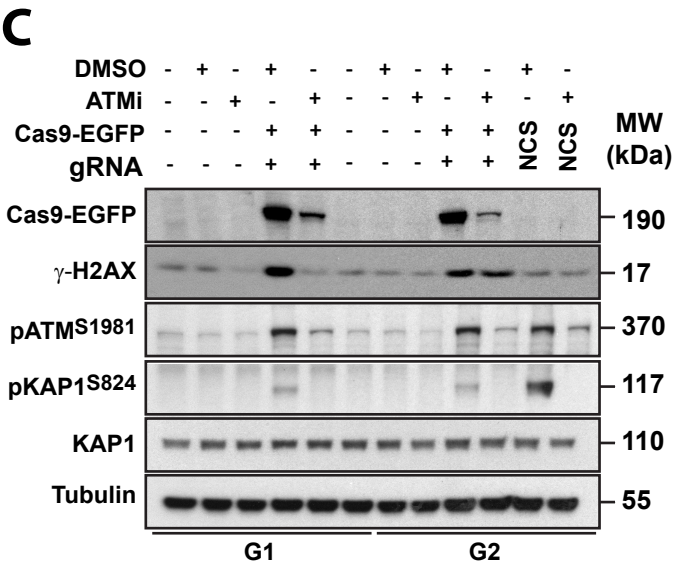

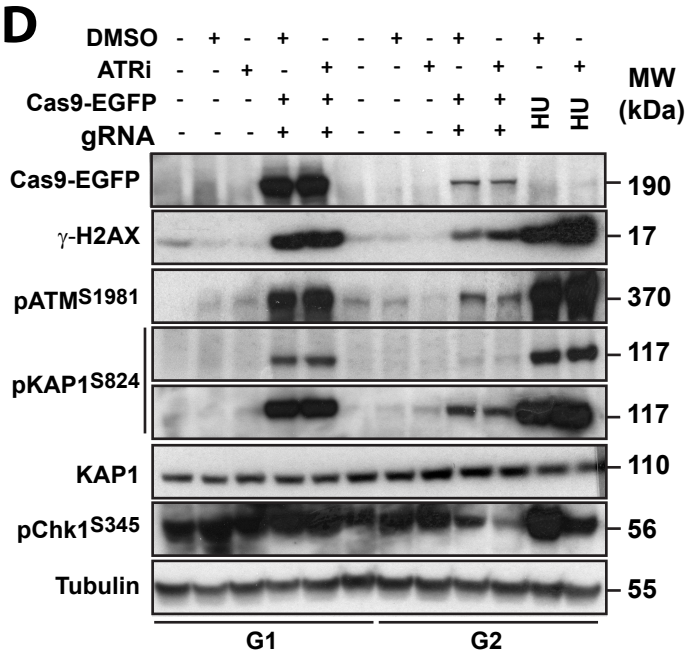

Figure S4 (Related to Figure 3).

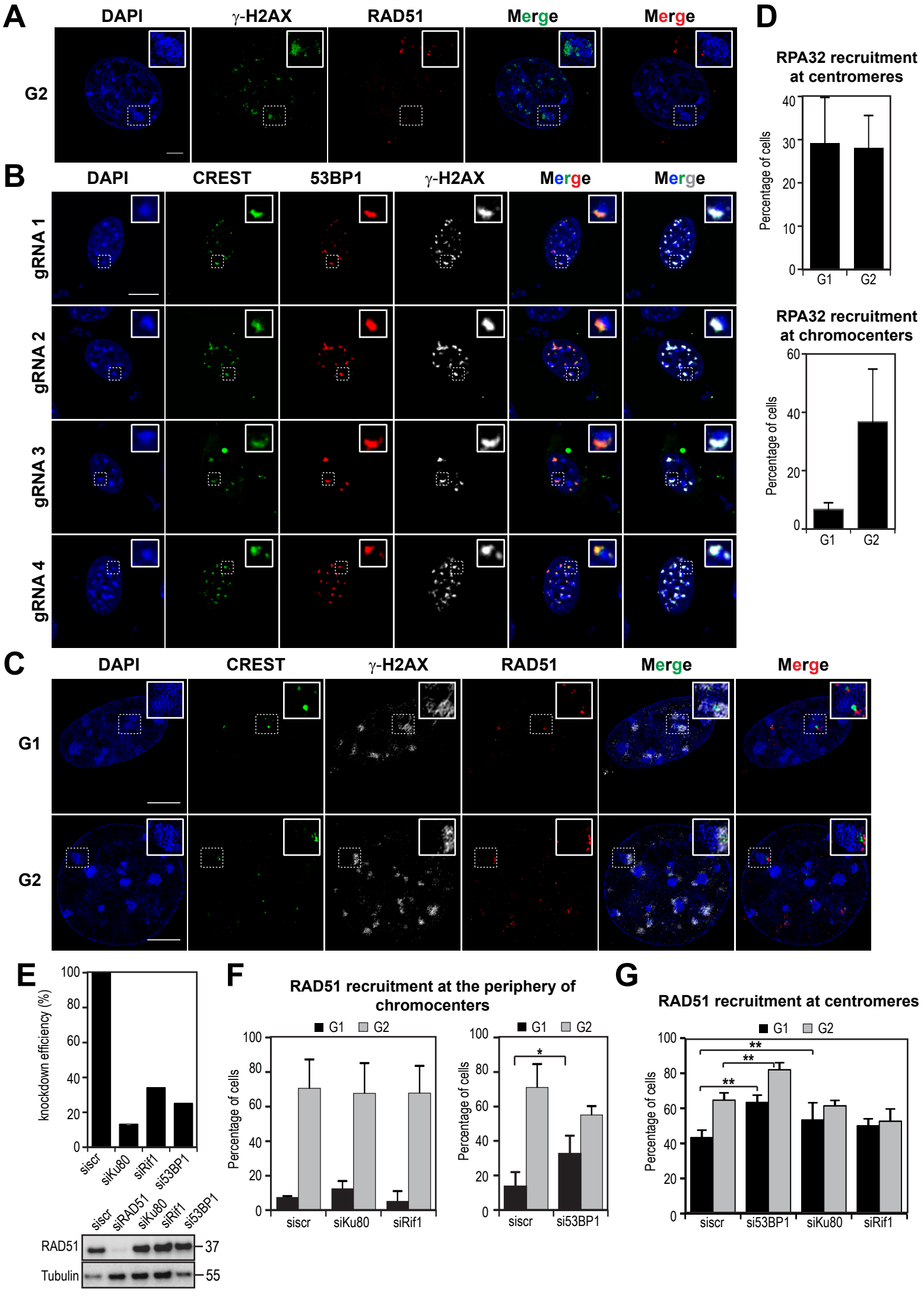

Figure S5 (Related to Figure 3).

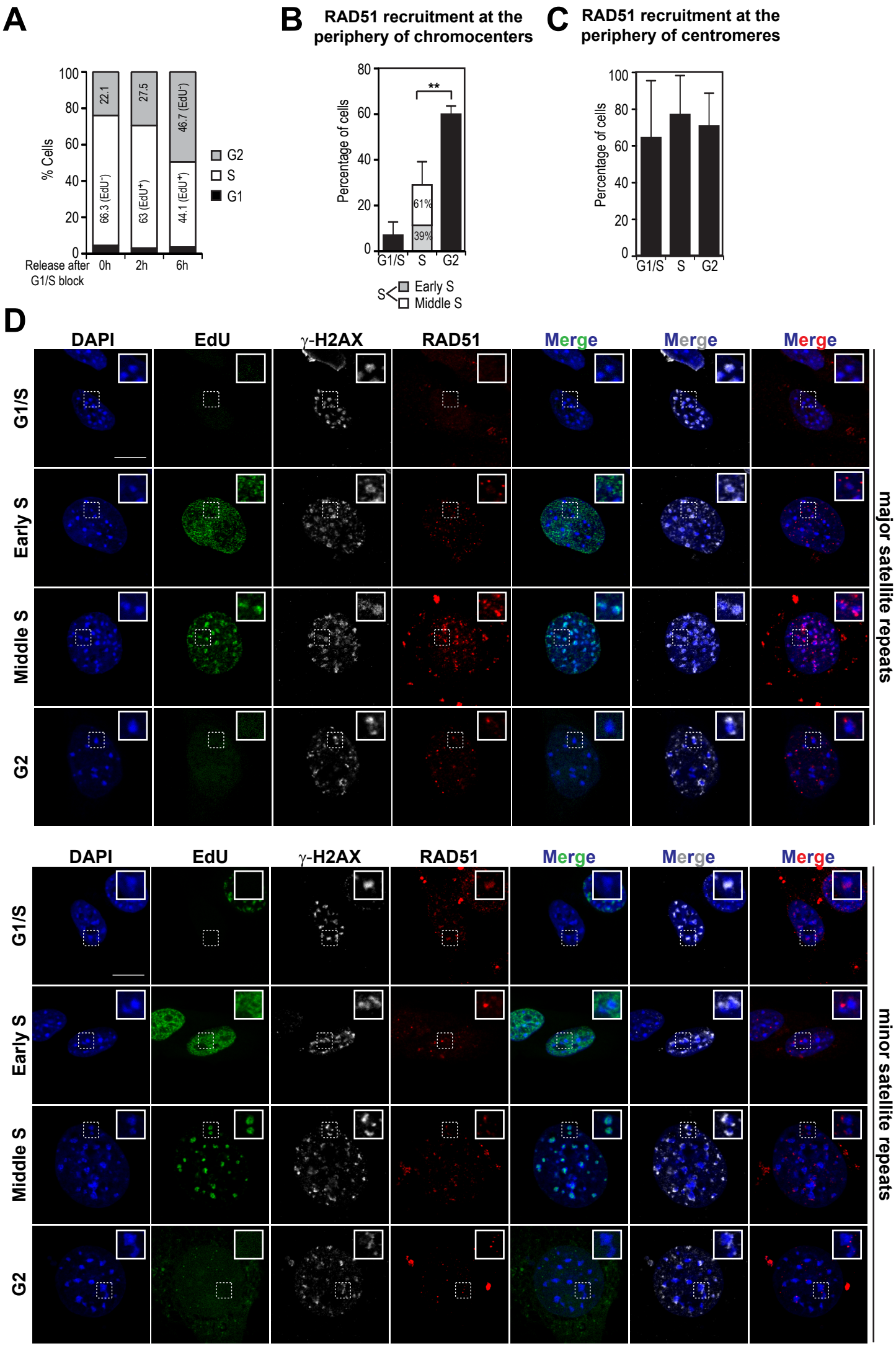

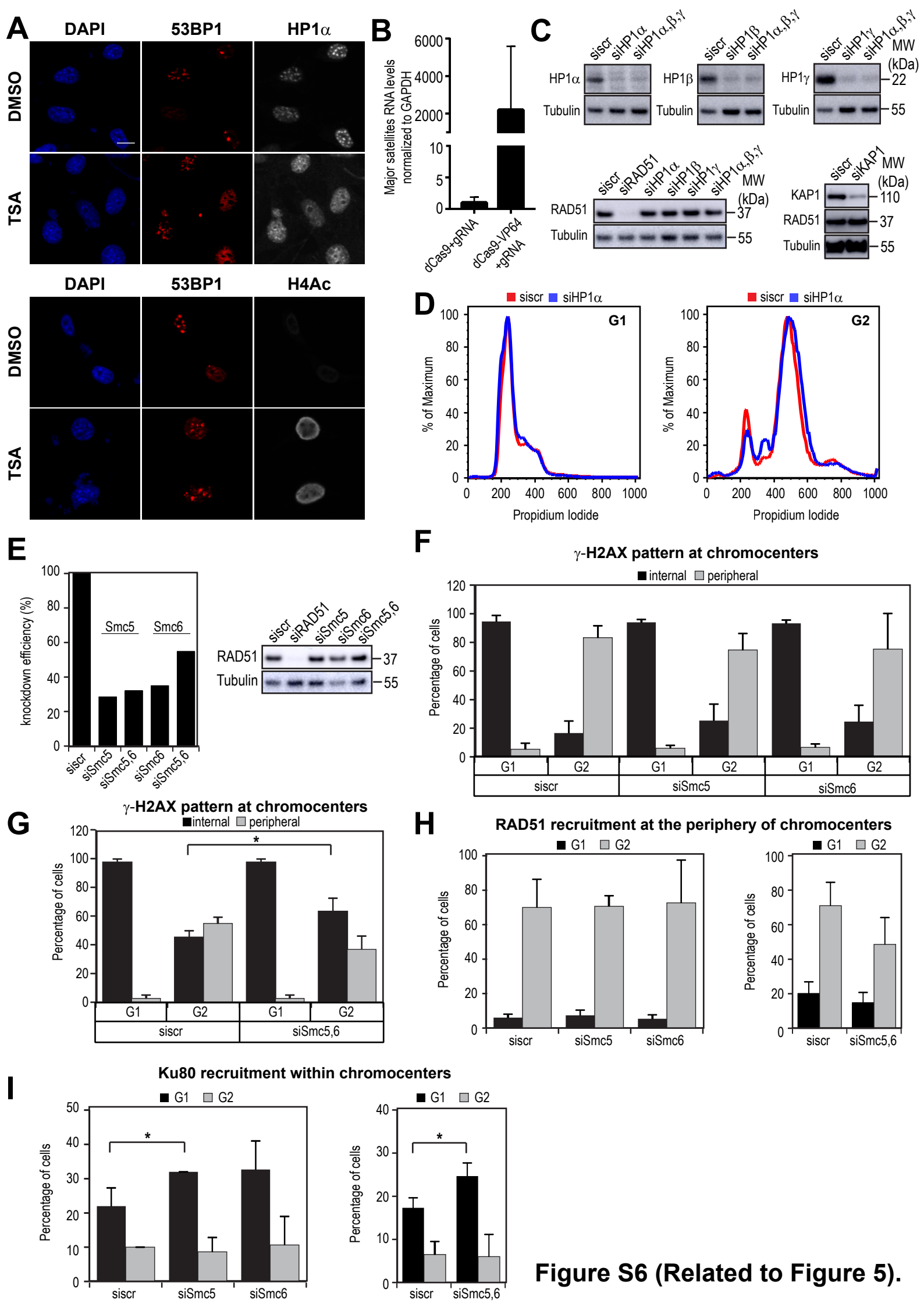

Figure S6 (Related to Figure 5).

Figure S7 (related to Figure 6 and Figure 7).

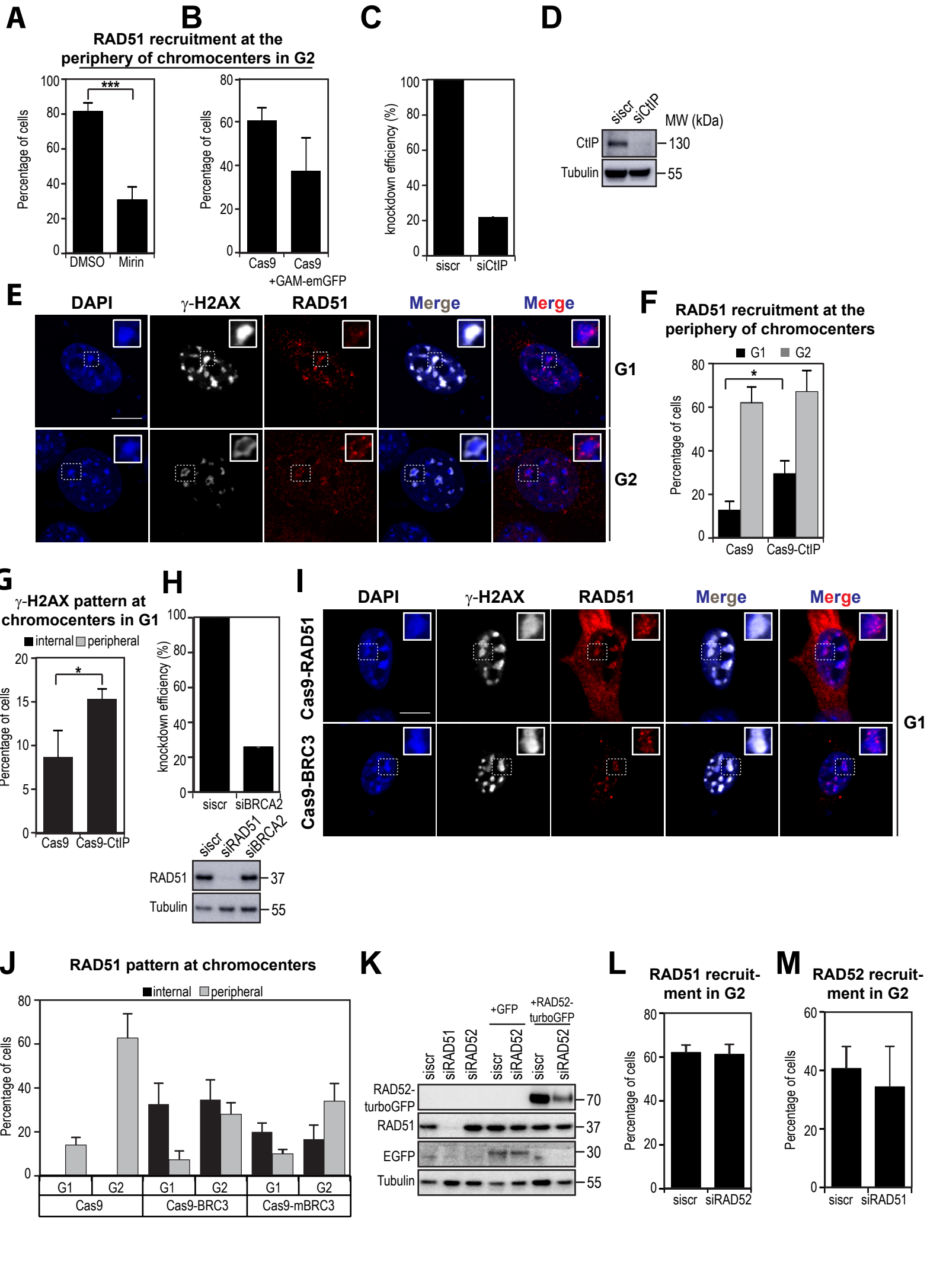

Supplemental Figure Legends.

Figure S1 (Related to Figure 1). Cas9-specific induction of DSBs at pericentric heterochromatin and robust ATM-dependent DDR activation. **A.** IF confocal analysis of cells expressing Cas9-EGFP ± four different gRNAs specific for major satellite DNA repeats and stained with DAPI and antibodies specific for γ-H2AX and 53BP1. **B-D.** Western blot analysis for Cas9-EGFP (EGFP), γ-H2AX, pATM^{S1981}, pKAP1^{S824}, KAP1 and tubulin in protein extracts prepared from cells expressing Cas9-EGFP + gRNA after treatment with an ATM (ATMi) (**B**), ATR (ATRi) (**C**), DNAPK$_{CS}$ (DNAPKi) and ATM inhibitor (**D**) or vehicle only (DMSO). Theoretical molecular weights are indicated on the right. For confocal images, scale bar represents 10 μm. **A:** 8h post-transfection, plasmids used: Cas9-EGFP (pCX-5), gRNA#1 (pG-57), gRNA#2 (pG-58), gRNA#3 (pG-56), gRNA#4 (pG-59). **B-D:** 8h post-transfection, plasmids used: Cas9-EGFP (pCX-5), gRNA (pG-56).

Figure S2 (Related to Figure 2). Quantification of 53BP1 foci per chromocenter using super-resolution microscopy, cell cycle analysis and kinetic distribution of γ-H2AX. **A.** Representative super-resolution image used to measure the size and the number of 53BP1 foci per chromocenter (Imaris software) of a cell expressing Cas9-EGFP + gRNA and stained with DAPI and an antibody specific for 53BP1. Scale bar represents 2 μm. **B.** Mean 53BP1 foci number per chromocenter of five cells analyzed as described in A. **C.** Western blot analysis for AID-Cas9-EGFP-AID (Cas9), γ-H2AX, pATM^{S1981}, pKAP1^{S824}, KAP1 and tubulin in protein extracts prepared from cells expressing Doxycycline (DOX) inducible Cas9-EGFP fused to Auxin-Induced Degron (AID), gRNA for major satellite repeats, TIR1 and rtTA after treatment with DOX and Auxin for the indicated timepoints. Theoretical molecular weights are indicated on the right. **D.** Cell cycle analysis of cells expressing Cas9-EGFP + gRNA. **E.** Cell cycle analysis of untreated and RO-3306 treated cells (24h). **F.** IF confocal analysis of cells expressing Cas9-EGFP + gRNA in G1 (EdU$^-$/H3S10p$^-$ cells - upper panel) and RO-3306 arrested cells in G2 (EdU$^-$/H3S10p$^+$ cells - lower panel) and stained with DAPI and antibodies specific for γ-H2AX and H3S10p. Quantification of γ-H2AX (**G**), H3S10p (**H**) and γ-H2AX/H3S10p (**I**) intensity at the core of chromocenters in cells as described in F. Individual cell values are represented as a box-and-whisker plot (median and quartile with outliers representing 1% of the population) of one representative experiment with n>50 cells for G1 and G2. Three independent experiments were performed with n>50 cells for G1 and G2. Cell by cell data were plotted using GraphPad Prism and t-test was used for statistical analysis. (*) $p<0.05$; (**) $p<0.01$; (***) $p<0.001$; (****) $p<0.0001$. **J**. Schematic representation and cell cycle analysis by flow cytometry of cells blocked in G1/S phase (by double thymidine) and released for 2h (S phase) or 6h (G2). **K**. Quantification of γ-H2AX pattern in G1/S, S and G2 cells expressing Cas9-EGFP + gRNA as described in J. Cells in S or G2 were identified on the basis of EdU incorporation: S (EdU$^+$), G2 (EdU$^-$). Values represent mean + SD of three independent experiments with n>30 cells. **L**. IF confocal analysis of cells in G1 (EdU$^-$/H3S10p$^-$ cells - left panel) and G2 (RO-3306 arrested cells) (EdU$^-$/H3S10p$^+$ cells - right panel) stably expressing Cas9 and transfected with *in vitro* transcribed gRNA for major satellite repeats for the indicated timepoints and stained with DAPI and antibody specific for γ-H2AX. **A, D, F-I, K**: 8h post-transfection, plasmids used: Cas9-EGFP (pCX-5), gRNA (pG-56). For confocal images, scale bar represents 10 μm.

Figure S3 (Related to Figure 2). DDR in pericentric heteromatin in G2 is ATM- and ATR-dependent. **A**. IF confocal analysis of G2 (RO-3306 treated) cells expressing Cas9-EGFP+gRNA and stained with DAPI and a γ-H2AX specific antibody after treatment with an ATM (ATMi) or ATR (ATRi) inhibitor or vehicle only (DMSO). **B.** Quantification of cells as described in A. **C-D**. Western blot analysis for Cas9-EGFP (EGFP), γ-H2AX, pATM^{S1981}, pKAP1^{S824}, KAP1, pChk1^{S345} and tubulin in protein extracts prepared from cells expressing Cas9-EGFP+gRNA after treatment with an ATM (ATMi) (**C**) or ATR (ATRi) (**D**) inhibitor or vehicle only (DMSO). Theoretical molecular weights are indicated on the right. For confocal images, scale bar represents 10 μm. **A-D**: 8h post-transfection, plasmids used: Cas9-EGFP (pCX-5), gRNA (pG-56).

Figure S4 ***(Related to Figure 3). Cas9-specific induction of DSBs at centromeric heterochromatin and regulation of end-resection in the centromeric and pericentromeric lesions.*** **A.** IF super-resolution imaging analysis of cells expressing Cas9-EGFP + gRNA in G2 and stained with DAPI and antibodies specific for γ-H2AX and RAD51 (see also Movie S5). Plasmids used: Cas9-EGFP (pCX-5), gRNA (pG-56). **B.** IF confocal analysis of cells expressing Cas9-EGFP ± four different gRNAs specific for minor satellite DNA repeats and stained with DAPI and antibodies specific for centromeres (CREST), γ-H2AX and 53BP1. Plasmids used: Cas9-EGFP (pCX-5), gRNA#1 (pG-35), gRNA#2 (pG-36), gRNA#3 (pG-37), gRNA#4 (pG-38). **C**. IF super-resolution imaging analysis of cells expressing Cas9-EGFP + gRNA2 against minor satellite DNA repeats in G1 and G2 (RO-3306 treated cells) stained with DAPI and antibodies specific for centromeres (CREST), γ-H2AX and RAD51 (see also Movie S6 for G1 and Movie S7 for G2). **D.** Quantification of RPA32 recruitment in G1 and G2 cells expressing Cas9-EGFP+gRNA2 (minor satellites; upper panel) or Cas9-EGFP+gRNA (major satellites; lower panel) after IF confocal analysis and staining with an RPA32 specific antibody. Plasmids used: Cas9-EGFP (pCX-5), gRNA#2 (minor satellites; pG-36), gRNA (major satellites; pG-56). **E.** RT-qPCR measurement of Ku80, Rif1 and 53BP1 knockdown efficiency and Western blot analysis for RAD51 and tubulin of the corresponding cells. **F**. Quantification of RAD51 recruitment of G1 and G2 (RO-3306 treated) cells expressing Cas9-EGFP + gRNA after Ku80, Rif1 or 53BP1 knockdown. Plasmids used: Cas9-EGFP (pCX-5), gRNA

(pG-56). **G**. Quantification of RAD51 recruitment of G1 and G2 (RO-3306 treated) cells expressing Cas9-EGFP + gRNA2 after Ku80, Rif1 or 53BP1 knockdown. Plasmids used: Cas9-EGFP (pCX-5), gRNA#2 (pG-36). For super-resolution images, scale bar represents 5 μm. Values represent mean ± SD of three independent experiments with n=50 cells. For statistical analysis, t-test was performed. (*) $p<0.05$; (**) $p<0.01$; (***) $p<0.001$.) **A-D and F-G**: 8h post-transfection.

Figure S5 (Related to Figure 3). Rad51 binding at pericentric and centromeric heterochromatin throughout the cell cycle. **A.** EdU incorporation profile of cells blocked in G1/S phase (by double thymidine) and released for 2h (S) or 6h (G2). Quantification of RAD51 recruitment in pericentric **(B)** or centromeric **(C)** heterochromatin in cells expressing Cas9-EGFP + gRNA against major or minor satellite repeats in G1/S (thymidine blocked), early S (diffuse EdU pattern), middle S (EdU at pericentric heterochromatin) and G2 (EdU-). **D**. IF confocal analysis of cells expressing Cas9-EGFP + gRNA against major (upper panel) or minor satellite (lower panel) repeats in G1/S (thymidine blocked), early S (diffuse EdU pattern), middle S (EdU at pericentric heterochromatin) and G2 (EdU-) stained with DAPI and specific antibodies for EdU, γ-H2AX and RAD51. Scale bar represents 10 μm. Values represent mean ± SD of three independent experiments with n>30 cells. For statistical analysis, t-test was performed. (*) $p<0.05$; (**) $p<0.01$; (***) $p<0.001$.) **A-C**: 8h post-transfection, plasmids used: Cas9-EGFP (pCX-5), gRNA (major satellites; pG-56), gRNA (minor satellites; pG-36).

Figure S6 (Related to Figure 5). Chromatin compaction is not refractory to DNA repair. **A.** IF confocal analysis of cells expressing Cas9-EGFP +gRNA treated with TSA or vehicle only (DMSO), stained with DAPI and specific antibodies for 53BP1 and HP1α (upper panel) or 53BP1 and H4Ac (lower panel). **B.** RT-qPCR measurement of major satellites trascripts of cells expressing dCas9-EGFP (pCx-15) +gRNA or dCas9-VP64 (pCX-41) +gRNA.**C.** Western blot analysis for KAP1, HP1α, HP1β, HP1γ, RAD51 and tubulin in protein extracts prepared from cells after individual or simultaneous knockdown of HP1α, HP1β, HP1γ, KAP1 as well as of RAD51. Theoretical molecular weights are indicated on the right. **D.** Cell cycle analysis of G1 and G2 (RO-3306 treated) cells after HP1α knockdown. Cell cycle analysis plots are representative of all siRNAs used in the paper. **E**. RT-qPCR measurement of SMC5 and SMC6 knockdown efficiency and Western blot analysis for RAD51 and tubulin of the corresponding cells. **F**. Quantification of γ-H2AX pattern in G1 and G2 (RO-3306 treated) cells expressing Cas9-EGFP + gRNA after SMC5 or SMC6 knockdown. **G**. Quantification of γ-H2AX pattern in G1 and G2 (RO-3306 treated) cells expressing Cas9-EGFP + gRNA after simultaneous SMC5 and SMC6 knockdown. **H-I**. Quantification of RAD51 (**H**) and Ku80 (**I**) recruitment as in (**F-G)**. For confocal images, scale bar represents 10 μm. Values represent mean ± SD of three independent experiments with n=50 cells. For statistical analysis, t-test was performed. (*) $p<0.05$; (**) $p<0.01$; (***) $p<0.001$. **A and E-I**: 8h post-transfection, plasmids used: Cas9-EGFP (pCX-5), gRNA (pG-56).

Figure S7 (Related to Figure 6 and Figure 7). Rad51 binding at heterochromatic DSBs depends on the level of resection and tethering of BRC3 at the core of pericentric heterochromatin is sufficient to recruit RAD51. **A-B**. Quantification of RAD51 recruitment in G2 (RO-3306 treated) cells expressing Cas9-EGFP + gRNA after treatment with Mirin inhibitor or vehicle only (DMSO) (**A**) or GAM-emGFP expression (**B**). **C**. RT-qPCR measurement of CtIP knockdown efficiency. **D**. Western blot analysis for CtIP and tubulin in protein extracts prepared from cells after knockdown of CtIP. Theoretical molecular weights are indicated on the right. **E**. IF confocal analysis of G1 and G2 (RO-treated) cells expressing Cas9-CtIP + gRNA, stained with DAPI and specific antibodies for γ-H2AX and Rad51. **F**. Quantification of RAD51 recruitment in G1 and G2 (RO-treated) cells expressing Cas9-CtIP + gRNA. **G**. Quantification of γ-H2AX pattern in G1 cells expressing Cas9-CtIP +gRNA. **H**. RT-qPCR measurement of BRCA2 knockdown efficiency and Western blot analysis of RAD51 and tubulin in the corresponding cells. **I**. IF confocal analysis of G1 cells expressing Cas9-RAD51 (upper panel) or Cas9-BRC3 (lower panel), stained with DAPI and specific antibodies for γ-H2AX and RAD51. **J**. Quantification of RAD51 pattern in G1 and G2 (RO-3306 treated) cells expressing Cas9-BRC3 or Cas9-mBRC3 +gRNA. **K**. Western blot analysis of RAD52-turboGFP (RAD52), RAD51, EGFP and tubulin in protein extracts prepared from cells after RAD51 or RAD52 knockdown or RAD52 knockdown and overexpression of either EGFP or RAD52-turboGFP . Theoretical molecular weights are indicated on the right. **L**. Quantification of RAD51 recruitment in G2 (RO-3306 treated) cells expressing Cas9-EGFP +gRNA upon RAD52 knockdown. **M**. Quantification of RAD52 recruitment in G2 (RO-3306 treated) cells expressing Cas9-EGFP +gRNA upon RAD51 knockdown. For confocal images, scale bar represents 10 μm. Values represent mean ± SD of three independent experiments with n=50 cells. For statistical analysis, t-test was performed. (*) $p<0.05$; (**) $p<0.01$; (***) $p<0.001$. **A**: 8h post-transfection. Plasmids used: Cas9-EGFP (pCX-5), gRNA (pG-56). **B**: 16h post-transfection, plasmids used: Cas9-mCherry+gRNA (pX-86) and GAM-emGFP. **E-G**: 16h post-transfection, plasmids used: Cas9-mCherry (pX-86) and Cas9-CtIP (pX-147). **I and G**: 16h post-transfection, plasmids used: Cas9-mCherry+gRNA (pX-86), Cas9-BRC3 (pX-189), Cas9-mBRC3 (pX-190). **K**: 72h post-knockdown and 16h post-transfection with RAD52-turboGFP. **L and M**: Plasmids used: Cas9-EGFP (pCX-5), gRNA (pG-56).

Movie S1 (Related to Figure 2): γ-H2AX internal pattern after Cas9-induced DSBs at chromocenters. Movie of the Z-stack series of the cell shown in Figure 2A (upper panel) expressing Cas9-EGFP+gRNA and stained with DAPI

(Blue) and a γ-H2AX specific antibody (Green). 46 stacks (0.125 μm spacing) across the entire nuclear volume were used for the movie reconstruction.

Movie S2 (Related to Figure 2): 53BP1 internal pattern after Cas9-induced DSBs at chromocenters. Movie of the Z-stack series of the cell shown in Figure 2A (lower panel) expressing Cas9-EGFP+gRNA and stained with DAPI (Blue) and a 53BP1 specific antibody (Red). 67 stacks (0.125 μm spacing) across the entire nuclear volume were used for the movie reconstruction.

Movie S3 (Related to Figure 2): γ-H2AX peripheral pattern after Cas9-induced DSBs at chromocenters in G2. Movie of the Z-stack series of the cell in G2 shown in Figure 2B (upper panel) expressing Cas9-EGFP+gRNA and stained with DAPI (Blue) and a γ-H2AX specific antibody (Green). 59 stacks (0.125 μm spacing) across the entire nuclear volume were used for the movie reconstruction.

Movie S4 (Related to Figure 2): 53BP1 peripheral pattern after Cas9-induced DSBs at chromocenters in G2. Movie of the Z-stack series of the cell in G2 shown in Figure 2B (lower panel) expressing Cas9-EGFP+gRNA and stained with DAPI (Blue) and a 53BP1 specific antibody (Red). 100 stacks (0.125 μm spacing) across the entire nuclear volume were used for the movie reconstruction.

Movie S5 (Related to Figure S4): RAD51 peripheral localization after Cas9-induced DSBs at chromocenters in G2. Movie of the Z-stack series of the cell in G2 shown in Figure S5A expressing Cas9-EGFP+gRNA and stained with DAPI (Blue) and antibodies specific for γ-H2AX (Green) and RAD51 (Red). Colocalization of γ-H2AX and RAD51 is depicted in yellow. 54 stacks (0.125 μm spacing) across the entire nuclear volume were used for the movie reconstruction.

Movie S6 (Related to Figure S4): RAD51 peripheral localization after Cas9-induced DSBs at centromeres in G1. Movie of the Z-stack series of the cell in G1 shown in Figure S5C (upper panel) expressing Cas9-EGFP+gRNA and stained with DAPI (Blue) and antibodies specific for centromeres (CREST-Green), γ-H2AX (Gray) and RAD51 (Red). 73 stacks (0.125 μm spacing) across the entire nuclear volume were used for the movie reconstruction.

Movie S7 (Related to Figure S4): RAD51 peripheral localization after Cas9-induced DSBs at centromeres in G2. Movie of the Z-stack series of the cell in G2 shown in Figure S5C (lower panel) expressing Cas9-EGFP+gRNA and stained with DAPI (Blue) and antibodies specific for centromeres (CREST-Green), γ-H2AX (Gray) and RAD51 (Red). 84 stacks (0.125 μm spacing) across the entire nuclear volume were used for the movie reconstruction.

Supplemental Materials and Methods.

Cell treatments.

Neocarzinostatin (NCS; N9162-100 UG; Sigma) was added (50, 100 or 200 ng/ml), 15 min later medium was replaced and cells were harvested for Western blot analysis 1 h later. The Mre11 inhibitor (Mirin; M9948; Sigma-Aldrich) was added (50 μM) 5 min before transfection. The ATM inhibitor (Ku55933; Tocris Bioscience) was added (20 μM) 1 h before transfection. The ATR inhibitor (504972; Calbiochem) was added (0.5 μM) 1 h before transfection and refreshed 4h before fixation. The DNAPKi inhibitor (Nu7026; Sigma) was added (20 μM) 1 h before transfection. Trichostatin A (TSA; T-1952; Sigma) was added (0.5 μM) 16h before transfection. Cells were synchronized in the G2 phase of the cell cycle with the Cdk1 inhibitor IV (RO-3306; 217699; Calbiochem; 10 μM), which was added 16 h before transfection. Cells were arrested in G1/S phase of the cell cycle with double-thymidine (T1895; Sigma) block: 18h thymidine treatment (2 mM), 9h release, 16h thymidine treatment (2 mM). Cell-cycle arrest was confirmed by flow cytometry.

Cell cycle analysis.

Cells were fixed in 70% ethanol overnight at -20°C, then treated with RNAse A (100 μg/ml) and stained with propidium iodide (40 μg/ml). Data were collected on a FACSCalibur (Becton-Dickinson) and analyzed with FlowJo (TreeStar).

In vitro transcription of gRNA

The T7 promoter was added to the gRNA template (plasmid) by PCR amplification using specific primers (Fwd primer: 5'- TTAATACGACTCACTATAGGAAATGTCCACTGTAGGACG-3' and Rev. primer: 5'-AAAAAAAGCACCGACTCGGTGCCAC-3'). The T7-gRNA PCR product was used as the template for in vitro transcription. In vitro transcription is performed with the MEGAshortscript T7 kit (Life Technologies) following the manufacturer's instructions. The gRNA was purified with 2 mM LiCl and 100% EtOH and was resuspended in Ambion® Nuclease-Free Water.

3D-SIM super-resolution image analysis.

Image analysis of chromocenters and foci was conducted in automated fashion using the image analysis software Imaris (Bitplane, Switzerland) based on 3D-SIM super-resolution images.
Each image consisted of 3 channels: 1) DAPI (nuclei), 2) HP1a (Heterochromatin protein 1), 3) 53BP1 (DNA repair foci). Cells in G1 phase were analyzed. Using the Imaris "Cell" module, the chromocenters (DAPI dense regions) were defined using the 53BP1 channel. The DAPI channel was not suitable directly, as false positive regions could not be avoided due to the high intensity signal at the nuclear membrane.

High-throughput analysis of chromocenter area and heterochromatin markers before and after damage induction.

Images were acquired using the IN Cell Analyzer 1000 Cellular Imaging System (20 fields per well at 20x magnification) followed by a cell to cell analysis using Cellomics Cell-Insight software (Colocalization Bioapplication). Firstly, cells were selected based on DAPI staining and chromocenters were defined as the DAPI dense regions. Then cells expressing Cas9-EGFP - gRNA were chosen as GFP^+ and cells expressing Cas9-EGFP + gRNA were selected based on their characteristic γ-H2AX/53BP1 pattern colocalizing with chromocenters (Figure 1B-D). Subsequently, average chromocenter area per cell was measured as well as γ-H2AX, H3K9me3, HP1α, HP1β, HP1γ, KAP1 and $pKAP1^{S824}$ total intensities within chromocenter area.

Plasmid Construction.

The DNA sequences encoding Cas9 (Cong et al., 2013), dCas9 (Cong et al., 2013), EGFP, mCherry, VP64 (Mali et al., 2013), hCTIP (gift from Pablo Huertas), hRad51 (gift from Tom Misteli), BRC3 domain of Brca2 (Reuter et al., 2015) and BRC3DFK domain of Brca2(Reuter et al., 2015) were amplified by PCR and cloned by megawhop cloning (Miyazaki, 2011). Individual gRNAs (Table S4) were cloned into a vector containing the U6 promoter followed by a gRNA scaffold. All plasmids (Table S5) were assembled by golden gate cloning (Engler et al., 2009). wtCas9 was amplified from pX330-U6-Chimeric_BB-CBh-hSpCas9 and dCas9 was generated by mutagenesis and amplified from pX335-U6-Chimeric_BB-CBh-hSpCas9n(D10A). pX330-U6-Chimeric_BB-CBh-hSpCas9 and pX335-U6-Chimeric_BB-CBh-hSpCas9n(D10A) were a gift from Feng Zhang (Addgene plasmids # 42230 and # 42335). See Table S4 for plasmid details and sequences. RAD52-turboGFP plasmid was a gift from Madalena Tarsounas.

*siRNAs used.**	
siRNA	**Reference**
scramble	D-001810-10
HP1α (Cbx5)	L-040799-01
HP1β (Cbx1)	L-060281-01
HP1γ (Cbx3)	L-044218-01
CtIP	L-055713-01
Smc5	L-053946-01
Smc6	L-054453-01
Brca2	L-042993-00
Rad51	L-062730-00
Rad52	L-043751-00
KAP1	L-040800-01
53BP1	L-042290-01
Ku80	L-046264-01
Rif1	L-040028-01

* All siRNAs (ON-TARGETplus SMARTpool siRNAs) were purchased from Dharmacon.

Primers used.		
Target	**Forward primer**	**Reverse primer**
HPRT	GTTGGATACAGGCCAGACTTTGTTG	GATTCAACTTGCGCTCATCTTAGGC
SMC5	TCCAGACACAAGTACCCACCA	TGAGTACTCCTCAACCACCGAA
SMC6	CACCGCACTCATAGTTGGTCT	AAACCACGGTGCCTTTTTCA
CtIP	GGACGCGGCGAGAGGTAG	GATTGTTGAAATACCTCGGCGGG
BRCA2	CCAAAAGATAGGCCTGAGACTTCC	ACCAATTGAGGCTTATCGGTCC
Major Satellites	GACGACTTGAAAAATGACGAAATC	CATATTCCAGGTCCTTCAGTGTGC
GAPDH	AACTTTGGCATTGTGGAAGG	ACACATTGGGGGTAGGAACA
53BP1	GTTGCCAGTCTCCAGAAGCC	ACTCTGCCTGAGTTTTGGGG
Ku80	ACTGCTCAGGACGTTTTCCA	TGGAGACTCGCTTCCTCAAAG
Rif1	TGTACACGGTTTTAAAGGCTCA	AGCAGGAAACGTCTGTTTGGA

Antibodies used.		
Antibody	**Company (reference)**	**Dilution (Use)***
γ-H2AX (H2AX S139)	Abcam (ab22551)	1:1000 (IF & WB)
53BP1	Novus Biologicals (100-304)	1:1000 (IF)
pATM (S1981)	RockLand (200-301-400)	1:500 (IF), 1:1000 (WB)
pKAP1 (S824)	Bethyl (A300-767A)	1:1000 (IF & WB)
KAP1	Euromedex (1TB1A9)	1:1000 (IF & WB)
pChk1 (S345)	Cell Signalling (133D3)	1:500 (WB)
MDC1	Made in IGBMC	1:500 (IF)
RAD51	Calbiochem (PC130)	1:50 (IF), 1:1000 (WB)
Ku80	Santa Cruz (sc-56136)	1:50 (IF), 1:200 (WB)
EGFP	Abcam (6673-100)	1:3000 (WB)
RPA32	Novus Biologicals (600-565)	1:250 (IF)
H3K9me3	Abcam (8898)	1:500 (IF)
HP1α	Euromedex (2HP1H5)	1:500 (IF & WB)
HP1β	Euromedex (1MOD1A9)	1:1000 (IF & WB)
HP1γ	Euromedex (2MOD1G6)	1:3000 (IF & WB)
H4Ac	Active Motif (3HH4-2C2)	1:500 (IF)
α Tubulin	Sigma Aldrich (T5168)	1:5000 (WB)
CREST	Antibodies Incorporated (15-235-F)	1:500 (IF)
RAD52	Cell Signalling (3425)	1:1000 (WB)
H3S10p	Millipore (06-570)	1:1000 (IF)
CtIP	Gift from Richard Baer	1:500 (WB)

* WB: Western Blot; IF: Immunofluorescence.

gRNAs				
gRNA	**Sequence**	**PAM**	**Primers**	
Ma-Sat#1	GGCGAGAAAACTGAAAATCA	CGG	Fwd	AAAGAAGACAAACCGGCGAGAAAACTGAAAATCAGTTTAAGTCTTCTTT
			Rev	AAAGAAGACTTAAACCCTTTTTCAGTTTTCCTCGCGGTTTGTCTTCTTT
Ma-Sat#2	GCGAGGAAAACTGAAAAAGG	TGG	Fwd	AAAGAAGACAAACCGCGAGGAAAACTGAAAAAGGGTTTAAGTCTTCTTT
			Rev	AAAGAAGACTTAAACCGTCCTACAGTGGACATTTCGGTTTGTCTTCTTT
Ma-Sat#3	GAAATGTCCACTGTAGGACG	TGG	Fwd	AAAGAAGACAAACCGAAATGTCCACTGTAGGACGGTTTAAGTCTTCTTT
			Rev	AAAGAAGACTTAAACTGATTTTCAGTTTTCTCGCCGGTTTGTCTTCTTT
Ma-Sat#4	GAAATGTCCACTGTAGGACG	TGG	Fwd	AAAGAAGACAAACCGGCAAGAAAACTGAAAATCAGTTTAAGTCTTCTTT
			Rev	AAAGAAGACTTAAACTGATTTTCAGTTTTCTTGCCGGTTTGTCTTCTTT
Mi-Sat#1	ACACTGAAAAACACATTCGT	TGG	Fwd	AAAGAAGACAAACCGACACTGAAAAACACATTCGTGTTTAAGTCTTCTTT
			Rev	AAAGAAGACTTAAACACGAATGTGTTTTTCAGTGTCGGTTTGTCTTCTTT
Mi-Sat#2	AAAACACATTCGTTGGAAAC	CGG	Fwd	AAAGAAGACAAACCGAAAACACATTCGTTGGAAACGTTTAAGTCTTCTTT
			Rev	AAAGAAGACTTAAACGTTTCCAACGAATGTGTTTTCGGTTTGTCTTCTTT
Mi-Sat#3	ATGAGTTACAATTAGAAACA	TGG	Fwd	AAAGAAGACAAACCGATGAGTTACAATTAGAAACAGTTTAAGTCTTCTTT
			Rev	AAAGAAGACTTAAACTGTTTCTAATTGTAACTCATCGGTTTGTCTTCTTT
Mi-Sat#4	ATCTAATATGTTCTACAGTG	TGG	Fwd	AAAGAAGACAAACCGATCTAATATGTTCTACAGTGGTTTAAGTCTTCTTT
			Rev	AAAGAAGACTTAAACCACTGTAGAACATATTAGATCGGTTTGTCTTCTTT

Plasmids used*.	
pCX-5	CMVp-Cas9-EGFP-SV40p-PuroR-pA
pCX-15	CMVp-dCas9-EGFP-SV40-PuroR-pA
pCX-40	CMVp-EGFP-Cas9-VP64-SV40p-PuroR-pA
pCX-41	CMVp-EGFP-dCas9-VP64-SV40p-PuroR-pA
pX-86	U6p-gRNA(Ma-Sat#3)-CMVp-Cas9-mCherry-SV40p-HygroR-pA
pX-112	U6p-gRNA(Ma-Sat#3)-SV40p-EGFP-Cas9-hRad51-SV40p-HygroR-pA
pX-147	U6p-gRNA(Ma-Sat#3)-SV40p-EGFP-Cas9-hCTIP-SV40-HygroR-pA
pX-189	U6p-gRNA(Ma-Sat#3)-SV40p-BRC3-Cas9-EGFP-SV40-PuroR-pA
pX-190	U6p-gRNA(Ma-Sat#3)-SV40p-BRC3ΔFK-Cas9-EGFP-SV40-PuroR-pA
pG-56	U6p-gRNA (Ma-Sat#3)-gRNA Scaffold
pG-57	U6p-gRNA (Ma-Sat#1)-gRNA Scaffold
pG-58	U6p-gRNA (Ma-Sat#2)-gRNA Scaffold
pG-59	U6p-gRNA (Ma-Sat#4)-gRNA Scaffold
pG-35	U6p-gRNA (Mi-Sat#1)-gRNA Scaffold
pG-36	U6p-gRNA (Mi-Sat#2)-gRNA Scaffold
pG-37	U6p-gRNA (Mi-Sat#3)-gRNA Scaffold
pG-38	U6p-gRNA (Mi-Sat#4)-gRNA Scaffold
pR-18	pTRE-Cas9-EGFP-SV40-PuroR-pA
pX-243	CMV-HA-TIR1-IRES-rtTA-SV40-HygroR-pA
pX-303	U6p-gRNA(Ma-Sat#3)-pTRE-AID-Cas9-EGFP-AID-SV40-PuroR-pA

* Plasmids and sequences available upon request.

Supplemental References

Cong, L., Ran, F.A., Cox, D., Lin, S., Barretto, R., Habib, N., Hsu, P.D., Wu, X., Jiang, W., Marraffini, L.A., *et al.* (2013). Multiplex genome engineering using CRISPR/Cas systems. Science *339*, 819-823.

Engler, C., Gruetzner, R., Kandzia, R., and Marillonnet, S. (2009). Golden gate shuffling: a one-pot DNA shuffling method based on type IIs restriction enzymes. PLoS One *4*, e5553.

Mali, P., Aach, J., Stranges, P.B., Esvelt, K.M., Moosburner, M., Kosuri, S., Yang, L., and Church, G.M. (2013). CAS9 transcriptional activators for target specificity screening and paired nickases for cooperative genome engineering. Nat Biotechnol *31*, 833-838.

Miyazaki, K. (2011). MEGAWHOP cloning: a method of creating random mutagenesis libraries via megaprimer PCR of whole plasmids. Methods Enzymol *498*, 399-406.

Reuter, M., Zelensky, A., Smal, I., Meijering, E., van Cappellen, W.A., de Gruiter, H.M., van Belle, G.J., van Royen, M.E., Houtsmuller, A.B., Essers, J., *et al.* (2015). BRCA2 diffuses as oligomeric clusters with RAD51 and changes mobility after DNA damage in live cells. J Cell Biol *208*, 857.

3.2 Double Strand Break Repair pathways in centromeres

Following these recently published data, we are particularly interested in understanding the differences in the repair between centromeric and pericentromeric lesions. Although these two structures are highly condensed as typical examples of constitutive heterochromatin, they are characterized by different DNA sequence, chromatin modifications and histone variant composition (Figure 3.1C). These differences could have an impact on the DNA repair outcome. More specifically, pericentric heterochromatin is enriched in H3K9me3, H4K20me2/3 and HP1s that are considered the key markers of constitutive heterochromatin. On the other hand, nucleosomes of centromeres are enriched in CENP-A as well as in H3K36me2 and H3K4me2 that represent a more active chromatin environment. Our goal is to investigate if and how this unique structure of centromeric heterochromatin could allow RAD51 recruitment and thus HR activation throughout the cell cycle in comparison with pericentric heterochromatin where HR is inhibited in G1.

To address this question, we are using two approaches: a candidate approach and an unbiased proteomics approach. For the candidate approach, we are interested in individual factors and their impact on HR in G1 in centromeres in contrast to pericentromeres. In order to investigate these differences, we are currently constructing vectors expressing different proteins involved in resection such as Mre11, CtIP, EXO1, DNA2, BLM and EXD2 fused to EGFP in order to test their recruitment at these two heterochromatic structures. Moreover, we are currently performing immunofluorescence experiments regarding RAD51 and RPA recruitment under knockdown conditions of these resection factors. Combined results from these experiments will shed light on the precise activation of each step of HR, being potentially involved in the promotion of this pathway in G1 in centromeres

The unique nature of centromeric heterochromatin could also have a potential role in the licensing of HR in G1 (Muller and Almouzni, 2017). CENP-A is the centromeric H3 histone variant incorporated in chromatin in G1 through its specific chaperone HJURP (Muller and Almouzni, 2017). Thus these two proteins could be good candidates to positively affect HR specifically in this phase of cell cycle. Indeed, CENP-A seems to positively affect HR since RAD51 and RPA32 recruitment is decreased under *CENP-A* knockdown conditions (Figure 3.2A-C). Though the same tendency for RAD51 and RPA32 recruitment is observed under *HJURP* knockdown conditions, the results are not statistically significant (Figure 3.2D-F). Apart from CENP-A and HJURP, histone modifications could have a crucial role promoting H1 in G1. We are currently

working on two histone modifications, H3K36me2 and H4K20me2, and their potential role in this process. More specifically, in order to investigate the potential role of H3K36me2 that is enriched in centromeres and not in pericentromeres, we are currently constructing a vector expressing Cas9 fused to the KDM2A demethylase. Cas9-KDM2A will be targeted specifically to the centromeres through the expression of the corresponding gRNA, where it will induce DSBs and in parallel KDM2A will locally remove H3K36me2. On the other hand, centromeres are deprived of H4K20me2 that is essential for 53BP1 recruitment and thus promotion of NHEJ. Lack of this modification might allow for more efficient BRCA1 recruitment and thus resection and HR promotion. To test this hypothesis, we are constructing a vector expressing the MMSET methylase that will induce H4K20me2 fused to Cas9. These experiments will allow us to study the impact of each modification in HR in centromeres.

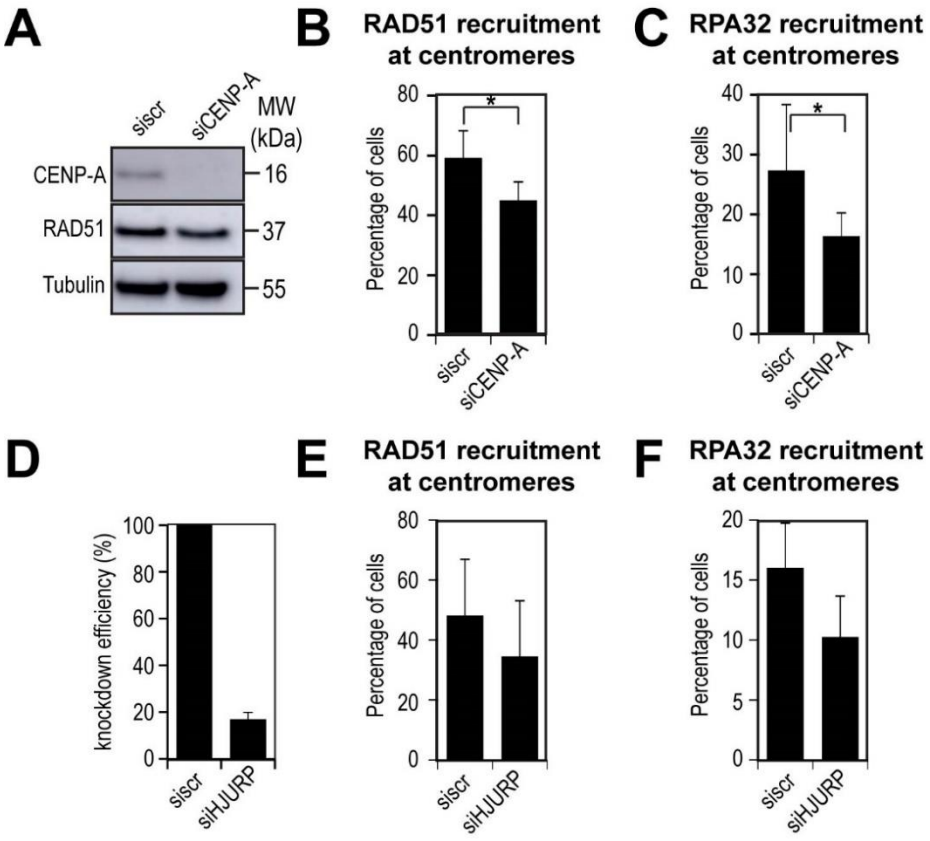

Figure 3.2: Effect of *CENP-A* and *HJURP* knockdown on HR in G1 phase of cell cycle of centromeres. A. Western blot analysis for CENP-A, RAD51 and tubulin in protein extracts prepared from cells after knockdown of *CENP-A*. **B-C.** Quantification of RAD51 and RPA32 recruitment of cells expressing Cas9-EGFP+gRNA specific for minor satellites upon *CENP-A* knockdown. **D.** RT-qPCR measurement of *HJURP* knockdown efficiency. **E-F.** Quantification of RAD51 and RPA32 recruitment of cells expressing Cas9-EGFP+gRNA specific for minor satellites upon *HJURP* knockdown. Quantification of RAD51 and RPA32 recruitment is based on single cell counting after IF confocal analysis using specific antibodies for each protein. Values represent mean ± SD of 5 for B, 6 for C and 4 for E-F independent experiments with n>50 cells. For statistical analysis, t-test was performed. (*) $p<0.05$; (**) $p<0.01$; (***) $p<0.001$.

Apart from the candidate approach and in order to identify novel factors that allow HR in centromeres in G1, we have performed unbiased proteomics experiments using the Bio-ID technology. In this technology, BirA* is used that is the promiscuous *E. coli* biotin ligase which biotinylates proteins in close proximity with it, in the presence of biotin (Roux et al., 2012). This allows for the efficient isolation of biotinylated proteins by using streptavidin-coupled beads that will then be submitted to identification by mass spectrometry (Roux et al., 2012). For our experiments, we have created NIH3T3 cell lines that stably express Cas9 or dCas9 (catalytically inactive) fused to BirA* (Figure 3.3A). This BirA*-Cas9 is efficiently targeted to centromeres or pericentromeres upon expression of the corresponding gRNA, induces DSBs and biotinylates proteins in proximity as we have detected by immunofluorescence checking for γ-H2AX as the hallmark of the DDR and streptavidin staining respectively (Figure 3.3A-B, B: one cell with DSBs and biotinylation in centromeres is representatively shown). BirA*-dCas9 targeted to centromeres or pericentromeres is used as a control. Moreover, since BirA*-Cas9/ dCas9 is stably expressed in the cells and it can consequently biotinylate proteins in the absence of DNA damage, the two corresponding cell lines have also been used as a control without expression of a gRNA. The biotinylated proteins from these different conditions have been isolated using streptavidin-coupled beads and submitted to identification by mass spectrometry. Two independent experiments have been performed with 356 proteins in common (Figure 3.3C). These proteins are further classified into different categories based on their functional role (Figure 3.3D). Among them, DNA repair proteins have been identified that are enriched after DSB induction in centromeres and pericentromeres (Figure 3.3D), suggesting that our mass spectrometry analysis gives reliable results. Among these results, some interesting candidates are revealed that could be implicated in the specific activation of DNA repair in centromeres or pericentromeres. This project will shed light on the differences in DSB repair between two heterochromatic structures with different characteristics highlighting the impact of chromatin environment and not only the compaction on the outcome of the repair.

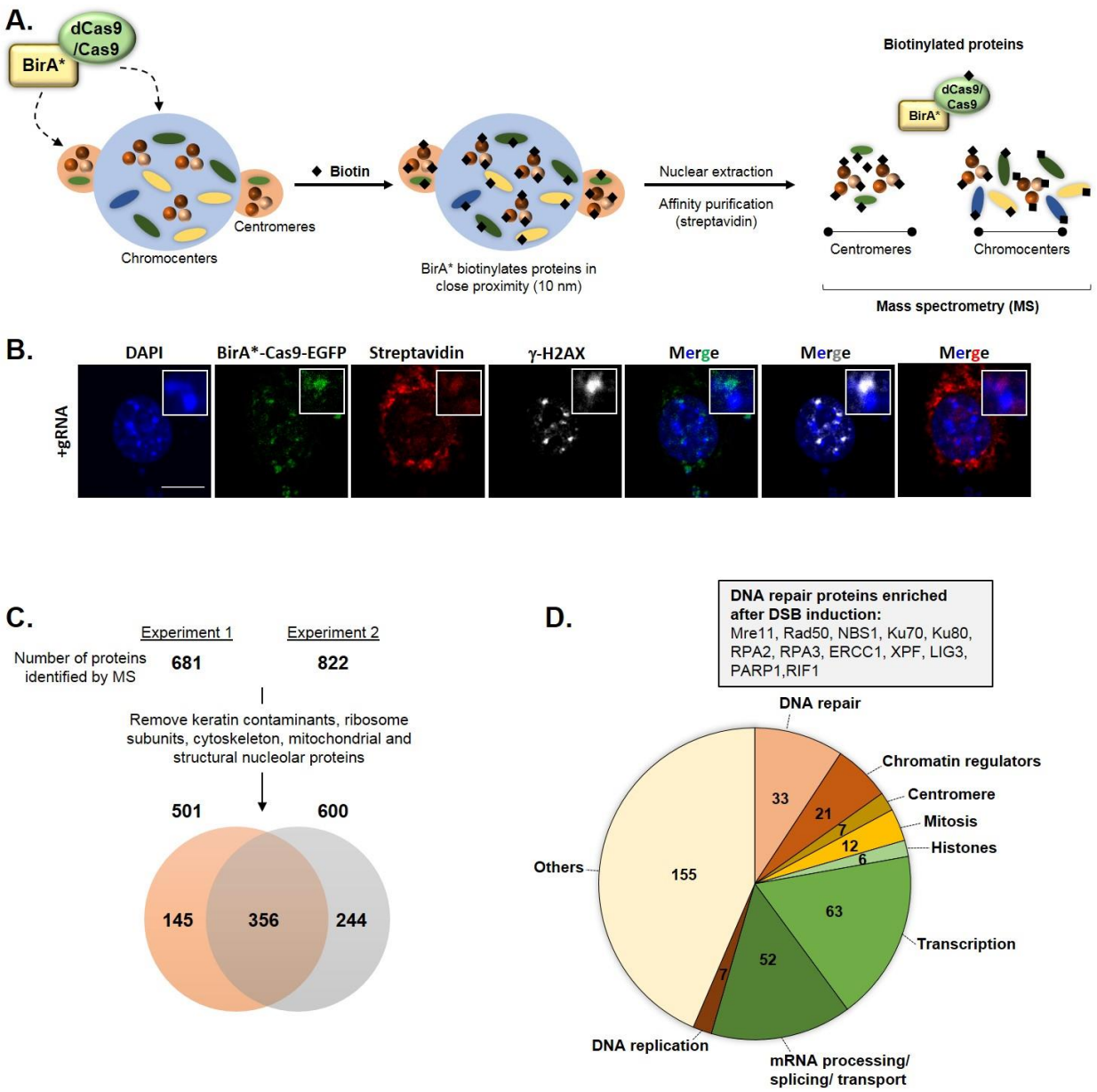

Figure 3.3: Proteomics of DSB repair within heterochromatin using the Bio-ID technology. A. dCas9 and Cas9 fused to BirA* are targeted to centromeres and pericentromeres/chromocenters through expression of a gRNA against minor and major satellite repeats, respectively. After addition of biotin, BirA* biotinylates proteins in close proximity. Biotinylated proteins are then isolated through nuclear extraction and subsequent streptavidin-based affinity purification and they are identified by mass spectrometry. **B.** IF confocal analysis of one cell expressing BirA*-Cas9-EGFP+gRNA specific for minor satellites DNA repeats in G1 and stained with DAPI, fluorescently labeled streptavidin and an antibody specific for γ-H2AX. Scale bar represents 10 μm. **C.** Number of proteins identified from two independent MS experiments. **D.** Gene Ontology (GO) analysis of the 356 common proteins identified between the two independent MS experiments. DNA repair proteins enriched after DSB induction in centromeres or pericentromeres are indicatively shown.

4. Discussion

Cas9-induced DSBs in pericentric heterochromatin and their cell-cycle regulated localization

In our recently published work, we took advantage of the CRISPR/Cas9 system to target and induce DSBs specifically in different heterochromatic structures of mammalian cells and study their repair (Tsouroula et al., 2016). More specifically, we designed a gRNA targeting major satellite repeats of pericentric heterochromatin, which in mouse cells corresponds to the DAPI-dense regions known as chromocenters. Using high-resolution imaging and 3D reconstruction, we firstly showed that these DSBs are homogenously distributed in the structure of chromocenters and they can also efficiently activate the DDR pathway. Although, these Cas9-induced DSBs were induced within the HC domain as revealed by γ-H2AX and 53BP1 staining using 3D-SIM super-resolution microscopy, their localization could be then altered depending on the cell cycle phases; in G1, breaks are positionally stable through time in contrast to S/G2 where they relocate to the HC periphery in order to be repaired. These results were confirmed through different experimental approaches. More specifically, the gRNA expression as a plasmid but also as *in vitro* transcribed gRNA gave us the possibility to investigate in detail the kinetics of the HC DSBs. Furthermore, cell cycle arrest was achieved through different inhibitors (RO-3306 for G2 and thymidine block for G1/S and further release in S and G2) and confirmed both by flow cytometry and IF confocal analysis with a specific antibody for H3S10p G2 marker, strengthening our cell-cycle regulated results for γ-H2AX and 53BP1 pattern. Although this peripheral localization of heterochromatic DSBs has also been reported in other studies (Chiolo et al., 2011; Jakob et al., 2011; Janssen et al., 2016; Torres-Rosell et al., 2007; Warmerdam et al., 2016), these data reveal for the first time the cell-cycle specific regulation of DSB relocation in HC, adding another key regulatory factor in HC DNA repair of mammalian cells.

Heterochromatic Cas9-induced DSBs and repair pathway choice

After confirming that Cas9-induced DSBs properly activate DDR and follow a differential distribution pattern during cell-cycle, we studied the activation of HR and NHEJ, the two main DSB repair pathways, and their correlation with the localization of the breaks. To address this question, we assessed the recruitment of Ku80 and RAD51 as representative factors for NHEJ and HR respectively in correlation with the γ-H2AX or 53BP1 pattern as indicative for the break localization. In the case of HR, we also performed similar experiments regarding the recruitment of RPA as a marker of end-resection. We found that in G1, NHEJ (but not HR) is activated within

the HC core domain, exemplified by the recruitment of Ku80 at the sites of breaks. In G2, however, both NHEJ and HR are activated. Although the majority of DSBs (70%) in G2 move to the periphery to be repaired, there are still some that are positionally stable and they are repaired within the HC core by NHEJ. On the other hand, the breaks that move to the periphery are repaired by HR. While RPA recruitment is observed at the core HC domain, RAD51 is entirely peripheral leading to the spatial restriction of HR to the HC periphery. This indicates that DNA-end resection and the search for homology are spatially separated and suggests that resected DNA ends relocate to the HC periphery to perform the late steps of HR.

Apart from the correlation of the HC DSBs with NHEJ and HR, we also revealed that SSA can be activated within this compacted structure. As mentioned above, the majority of DSBs in G2 relocate to the periphery to be repaired by HR. The rest of them (30%) remains in the HC core as revealed by γ-H2AX staining. RAD52, an indicative factor of SSA, is recruited to these breaks, suggesting that although the majority of lesions relocate to the periphery, resected breaks that fail to relocate recruit RAD52 and can be repaired *in situ* by SSA. Thus, HC breaks will primarily be repaired by HR moving to the HC periphery, but they can also activate NHEJ in the core of the structure. In case resection has happened but they fail to relocate, SSA can also be activated within HC. The activation of SSA within the core could be a safeguard mechanism to ensure that resected breaks that fail to relocate can still be repaired within the HC structure. Therefore, relocation might be essential to avoid highly mutagenic pathways such as SSA and instead inforce high-fidelity repair at the periphery.

The activation of these three repair pathways (HR, NHEJ, SSA) by heterochromatic DSBs was also recently confirmed in *D. melanogaster* (Janssen et al., 2016) in contrast to previous studies regarding exclusively HR as the repair pathway chosen for HC breaks in this model organism (Chiolo et al., 2011; Ryu et al., 2015). Apart from the fact that homologous chromosomes are almost always paired in somatic Drosophila cells serving as a potential template for HR, 95% of cultured Drosophila cells used in Chiolo et al. (2011) were in S and G2 phases of the cell cycle (Chiolo et al., 2011; Ryu et al., 2015). This is a possible explanation for considering HR the only pathway used for heterochromatic DSB repair in this study (Chiolo et al., 2011). On the other hand, only 50% of cells of larval tissues used in Janssen et al. (2016) were in S/G2, thus allowing the detection of other repair pathways being activated in different phases of cell cycle (Janssen et al., 2016). Moreover, the use of I-SceI to induce one single DSB (Janssen et al., 2016) compared to multiple and different breaks induced by IR (Chiolo et al., 2011) could allow for more

efficient observations regarding the utilization of different repair pathways in HC. I-SceI DSBs are more similar to Cas9-induced DSBs used in our study thus allowing for the activation and detection of HR, NHEJ and SSA in heterochromatin in Drosophila and mouse cells, respectively (Janssen et al., 2016; Tsouroula et al., 2016).

Role of resection and RAD51 in peripheral localization of heterochromatic DSBs

The spatial restriction of HR seems to be a conserved mechanism among species to avoid recombination of repetitive sequences that would threaten their genome integrity and cell viability. As it was previously mentioned, in *D. melanogaster*, DSBs move to the periphery and ultimately relocate to the pores to accomplish HR (Chiolo et al., 2011; Ryu et al., 2015). Similar results obtained for the damaged repetitive ribosomal locus that delocalizes outside of the nucleolus domain to be repaired by HR in yeast and in human cells (Torres-Rosell et al., 2007; van Sluis and McStay, 2015; Warmerdam et al., 2016). Both in *D. melanogaster* and in yeast, resection is the driving force of DSB relocation to the HC periphery, something that we also confirmed by our experiments. On the other hand, contrary to what was shown in *D. melanogaster* (Chiolo et al., 2011), the checkpoint kinase ATR does not play a role in the relocation of the breaks in mouse cells. This is also the case for ATM kinase since its inhibition does not affect the peripheral pattern of γ-H2AX (Jakob et al., 2011; Tsouroula et al., 2016). Thus, with our experiments, we confirmed the key role of resection for the relocation of the breaks in mammalian cells but we also showed that this is an ATM and ATR independent process.

Apart from resection as a first step of this mechanism, we also revealed the role of RAD51 in retention of the breaks at the HC periphery. Upon *BRCA2* depletion, RAD51 loading on resected DSBs was dramatically impaired and these breaks were stabilized at the core of the HC domain in G2. This suggests that though resected breaks have the potential to relocate, they are not engaged at the HC periphery in the absence of RAD51. We strengthened this idea by forcing the recruitment of RAD51 in the core of chromocenters through Cas9 fusion to BRC3 domain (responsible for BRCA2 interaction with RAD51) or RAD51 itself. In both cases, tethering of RAD51 within chromocenters blocked DSB relocation to the periphery of the structure. These data support a two-step mechanism of DSB movement in mammalian cells, the first being resection as the driving force and the second the retention of the breaks at the periphery by the RAD51/BRCA2 complex.

RAD51 is excluded from pericentric heterochromatin

The spatial restriction of HR is a result of the active exclusion of RAD51 from the core HC domain (Chiolo et al., 2011; Janssen et al., 2016; Torres-Rosell et al., 2007; Tsouroula et al., 2016; Warmerdam et al., 2016). It has been shown that chromatin compaction blocks RAD51 entrance in HC in *D.melanogaster* through a mechanism that involves HP1a; HP1a interacts with SMC5/6 complex that consequently blocks RAD51 entrance in HC through a SUMO-regulated pathway (Ryu et al., 2016; Ryu et al., 2015). The involvement of sumoylation and SMC5/6 complex in this process was also shown in yeast (Torres-Rosell et al., 2007). In contrast to the above data, we showed that chromatin compaction and SMC5/6 complex are not involved in RAD51's exclusion from HC in mammalian cells. More specifically, we assessed the localization of RAD51 in HC after induction of chromatin relaxation through three different ways: 1. Treatment with the histone deacetylase inhibitor Trichostatin A (TSA) that induces robust chromatin relaxation and loss of HP1s from heterochromatin. 2. Tethering of the transcriptional activator VP64 specifically to pericentric heterochromatin through its fusion to Cas9. 3. Individual and simultaneous knockdown of *HP1*α, *HP1*β and *HP1*γ as well as individual knockdown of *KAP1*. RAD51 peripheral localization did not change under any of the above conditions. More interestingly, RAD51 recruitment was significantly decreased upon simultaneous knockdown of HP1s, further supporting the existing data for the role of HP1α in HR (Baldeyron et al., 2011). Similar decrease in RAD51 levels was observed upon KAP1 depletion, suggesting an active role of KAP1 in HR. Moreover, individual or simultaneous knockdown of *Smc5* and Smc*6* did not change RAD51 peripheral recruitment. We conclude that, in contrast to yeast and *Drosophila* data, chromatin compaction and SMC5/6 complex are not involved in the exclusion of RAD51 from heterochromatin in mammalian cells. This could be explained by the protein complexity of mammalian heterochromatin compared to yeast and Drosophila. As it was previously described (see 1.7.3), mammalian heterochromatin consists of many different components that participate in the maintenance of its compacted nature that could potentially have a role in RAD51's exclusion. Thus, further studies are needed to show the molecular mechanism that mediates this exclusion of RAD51 in mammalian cells. Overall, exclusion of RAD51 from the core domain of heterochromatin seems to be a conserved mechanisms to prevent the activation of HR in order to avoid illegitimate recombination between repetitive sequences. More specifically, given the fact that pericentric domains of several mouse chromosomes are clustered, DSB relocation and restriction of RAD51 at the HC periphery could prevent HR between different chromosomes, hence preventing chromosomal translocations.

Cas9-induced DSBs trigger chromatin expansion independently of the release of HP1s or H3K9me3

As previously mentioned, chromatin is undergoing through different changes in response to DNA damage in order to facilitate repair. In order to study the chromatin changes at chromocenters after Cas9-induced DSBs, we measured the intensities of HP1 proteins, KAP1, H3K9me3 as well as the area of chromocenters defined as the DAPI-dense regions. Our results showed that chromatin expansion happens both in G1 and G2 after damage induction, as it has been previously reported (Chiolo et al., 2011; Jakob et al., 2011). This expansion was not accompanied by the loss of any heterochromatin marker. More specifically, H3K9m3 was increased both in G1 and G2 that is in agreement with data showing increase of H3K9me3 at a single locus after damage induction (Ayrapetov et al., 2014). Furthermore, HP1s and KAP1 levels were significantly increased after damage induction in G2, supporting the hypothesis that they might have an active role in the HR repair process. These results also agree with many studies showing recruitment of HP1s after damage (Baldeyron et al., 2011; Luijsterburg et al., 2009; Zarebski et al., 2009). This increase of HP1s at Cas9-induced DSBs could be possibly explained by their enhanced binding through recognition of H3K9me3 but also DSBs by their chromodomain and chromoshadow domain (Luijsterburg et al., 2009), respectively; this could lead to their stabilization on heterochromatin and thus a net increase of their signal.

Cas9-induced DSBs and repair pathway choice in centromeric heterochromatin

To investigate whether the above results are specific to pericentric HC, we also used the CRISPR/Cas9 system to induce DSBs in centromeric HC of mouse cells. In this case, we designed a gRNA against centromeric minor satellite repeats and we induced specifically DSBs in centromeres. We showed that Ku80 is recruited both in G1 and G2, similarly to pericentric heterochromatin. In contrast to DSBs induced in pericentric heterochromatin, we showed that RAD51 is efficiently recruited at centromeric lesions both in G1 and G2, suggesting that unlike pericentric HC, HR is active throughout the cell cycle. As centromeres from different chromosomes are spatially separated and they do not cluster together, we could speculate that the risk of chromosomal translocations could be minimal and this allows HR to happen throughout the cell cycle. On the other hand, similarly to what we showed for pericentromeric lesions, RAD51 localization is peripheral in line with γ-H2AX peripheral pattern. Although these two heterochromatic structures are highly compacted, they differ in their DNA sequence, chromatin modifications and histone variant composition. More specifically, pericentric heterochromatin is enriched in H3K9me3, H4K20me2/3 and HP1s that are considered the key markers of constitutive

heterochromatin (Maison and Almouzni, 2004). On the other hand, nucleosomes of centromeres are enriched in the H3 histone variant CENP-A that is incorporated in chromatin through its specific chaperone HJURP. Additionally, they are characterized by H3K36me2 and H3K4me2 that represent a more active chromatin environment (Chan and Wong, 2012). These features could differentially affect the DNA repair outcome. Indeed, our unpublished data regarding the role of CENP-A and HJURP show that both proteins positively affect HR in G1 since their depletion leads to impaired RAD51 and RPA recruitment.

Except for CENP-A and HJURP, histone modifications could affect DNA repair. It has been shown that H3K36me3 promotes resection by recruiting CtIP through LEDGF, a chromatin binding protein that binds H3K36me3 (Aymard et al., 2014). The presence of H3K36me2 in centromeres might facilitate the induction of H3K36me3 creating a permissive environment for resection and thus HR. On the other hand, centromeres do not have H4K20me2/3 that exists in pericentromeric HC. Since this modification is recognized by 53BP1 that favors NHEJ, its lack maybe leads to decrease 53BP1 accumulation at the sites of breaks and thus HR is favored in these structures. Another scenario regarding the cell-cycle regulated HR in centromeres could involve the deubiquitinase USP11 that promotes interaction of BRCA1 and PALB2/BRCA2 in G2 (Orthwein et al., 2015). Though it has been shown that USP11 is degraded in G1 after damage induction (Orthwein et al., 2015), it might be protected from degradation specifically at centromeres promoting the BRCA1-PALB2 interaction and thus repair by HR.

Although testing the role of the above-mentioned individual factors can be very informative for the molecular mechanism that favors repair of centromeric lesions by HR in G1, we also proceeded to proteomic analysis of DSB repair in centromeres and pericentromeres using the Bio-ID technology. In this case, we took advantage of BirA*, the promiscuous strain of the corresponding *E.coli* biotin ligase, that biotinylates proteins in close proximity. By fusing this BirA* with Cas9, we targeted it at the centromeres and pericentromeres where it biotinylates proteins after damage induction. We subsequently isolated these biotinylated proteins using streptavidin-coupled beads and identified them by mass spectrometry (MS). Among these proteins, DNA repair factors are enriched after damage induction, suggesting that our MS analysis gives reliable results. Novel factors are also enriched after damage, suggesting their potential role in the repair process. This unbiased proteomics approach in combination with the study of individual factors will allow as to reveal the molecular mechanism that promotes HR in G1 in centromeres and not in pericentromeres.

Spatial distribution of Double Strand Breaks and repair pathway choice in heterochromatin

Katerina Tsouroula, Bernardo Reina-San-Martin and Evi Soutoglou#

Institut de Génétique et de Biologie Moléculaire et Cellulaire (IGBMC), UMR 7104 CNRS, UdS, INSERM U964, BP 10142, F-67404 Illkirch Cedex, CU de Strasbourg, France

#corresponding author: evisou@igbmc.fr

Original paper:

Title: Temporal and spatial uncoupling of DNA Double Strand Break repair pathways within mammalian heterochromatin.

Authors: Katerina Tsouroula, Audrey Furst, Melanie Rogier, Vincent Heyer, Anne Maglott-Roth[1], Alexia Loynton-Ferrand, Bernardo Reina-San-Martin and Evi Soutoglou.

Journal: Molecular Cell 63, 293-305, July 21, 2016.

Abstract

Heterochromatin is the tightly packed form of repetitive DNA, essential for cell viability. Its highly compacted and repetitive nature renders DSB repair a challenging process that cells need to overcome in order to maintain their genome integrity. Developing a highly specific and robust CRISPR/Cas9 system to target pericentric heterochromatin, we showed that DSBs in G1 are positionally stable and repaired by NHEJ. In S/G2, they relocate to the periphery of this domain to be repaired by HR. This relocation process is dependent of resection and RAD51 exclusion from the core domain of heterochromatin. If these breaks fail to relocate, they are repaired within heterochromatin by NHEJ or SSA. On the other hand, DSBs in centromeric heterochromatin activate both NHEJ and HR throughout the cell cycle. Our results reveal the differential repair pathway choice between centromeric and pericentric heterochromatin that also regulates the DSB position.

Double Strand Break Repair in heterochromatin

Double-strand Breaks (DSBs) are among the rarest but also the most cytotoxic lesions, leading to genomic instability, chromosomal translocations, cellular transformation and cancer[1]. These DSBs activate the DNA Damage Response (DDR) pathway, a complex network of processes that allows recognition of the break and activation of checkpoints, which pause cell cycle progression, leaving time for the cell to repair the breaks before dividing[2]. Two are the main repair pathways for DSBs: homologous recombination (HR) that is active during S and G2 when the sister chromatin is present to be used as a template for the repair and non-homologous end joining (NHEJ) that is active throughout the cell cycle[3].

These DSBs happen in the context of highly-ordered chromatin. Heterochromatin (HC) is the stably compacted part of chromatin, characterized by highly repetitive sequences and complex protein composition[4]. More specifically, Heterochromatin Protein 1 (HP1) directly recognizes tri-methylated lysine 9 of H3 (H3K9me3), a key feature of heterochromatin[4]. Mammalian cells have 3 isoforms, HP1α, HP1β and HP1γ that could increase the level of complexity in comparison to *D. melanogaster* that has only HP1a and *S. pombe* that has its homologue Swi6[4]. Moreover, there are other proteins ensuring the compacted nature of the domain like the methyltransferases Suv3-9 and Suv4-20 catalyzing H3K9me3 and H4K20me2/me3 respectively as well as the co-repressor KAP1, interacting with SETDB1 (histone methyltransferase), HDAC1 and HDAC2 (histone de-acetylases) and CHD3/Mi-2a (nucleosome remodeling factor). These features make DNA

repair in heterochromatin a challenging process that cells need to overcome in order to preserve their genome integrity.

It has been proposed that chromatin relaxation is a necessary step for the repair of heterochromatic breaks, with ATM kinase being a key factor in this process[5, 6]. It has been shown that KAP1 is phosphorylated by ATM[7], interrupting its interaction with CHD3 and thus allowing chromatin to have a more open configuration[8]. Another proposed mechanism for chromatin relaxation is the release of HP1β from the sites of damage[9] that is contradictory to many studies showing HP1s' recruitment and active role in the repair process [10],[11],[12]. Furthermore, in *D. melanogaster*, chromatin expansion is necessary for DSB relocation to the periphery of the HC domain in order to be repaired by HR that will be finally accomplished at the nuclear pores[13, 14]. Chromatin expansion and DSB relocation to the periphery of HC was also observed for mouse cells after α-particle induced DNA damage[15]. On the other hand, it was reported that in DSBs induced at the heterochromatin associated with the nuclear lamina, DDR activation is delayed and HR is defective and the DNA lesions do not migrate to a more permissive environment for their repair but instead they are immobile and are repaired by alt-NHEJ pathway[16]. These studies have set the basis for understanding how DNA repair proceeds in chromatin dense regions, proposing that different organisms with distinct heterochromatic structures have developed different mechanisms to repair heterochromatic DSBs (reviewed in detail in [17, 18]).

Cas9-induced DSBs in pericentric heterochromatin and their cell-cycle regulated localization

In our recently published work, we took advantage of the CRISPR/Cas9 system[19] to target and induce DSBs specifically in different heterochromatic structures of mammalian cells and study their repair[20]. More specifically, we designed a gRNA targeting major satellite repeats of pericentric heterochromatin, which in mouse cells corresponds to the DAPI-dense regions known as chromocenters[20]. Using high-resolution imaging and 3D reconstruction, we firstly showed that these DSBs are homogenously distributed in the structure of chromocenters and they can also activate DDR pathway very efficiently[20]. Although, these Cas9-induced DSBs were induced within the HC domain as revealed by γ-H2AX and 53BP1 staining, their localization was then changed depending of the cell-cycle phase; in G1, breaks are positionally stable through time in contrast to G2 where they re-locate to the HC periphery in order to be repaired[20]. In order to investigate in more detail the differential localization of HC DSBs, we also blocked cells in G1/S and released them to enter S and G2. In G1/S, breaks were stably in the HC core in contrast to S and G2 where they were peripheral. Although this peripheral localization of heterochromatic DSBs has also been reported in other studies[13, 15, 21-23], these data reveal for the first time the cell-cycle regulation for the break localization in HC, adding another key regulatory factor in HC DNA repair of mammalian cells.

Heterochromatic Cas9-induced DSBs and repair pathway choice

Then, we studied the activation of the two main DSB repair pathways (HR and NHEJ) and their correlation with the localization of the breaks. To do this, we assessed the recruitment of specific NHEJ (Ku80) and HR (RPA and RAD51) factors in correlation with γ-H2AX or 53BP1 pattern as indicative for the break localization. We found that in G1, both DDR and NHEJ (but not HR) are activated within the HC core domain, exemplified by the recruitment of Ku80 and several DDR markers. In G2, however, both NHEJ and HR are activated. Although the majority of DSBs (70%) in G2 move to the periphery to be repaired, there are still some that are positionally stable and they are repaired within the HC core by NHEJ. On the other hand, the breaks that move to the periphery are repaired by HR. While RPA recruitment is observed at the core HC domain, RAD51 is entirely peripheral leading to the spatial restriction of HR to the HC periphery. This indicates that DNA-end resection and the search for homology are spatially separated and suggests that resected DNA ends relocate to the HC periphery to perform the late steps of HR.

Apart from the correlation of DSBs in HC with the two main repair pathways NHEJ and HR, we also revealed that SSA can be also activated within this compacted structure. As mentioned above, the majority of DSBs in G2 relocate to the periphery to be repaired by HR. The rest of them (30%) remains in the HC core as revealed by γ-H2AX staining. RAD52, a major factor for SSA, is recruited to these breaks, suggesting that although the majority of lesions relocate to the periphery, resected breaks that fail to relocate recruit RAD52 and can be repaired by SSA that is a highly mutagenic pathway. To conclude, HC

breaks will primarily be repaired by HR moving to the HC periphery, but they can also activate NHEJ in the core of the structure. In case resection has happened but they fail to relocate, SSA can also be activated within HC. The activation of these three repair pathways by heterochromatic DSBs was also recently shown in *D. melanogaster*[21] in contrast to previous studies regarding exclusively HR as the repair pathway chosen for HC breaks in this organism[13, 14].

Role of resection and RAD51 in peripheral localization of heterochromatic DSBs

The spatial restriction of HR seems to be a conserved mechanism among species to avoid recombination of repetitive sequences that would threaten their genome integrity and cell viability. As it was previously mentioned, in *D. melanogaster*, DSBs move to the periphery and ultimately relocate to the pores to accomplish HR[13, 14]. Similar results obtained for the damaged repetitive ribosomal locus that delocalizes outside of the nucleolus domain to be repaired by HR in yeast and in human cells[22-24]. Both in *D. melanogaster* and in yeast, resection is the driving force of DSB relocation to the HC periphery[13, 20], something that we also confirmed with our experiments. On the other hand, contrary to what was shown in *D. melanogaster*, the checkpoint kinase ATR does not play a role in the relocation of the breaks. This was also the case for ATM kinase, as it has been shown again for mouse cells[15]. Thus, with our experiments, we confirmed the key role of resection for the relocation of the breaks in mammalian cells but we also showed that this is an ATM and ATR independent process.

Apart from resection as a first step of this mechanism, we also revealed RAD51's role in retention of the breaks at the HC periphery. Upon BRCA2 depletion, RAD51 loading to DSBs was dramatically impaired and these breaks were stabilized at the core of the HC domain in G2. This suggests that though resected breaks have the potential to relocate, they are not engaged at the HC periphery in the absence of RAD51. We strengthened this idea by forcing the recruitment of RAD51 in the core of chromocenters through Cas9 fusion to BRC3 domain (responsible for BRCA2 interaction with RAD51) or RAD51 itself. In both cases, tethering of RAD51 within chromocenters blocked DSB relocalization to the periphery of the structure. These data support a two-step mechanism of DSB relocalization in mammalian cells, the first being resection as the driving force and the second the retention of the breaks at the periphery by the RAD51/BRCA2 complex.

RAD51 is excluded from pericentric heterochromatin

The spatial restriction of HR is a result of the active exclusion of RAD51 from the core HC domain[13, 20, 22, 23]. It has been shown that chromatin compaction blocks RAD51 entrance in HC in *D.melanogaster* through a mechanism that involves HP1a; HP1a interacts with SMC5/6 complex that consequently blocks RAD51 entrance in HC through a SUMO-regulated pathway[14, 25]. The involvement of sumoylation and SMC5/6 complex in this process was also shown in yeast[22]. In contrast to the above data, we showed that chromatin compaction and SMC5/6 complex are not involved in RAD51's exclusion from HC in mammalian cells[20]. More specifically, we assessed RAD51's localization after

induction of chromatin relaxation through three different ways: 1. Treatment with the histone deacetylase inhibitor Trichostatin A (TSA) that induces robust chromatin relaxation and loss of HP1s from heterochromatin. 2. Tethering of the transcriptional activator VP64 specifically to pericentric heterochromatin through its fusion to Cas9. 3. Individual and simultaneous knockdown of HP1α, HP1β and HP1γ as well as individual knockdown of KAP1[20]. RAD51 peripheral localization did not change under any of the above conditions. More interestingly, RAD51 recruitment was significantly decreased upon simultaneous knockdown of HP1s, further supporting the existing data for HP1α's role in HR[10]. Similar decrease in RAD51 levels was observed upon KAP1 depletion, suggesting an active role of KAP1 in HR as it has been recently proposed in lymphocytes after damage induction[26]. Moreover, individual or simultaneous knockdown of Smc5 and 6 did not change RAD51 peripheral recruitment[20]. We conclude that chromatin compaction and SMC5/6 complex are not involved in RAD51's exclusion from HC in mammalian cells.

Cas9-induced DSBs trigger chromatin expansion independently of the release of HP1s or H3K9me3

As previously mentioned, chromatin expansion is a major step for DSB relocation to the periphery of HC in *D. melanogaster*[13]. Moreover, chromatin is undergoing through different changes in response to DNA damage in order to facilitate repair[27, 28]. In order to study the chromatin changes at chromocenters after Cas9-induced DSBs, we measured

the intensities of HP1 proteins, KAP1, H3K9me3 as well as the area of chromocenters defined as the DAPI-dense regions. Our results showed that chromatin expansion happens both in G1 and G2 after damage induction, as it has been previously reported[13, 15]. This expansion was not accompanied by the loss of any heterochromatin marker. More specifically, H3K9m3 was increased both in G1 and G2 that is in agreement with data showing increase of H3K9me3 at a single locus after damage induction[29]. Furthermore, HP1s and KAP1 levels were significantly increased after damage induction in G2, supporting the hypothesis emerging from previously mentioned data that they might have an active role in the HR repair process. These results also agree with many studies showing recruitment of HP1s after damage[10,11,12].

Cas9-induced DSBs and repair pathway choice in centromeric heterochromatin

To investigate whether the above results are specific to pericentric HC, we also used the CRISPR/Cas9 system to induce DSBs in centromeric HC of mouse cells. In this case, we designed a gRNA against centromeric minor satellite repeats and we induced specifically DSBs in centromeres. We showed that Ku80 is recruited in the same way as in pericentric heterochromatin. In contrast to DSBs induced in pericentric heterochromatin, we showed that RAD51 is efficiently recruited at centromeric lesions both in G1 and G2, suggesting that unlike in pericentric HC, HR is active throughout the cell cycle. On the other hand, similarly to what we showed for pericentromeric lesions, RAD51 localization is peripheral in accordance with γ-H2AX peripheral pattern. Although these two structures are highly condensed as typical examples of constitutive heterochromatin, they are

characterized by different DNA sequence, chromatin modifications and histone variant composition. More specifically, pericentric heterochromatin is enriched in H3K9me3, H4K20me2/3 and HP1s that are considered the key markers of constitutive heterochromatin[4]. On the other hand, nucleosomes of centromeres are enriched in CENP-A, an H3 histone variant (specific for centromeres) as well as in H3K36me2 and H3K4me2 that represent a more active chromatin environment[30]. These features could have an impact on the DNA repair outcome. It has been shown that H3K36me3 promote resection by recruiting CtIP through LEDGF, a chromatin binding protein that binds H3K36me3[31]. The presence of this modification in centromeres might create a permissive environment for resection and thus HR. On the other hand, centromeres do not have H4K20me2/3 that exists in pericentromeric HC. Since this modification is recognized by 53BP1 that favors NHEJ[32, 33], its lack maybe leads to decrease 53BP1 accumulation at the sites of breaks and thus HR is favored in these structures. Another scenario could involve the deubiquitylase USP11 that promotes interaction of BRCA1 and PALB2/BRCA2 in G2[34]. Though it has been shown that USP11 is degraded in G1 and thus the BRCA1-PALB2 interaction is blocked[34], it might be protected from degradation specifically at centromeres allowing HR to happen.

Concluding remarks

In our study, we have developed a CRISPR/Cas9 experimental system with unprecedented specificity and robustness to study DSB repair in the context of heterochromatin. We showed that DNA repair pathways activated in pericentric

heterochromatin are linked to cell cycle progression and are temporally and spatially regulated. In G1 DSBs are positionally stable and are repaired by NHEJ, while in S/G2 DSBs are mobile and relocate to the periphery of heterochromatin to be repaired by HR. In case they fail to relocate, they can also be repaired in the HC core by SSA. Moreover, contrary to what was believed before, we found that compacted chromatin is not refractory to DNA repair and that DSB relocation is dependent on DNA end-resection and RAD51 exclusion from the core domain. Interestingly, we also revealed fundamental differences between DSB repair in centromeric and pericentromeric heterochromatin, suggesting that different chromatin environment and not only the compaction level can affect the DNA repair outcome.

References

1. Jackson SP, Bartek J. The DNA-damage response in human biology and disease. Nature 2009; 461:1071-8.
2. Chapman JR, Taylor MR, Boulton SJ. Playing the end game: DNA double-strand break repair pathway choice. Molecular cell 2012; 47:497-510.
3. Ciccia A, Elledge SJ. The DNA damage response: making it safe to play with knives. Molecular cell 2010; 40:179-204.
4. Maison C, Almouzni G. HP1 and the dynamics of heterochromatin maintenance. Nature reviews Molecular cell biology 2004; 5:296-304.
5. Goodarzi AA, Noon AT, Deckbar D, Ziv Y, Shiloh Y, Lobrich M, et al. ATM signaling facilitates repair of DNA double-strand breaks associated with heterochromatin. Molecular cell 2008; 31:167-77.
6. Noon AT, Shibata A, Rief N, Lobrich M, Stewart GS, Jeggo PA, et al. 53BP1-dependent robust localized KAP-1 phosphorylation is essential for heterochromatic DNA double-strand break repair. Nature cell biology 2010; 12:177-84.
7. Ziv Y, Bielopolski D, Galanty Y, Lukas C, Taya Y, Schultz DC, et al. Chromatin relaxation in response to DNA double-strand breaks is modulated by a novel ATM- and KAP-1 dependent pathway. Nature cell biology 2006; 8:870-6.
8. Goodarzi AA, Kurka T, Jeggo PA. KAP-1 phosphorylation regulates CHD3 nucleosome remodeling during the DNA double-strand break response. Nature structural & molecular biology 2011; 18:831-9.
9. Ayoub N, Jeyasekharan AD, Bernal JA, Venkitaraman AR. HP1-beta mobilization promotes chromatin changes that initiate the DNA damage response. Nature 2008; 453:682-6.

10. Baldeyron C, Soria G, Roche D, Cook AJ, Almouzni G. HP1alpha recruitment to DNA damage by p150CAF-1 promotes homologous recombination repair. The Journal of cell biology 2011; 193:81-95.
11. Luijsterburg MS, Dinant C, Lans H, Stap J, Wiernasz E, Lagerwerf S, et al. Heterochromatin protein 1 is recruited to various types of DNA damage. The Journal of cell biology 2009; 185:577-86.
12. Zarebski M, Wiernasz E, Dobrucki JW. Recruitment of heterochromatin protein 1 to DNA repair sites. Cytometry Part A : the journal of the International Society for Analytical Cytology 2009; 75:619-25.
13. Chiolo I, Minoda A, Colmenares SU, Polyzos A, Costes SV, Karpen GH. Double-strand breaks in heterochromatin move outside of a dynamic HP1a domain to complete recombinational repair. Cell 2011; 144:732-44.
14. Ryu T, Spatola B, Delabaere L, Bowlin K, Hopp H, Kunitake R, et al. Heterochromatic breaks move to the nuclear periphery to continue recombinational repair. Nature cell biology 2015; 17:1401-11.
15. Jakob B, Splinter J, Conrad S, Voss KO, Zink D, Durante M, et al. DNA double-strand breaks in heterochromatin elicit fast repair protein recruitment, histone H2AX phosphorylation and relocation to euchromatin. Nucleic acids research 2011; 39:6489-99.
16. Lemaitre C, Grabarz A, Tsouroula K, Andronov L, Furst A, Pankotai T, et al. Nuclear position dictates DNA repair pathway choice. Genes & development 2014.
17. Goodarzi AA, Jeggo PA. The heterochromatic barrier to DNA double strand break repair: how to get the entry visa. International journal of molecular sciences 2012; 13:11844-60.
18. Lemaitre C, Soutoglou E. Double strand break (DSB) repair in heterochromatin and heterochromatin proteins in DSB repair. DNA repair 2014; 19:163-8.
19. Cong L, Ran FA, Cox D, Lin S, Barretto R, Habib N, et al. Multiplex genome engineering using CRISPR/Cas systems. Science 2013; 339:819-23.
20. Tsouroula K, Furst A, Rogier M, Heyer V, Maglott-Roth A, Ferrand A, et al. Temporal and Spatial Uncoupling of DNA Double Strand Break Repair Pathways within Mammalian Heterochromatin. Molecular cell 2016; 63:293-305.
21. Janssen A, Breuer GA, Brinkman EK, van der Meulen AI, Borden SV, van Steensel B, et al. A single double-strand break system reveals repair dynamics and mechanisms in heterochromatin and euchromatin. Genes & development 2016; 30:1645-57.
22. Torres-Rosell J, Sunjevaric I, De Piccoli G, Sacher M, Eckert-Boulet N, Reid R, et al. The Smc5-Smc6 complex and SUMO modification of Rad52 regulates recombinational repair at the ribosomal gene locus. Nature cell biology 2007; 9:923-31.
23. Warmerdam DO, van den Berg J, Medema RH. Breaks in the 45S rDNA Lead to Recombination-Mediated Loss of Repeats. Cell Rep 2016; 14:2519-27.
24. van Sluis M, McStay B. A localized nucleolar DNA damage response facilitates recruitment of the homology-directed repair machinery independent of cell cycle stage. Genes & development 2015; 29:1151-63.
25. Ryu T, Bonner MR, Chiolo I. Cervantes and Quijote protect heterochromatin from aberrant recombination and lead the way to the nuclear periphery. Nucleus 2016; 7:485-97.
26. Tubbs AT, Dorsett Y, Chan E, Helmink B, Lee BS, Hung P, et al. KAP-1 promotes resection of broken DNA ends not protected by gamma-H2AX and 53BP1 in G(1)-phase lymphocytes. Molecular and cellular biology 2014; 34:2811-21.
27. Misteli T, Soutoglou E. The emerging role of nuclear architecture in DNA repair and genome maintenance. Nature reviews Molecular cell biology 2009; 10:243-54.
28. Price BD, D'Andrea AD. Chromatin remodeling at DNA double-strand breaks. Cell 2013; 152:1344-54.
29. Ayrapetov MK, Gursoy-Yuzugullu O, Xu C, Xu Y, Price BD. DNA double-strand breaks promote methylation of histone H3 on lysine 9 and transient formation of repressive chromatin. Proceedings of the National Academy of Sciences of the United States of America 2014; 111:9169-74.

30. Chan FL, Wong LH. Transcription in the maintenance of centromere chromatin identity. Nucleic acids research 2012; 40:11178-88.
31. Aymard F, Bugler B, Schmidt CK, Guillou E, Caron P, Briois S, et al. Transcriptionally active chromatin recruits homologous recombination at DNA double-strand breaks. Nature structural & molecular biology 2014; 21:366-74.
32. Hsiao KY, Mizzen CA. Histone H4 deacetylation facilitates 53BP1 DNA damage signaling and double-strand break repair. Journal of molecular cell biology 2013; 5:157-65.
33. Daley JM, Sung P. 53BP1, BRCA1, and the choice between recombination and end joining at DNA double-strand breaks. Molecular and cellular biology 2014; 34:1380-8.
34. Orthwein A, Noordermeer SM, Wilson MD, Landry S, Enchev RI, Sherker A, et al. A mechanism for the suppression of homologous recombination in G1 cells. Nature 2015; 528:422-6.

5. Perspectives

5.1 Double Strand Break Repair pathways in centromeres versus pericentromeres

As mentioned above, following our published data, one of our main questions is to understand why HR is activated in G1 after Cas9-induced DSBs in centromeres but not in pericentromeres. In order to address this question, we are firstly interested in the differential recruitment of various HR factors that could potentially explain the differential activation of HR between these two structures. Apart from our published data regarding RAD51 and RPA recruitment at centromeric lesions in G1, we are currently interested in testing the recruitment of different key resection factors. Due to lack of specific antibodies that work in mouse cells, we are currently constructing vectors expressing different proteins involved in resection such as Mre11, CtIP, EXO1, DNA2, BLM and EXD2 fused to EGFP in order to test their recruitment after co-expression with Cas9 and the gRNA against major or minor satellite repeats. Moreover, we are currently performing immunofluorescence experiments regarding RAD51 and RPA recruitment under knockdown conditions of these resection factors. Combined results from these experiments will reveal the precise activation of each step of HR, being potentially involved in the promotion of this pathway in G1 in centromeres.

Regarding the chromatin aspect, since we observed a positive role of CENP-A and its chaperone HJURP in HR, we would like to further investigate their role in this process. In order to do this, we will induce DSBs in centromeres both in G1 and G2 phases of cell cycle, under *CENP-A* and *HJURP* knockdown conditions and we will observe the recruitment of RAD51 and RPA by immunofluorescence experiments. Since CENP-A is incorporated in the centromeric sequence in G1 but is diluted after S phase with H3.3 incorporation (Muller and Almouzni, 2017), it would be interesting to observe if this difference in the amount of CENP-A will impact on HR in G2 similarly to G1. Moreover, since CENP-A incorporation happens exclusively in G1, knockdown of its chaperone HJURP should not affect HR in G2 except if this protein has an additional role in this process at this phase of cell cycle. This role could be uncoupled of its function as a chaperone or it could involve *de novo* incorporation of CENPA in G2. In order to test this hypothesis, we will use the SNAP-tag technology (described in (Adam et al., 2013)) to observe the potential further incorporation of CENP-A at the sites of centromeric damage. Moreover, as previously described, the different histone modifications of centromeres might affect the outcome of the repair. In order to address the role of each modification in this process, we will fuse Cas9 with the corresponding enzymes working as “writers” or “erasers” for these modifications. This will allow us to target them

specifically to centromeres where Cas9 will induce DSBs, revealing their potential role in HR in G1.

Furthermore, we will investigate the potential involvement of USP11 in HR in G1 at centromeres. Though it has been shown that USP11 is degraded in G1 after damage induction (Orthwein et al., 2015), it might be protected from degradation specifically at centromeres promoting the BRCA1-PALB2 interaction and thus repair by HR. To test this hypothesis, we firstly wanted to address its localization in the mouse nucleus using immunofluorescence experiments. Since the USP11 antibody we used is not working in mouse cells, we are currently constructing a vector expressing USP11 fused to EGFP to detect its potential recruitment at centromeres after damage induction. Additionally, we will perform immunoprecipitation experiments using a specific antibody for CENP-A or EGFP (for USP11-EGFP) to investigate the potential interaction between these two proteins before and after DSBs induction. In parallel, we will test the effect of *USP11* knockdown on HR by immunofluorescence experiments to detect RAD51 and RPA recruitment at centromeric lesions in G1.

Apart from testing the role of the above-mentioned individual factors, we have also performed proteomics analysis of DNA repair in these structures using the Bio-ID technology as described in the section of Results (3.2). Analysis of these experiments has revealed novel factors that are enriched at centromeres or pericentromeres after damage induction. Apart from the common factors between these two structures that might have a role in DDR activation, it would be interesting to investigate the role of the unique identified proteins for each structure in their repair. To do this, we will firstly assess their recruitment at the breaks using specific antibodies for immunofluorescence confocal analysis as well as test the effect of their depletion on RAD51 and RPA recruitment.

5.2 Exclusion of RAD51 from constitutive heterochromatin in mammalian cells

Our second goal is to gain insight into the mechanism that excludes RAD51 from heterochromatin in mammalian cells. To address this question, we will use the Bio-ID technology. More specifically we are currently constructing a vector expressing BirA* fused to RAD51. Since it has been observed that overexpression of RAD51 under strong promoters leads to RAD51 filament formation at the cytoplasm and thus renders RAD51 non-functional, we will use the TRE (Tetracycline Inducible Expression) promoter to express the BirA*-RAD51 fused protein. Based on our experience in the laboratory, although TRE is an inducible promoter, it is leaky leading to

very low expression of the locus that is under its control. It will be interesting to test if we will overcome the problem of RAD51 overexpression by using this low expression promoter. After DSBs induction, BirA*-RAD51 will be targeted to pericentric heterochromatin in G2 and will biotinylate proteins in proximity with it. These biotinylated proteins will be isolated using streptavidin-coupled beads and will then be submitted to identification by mass spectrometry. As an alternative strategy, we will also use the wild type BirA that biotinylates a specific small protein sequence (BioTag) in *E.coli*. Thus, we are currently constructing a vector that expresses separately the wild type BirA and RAD51 fused to this BioTag under the control of TRE promoter. In this case, BirA will specifically biotinylate the BioTag that is fused to RAD51. Thus, immunoprecipitation of the biotinylated BioTAg-RAD51 using streptavidin-coupled beads will allow for isolation of proteins that physically interact with it before and after damage induction. These proteins will be identified by mass spectrometry.

The above-mentioned vectors will be used for the ectopic expression of RAD51 in the cells. In order to perform our experiments under more physiological conditions, we are also engineering two differentially tagged RAD51 knock-in NIH3T3 cell lines using the CRISPR/Cas9 technology. In one cell line, a flag-EGFP tag will be introduced at the N-terminus of RAD51. After DSBs induction at chromocenters, we will isolate proteins that interact with RAD51 at the sites of breaks by immunoprecipitation using antibodies against flag and EGFP. As an alternative approach, we will also fuse RAD51 with BirA* which will biotinylate proteins in proximity to RAD51 that will be isolated as described above. After DSBs induction, proteins isolated from these different cell lines will then be submitted to identification by mass spectrometry. Mass spectrometry results from all the experiments will be compared, highlighting proteins or protein modifications as strong candidates for RAD51's exclusion from HC. These candidates will be subsequently validated with various experiments. Immunofluorescence experiments and confocal analysis will be used to test their specific recruitment at the sites of breaks, immunoprecipitation experiments to verify their interaction with RAD51 and knockdown experiments to check the effect on RAD51 localization. To conclude, these experiments will reveal the molecular mechanism through which RAD51 and thus HR is blocked at the HC core in mammalian cells.

6. Concluding remarks

In our study, we have developed a CRISPR/Cas9 experimental system with unprecedented specificity and robustness to study DSB repair in the context of constitutive heterochromatin. We showed that DNA repair pathways activated in pericentric heterochromatin are linked to cell cycle progression and are temporally and spatially regulated. In G1, DSBs are positionally stable and are repaired by NHEJ, while in S/G2 DSBs are mobile and relocate to the periphery of heterochromatin to be repaired by HR. DSB relocation is dependent on DNA end-resection and RAD51 exclusion from the core domain. In case they fail to relocate, they can also be repaired in the HC core by SSA. In contrast to previous studies in yeast and Drosophila, we showed that compacted chromatin is not refractory to DNA repair. Our current and future unbiased experiments using the Bio-ID technology will shed light on the distinct molecular mechanism that does not allow RAD51 to enter in constitutive heterochromatin of mammalian cells. Interestingly, we also revealed fundamental differences between DSB repair in centromeric and pericentromeric heterochromatin supported also by our unpublished data, suggesting that different chromatin environment and not only the compaction level can affect the DNA repair outcome. Our future experiments will reveal the exact molecular mechanism that controls the repair differences between these two heterochromatic structures.

7. Materials and methods

7.1 Materials

siRNAs used.*	
siRNA	**Reference**
scramble	D-001810-10
CENP-A	L-044345-00
HJURP	L-057537-00

* All siRNAs (ON-TARGETplus SMARTpool siRNAs) were purchased from Dharmacon.

Primers used.		
Target	**Forward primer**	**Reverse primer**
GAPDH	AACTTTGGCATTGTGGAAGG	ACACATTGGGGGTAGGAACA
HJURP	GCGGCTGATAGCGAAGTACAA	CCTTCTGGAGCTTGCCCATTTA

Antibodies used.		
Antibody	**Company (Reference)**	**Dilution (Use)***
γ-H2AX (H2AX S139)	Abcam (ab22551)	1:1000 (IF & WB)
53BP1	Novus Biologicals (100-304)	1:1000 (IF)
RAD51	Calbiochem (PC130)	1:50 (IF), 1:1000 (WB)
RPA32	Novus Biologicals (600-565)	1:250 (IF)
CENPA	Cell Signaling Technology (2048)	1:500 (IF & WB)
Streptavidin Alexa Fluor® 568 conjugate	ThermoFisher Scientific	1:1000 (IF)
α Tubulin	Sigma Aldrich (T5168)	1:5000 (WB)

* WB: Western Blot; IF: Immunofluorescence.

Plasmids used.*	
pR24	pTRE-BirA*-Cas9-EGFP-SV40-PuroR-pA
pR26	pTRE-BirA*-dCas9-EGFP-SV40-PuroR-pA
pG-56	U6p-gRNA (Ma-Sat#3)-gRNA Scaffold
pG-36	U6p-gRNA (Mi-Sat#2)-gRNA Scaffold

* NIH3T3 cells stably expressing pR24 or pR26 were generated by infection of cells with the corresponding vectors followed by puromycin selection for 10 days.

7.2 Methods

7.2.1 Nuclear Extraction and Streptavidin based affinity purification.

Cells are harvested and washed twice with ice cold PBS. After the Pellet Cell Volume (PCV) is defined, they are resuspended in 10xPCV ice cold HBSS buffer (340 mM sucrose, 15mM Tris pH. 7.5, 15mM NaCl, 60mM KCl, 10mM DTT, 0.15mM spermine, 0.5 mM spermidine, 0.5% Triton). After they are lysed for 5 min in ice with periodic mixing, they are centrifuged at 11000 rpm, for 5 min, at 4°C. The pellet formed after centrifugation is resuspended in 5xPCV ice cold HBSS buffer, incubated for 5 min and centrifuged again at 11000 rpm, for 5 min, at 4°C.

Nuclei are then lysed in 5xPCV ice cold RIPA buffer (50mM Tris pH 7.7, 1% NP40, 150 mM NaCl, 1mM EDTA, 1mM EGTA, 0.1% SDS, 0.5% sodium deoxycholate) for 20 min and centrifuged at 14000 rpm for 20 min at 4°C. The supernatant is incubated with streptavidin dynabeads (Invitrogen Dynabeads M-280 streptavidin, Reference 11205D) for 2h at 4°C. The beads are subsequently washed 2 times with RIPA buffer and 2 times with TAP buffer (10% glycerol, 50mM Hepes pH 8, 150 mM NaCl, 2mM EDTA, 0.1% NP40). Each wash is 10 min on rotation at 4°C. Biotinylated proteins are eluted in 2x NuPAGE LDS Sample Buffer (ThermoFisher Scinetific), at 75°C for 15 min.

7.2.2 Isolation of biotinylated proteins for mass spectrometry analysis.

NIH3T3 pR24 and pR26 cells were seeded in 10 cm plates (24 plates/condition). The next day, D-Biotin (Euromedex, Reference: UB1750-A) was added (50 mM) 5h before transfection with a plasmid expressing a gRNA against minor (pG-36) or major satellite repeats (pG-56) for 16h. Transient transfections were done with Lipofectamine 2000 (Invitrogen^{TM} Life Technologies) according to the manufacturer's instructions. Cells were harvested (~55x10^6 cells/condition) and nuclei were extracted as described in 7.2.1. Streptavidin based affinity purification was then used to isolate the biotinylated proteins. 1/10 of the volume of the eluted proteins was run in NuPAGE 10% Bis-Tris Protein Gels (ThermoFisher Scientific) and stained with Coomassie Brilliant Blue R-250 Dye (ThermoFisher Scientific).

Gel bands were reduced, alkylated and digested with trypsin at 37°C overnight. Extracted peptides were then analyzed using an Ultimate 3000 nano-RSLC (Thermo Scientific, San Jose California) coupled in line with an Orbitrap ELITE (Thermo Scientific, San Jose Califronia). Briefly, peptides were separated on a C18 nano-column with a linear gradient of acetonitrile and analyzed in a Top 20 CID (Collision-induced dissociation) data-dependent mass spectrometry. Data were processed by database searching using SequestHT (Thermo Fisher Scientific) with Proteome Discoverer 1.4 software (Thermo Fisher Scientific) against a mouse database. Precursor and fragment mass tolerance were set at 7 ppm and 0.5 Da respectively. Trypsin was set as enzyme, and up to 2 missed cleavages were allowed. Oxidation (M) and deamidation (N,Q) are set as variable modification, and carbamidomethylation (C) as fixed modification. Proteins were identified with a minimum of two unique peptides and filtered with Percolator and 1% False Discoverer Rate.

8. References

Adam, S., Polo, S.E., and Almouzni, G. (2013). Transcription recovery after DNA damage requires chromatin priming by the H3.3 histone chaperone HIRA. Cell *155*, 94-106.

Agmon, N., Liefshitz, B., Zimmer, C., Fabre, E., and Kupiec, M. (2013). Effect of nuclear architecture on the efficiency of double-strand break repair. Nature cell biology *15*, 694-699.

Aguilera, A., and Garcia-Muse, T. (2013). Causes of genome instability. Annual review of genetics *47*, 1-32.

Ahel, D., Horejsi, Z., Wiechens, N., Polo, S.E., Garcia-Wilson, E., Ahel, I., Flynn, H., Skehel, M., West, S.C., Jackson, S.P*., et al.* (2009). Poly(ADP-ribose)-dependent regulation of DNA repair by the chromatin remodeling enzyme ALC1. Science *325*, 1240-1243.

Ahnesorg, P., Smith, P., and Jackson, S.P. (2006). XLF interacts with the XRCC4-DNA ligase IV complex to promote DNA nonhomologous end-joining. Cell *124*, 301-313.

Ahrabi, S., Sarkar, S., Pfister, S.X., Pirovano, G., Higgins, G.S., Porter, A.C., and Humphrey, T.C. (2016). A role for human homologous recombination factors in suppressing microhomology-mediated end joining. Nucleic acids research *44*, 5743-5757.

Akopiants, K., Zhou, R.Z., Mohapatra, S., Valerie, K., Lees-Miller, S.P., Lee, K.J., Chen, D.J., Revy, P., de Villartay, J.P., and Povirk, L.F. (2009). Requirement for XLF/Cernunnos in alignment-based gap filling by DNA polymerases lambda and mu for nonhomologous end joining in human whole-cell extracts. Nucleic acids research *37*, 4055-4062.

Alani, E., Padmore, R., and Kleckner, N. (1990). Analysis of wild-type and rad50 mutants of yeast suggests an intimate relationship between meiotic chromosome synapsis and recombination. Cell *61*, 419-436.

Albig, W., Kioschis, P., Poustka, A., Meergans, K., and Doenecke, D. (1997). Human histone gene organization: nonregular arrangement within a large cluster. Genomics *40*, 314-322.

Alt, F.W., Zhang, Y., Meng, F.L., Guo, C., and Schwer, B. (2013). Mechanisms of programmed DNA lesions and genomic instability in the immune system. Cell *152*, 417-429.

Andres, S.N., Modesti, M., Tsai, C.J., Chu, G., and Junop, M.S. (2007). Crystal structure of human XLF: a twist in nonhomologous DNA end-joining. Molecular cell *28*, 1093-1101.

Andres, S.N., Vergnes, A., Ristic, D., Wyman, C., Modesti, M., and Junop, M. (2012). A human XRCC4-XLF complex bridges DNA. Nucleic acids research *40*, 1868-1878.

Aravind, L., and Koonin, E.V. (2001). Prokaryotic homologs of the eukaryotic DNA-end-binding protein Ku, novel domains in the Ku protein and prediction of a prokaryotic double-strand break repair system. Genome research *11*, 1365-1374.

Aten, J.A., Stap, J., Krawczyk, P.M., van Oven, C.H., Hoebe, R.A., Essers, J., and Kanaar, R. (2004). Dynamics of DNA double-strand breaks revealed by clustering of damaged chromosome domains. Science *303*, 92-95.

Atsumi, Y., Minakawa, Y., Ono, M., Dobashi, S., Shinohe, K., Shinohara, A., Takeda, S., Takagi, M., Takamatsu, N., Nakagama, H*., et al.* (2015). ATM and SIRT6/SNF2H Mediate Transient H2AX Stabilization When DSBs Form by Blocking HUWE1 to Allow Efficient gammaH2AX Foci Formation. Cell Rep *13*, 2728-2740.

Audebert, M., Salles, B., and Calsou, P. (2004). Involvement of poly(ADP-ribose) polymerase-1 and XRCC1/DNA ligase III in an alternative route for DNA double-strand breaks rejoining. The Journal of biological chemistry *279*, 55117-55126.

Aydin, O.Z., Vermeulen, W., and Lans, H. (2014). ISWI chromatin remodeling complexes in the DNA damage response. Cell cycle *13*, 3016-3025.

Aymard, F., Aguirrebengoa, M., Guillou, E., Javierre, B.M., Bugler, B., Arnould, C., Rocher, V., Iacovoni, J.S., Biernacka, A., Skrzypczak, M*., et al.* (2017). Genome-wide mapping of long-range contacts unveils

clustering of DNA double-strand breaks at damaged active genes. Nature structural & molecular biology.

Aymard, F., Bugler, B., Schmidt, C.K., Guillou, E., Caron, P., Briois, S., Iacovoni, J.S., Daburon, V., Miller, K.M., Jackson, S.P*., et al.* (2014). Transcriptionally active chromatin recruits homologous recombination at DNA double-strand breaks. Nature structural & molecular biology *21*, 366-374.

Ayoub, N., Jeyasekharan, A.D., Bernal, J.A., and Venkitaraman, A.R. (2008). HP1-beta mobilization promotes chromatin changes that initiate the DNA damage response. Nature *453*, 682-686.

Ayrapetov, M.K., Gursoy-Yuzugullu, O., Xu, C., Xu, Y., and Price, B.D. (2014). DNA double-strand breaks promote methylation of histone H3 on lysine 9 and transient formation of repressive chromatin. Proceedings of the National Academy of Sciences of the United States of America *111*, 9169-9174.

Badie, S., Carlos, A.R., Folio, C., Okamoto, K., Bouwman, P., Jonkers, J., and Tarsounas, M. (2015). BRCA1 and CtIP promote alternative non-homologous end-joining at uncapped telomeres. The EMBO journal *34*, 828.

Bakkenist, C.J., and Kastan, M.B. (2003). DNA damage activates ATM through intermolecular autophosphorylation and dimer dissociation. Nature *421*, 499-506.

Bakr, A., Oing, C., Kocher, S., Borgmann, K., Dornreiter, I., Petersen, C., Dikomey, E., and Mansour, W.Y. (2015). Involvement of ATM in homologous recombination after end resection and RAD51 nucleofilament formation. Nucleic acids research *43*, 3154-3166.

Baldeyron, C., Soria, G., Roche, D., Cook, A.J., and Almouzni, G. (2011). HP1alpha recruitment to DNA damage by p150CAF-1 promotes homologous recombination repair. The Journal of cell biology *193*, 81-95.

Bannister, A.J., and Kouzarides, T. (2011). Regulation of chromatin by histone modifications. Cell Res *21*, 381-395.

Bannister, A.J., Zegerman, P., Partridge, J.F., Miska, E.A., Thomas, J.O., Allshire, R.C., and Kouzarides, T. (2001). Selective recognition of methylated lysine 9 on histone H3 by the HP1 chromo domain. Nature *410*, 120-124.

Bantele, S.C., Ferreira, P., Gritenaite, D., Boos, D., and Pfander, B. (2017). Targeting of the Fun30 nucleosome remodeller by the Dpb11 scaffold facilitates cell cycle-regulated DNA end resection. Elife *6*.

Barnes, D.E., Stamp, G., Rosewell, I., Denzel, A., and Lindahl, T. (1998). Targeted disruption of the gene encoding DNA ligase IV leads to lethality in embryonic mice. Current biology : CB *8*, 1395-1398.

Barski, A., Cuddapah, S., Cui, K., Roh, T.Y., Schones, D.E., Wang, Z., Wei, G., Chepelev, I., and Zhao, K. (2007). High-resolution profiling of histone methylations in the human genome. Cell *129*, 823-837.

Bartek, J., and Lukas, J. (2003). Chk1 and Chk2 kinases in checkpoint control and cancer. Cancer cell *3*, 421-429.

Bass, T.E., Luzwick, J.W., Kavanaugh, G., Carroll, C., Dungrawala, H., Glick, G.G., Feldkamp, M.D., Putney, R., Chazin, W.J., and Cortez, D. (2016). ETAA1 acts at stalled replication forks to maintain genome integrity. Nature cell biology *18*, 1185-1195.

Baudat, F., Imai, Y., and de Massy, B. (2013). Meiotic recombination in mammals: localization and regulation. Nat Rev Genet *14*, 794-806.

Beck, C., Boehler, C., Guirouilh Barbat, J., Bonnet, M.E., Illuzzi, G., Ronde, P., Gauthier, L.R., Magroun, N., Rajendran, A., Lopez, B.S*., et al.* (2014a). PARP3 affects the relative contribution of homologous recombination and nonhomologous end-joining pathways. Nucleic acids research *42*, 5616-5632.

Beck, C., Robert, I., Reina-San-Martin, B., Schreiber, V., and Dantzer, F. (2014b). Poly(ADP-ribose) polymerases in double-strand break repair: Focus on PARP1, PARP2 and PARP3. Experimental cell research.

Beck, M., and Hurt, E. (2017). The nuclear pore complex: understanding its function through structural insight. Nature reviews Molecular cell biology *18*, 73-89.

Becker, A., Durante, M., Taucher-Scholz, G., and Jakob, B. (2014). ATM alters the otherwise robust chromatin mobility at sites of DNA double-strand breaks (DSBs) in human cells. PloS one *9*, e92640.

Bekker-Jensen, S., and Mailand, N. (2010). Assembly and function of DNA double-strand break repair foci in mammalian cells. DNA repair *9*, 1219-1228.

Bekker-Jensen, S., Rendtlew Danielsen, J., Fugger, K., Gromova, I., Nerstedt, A., Lukas, C., Bartek, J., Lukas, J., and Mailand, N. (2010). HERC2 coordinates ubiquitin-dependent assembly of DNA repair factors on damaged chromosomes. Nature cell biology *12*, 80-86; sup pp 81-12.

Bennardo, N., Cheng, A., Huang, N., and Stark, J.M. (2008). Alternative-NHEJ is a mechanistically distinct pathway of mammalian chromosome break repair. PLoS genetics *4*, e1000110.

Bennett, G., Papamichos-Chronakis, M., and Peterson, C.L. (2013). DNA repair choice defines a common pathway for recruitment of chromatin regulators. Nature communications *4*, 2084.

Bennett, G., and Peterson, C.L. (2015). SWI/SNF recruitment to a DNA double-strand break by the NuA4 and Gcn5 histone acetyltransferases. DNA repair *30*, 38-45.

Bentley, J., Diggle, C.P., Harnden, P., Knowles, M.A., and Kiltie, A.E. (2004). DNA double strand break repair in human bladder cancer is error prone and involves microhomology-associated end-joining. Nucleic acids research *32*, 5249-5259.

Bentley, J., L'Hote, C., Platt, F., Hurst, C.D., Lowery, J., Taylor, C., Sak, S.C., Harnden, P., Knowles, M.A., and Kiltie, A.E. (2009). Papillary and muscle invasive bladder tumors with distinct genomic stability profiles have different DNA repair fidelity and KU DNA-binding activities. Genes Chromosomes Cancer *48*, 310-321.

Bhargava, R., Onyango, D.O., and Stark, J.M. (2016). Regulation of Single-Strand Annealing and its Role in Genome Maintenance. Trends Genet *32*, 566-575.

Bhaskara, V., Dupre, A., Lengsfeld, B., Hopkins, B.B., Chan, A., Lee, J.H., Zhang, X., Gautier, J., Zakian, V., and Paull, T.T. (2007). Rad50 adenylate kinase activity regulates DNA tethering by Mre11/Rad50 complexes. Molecular cell *25*, 647-661.

Bickmore, W.A., and van Steensel, B. (2013). Genome architecture: domain organization of interphase chromosomes. Cell *152*, 1270-1284.

Biehs, R., Steinlage, M., Barton, O., Juhasz, S., Kunzel, J., Spies, J., Shibata, A., Jeggo, P.A., and Lobrich, M. (2017). DNA Double-Strand Break Resection Occurs during Non-homologous End Joining in G1 but Is Distinct from Resection during Homologous Recombination. Molecular cell *65*, 671-684 e675.

Bird, A.W., Yu, D.Y., Pray-Grant, M.G., Qiu, Q., Harmon, K.E., Megee, P.C., Grant, P.A., Smith, M.M., and Christman, M.F. (2002). Acetylation of histone H4 by Esa1 is required for DNA double-strand break repair. Nature *419*, 411-415.

Bishop, D.K., Ear, U., Bhattacharyya, A., Calderone, C., Beckett, M., Weichselbaum, R.R., and Shinohara, A. (1998). Xrcc3 is required for assembly of Rad51 complexes in vivo. The Journal of biological chemistry *273*, 21482-21488.

Block, W.D., Yu, Y., and Lees-Miller, S.P. (2004). Phosphatidyl inositol 3-kinase-like serine/threonine protein kinases (PIKKs) are required for DNA damage-induced phosphorylation of the 32 kDa subunit of replication protein A at threonine 21. Nucleic acids research *32*, 997-1005.

Boboila, C., Jankovic, M., Yan, C.T., Wang, J.H., Wesemann, D.R., Zhang, T., Fazeli, A., Feldman, L., Nussenzweig, A., Nussenzweig, M*., et al.* (2010). Alternative end-joining catalyzes robust IgH locus deletions and translocations in the combined absence of ligase 4 and Ku70. Proceedings of the National Academy of Sciences of the United States of America *107*, 3034-3039.

Boboila, C., Oksenych, V., Gostissa, M., Wang, J.H., Zha, S., Zhang, Y., Chai, H., Lee, C.S., Jankovic, M., Saez, L.M*., et al.* (2012). Robust chromosomal DNA repair via alternative end-joining in the absence of X-ray repair cross-complementing protein 1 (XRCC1). Proceedings of the National Academy of Sciences of the United States of America *109*, 2473-2478.

Boehler, C., Gauthier, L.R., Mortusewicz, O., Biard, D.S., Saliou, J.M., Bresson, A., Sanglier-Cianferani, S., Smith, S., Schreiber, V., Boussin, F.*, et al.* (2011). Poly(ADP-ribose) polymerase 3 (PARP3), a newcomer in cellular response to DNA damage and mitotic progression. Proceedings of the National Academy of Sciences of the United States of America *108*, 2783-2788.

Bonev, B., and Cavalli, G. (2016). Organization and function of the 3D genome. Nat Rev Genet *17*, 661-678.

Bothmer, A., Robbiani, D.F., Di Virgilio, M., Bunting, S.F., Klein, I.A., Feldhahn, N., Barlow, J., Chen, H.T., Bosque, D., Callen, E.*, et al.* (2011). Regulation of DNA end joining, resection, and immunoglobulin class switch recombination by 53BP1. Molecular cell *42*, 319-329.

Bothmer, A., Robbiani, D.F., Feldhahn, N., Gazumyan, A., Nussenzweig, A., and Nussenzweig, M.C. (2010). 53BP1 regulates DNA resection and the choice between classical and alternative end joining during class switch recombination. J Exp Med *207*, 855-865.

Botuyan, M.V., Lee, J., Ward, I.M., Kim, J.E., Thompson, J.R., Chen, J., and Mer, G. (2006). Structural basis for the methylation state-specific recognition of histone H4-K20 by 53BP1 and Crb2 in DNA repair. Cell *127*, 1361-1373.

Boulton, S., Kyle, S., and Durkacz, B.W. (1999). Interactive effects of inhibitors of poly(ADP-ribose) polymerase and DNA-dependent protein kinase on cellular responses to DNA damage. Carcinogenesis *20*, 199-203.

Boulton, S.J., and Jackson, S.P. (1996). Saccharomyces cerevisiae Ku70 potentiates illegitimate DNA double-strand break repair and serves as a barrier to error-prone DNA repair pathways. The EMBO journal *15*, 5093-5103.

Bouwman, P., Aly, A., Escandell, J.M., Pieterse, M., Bartkova, J., van der Gulden, H., Hiddingh, S., Thanasoula, M., Kulkarni, A., Yang, Q.*, et al.* (2010). 53BP1 loss rescues BRCA1 deficiency and is associated with triple-negative and BRCA-mutated breast cancers. Nature structural & molecular biology *17*, 688-695.

Broderick, R., Nieminuszczy, J., Baddock, H.T., Deshpande, R.A., Gileadi, O., Paull, T.T., McHugh, P.J., and Niedzwiedz, W. (2016). EXD2 promotes homologous recombination by facilitating DNA end resection. Nature cell biology *18*, 271-280.

Brouwer, I., Sitters, G., Candelli, A., Heerema, S.J., Heller, I., de Melo, A.J., Zhang, H., Normanno, D., Modesti, M., Peterman, E.J.*, et al.* (2016). Sliding sleeves of XRCC4-XLF bridge DNA and connect fragments of broken DNA. Nature *535*, 566-569.

Brown, J.S., Lukashchuk, N., Sczaniecka-Clift, M., Britton, S., le Sage, C., Calsou, P., Beli, P., Galanty, Y., and Jackson, S.P. (2015). Neddylation promotes ubiquitylation and release of Ku from DNA-damage sites. Cell Rep *11*, 704-714.

Bryant, H.E., Petermann, E., Schultz, N., Jemth, A.S., Loseva, O., Issaeva, N., Johansson, F., Fernandez, S., McGlynn, P., and Helleday, T. (2009). PARP is activated at stalled forks to mediate Mre11-dependent replication restart and recombination. The EMBO journal *28*, 2601-2615.

Buck, D., Malivert, L., de Chasseval, R., Barraud, A., Fondaneche, M.C., Sanal, O., Plebani, A., Stephan, J.L., Hufnagel, M., le Deist, F.*, et al.* (2006). Cernunnos, a novel nonhomologous end-joining factor, is mutated in human immunodeficiency with microcephaly. Cell *124*, 287-299.

Bunting, S.F., Callen, E., Kozak, M.L., Kim, J.M., Wong, N., Lopez-Contreras, A.J., Ludwig, T., Baer, R., Faryabi, R.B., Malhowski, A.*, et al.* (2012). BRCA1 functions independently of homologous recombination in DNA interstrand crosslink repair. Molecular cell *46*, 125-135.

Bunting, S.F., Callen, E., Wong, N., Chen, H.T., Polato, F., Gunn, A., Bothmer, A., Feldhahn, N., Fernandez-Capetillo, O., Cao, L.*, et al.* (2010). 53BP1 inhibits homologous recombination in Brca1-deficient cells by blocking resection of DNA breaks. Cell *141*, 243-254.

Buschbeck, M., and Hake, S.B. (2017). Variants of core histones and their roles in cell fate decisions, development and cancer. Nature reviews Molecular cell biology.

Callen, E., Di Virgilio, M., Kruhlak, M.J., Nieto-Soler, M., Wong, N., Chen, H.T., Faryabi, R.B., Polato, F., Santos, M., Starnes, L.M.*, et al.* (2013). 53BP1 mediates productive and mutagenic DNA repair through distinct phosphoprotein interactions. Cell *153*, 1266-1280.

Cannavo, E., and Cejka, P. (2014). Sae2 promotes dsDNA endonuclease activity within Mre11-Rad50-Xrs2 to resect DNA breaks. Nature *514*, 122-125.

Cao, L., Xu, X., Bunting, S.F., Liu, J., Wang, R.H., Cao, L.L., Wu, J.J., Peng, T.N., Chen, J., Nussenzweig, A.*, et al.* (2009). A selective requirement for 53BP1 in the biological response to genomic instability induced by Brca1 deficiency. Molecular cell *35*, 534-541.

Caron, P., Choudjaye, J., Clouaire, T., Bugler, B., Daburon, V., Aguirrebengoa, M., Mangeat, T., Iacovoni, J.S., Alvarez-Quilon, A., Cortes-Ledesma, F.*, et al.* (2015). Non-redundant Functions of ATM and DNA-PKcs in Response to DNA Double-Strand Breaks. Cell Rep *13*, 1598-1609.

Carreira, A., and Kowalczykowski, S.C. (2011). Two classes of BRC repeats in BRCA2 promote RAD51 nucleoprotein filament function by distinct mechanisms. Proceedings of the National Academy of Sciences of the United States of America *108*, 10448-10453.

Carvalho, S., Vitor, A.C., Sridhara, S.C., Martins, F.B., Raposo, A.C., Desterro, J.M., Ferreira, J., and de Almeida, S.F. (2014). SETD2 is required for DNA double-strand break repair and activation of the p53-mediated checkpoint. Elife *3*, e02482.

Ceccaldi, R., Liu, J.C., Amunugama, R., Hajdu, I., Primack, B., Petalcorin, M.I., O'Connor, K.W., Konstantinopoulos, P.A., Elledge, S.J., Boulton, S.J.*, et al.* (2015). Homologous-recombination-deficient tumours are dependent on Poltheta-mediated repair. Nature *518*, 258-262.

Ceccaldi, R., Rondinelli, B., and D'Andrea, A.D. (2016). Repair Pathway Choices and Consequences at the Double-Strand Break. Trends in cell biology *26*, 52-64.

Celeste, A., Difilippantonio, S., Difilippantonio, M.J., Fernandez-Capetillo, O., Pilch, D.R., Sedelnikova, O.A., Eckhaus, M., Ried, T., Bonner, W.M., and Nussenzweig, A. (2003a). H2AX haploinsufficiency modifies genomic stability and tumor susceptibility. Cell *114*, 371-383.

Celeste, A., Fernandez-Capetillo, O., Kruhlak, M.J., Pilch, D.R., Staudt, D.W., Lee, A., Bonner, R.F., Bonner, W.M., and Nussenzweig, A. (2003b). Histone H2AX phosphorylation is dispensable for the initial recognition of DNA breaks. Nature cell biology *5*, 675-679.

Celli, G.B., and de Lange, T. (2005). DNA processing is not required for ATM-mediated telomere damage response after TRF2 deletion. Nature cell biology *7*, 712-718.

Chai, B., Huang, J., Cairns, B.R., and Laurent, B.C. (2005). Distinct roles for the RSC and Swi/Snf ATP-dependent chromatin remodelers in DNA double-strand break repair. Genes & development *19*, 1656-1661.

Chan, D.W., Ye, R., Veillette, C.J., and Lees-Miller, S.P. (1999). DNA-dependent protein kinase phosphorylation sites in Ku 70/80 heterodimer. Biochemistry *38*, 1819-1828.

Chan, F.L., and Wong, L.H. (2012). Transcription in the maintenance of centromere chromatin identity. Nucleic acids research *40*, 11178-11188.

Chan, S.H., Yu, A.M., and McVey, M. (2010). Dual roles for DNA polymerase theta in alternative end-joining repair of double-strand breaks in Drosophila. PLoS genetics *6*, e1001005.

Chapman, J.R., Barral, P., Vannier, J.B., Borel, V., Steger, M., Tomas-Loba, A., Sartori, A.A., Adams, I.R., Batista, F.D., and Boulton, S.J. (2013). RIF1 is essential for 53BP1-dependent nonhomologous end joining and suppression of DNA double-strand break resection. Molecular cell *49*, 858-871.

Chapman, J.R., and Jackson, S.P. (2008). Phospho-dependent interactions between NBS1 and MDC1 mediate chromatin retention of the MRN complex at sites of DNA damage. EMBO reports *9*, 795-801.

Chapman, J.R., Sossick, A.J., Boulton, S.J., and Jackson, S.P. (2012a). BRCA1-associated exclusion of 53BP1 from DNA damage sites underlies temporal control of DNA repair. Journal of cell science *125*, 3529-3534.

Chapman, J.R., Taylor, M.R., and Boulton, S.J. (2012b). Playing the end game: DNA double-strand break repair pathway choice. Molecular cell *47*, 497-510.

Chappell, C., Hanakahi, L.A., Karimi-Busheri, F., Weinfeld, M., and West, S.C. (2002). Involvement of human polynucleotide kinase in double-strand break repair by non-homologous end joining. The EMBO journal *21*, 2827-2832.

Chayot, R., Montagne, B., Mazel, D., and Ricchetti, M. (2010). An end-joining repair mechanism in Escherichia coli. Proceedings of the National Academy of Sciences of the United States of America *107*, 2141-2146.

Chen, B., Gilbert, L.A., Cimini, B.A., Schnitzbauer, J., Zhang, W., Li, G.W., Park, J., Blackburn, E.H., Weissman, J.S., Qi, L.S*., et al.* (2013). Dynamic imaging of genomic loci in living human cells by an optimized CRISPR/Cas system. Cell *155*, 1479-1491.

Chen, L., Nievera, C.J., Lee, A.Y., and Wu, X. (2008a). Cell cycle-dependent complex formation of BRCA1.CtIP.MRN is important for DNA double-strand break repair. The Journal of biological chemistry *283*, 7713-7720.

Chen, X., Cui, D., Papusha, A., Zhang, X., Chu, C.D., Tang, J., Chen, K., Pan, X., and Ira, G. (2012). The Fun30 nucleosome remodeller promotes resection of DNA double-strand break ends. Nature *489*, 576-580.

Chen, X., Niu, H., Chung, W.H., Zhu, Z., Papusha, A., Shim, E.Y., Lee, S.E., Sung, P., and Ira, G. (2011). Cell cycle regulation of DNA double-strand break end resection by Cdk1-dependent Dna2 phosphorylation. Nature structural & molecular biology *18*, 1015-1019.

Chen, Z., Yang, H., and Pavletich, N.P. (2008b). Mechanism of homologous recombination from the RecA-ssDNA/dsDNA structures. Nature *453*, 489-484.

Chiolo, I., Carotenuto, W., Maffioletti, G., Petrini, J.H., Foiani, M., and Liberi, G. (2005). Srs2 and Sgs1 DNA helicases associate with Mre11 in different subcomplexes following checkpoint activation and CDK1-mediated Srs2 phosphorylation. Molecular and cellular biology *25*, 5738-5751.

Chiolo, I., Minoda, A., Colmenares, S.U., Polyzos, A., Costes, S.V., and Karpen, G.H. (2011). Double-strand breaks in heterochromatin move outside of a dynamic HP1a domain to complete recombinational repair. Cell *144*, 732-744.

Cho, N.W., Dilley, R.L., Lampson, M.A., and Greenberg, R.A. (2014). Interchromosomal Homology Searches Drive Directional ALT Telomere Movement and Synapsis. Cell *159*, 108-121.

Chou, D.M., Adamson, B., Dephoure, N.E., Tan, X., Nottke, A.C., Hurov, K.E., Gygi, S.P., Colaiacovo, M.P., and Elledge, S.J. (2010). A chromatin localization screen reveals poly (ADP ribose)-regulated recruitment of the repressive polycomb and NuRD complexes to sites of DNA damage. Proceedings of the National Academy of Sciences of the United States of America *107*, 18475-18480.

Clapier, C.R., and Cairns, B.R. (2009). The biology of chromatin remodeling complexes. Annu Rev Biochem *78*, 273-304.

Clarke, T.L., Sanchez-Bailon, M.P., Chiang, K., Reynolds, J.J., Herrero-Ruiz, J., Bandeiras, T.M., Matias, P.M., Maslen, S.L., Skehel, J.M., Stewart, G.S*., et al.* (2017). PRMT5-Dependent Methylation of the TIP60 Coactivator RUVBL1 Is a Key Regulator of Homologous Recombination. Molecular cell *65*, 900-916 e907.

Clerici, M., Mantiero, D., Guerini, I., Lucchini, G., and Longhese, M.P. (2008). The Yku70-Yku80 complex contributes to regulate double-strand break processing and checkpoint activation during the cell cycle. EMBO reports *9*, 810-818.

Cong, L., Ran, F.A., Cox, D., Lin, S., Barretto, R., Habib, N., Hsu, P.D., Wu, X., Jiang, W., Marraffini, L.A*., et al.* (2013). Multiplex genome engineering using CRISPR/Cas systems. Science *339*, 819-823.

Cook, P.J., Ju, B.G., Telese, F., Wang, X., Glass, C.K., and Rosenfeld, M.G. (2009). Tyrosine dephosphorylation of H2AX modulates apoptosis and survival decisions. Nature *458*, 591-596.

Cooper, M.P., Machwe, A., Orren, D.K., Brosh, R.M., Ramsden, D., and Bohr, V.A. (2000). Ku complex interacts with and stimulates the Werner protein. Genes & development *14*, 907-912.

Corneo, B., Wendland, R.L., Deriano, L., Cui, X., Klein, I.A., Wong, S.Y., Arnal, S., Holub, A.J., Weller, G.R., Pancake, B.A*., et al.* (2007). Rag mutations reveal robust alternative end joining. Nature *449*, 483-486.

Costelloe, T., Louge, R., Tomimatsu, N., Mukherjee, B., Martini, E., Khadaroo, B., Dubois, K., Wiegant, W.W., Thierry, A., Burma, S*., et al.* (2012). The yeast Fun30 and human SMARCAD1 chromatin remodellers promote DNA end resection. Nature *489*, 581-584.

Courilleau, C., Chailleux, C., Jauneau, A., Grimal, F., Briois, S., Boutet-Robinet, E., Boudsocq, F., Trouche, D., and Canitrot, Y. (2012). The chromatin remodeler p400 ATPase facilitates Rad51-mediated repair of DNA double-strand breaks. The Journal of cell biology *199*, 1067-1081.

Cui, X., Yu, Y., Gupta, S., Cho, Y.M., Lees-Miller, S.P., and Meek, K. (2005). Autophosphorylation of DNA-dependent protein kinase regulates DNA end processing and may also alter double-strand break repair pathway choice. Molecular and cellular biology *25*, 10842-10852.

d'Adda di Fagagna, F. (2008). Living on a break: cellular senescence as a DNA-damage response. Nat Rev Cancer *8*, 512-522.

D'Amours, D., and Jackson, S.P. (2002). The Mre11 complex: at the crossroads of dna repair and checkpoint signalling. Nature reviews Molecular cell biology *3*, 317-327.

Das, C., Lucia, M.S., Hansen, K.C., and Tyler, J.K. (2009). CBP/p300-mediated acetylation of histone H3 on lysine 56. Nature *459*, 113-117.

Daugaard, M., Baude, A., Fugger, K., Povlsen, L.K., Beck, H., Sorensen, C.S., Petersen, N.H., Sorensen, P.H., Lukas, C., Bartek, J*., et al.* (2012). LEDGF (p75) promotes DNA-end resection and homologous recombination. Nature structural & molecular biology *19*, 803-810.

de Lange, T. (2002). Protection of mammalian telomeres. Oncogene *21*, 532-540.

Deans, B., Griffin, C.S., Maconochie, M., and Thacker, J. (2000). Xrcc2 is required for genetic stability, embryonic neurogenesis and viability in mice. The EMBO journal *19*, 6675-6685.

Deng, S.K., Gibb, B., de Almeida, M.J., Greene, E.C., and Symington, L.S. (2014). RPA antagonizes microhomology-mediated repair of DNA double-strand breaks. Nature structural & molecular biology *21*, 405-412.

Densham, R.M., Garvin, A.J., Stone, H.R., Strachan, J., Baldock, R.A., Daza-Martin, M., Fletcher, A., Blair-Reid, S., Beesley, J., Johal, B*., et al.* (2016). Human BRCA1-BARD1 ubiquitin ligase activity counteracts chromatin barriers to DNA resection. Nature structural & molecular biology *23*, 647-655.

Deriano, L., and Roth, D.B. (2013). Modernizing the nonhomologous end-joining repertoire: alternative and classical NHEJ share the stage. Annual review of genetics *47*, 433-455.

Deriano, L., Stracker, T.H., Baker, A., Petrini, J.H., and Roth, D.B. (2009). Roles for NBS1 in alternative nonhomologous end-joining of V(D)J recombination intermediates. Molecular cell *34*, 13-25.

Di Virgilio, M., Callen, E., Yamane, A., Zhang, W., Jankovic, M., Gitlin, A.D., Feldhahn, N., Resch, W., Oliveira, T.Y., Chait, B.T*., et al.* (2013). Rif1 prevents resection of DNA breaks and promotes immunoglobulin class switching. Science *339*, 711-715.

Difilippantonio, M.J., Zhu, J., Chen, H.T., Meffre, E., Nussenzweig, M.C., Max, E.E., Ried, T., and Nussenzweig, A. (2000). DNA repair protein Ku80 suppresses chromosomal aberrations and malignant transformation. Nature *404*, 510-514.

Difilippantonio, S., Celeste, A., Fernandez-Capetillo, O., Chen, H.T., Reina San Martin, B., Van Laethem, F., Yang, Y.P., Petukhova, G.V., Eckhaus, M., Feigenbaum, L*., et al.* (2005). Role of Nbs1 in the activation of the Atm kinase revealed in humanized mouse models. Nature cell biology *7*, 675-685.

Dimitrova, N., Chen, Y.C., Spector, D.L., and de Lange, T. (2008). 53BP1 promotes non-homologous end joining of telomeres by increasing chromatin mobility. Nature *456*, 524-528.

Dinant, C., Ampatziadis-Michailidis, G., Lans, H., Tresini, M., Lagarou, A., Grosbart, M., Theil, A.F., van Cappellen, W.A., Kimura, H., Bartek, J.*, et al.* (2013). Enhanced chromatin dynamics by FACT promotes transcriptional restart after UV-induced DNA damage. Molecular cell *51*, 469-479.

Dion, V., and Gasser, S.M. (2013). Chromatin movement in the maintenance of genome stability. Cell *152*, 1355-1364.

Dion, V., Kalck, V., Horigome, C., Towbin, B.D., and Gasser, S.M. (2012). Increased mobility of double-strand breaks requires Mec1, Rad9 and the homologous recombination machinery. Nature cell biology *14*, 502-509.

Dion, V., Kalck, V., Seeber, A., Schleker, T., and Gasser, S.M. (2013). Cohesin and the nucleolus constrain the mobility of spontaneous repair foci. EMBO reports *14*, 984-991.

Dixon, J.R., Selvaraj, S., Yue, F., Kim, A., Li, Y., Shen, Y., Hu, M., Liu, J.S., and Ren, B. (2012). Topological domains in mammalian genomes identified by analysis of chromatin interactions. Nature *485*, 376-380.

Dobbs, T.A., Tainer, J.A., and Lees-Miller, S.P. (2010). A structural model for regulation of NHEJ by DNA-PKcs autophosphorylation. DNA repair *9*, 1307-1314.

Dohrn, L., Salles, D., Siehler, S.Y., Kaufmann, J., and Wiesmuller, L. (2012). BRCA1-mediated repression of mutagenic end-joining of DNA double-strand breaks requires complex formation with BACH1. Biochem J *441*, 919-926.

Doil, C., Mailand, N., Bekker-Jensen, S., Menard, P., Larsen, D.H., Pepperkok, R., Ellenberg, J., Panier, S., Durocher, D., Bartek, J.*, et al.* (2009). RNF168 binds and amplifies ubiquitin conjugates on damaged chromosomes to allow accumulation of repair proteins. Cell *136*, 435-446.

Drane, P., Brault, M.E., Cui, G., Meghani, K., Chaubey, S., Detappe, A., Parnandi, N., He, Y., Zheng, X.F., Botuyan, M.V.*, et al.* (2017). TIRR regulates 53BP1 by masking its histone methyl-lysine binding function. Nature *543*, 211-216.

Dundr, M., and Misteli, T. (2001). Functional architecture in the cell nucleus. Biochem J *356*, 297-310.

Dutta, A., Eckelmann, B., Adhikari, S., Ahmed, K.M., Sengupta, S., Pandey, A., Hegde, P.M., Tsai, M.S., Tainer, J.A., Weinfeld, M.*, et al.* (2016). Microhomology-mediated end joining is activated in irradiated human cells due to phosphorylation-dependent formation of the XRCC1 repair complex. Nucleic acids research.

Dynan, W.S., and Yoo, S. (1998). Interaction of Ku protein and DNA-dependent protein kinase catalytic subunit with nucleic acids. Nucleic acids research *26*, 1551-1559.

Eapen, V.V., Sugawara, N., Tsabar, M., Wu, W.H., and Haber, J.E. (2012). The Saccharomyces cerevisiae chromatin remodeler Fun30 regulates DNA end resection and checkpoint deactivation. Molecular and cellular biology *32*, 4727-4740.

Ellison, V., and Stillman, B. (2003). Biochemical characterization of DNA damage checkpoint complexes: clamp loader and clamp complexes with specificity for 5' recessed DNA. PLoS Biol *1*, E33.

Esashi, F., Galkin, V.E., Yu, X., Egelman, E.H., and West, S.C. (2007). Stabilization of RAD51 nucleoprotein filaments by the C-terminal region of BRCA2. Nature structural & molecular biology *14*, 468-474.

Escribano-Diaz, C., Orthwein, A., Fradet-Turcotte, A., Xing, M., Young, J.T., Tkac, J., Cook, M.A., Rosebrock, A.P., Munro, M., Canny, M.D.*, et al.* (2013). A cell cycle-dependent regulatory circuit composed of 53BP1-RIF1 and BRCA1-CtIP controls DNA repair pathway choice. Molecular cell *49*, 872-883.

Falck, J., Coates, J., and Jackson, S.P. (2005). Conserved modes of recruitment of ATM, ATR and DNA-PKcs to sites of DNA damage. Nature *434*, 605-611.

Falck, J., Forment, J.V., Coates, J., Mistrik, M., Lukas, J., Bartek, J., and Jackson, S.P. (2012). CDK targeting of NBS1 promotes DNA-end resection, replication restart and homologous recombination. EMBO reports *13*, 561-568.

Faucher, D., and Wellinger, R.J. (2010). Methylated H3K4, a transcription-associated histone modification, is involved in the DNA damage response pathway. PLoS genetics *6*.

Feng, L., Fong, K.W., Wang, J., Wang, W., and Chen, J. (2013). RIF1 counteracts BRCA1-mediated end resection during DNA repair. The Journal of biological chemistry *288*, 11135-11143.

Fernandez-Capetillo, O., Allis, C.D., and Nussenzweig, A. (2004). Phosphorylation of histone H2B at DNA double-strand breaks. J Exp Med *199*, 1671-1677.

Fnu, S., Williamson, E.A., De Haro, L.P., Brenneman, M., Wray, J., Shaheen, M., Radhakrishnan, K., Lee, S.H., Nickoloff, J.A., and Hromas, R. (2011). Methylation of histone H3 lysine 36 enhances DNA repair by nonhomologous end-joining. Proceedings of the National Academy of Sciences of the United States of America *108*, 540-545.

Fradet-Turcotte, A., Canny, M.D., Escribano-Diaz, C., Orthwein, A., Leung, C.C., Huang, H., Landry, M.C., Kitevski-LeBlanc, J., Noordermeer, S.M., Sicheri, F*., et al.* (2013). 53BP1 is a reader of the DNA-damage-induced H2A Lys 15 ubiquitin mark. Nature *499*, 50-54.

Frank, K.M., Sekiguchi, J.M., Seidl, K.J., Swat, W., Rathbun, G.A., Cheng, H.L., Davidson, L., Kangaloo, L., and Alt, F.W. (1998). Late embryonic lethality and impaired V(D)J recombination in mice lacking DNA ligase IV. Nature *396*, 173-177.

Fraser, P., and Bickmore, W. (2007). Nuclear organization of the genome and the potential for gene regulation. Nature *447*, 413-417.

French, C.A., Masson, J.Y., Griffin, C.S., O'Regan, P., West, S.C., and Thacker, J. (2002). Role of mammalian RAD51L2 (RAD51C) in recombination and genetic stability. The Journal of biological chemistry *277*, 19322-19330.

Fritsch, O., Benvenuto, G., Bowler, C., Molinier, J., and Hohn, B. (2004). The INO80 protein controls homologous recombination in Arabidopsis thaliana. Molecular cell *16*, 479-485.

Frohns, A., Frohns, F., Naumann, S.C., Layer, P.G., and Lobrich, M. (2014). Inefficient double-strand break repair in murine rod photoreceptors with inverted heterochromatin organization. Current biology : CB *24*, 1080-1090.

Gao, Y., Chaudhuri, J., Zhu, C., Davidson, L., Weaver, D.T., and Alt, F.W. (1998). A targeted DNA-PKcs-null mutation reveals DNA-PK-independent functions for KU in V(D)J recombination. Immunity *9*, 367-376.

Gao, Y., Ferguson, D.O., Xie, W., Manis, J.P., Sekiguchi, J., Frank, K.M., Chaudhuri, J., Horner, J., DePinho, R.A., and Alt, F.W. (2000). Interplay of p53 and DNA-repair protein XRCC4 in tumorigenesis, genomic stability and development. Nature *404*, 897-900.

Garcia, V., Phelps, S.E., Gray, S., and Neale, M.J. (2011). Bidirectional resection of DNA double-strand breaks by Mre11 and Exo1. Nature *479*, 241-244.

Garinis, G.A., van der Horst, G.T., Vijg, J., and Hoeijmakers, J.H. (2008). DNA damage and ageing: new-age ideas for an age-old problem. Nature cell biology *10*, 1241-1247.

Gatti, M., Pinato, S., Maiolica, A., Rocchio, F., Prato, M.G., Aebersold, R., and Penengo, L. (2015). RNF168 promotes noncanonical K27 ubiquitination to signal DNA damage. Cell Rep *10*, 226-238.

Gatti, M., Pinato, S., Maspero, E., Soffientini, P., Polo, S., and Penengo, L. (2012). A novel ubiquitin mark at the N-terminal tail of histone H2As targeted by RNF168 ubiquitin ligase. Cell cycle *11*, 2538-2544.

Geuting, V., Reul, C., and Lobrich, M. (2013). ATM release at resected double-strand breaks provides heterochromatin reconstitution to facilitate homologous recombination. PLoS genetics *9*, e1003667.

Ghezraoui, H., Piganeau, M., Renouf, B., Renaud, J.B., Sallmyr, A., Ruis, B., Oh, S., Tomkinson, A.E., Hendrickson, E.A., Giovannangeli, C*., et al.* (2014). Chromosomal translocations in human cells are generated by canonical nonhomologous end-joining. Molecular cell *55*, 829-842.

Ginjala, V., Nacerddine, K., Kulkarni, A., Oza, J., Hill, S.J., Yao, M., Citterio, E., van Lohuizen, M., and Ganesan, S. (2011). BMI1 is recruited to DNA breaks and contributes to DNA damage-induced H2A ubiquitination and repair. Molecular and cellular biology *31*, 1972-1982.

Goedecke, W., Eijpe, M., Offenberg, H.H., van Aalderen, M., and Heyting, C. (1999). Mre11 and Ku70 interact in somatic cells, but are differentially expressed in early meiosis. Nature genetics *23*, 194-198.

Gong, Y., Handa, N., Kowalczykowski, S.C., and de Lange, T. (2017). PHF11 promotes DSB resection, ATR signaling, and HR. Genes & development *31*, 46-58.

Gong, Z., Cho, Y.W., Kim, J.E., Ge, K., and Chen, J. (2009). Accumulation of Pax2 transactivation domain interaction protein (PTIP) at sites of DNA breaks via RNF8-dependent pathway is required for cell survival after DNA damage. The Journal of biological chemistry *284*, 7284-7293.

Goodarzi, A.A., Kurka, T., and Jeggo, P.A. (2011). KAP-1 phosphorylation regulates CHD3 nucleosome remodeling during the DNA double-strand break response. Nature structural & molecular biology *18*, 831-839.

Goodarzi, A.A., Noon, A.T., Deckbar, D., Ziv, Y., Shiloh, Y., Lobrich, M., and Jeggo, P.A. (2008). ATM signaling facilitates repair of DNA double-strand breaks associated with heterochromatin. Molecular cell *31*, 167-177.

Goodarzi, A.A., Yu, Y., Riballo, E., Douglas, P., Walker, S.A., Ye, R., Harer, C., Marchetti, C., Morrice, N., Jeggo, P.A*., et al.* (2006). DNA-PK autophosphorylation facilitates Artemis endonuclease activity. The EMBO journal *25*, 3880-3889.

Gospodinov, A., Vaissiere, T., Krastev, D.B., Legube, G., Anachkova, B., and Herceg, Z. (2011). Mammalian Ino80 mediates double-strand break repair through its role in DNA end strand resection. Molecular and cellular biology *31*, 4735-4745.

Gottlieb, T.M., and Jackson, S.P. (1993). The DNA-dependent protein kinase: requirement for DNA ends and association with Ku antigen. Cell *72*, 131-142.

Gottschalk, A.J., Timinszky, G., Kong, S.E., Jin, J., Cai, Y., Swanson, S.K., Washburn, M.P., Florens, L., Ladurner, A.G., Conaway, J.W*., et al.* (2009). Poly(ADP-ribosyl)ation directs recruitment and activation of an ATP-dependent chromatin remodeler. Proceedings of the National Academy of Sciences of the United States of America *106*, 13770-13774.

Grawunder, U., Wilm, M., Wu, X., Kulesza, P., Wilson, T.E., Mann, M., and Lieber, M.R. (1997). Activity of DNA ligase IV stimulated by complex formation with XRCC4 protein in mammalian cells. Nature *388*, 492-495.

Grawunder, U., Zimmer, D., Fugmann, S., Schwarz, K., and Lieber, M.R. (1998). DNA ligase IV is essential for V(D)J recombination and DNA double-strand break repair in human precursor lymphocytes. Molecular cell *2*, 477-484.

Greenberg, R.A., Sobhian, B., Pathania, S., Cantor, S.B., Nakatani, Y., and Livingston, D.M. (2006). Multifactorial contributions to an acute DNA damage response by BRCA1/BARD1-containing complexes. Genes & development *20*, 34-46.

Greer, E.L., and Shi, Y. (2012). Histone methylation: a dynamic mark in health, disease and inheritance. Nat Rev Genet *13*, 343-357.

Grundy, G.J., Rulten, S.L., Zeng, Z., Arribas-Bosacoma, R., Iles, N., Manley, K., Oliver, A., and Caldecott, K.W. (2013). APLF promotes the assembly and activity of non-homologous end joining protein complexes. The EMBO journal *32*, 112-125.

Grundy, G.J., Yang, W., and Gellert, M. (2010). Autoinhibition of DNA cleavage mediated by RAG1 and RAG2 is overcome by an epigenetic signal in V(D)J recombination. Proceedings of the National Academy of Sciences of the United States of America *107*, 22487-22492.

Gupta, A., Hunt, C.R., Hegde, M.L., Chakraborty, S., Udayakumar, D., Horikoshi, N., Singh, M., Ramnarain, D.B., Hittelman, W.N., Namjoshi, S*., et al.* (2014). MOF phosphorylation by ATM regulates 53BP1-mediated double-strand break repair pathway choice. Cell Rep *8*, 177-189.

Gurard-Levin, Z.A., Quivy, J.P., and Almouzni, G. (2014). Histone chaperones: assisting histone traffic and nucleosome dynamics. Annu Rev Biochem *83*, 487-517.

Gursoy-Yuzugullu, O., Ayrapetov, M.K., and Price, B.D. (2015). Histone chaperone Anp32e removes H2A.Z from DNA double-strand breaks and promotes nucleosome reorganization and DNA repair. Proceedings of the National Academy of Sciences of the United States of America *112*, 7507-7512.

Haahr, P., Hoffmann, S., Tollenaere, M.A., Ho, T., Toledo, L.I., Mann, M., Bekker-Jensen, S., Raschle, M., and Mailand, N. (2016). Activation of the ATR kinase by the RPA-binding protein ETAA1. Nature cell biology *18*, 1196-1207.

Haince, J.F., Kozlov, S., Dawson, V.L., Dawson, T.M., Hendzel, M.J., Lavin, M.F., and Poirier, G.G. (2007). Ataxia telangiectasia mutated (ATM) signaling network is modulated by a novel poly(ADP-ribose)-dependent pathway in the early response to DNA-damaging agents. The Journal of biological chemistry *282*, 16441-16453.

Haince, J.F., McDonald, D., Rodrigue, A., Dery, U., Masson, J.Y., Hendzel, M.J., and Poirier, G.G. (2008). PARP1-dependent kinetics of recruitment of MRE11 and NBS1 proteins to multiple DNA damage sites. The Journal of biological chemistry *283*, 1197-1208.

Hammond, C.M., Stromme, C.B., Huang, H., Patel, D.J., and Groth, A. (2017). Histone chaperone networks shaping chromatin function. Nature reviews Molecular cell biology *18*, 141-158.

Hansen, R.K., Mund, A., Poulsen, S.L., Sandoval, M., Klement, K., Tsouroula, K., Tollenaere, M.A., Raschle, M., Soria, R., Offermanns, S*., et al.* (2016). SCAI promotes DNA double-strand break repair in distinct chromosomal contexts. Nature cell biology *18*, 1357-1366.

Harding, S.M., Boiarsky, J.A., and Greenberg, R.A. (2015). ATM Dependent Silencing Links Nucleolar Chromatin Reorganization to DNA Damage Recognition. Cell Rep *13*, 251-259.

Helfricht, A., Wiegant, W.W., Thijssen, P.E., Vertegaal, A.C., Luijsterburg, M.S., and van Attikum, H. (2013). Remodeling and spacing factor 1 (RSF1) deposits centromere proteins at DNA double-strand breaks to promote non-homologous end-joining. Cell cycle *12*, 3070-3082.

Hergeth, S.P., and Schneider, R. (2015). The H1 linker histones: multifunctional proteins beyond the nucleosomal core particle. EMBO reports *16*, 1439-1453.

Heyer, W.D., Ehmsen, K.T., and Liu, J. (2010). Regulation of homologous recombination in eukaryotes. Annual review of genetics *44*, 113-139.

Heyer, W.D., Li, X., Rolfsmeier, M., and Zhang, X.P. (2006). Rad54: the Swiss Army knife of homologous recombination? Nucleic acids research *34*, 4115-4125.

Hochegger, H., Dejsuphong, D., Fukushima, T., Morrison, C., Sonoda, E., Schreiber, V., Zhao, G.Y., Saberi, A., Masutani, M., Adachi, N*., et al.* (2006). Parp-1 protects homologous recombination from interference by Ku and Ligase IV in vertebrate cells. The EMBO journal *25*, 1305-1314.

Hoeijmakers, J.H. (2001). Genome maintenance mechanisms for preventing cancer. Nature *411*, 366-374.

Hon, G.C., Hawkins, R.D., and Ren, B. (2009). Predictive chromatin signatures in the mammalian genome. Hum Mol Genet *18*, R195-201.

Horigome, C., Oma, Y., Konishi, T., Schmid, R., Marcomini, I., Hauer, M.H., Dion, V., Harata, M., and Gasser, S.M. (2014). SWR1 and INO80 chromatin remodelers contribute to DNA double-strand break perinuclear anchorage site choice. Molecular cell *55*, 626-639.

Hsiao, K.Y., and Mizzen, C.A. (2013). Histone H4 deacetylation facilitates 53BP1 DNA damage signaling and double-strand break repair. Journal of molecular cell biology *5*, 157-165.

Hu, Y., Scully, R., Sobhian, B., Xie, A., Shestakova, E., and Livingston, D.M. (2011). RAP80-directed tuning of BRCA1 homologous recombination function at ionizing radiation-induced nuclear foci. Genes & development *25*, 685-700.

Huang, H., Sabari, B.R., Garcia, B.A., Allis, C.D., and Zhao, Y. (2014). SnapShot: histone modifications. Cell *159*, 458-458 e451.

Huen, M.S., Grant, R., Manke, I., Minn, K., Yu, X., Yaffe, M.B., and Chen, J. (2007). RNF8 transduces the DNA-damage signal via histone ubiquitylation and checkpoint protein assembly. Cell *131*, 901-914.

Huen, M.S., Sy, S.M., and Chen, J. (2010). BRCA1 and its toolbox for the maintenance of genome integrity. Nature reviews Molecular cell biology *11*, 138-148.

Huertas, P., Cortes-Ledesma, F., Sartori, A.A., Aguilera, A., and Jackson, S.P. (2008). CDK targets Sae2 to control DNA-end resection and homologous recombination. Nature *455*, 689-692.

Huertas, P., and Jackson, S.P. (2009). Human CtIP mediates cell cycle control of DNA end resection and double strand break repair. The Journal of biological chemistry *284*, 9558-9565.

Huyen, Y., Zgheib, O., Ditullio, R.A., Jr., Gorgoulis, V.G., Zacharatos, P., Petty, T.J., Sheston, E.A., Mellert, H.S., Stavridi, E.S., and Halazonetis, T.D. (2004). Methylated lysine 79 of histone H3 targets 53BP1 to DNA double-strand breaks. Nature *432*, 406-411.

Ikura, T., Tashiro, S., Kakino, A., Shima, H., Jacob, N., Amunugama, R., Yoder, K., Izumi, S., Kuraoka, I., Tanaka, K.*, et al.* (2007). DNA damage-dependent acetylation and ubiquitination of H2AX enhances chromatin dynamics. Molecular and cellular biology *27*, 7028-7040.

Islam, M.N., Paquet, N., Fox, D., 3rd, Dray, E., Zheng, X.F., Klein, H., Sung, P., and Wang, W. (2012). A variant of the breast cancer type 2 susceptibility protein (BRC) repeat is essential for the RECQL5 helicase to interact with RAD51 recombinase for genome stabilization. The Journal of biological chemistry *287*, 23808-23818.

Ismail, I.H., Andrin, C., McDonald, D., and Hendzel, M.J. (2010). BMI1-mediated histone ubiquitylation promotes DNA double-strand break repair. The Journal of cell biology *191*, 45-60.

Isono, M., Niimi, A., Oike, T., Hagiwara, Y., Sato, H., Sekine, R., Yoshida, Y., Isobe, S.Y., Obuse, C., Nishi, R.*, et al.* (2017). BRCA1 Directs the Repair Pathway to Homologous Recombination by Promoting 53BP1 Dephosphorylation. Cell Rep *18*, 520-532.

Jackson, S.P., and Bartek, J. (2009). The DNA-damage response in human biology and disease. Nature *461*, 1071-1078.

Jacquet, K., Fradet-Turcotte, A., Avvakumov, N., Lambert, J.P., Roques, C., Pandita, R.K., Paquet, E., Herst, P., Gingras, A.C., Pandita, T.K.*, et al.* (2016). The TIP60 Complex Regulates Bivalent Chromatin Recognition by 53BP1 through Direct H4K20me Binding and H2AK15 Acetylation. Molecular cell *62*, 409-421.

Jakob, B., Splinter, J., Conrad, S., Voss, K.O., Zink, D., Durante, M., Lobrich, M., and Taucher-Scholz, G. (2011). DNA double-strand breaks in heterochromatin elicit fast repair protein recruitment, histone H2AX phosphorylation and relocation to euchromatin. Nucleic acids research *39*, 6489-6499.

Jakob, B., Splinter, J., Durante, M., and Taucher-Scholz, G. (2009). Live cell microscopy analysis of radiation-induced DNA double-strand break motion. Proceedings of the National Academy of Sciences of the United States of America *106*, 3172-3177.

Janssen, A., Breuer, G.A., Brinkman, E.K., van der Meulen, A.I., Borden, S.V., van Steensel, B., Bindra, R.S., LaRocque, J.R., and Karpen, G.H. (2016). A single double-strand break system reveals repair dynamics and mechanisms in heterochromatin and euchromatin. Genes & development *30*, 1645-1657.

Jasin, M., de Villiers, J., Weber, F., and Schaffner, W. (1985). High frequency of homologous recombination in mammalian cells between endogenous and introduced SV40 genomes. Cell *43*, 695-703.

Jasin, M., and Rothstein, R. (2013). Repair of strand breaks by homologous recombination. Cold Spring Harbor perspectives in biology *5*, a012740.

Jazayeri, A., Falck, J., Lukas, C., Bartek, J., Smith, G.C., Lukas, J., and Jackson, S.P. (2006). ATM- and cell cycle-dependent regulation of ATR in response to DNA double-strand breaks. Nature cell biology *8*, 37-45.

Jenuwein, T., and Allis, C.D. (2001). Translating the histone code. Science *293*, 1074-1080.

Jha, D.K., and Strahl, B.D. (2014). An RNA polymerase II-coupled function for histone H3K36 methylation in checkpoint activation and DSB repair. Nature communications *5*, 3965.

Jiang, W., Crowe, J.L., Liu, X., Nakajima, S., Wang, Y., Li, C., Lee, B.J., Dubois, R.L., Liu, C., Yu, X.*, et al.* (2015). Differential phosphorylation of DNA-PKcs regulates the interplay between end-processing and end-ligation during nonhomologous end-joining. Molecular cell *58*, 172-185.

Jiang, X., Xu, Y., and Price, B.D. (2010). Acetylation of H2AX on lysine 36 plays a key role in the DNA double-strand break repair pathway. FEBS Lett *584*, 2926-2930.

Jowsey, P.A., Doherty, A.J., and Rouse, J. (2004). Human PTIP facilitates ATM-mediated activation of p53 and promotes cellular resistance to ionizing radiation. The Journal of biological chemistry *279*, 55562-55569.

Kakarougkas, A., Ismail, A., Klement, K., Goodarzi, A.A., Conrad, S., Freire, R., Shibata, A., Lobrich, M., and Jeggo, P.A. (2013). Opposing roles for 53BP1 during homologous recombination. Nucleic acids research *41*, 9719-9731.

Kalb, R., Mallery, D.L., Larkin, C., Huang, J.T., and Hiom, K. (2014). BRCA1 is a histone-H2A-specific ubiquitin ligase. Cell Rep *8*, 999-1005.

Kalocsay, M., Hiller, N.J., and Jentsch, S. (2009). Chromosome-wide Rad51 spreading and SUMO-H2A.Z-dependent chromosome fixation in response to a persistent DNA double-strand break. Molecular cell *33*, 335-343.

Kashiwaba, S., Kitahashi, K., Watanabe, T., Onoda, F., Ohtsu, M., and Murakami, Y. (2010). The mammalian INO80 complex is recruited to DNA damage sites in an ARP8 dependent manner. Biochem Biophys Res Commun *402*, 619-625.

Kato, T., Sato, N., Hayama, S., Yamabuki, T., Ito, T., Miyamoto, M., Kondo, S., Nakamura, Y., and Daigo, Y. (2007). Activation of Holliday junction recognizing protein involved in the chromosomal stability and immortality of cancer cells. Cancer Res *67*, 8544-8553.

Keeney, S., Giroux, C.N., and Kleckner, N. (1997). Meiosis-specific DNA double-strand breaks are catalyzed by Spo11, a member of a widely conserved protein family. Cell *88*, 375-384.

Kent, N.A., Chambers, A.L., and Downs, J.A. (2007). Dual chromatin remodeling roles for RSC during DNA double strand break induction and repair at the yeast MAT locus. The Journal of biological chemistry *282*, 27693-27701.

Kent, T., Chandramouly, G., McDevitt, S.M., Ozdemir, A.Y., and Pomerantz, R.T. (2015). Mechanism of microhomology-mediated end-joining promoted by human DNA polymerase theta. Nature structural & molecular biology *22*, 230-237.

Khadaroo, B., Teixeira, M.T., Luciano, P., Eckert-Boulet, N., Germann, S.M., Simon, M.N., Gallina, I., Abdallah, P., Gilson, E., Geli, V.*, et al.* (2009). The DNA damage response at eroded telomeres and tethering to the nuclear pore complex. Nature cell biology *11*, 980-987.

Khurana, S., Kruhlak, M.J., Kim, J., Tran, A.D., Liu, J., Nyswaner, K., Shi, L., Jailwala, P., Sung, M.H., Hakim, O.*, et al.* (2014). A macrohistone variant links dynamic chromatin compaction to BRCA1-dependent genome maintenance. Cell Rep *8*, 1049-1062.

Kim, H., Huang, J., and Chen, J. (2007). CCDC98 is a BRCA1-BRCT domain-binding protein involved in the DNA damage response. Nature structural & molecular biology *14*, 710-715.

Kim, Y.C., Gerlitz, G., Furusawa, T., Catez, F., Nussenzweig, A., Oh, K.S., Kraemer, K.H., Shiloh, Y., and Bustin, M. (2009). Activation of ATM depends on chromatin interactions occurring before induction of DNA damage. Nature cell biology *11*, 92-96.

Klement, K., Luijsterburg, M.S., Pinder, J.B., Cena, C.S., Del Nero, V., Wintersinger, C.M., Dellaire, G., van Attikum, H., and Goodarzi, A.A. (2014). Opposing ISWI- and CHD-class chromatin remodeling activities orchestrate heterochromatic DNA repair. The Journal of cell biology *207*, 717-733.

Kolas, N.K., Chapman, J.R., Nakada, S., Ylanko, J., Chahwan, R., Sweeney, F.D., Panier, S., Mendez, M., Wildenhain, J., Thomson, T.M.*, et al.* (2007). Orchestration of the DNA-damage response by the RNF8 ubiquitin ligase. Science *318*, 1637-1640.

Kouzarides, T. (2007). Chromatin modifications and their function. Cell *128*, 693-705.

Krawczyk, P.M., Borovski, T., Stap, J., Cijsouw, T., ten Cate, R., Medema, J.P., Kanaar, R., Franken, N.A., and Aten, J.A. (2012). Chromatin mobility is increased at sites of DNA double-strand breaks. Journal of cell science *125*, 2127-2133.

Krejci, L., Van Komen, S., Li, Y., Villemain, J., Reddy, M.S., Klein, H., Ellenberger, T., and Sung, P. (2003). DNA helicase Srs2 disrupts the Rad51 presynaptic filament. Nature *423*, 305-309.

Kruhlak, M.J., Celeste, A., Dellaire, G., Fernandez-Capetillo, O., Muller, W.G., McNally, J.G., Bazett-Jones, D.P., and Nussenzweig, A. (2006). Changes in chromatin structure and mobility in living cells at sites of DNA double-strand breaks. The Journal of cell biology *172*, 823-834.

Kulkarni, A., and Wilson, D.M., 3rd (2008). The involvement of DNA-damage and -repair defects in neurological dysfunction. Am J Hum Genet *82*, 539-566.

Kumagai, A., and Dunphy, W.G. (2003). Repeated phosphopeptide motifs in Claspin mediate the regulated binding of Chk1. Nature cell biology *5*, 161-165.

Kumagai, A., Lee, J., Yoo, H.Y., and Dunphy, W.G. (2006). TopBP1 activates the ATR-ATRIP complex. Cell *124*, 943-955.

Kusumoto, R., Dawut, L., Marchetti, C., Wan Lee, J., Vindigni, A., Ramsden, D., and Bohr, V.A. (2008). Werner protein cooperates with the XRCC4-DNA ligase IV complex in end-processing. Biochemistry *47*, 7548-7556.

Kwon, S.J., Park, J.H., Park, E.J., Lee, S.A., Lee, H.S., Kang, S.W., and Kwon, J. (2015). ATM-mediated phosphorylation of the chromatin remodeling enzyme BRG1 modulates DNA double-strand break repair. Oncogene *34*, 303-313.

Lachner, M., O'Carroll, D., Rea, S., Mechtler, K., and Jenuwein, T. (2001). Methylation of histone H3 lysine 9 creates a binding site for HP1 proteins. Nature *410*, 116-120.

Lafon-Hughes, L., Di Tomaso, M.V., Liddle, P., Toledo, A., Reyes-Abalos, A.L., and Folle, G.A. (2013). Preferential localization of gammaH2AX foci in euchromatin of retina rod cells after DNA damage induction. Chromosome research : an international journal on the molecular, supramolecular and evolutionary aspects of chromosome biology *21*, 789-803.

Lan, L., Ui, A., Nakajima, S., Hatakeyama, K., Hoshi, M., Watanabe, R., Janicki, S.M., Ogiwara, H., Kohno, T., Kanno, S.*, et al.* (2010). The ACF1 complex is required for DNA double-strand break repair in human cells. Molecular cell *40*, 976-987.

Langelier, M.F., Planck, J.L., Roy, S., and Pascal, J.M. (2012). Structural basis for DNA damage-dependent poly(ADP-ribosyl)ation by human PARP-1. Science *336*, 728-732.

Larsen, D.H., Poinsignon, C., Gudjonsson, T., Dinant, C., Payne, M.R., Hari, F.J., Rendtlew Danielsen, J.M., Menard, P., Sand, J.C., Stucki, M.*, et al.* (2010). The chromatin-remodeling factor CHD4 coordinates signaling and repair after DNA damage. The Journal of cell biology *190*, 731-740.

Leber, R., Wise, T.W., Mizuta, R., and Meek, K. (1998). The XRCC4 gene product is a target for and interacts with the DNA-dependent protein kinase. The Journal of biological chemistry *273*, 1794-1801.

Lee-Theilen, M., Matthews, A.J., Kelly, D., Zheng, S., and Chaudhuri, J. (2011). CtIP promotes microhomology-mediated alternative end joining during class-switch recombination. Nature structural & molecular biology *18*, 75-79.

Lee, H.S., Park, J.H., Kim, S.J., Kwon, S.J., and Kwon, J. (2010). A cooperative activation loop among SWI/SNF, gamma-H2AX and H3 acetylation for DNA double-strand break repair. The EMBO journal *29*, 1434-1445.

Lee, J.H., and Paull, T.T. (2004). Direct activation of the ATM protein kinase by the Mre11/Rad50/Nbs1 complex. Science *304*, 93-96.

Lee, J.H., and Paull, T.T. (2005). ATM activation by DNA double-strand breaks through the Mre11-Rad50-Nbs1 complex. Science *308*, 551-554.

Lee, Y.C., Zhou, Q., Chen, J., and Yuan, J. (2016). RPA-Binding Protein ETAA1 Is an ATR Activator Involved in DNA Replication Stress Response. Current biology : CB *26*, 3257-3268.

Lemaitre, C., Grabarz, A., Tsouroula, K., Andronov, L., Furst, A., Pankotai, T., Heyer, V., Rogier, M., Attwood, K.M., Kessler, P*., et al.* (2014). Nuclear position dictates DNA repair pathway choice. Genes & development.

Lemaitre, C., and Soutoglou, E. (2014). DSB (im)mobility and DNA repair compartmentalization in mammalian cells. Journal of molecular biology.

Lengauer, C., Kinzler, K.W., and Vogelstein, B. (1998). Genetic instabilities in human cancers. Nature *396*, 643-649.

Lescale, C., Lenden Hasse, H., Blackford, A.N., Balmus, G., Bianchi, J.J., Yu, W., Bacoccina, L., Jarade, A., Clouin, C., Sivapalan, R*., et al.* (2016). Specific Roles of XRCC4 Paralogs PAXX and XLF during V(D)J Recombination. Cell Rep *16*, 2967-2979.

Leung, J.W., Agarwal, P., Canny, M.D., Gong, F., Robison, A.D., Finkelstein, I.J., Durocher, D., and Miller, K.M. (2014). Nucleosome acidic patch promotes RNF168- and RING1B/BMI1-dependent H2AX and H2A ubiquitination and DNA damage signaling. PLoS genetics *10*, e1004178.

Leung, J.W., Makharashvili, N., Agarwal, P., Chiu, L.Y., Pourpre, R., Cammarata, M.B., Cannon, J.R., Sherker, A., Durocher, D., Brodbelt, J.S*., et al.* (2017). ZMYM3 regulates BRCA1 localization at damaged chromatin to promote DNA repair. Genes & development *31*, 260-274.

Li, M., and Yu, X. (2013). Function of BRCA1 in the DNA damage response is mediated by ADP-ribosylation. Cancer cell *23*, 693-704.

Li, X., Corsa, C.A., Pan, P.W., Wu, L., Ferguson, D., Yu, X., Min, J., and Dou, Y. (2010). MOF and H4 K16 acetylation play important roles in DNA damage repair by modulating recruitment of DNA damage repair protein Mdc1. Molecular and cellular biology *30*, 5335-5347.

Li, X., and Tyler, J.K. (2016). Nucleosome disassembly during human non-homologous end joining followed by concerted HIRA- and CAF-1-dependent reassembly. Elife *5*.

Liang, B., Qiu, J., Ratnakumar, K., and Laurent, B.C. (2007). RSC functions as an early double-strand-break sensor in the cell's response to DNA damage. Current biology : CB *17*, 1432-1437.

Liang, F., Han, M., Romanienko, P.J., and Jasin, M. (1998). Homology-directed repair is a major double-strand break repair pathway in mammalian cells. Proceedings of the National Academy of Sciences of the United States of America *95*, 5172-5177.

Liaw, H., Lee, D., and Myung, K. (2011). DNA-PK-dependent RPA2 hyperphosphorylation facilitates DNA repair and suppresses sister chromatid exchange. PloS one *6*, e21424.

Lichter, P., Cremer, T., Borden, J., Manuelidis, L., and Ward, D.C. (1988). Delineation of individual human chromosomes in metaphase and interphase cells by in situ suppression hybridization using recombinant DNA libraries. Hum Genet *80*, 224-234.

Lieberman-Aiden, E., van Berkum, N.L., Williams, L., Imakaev, M., Ragoczy, T., Telling, A., Amit, I., Lajoie, B.R., Sabo, P.J., Dorschner, M.O*., et al.* (2009). Comprehensive mapping of long-range interactions reveals folding principles of the human genome. Science *326*, 289-293.

Lindahl, T. (1993). Instability and decay of the primary structure of DNA. Nature *362*, 709-715.

Lisby, M., Barlow, J.H., Burgess, R.C., and Rothstein, R. (2004). Choreography of the DNA damage response: spatiotemporal relationships among checkpoint and repair proteins. Cell *118*, 699-713.

Lisby, M., Mortensen, U.H., and Rothstein, R. (2003). Colocalization of multiple DNA double-strand breaks at a single Rad52 repair centre. Nature cell biology *5*, 572-577.

Liu, S., Bekker-Jensen, S., Mailand, N., Lukas, C., Bartek, J., and Lukas, J. (2006). Claspin operates downstream of TopBP1 to direct ATR signaling towards Chk1 activation. Molecular and cellular biology *26*, 6056-6064.

Liu, S., Opiyo, S.O., Manthey, K., Glanzer, J.G., Ashley, A.K., Amerin, C., Troksa, K., Shrivastav, M., Nickoloff, J.A., and Oakley, G.G. (2012a). Distinct roles for DNA-PK, ATM and ATR in RPA phosphorylation and checkpoint activation in response to replication stress. Nucleic acids research *40*, 10780-10794.

Liu, X., Jiang, W., Dubois, R.L., Yamamoto, K., Wolner, Z., and Zha, S. (2012b). Overlapping functions between XLF repair protein and 53BP1 DNA damage response factor in end joining and lymphocyte development. Proceedings of the National Academy of Sciences of the United States of America *109*, 3903-3908.

Liu, X., Shao, Z., Jiang, W., Lee, B.J., and Zha, S. (2017). PAXX promotes KU accumulation at DNA breaks and is essential for end-joining in XLF-deficient mice. Nature communications *8*, 13816.

Lok, B.H., Carley, A.C., Tchang, B., and Powell, S.N. (2013). RAD52 inactivation is synthetically lethal with deficiencies in BRCA1 and PALB2 in addition to BRCA2 through RAD51-mediated homologous recombination. Oncogene *32*, 3552-3558.

Lorat, Y., Schanz, S., Schuler, N., Wennemuth, G., Rube, C., and Rube, C.E. (2012). Beyond repair foci: DNA double-strand break repair in euchromatic and heterochromatic compartments analyzed by transmission electron microscopy. PloS one *7*, e38165.

Lorat, Y., Timm, S., Jakob, B., Taucher-Scholz, G., and Rube, C.E. (2016). Clustered double-strand breaks in heterochromatin perturb DNA repair after high linear energy transfer irradiation. Radiother Oncol *121*, 154-161.

Luger, K., Dechassa, M.L., and Tremethick, D.J. (2012). New insights into nucleosome and chromatin structure: an ordered state or a disordered affair? Nature reviews Molecular cell biology *13*, 436-447.

Luger, K., Mader, A.W., Richmond, R.K., Sargent, D.F., and Richmond, T.J. (1997). Crystal structure of the nucleosome core particle at 2.8 A resolution. Nature *389*, 251-260.

Luijsterburg, M.S., de Krijger, I., Wiegant, W.W., Shah, R.G., Smeenk, G., de Groot, A.J., Pines, A., Vertegaal, A.C., Jacobs, J.J., Shah, G.M.*, et al.* (2016). PARP1 Links CHD2-Mediated Chromatin Expansion and H3.3 Deposition to DNA Repair by Non-homologous End-Joining. Molecular cell *61*, 547-562.

Luijsterburg, M.S., Dinant, C., Lans, H., Stap, J., Wiernasz, E., Lagerwerf, S., Warmerdam, D.O., Lindh, M., Brink, M.C., Dobrucki, J.W.*, et al.* (2009). Heterochromatin protein 1 is recruited to various types of DNA damage. The Journal of cell biology *185*, 577-586.

Luijsterburg, M.S., Typas, D., Caron, M.C., Wiegant, W.W., van den Heuvel, D., Boonen, R.A., Couturier, A.M., Mullenders, L.H., Masson, J.Y., and van Attikum, H. (2017). A PALB2-interacting domain in RNF168 couples homologous recombination to DNA break-induced chromatin ubiquitylation. Elife *6*.

Lukas, C., Melander, F., Stucki, M., Falck, J., Bekker-Jensen, S., Goldberg, M., Lerenthal, Y., Jackson, S.P., Bartek, J., and Lukas, J. (2004). Mdc1 couples DNA double-strand break recognition by Nbs1 with its H2AX-dependent chromatin retention. The EMBO journal *23*, 2674-2683.

Luo, K., Li, L., Li, Y., Wu, C., Yin, Y., Chen, Y., Deng, M., Nowsheen, S., Yuan, J., and Lou, Z. (2016). A phosphorylation-deubiquitination cascade regulates the BRCA2-RAD51 axis in homologous recombination. Genes & development *30*, 2581-2595.

Ma, J.L., Kim, E.M., Haber, J.E., and Lee, S.E. (2003). Yeast Mre11 and Rad1 proteins define a Ku-independent mechanism to repair double-strand breaks lacking overlapping end sequences. Molecular and cellular biology *23*, 8820-8828.

Ma, Y., Pannicke, U., Lu, H., Niewolik, D., Schwarz, K., and Lieber, M.R. (2005). The DNA-dependent protein kinase catalytic subunit phosphorylation sites in human Artemis. The Journal of biological chemistry *280*, 33839-33846.

Ma, Y., Pannicke, U., Schwarz, K., and Lieber, M.R. (2002). Hairpin opening and overhang processing by an Artemis/DNA-dependent protein kinase complex in nonhomologous end joining and V(D)J recombination. Cell *108*, 781-794.

Mailand, N., Bekker-Jensen, S., Faustrup, H., Melander, F., Bartek, J., Lukas, C., and Lukas, J. (2007). RNF8 ubiquitylates histones at DNA double-strand breaks and promotes assembly of repair proteins. Cell *131*, 887-900.

Maison, C., and Almouzni, G. (2004). HP1 and the dynamics of heterochromatin maintenance. Nature reviews Molecular cell biology *5*, 296-304.

Majka, J., Niedziela-Majka, A., and Burgers, P.M. (2006). The checkpoint clamp activates Mec1 kinase during initiation of the DNA damage checkpoint. Molecular cell *24*, 891-901.

Mateos-Gomez, P.A., Gong, F., Nair, N., Miller, K.M., Lazzerini-Denchi, E., and Sfeir, A. (2015). Mammalian polymerase theta promotes alternative NHEJ and suppresses recombination. Nature *518*, 254-257.

Matsuoka, S., Rotman, G., Ogawa, A., Shiloh, Y., Tamai, K., and Elledge, S.J. (2000). Ataxia telangiectasia-mutated phosphorylates Chk2 in vivo and in vitro. Proceedings of the National Academy of Sciences of the United States of America *97*, 10389-10394.

Mattiroli, F., Vissers, J.H., van Dijk, W.J., Ikpa, P., Citterio, E., Vermeulen, W., Marteijn, J.A., and Sixma, T.K. (2012). RNF168 ubiquitinates K13-15 on H2A/H2AX to drive DNA damage signaling. Cell *150*, 1182-1195.

Matzuk, M.M., and Lamb, D.J. (2008). The biology of infertility: research advances and clinical challenges. Nat Med *14*, 1197-1213.

McKean, D., Huppi, K., Bell, M., Staudt, L., Gerhard, W., and Weigert, M. (1984). Generation of antibody diversity in the immune response of BALB/c mice to influenza virus hemagglutinin. Proceedings of the National Academy of Sciences of the United States of America *81*, 3180-3184.

McKinley, K.L., and Cheeseman, I.M. (2016). The molecular basis for centromere identity and function. Nature reviews Molecular cell biology *17*, 16-29.

Mehrotra, P.V., Ahel, D., Ryan, D.P., Weston, R., Wiechens, N., Kraehenbuehl, R., Owen-Hughes, T., and Ahel, I. (2011). DNA repair factor APLF is a histone chaperone. Molecular cell *41*, 46-55.

Miller, K.M., Tjeertes, J.V., Coates, J., Legube, G., Polo, S.E., Britton, S., and Jackson, S.P. (2010). Human HDAC1 and HDAC2 function in the DNA-damage response to promote DNA nonhomologous end-joining. Nature structural & molecular biology *17*, 1144-1151.

Mimitou, E.P., and Symington, L.S. (2008). Sae2, Exo1 and Sgs1 collaborate in DNA double-strand break processing. Nature *455*, 770-774.

Min, S., Jo, S., Lee, H.S., Chae, S., Lee, J.S., Ji, J.H., and Cho, H. (2014). ATM-dependent chromatin remodeler Rsf-1 facilitates DNA damage checkpoints and homologous recombination repair. Cell cycle *13*, 666-677.

Mine-Hattab, J., and Rothstein, R. (2012). Increased chromosome mobility facilitates homology search during recombination. Nature cell biology *14*, 510-517.

Mine-Hattab, J., and Rothstein, R. (2013). DNA in motion during double-strand break repair. Trends in cell biology *23*, 529-536.

Misteli, T., and Soutoglou, E. (2009). The emerging role of nuclear architecture in DNA repair and genome maintenance. Nature reviews Molecular cell biology *10*, 243-254.

Moldovan, G.L., Dejsuphong, D., Petalcorin, M.I., Hofmann, K., Takeda, S., Boulton, S.J., and D'Andrea, A.D. (2012). Inhibition of homologous recombination by the PCNA-interacting protein PARI. Molecular cell *45*, 75-86.

Mordes, D.A., Glick, G.G., Zhao, R., and Cortez, D. (2008). TopBP1 activates ATR through ATRIP and a PIKK regulatory domain. Genes & development *22*, 1478-1489.

Morrison, A.J., Highland, J., Krogan, N.J., Arbel-Eden, A., Greenblatt, J.F., Haber, J.E., and Shen, X. (2004). INO80 and gamma-H2AX interaction links ATP-dependent chromatin remodeling to DNA damage repair. Cell *119*, 767-775.

Mosbech, A., Lukas, C., Bekker-Jensen, S., and Mailand, N. (2013). The deubiquitylating enzyme USP44 counteracts the DNA double-strand break response mediated by the RNF8 and RNF168 ubiquitin ligases. The Journal of biological chemistry *288*, 16579-16587.

Moshous, D., Callebaut, I., de Chasseval, R., Corneo, B., Cavazzana-Calvo, M., Le Deist, F., Tezcan, I., Sanal, O., Bertrand, Y., Philippe, N.*, et al.* (2001). Artemis, a novel DNA double-strand break repair/V(D)J

recombination protein, is mutated in human severe combined immune deficiency. Cell *105*, 177-186.

Motycka, T.A., Bessho, T., Post, S.M., Sung, P., and Tomkinson, A.E. (2004). Physical and functional interaction between the XPF/ERCC1 endonuclease and hRad52. The Journal of biological chemistry *279*, 13634-13639.

Moyal, L., Lerenthal, Y., Gana-Weisz, M., Mass, G., So, S., Wang, S.Y., Eppink, B., Chung, Y.M., Shalev, G., Shema, E.*, et al.* (2011). Requirement of ATM-dependent monoubiquitylation of histone H2B for timely repair of DNA double-strand breaks. Molecular cell *41*, 529-542.

Moynahan, M.E., Pierce, A.J., and Jasin, M. (2001). BRCA2 is required for homology-directed repair of chromosomal breaks. Molecular cell *7*, 263-272.

Muller, S., and Almouzni, G. (2017). Chromatin dynamics during the cell cycle at centromeres. Nat Rev Genet *18*, 192-208.

Munoz, I.M., Jowsey, P.A., Toth, R., and Rouse, J. (2007). Phospho-epitope binding by the BRCT domains of hPTIP controls multiple aspects of the cellular response to DNA damage. Nucleic acids research *35*, 5312-5322.

Murr, R., Loizou, J.I., Yang, Y.G., Cuenin, C., Li, H., Wang, Z.Q., and Herceg, Z. (2006). Histone acetylation by Trrap-Tip60 modulates loading of repair proteins and repair of DNA double-strand breaks. Nature cell biology *8*, 91-99.

Myers, J.S., and Cortez, D. (2006). Rapid activation of ATR by ionizing radiation requires ATM and Mre11. The Journal of biological chemistry *281*, 9346-9350.

Nagai, S., Dubrana, K., Tsai-Pflugfelder, M., Davidson, M.B., Roberts, T.M., Brown, G.W., Varela, E., Hediger, F., Gasser, S.M., and Krogan, N.J. (2008). Functional targeting of DNA damage to a nuclear pore-associated SUMO-dependent ubiquitin ligase. Science *322*, 597-602.

Nagarajan, P., Onami, T.M., Rajagopalan, S., Kania, S., Donnell, R., and Venkatachalam, S. (2009). Role of chromodomain helicase DNA-binding protein 2 in DNA damage response signaling and tumorigenesis. Oncogene *28*, 1053-1062.

Nakamura, K., Kato, A., Kobayashi, J., Yanagihara, H., Sakamoto, S., Oliveira, D.V., Shimada, M., Tauchi, H., Suzuki, H., Tashiro, S.*, et al.* (2011). Regulation of homologous recombination by RNF20-dependent H2B ubiquitination. Molecular cell *41*, 515-528.

Navadgi-Patil, V.M., and Burgers, P.M. (2008). Yeast DNA replication protein Dpb11 activates the Mec1/ATR checkpoint kinase. The Journal of biological chemistry *283*, 35853-35859.

Neal, J.A., Dang, V., Douglas, P., Wold, M.S., Lees-Miller, S.P., and Meek, K. (2011). Inhibition of homologous recombination by DNA-dependent protein kinase requires kinase activity, is titratable, and is modulated by autophosphorylation. Molecular and cellular biology *31*, 1719-1733.

Neal, J.A., and Meek, K. (2011). Choosing the right path: does DNA-PK help make the decision? Mutation research *711*, 73-86.

Nepomuceno, T.C., Fernandes, V.C., Gomes, T.T., Carvalho, R.S., Suarez-Kurtz, G., Monteiro, A.N., and Carvalho, M.A. (2017). BRCA1 recruitment to damaged DNA sites is dependent on CDK9. Cell cycle *16*, 665-672.

Neumann, F.R., Dion, V., Gehlen, L.R., Tsai-Pflugfelder, M., Schmid, R., Taddei, A., and Gasser, S.M. (2012). Targeted INO80 enhances subnuclear chromatin movement and ectopic homologous recombination. Genes & development *26*, 369-383.

Nicassio, F., Corrado, N., Vissers, J.H., Areces, L.B., Bergink, S., Marteijn, J.A., Geverts, B., Houtsmuller, A.B., Vermeulen, W., Di Fiore, P.P.*, et al.* (2007). Human USP3 is a chromatin modifier required for S phase progression and genome stability. Current biology : CB *17*, 1972-1977.

Nimonkar, A.V., Genschel, J., Kinoshita, E., Polaczek, P., Campbell, J.L., Wyman, C., Modrich, P., and Kowalczykowski, S.C. (2011). BLM-DNA2-RPA-MRN and EXO1-BLM-RPA-MRN constitute two DNA end resection machineries for human DNA break repair. Genes & development *25*, 350-362.

Noon, A.T., Shibata, A., Rief, N., Lobrich, M., Stewart, G.S., Jeggo, P.A., and Goodarzi, A.A. (2010). 53BP1-dependent robust localized KAP-1 phosphorylation is essential for heterochromatic DNA double-strand break repair. Nature cell biology *12*, 177-184.

Nora, E.P., Lajoie, B.R., Schulz, E.G., Giorgetti, L., Okamoto, I., Servant, N., Piolot, T., van Berkum, N.L., Meisig, J., Sedat, J.*, et al.* (2012). Spatial partitioning of the regulatory landscape of the X-inactivation centre. Nature *485*, 381-385.

Nussenzweig, A., Chen, C., da Costa Soares, V., Sanchez, M., Sokol, K., Nussenzweig, M.C., and Li, G.C. (1996). Requirement for Ku80 in growth and immunoglobulin V(D)J recombination. Nature *382*, 551-555.

Ochi, T., Blackford, A.N., Coates, J., Jhujh, S., Mehmood, S., Tamura, N., Travers, J., Wu, Q., Draviam, V.M., Robinson, C.V.*, et al.* (2015). DNA repair. PAXX, a paralog of XRCC4 and XLF, interacts with Ku to promote DNA double-strand break repair. Science *347*, 185-188.

Ochs, F., Somyajit, K., Altmeyer, M., Rask, M.B., Lukas, J., and Lukas, C. (2016). 53BP1 fosters fidelity of homology-directed DNA repair. Nature structural & molecular biology *23*, 714-721.

Ogiwara, H., Ui, A., Otsuka, A., Satoh, H., Yokomi, I., Nakajima, S., Yasui, A., Yokota, J., and Kohno, T. (2011). Histone acetylation by CBP and p300 at double-strand break sites facilitates SWI/SNF chromatin remodeling and the recruitment of non-homologous end joining factors. Oncogene *30*, 2135-2146.

Oksenych, V., Alt, F.W., Kumar, V., Schwer, B., Wesemann, D.R., Hansen, E., Patel, H., Su, A., and Guo, C. (2012). Functional redundancy between repair factor XLF and damage response mediator 53BP1 in V(D)J recombination and DNA repair. Proceedings of the National Academy of Sciences of the United States of America *109*, 2455-2460.

Orthwein, A., Noordermeer, S.M., Wilson, M.D., Landry, S., Enchev, R.I., Sherker, A., Munro, M., Pinder, J., Salsman, J., Dellaire, G.*, et al.* (2015). A mechanism for the suppression of homologous recombination in G1 cells. Nature *528*, 422-426.

Oum, J.H., Seong, C., Kwon, Y., Ji, J.H., Sid, A., Ramakrishnan, S., Ira, G., Malkova, A., Sung, P., Lee, S.E.*, et al.* (2011). RSC facilitates Rad59-dependent homologous recombination between sister chromatids by promoting cohesin loading at DNA double-strand breaks. Molecular and cellular biology *31*, 3924-3937.

Oza, P., Jaspersen, S.L., Miele, A., Dekker, J., and Peterson, C.L. (2009). Mechanisms that regulate localization of a DNA double-strand break to the nuclear periphery. Genes & development *23*, 912-927.

Paddock, M.N., Bauman, A.T., Higdon, R., Kolker, E., Takeda, S., and Scharenberg, A.M. (2011). Competition between PARP-1 and Ku70 control the decision between high-fidelity and mutagenic DNA repair. DNA repair *10*, 338-343.

Pai, C.C., Deegan, R.S., Subramanian, L., Gal, C., Sarkar, S., Blaikley, E.J., Walker, C., Hulme, L., Bernhard, E., Codlin, S.*, et al.* (2014). A histone H3K36 chromatin switch coordinates DNA double-strand break repair pathway choice. Nature communications *5*, 4091.

Pan, M.R., Peng, G., Hung, W.C., and Lin, S.Y. (2011). Monoubiquitination of H2AX protein regulates DNA damage response signaling. The Journal of biological chemistry *286*, 28599-28607.

Panier, S., and Boulton, S.J. (2014). Double-strand break repair: 53BP1 comes into focus. Nature reviews Molecular cell biology *15*, 7-18.

Papamichos-Chronakis, M., Krebs, J.E., and Peterson, C.L. (2006). Interplay between Ino80 and Swr1 chromatin remodeling enzymes regulates cell cycle checkpoint adaptation in response to DNA damage. Genes & development *20*, 2437-2449.

Papamichos-Chronakis, M., and Peterson, C.L. (2013). Chromatin and the genome integrity network. Nat Rev Genet *14*, 62-75.

Papamichos-Chronakis, M., Watanabe, S., Rando, O.J., and Peterson, C.L. (2011). Global regulation of H2A.Z localization by the INO80 chromatin-remodeling enzyme is essential for genome integrity. Cell *144*, 200-213.

Park, E.J., Hur, S.K., and Kwon, J. (2010). Human INO80 chromatin-remodelling complex contributes to DNA double-strand break repair via the expression of Rad54B and XRCC3 genes. Biochem J *431*, 179-187.

Park, J.H., Park, E.J., Lee, H.S., Kim, S.J., Hur, S.K., Imbalzano, A.N., and Kwon, J. (2006). Mammalian SWI/SNF complexes facilitate DNA double-strand break repair by promoting gamma-H2AX induction. The EMBO journal *25*, 3986-3997.

Pavri, R., and Nussenzweig, M.C. (2011). AID targeting in antibody diversity. Adv Immunol *110*, 1-26.

Pei, H., Zhang, L., Luo, K., Qin, Y., Chesi, M., Fei, F., Bergsagel, P.L., Wang, L., You, Z., and Lou, Z. (2011). MMSET regulates histone H4K20 methylation and 53BP1 accumulation at DNA damage sites. Nature *470*, 124-128.

Pellegrini, M., Celeste, A., Difilippantonio, S., Guo, R., Wang, W., Feigenbaum, L., and Nussenzweig, A. (2006). Autophosphorylation at serine 1987 is dispensable for murine Atm activation in vivo. Nature *443*, 222-225.

Peng, G., Yim, E.K., Dai, H., Jackson, A.P., Burgt, I., Pan, M.R., Hu, R., Li, K., and Lin, S.Y. (2009). BRIT1/MCPH1 links chromatin remodelling to DNA damage response. Nature cell biology *11*, 865-872.

Perry, J.J., Yannone, S.M., Holden, L.G., Hitomi, C., Asaithamby, A., Han, S., Cooper, P.K., Chen, D.J., and Tainer, J.A. (2006). WRN exonuclease structure and molecular mechanism imply an editing role in DNA end processing. Nature structural & molecular biology *13*, 414-422.

Pessina, F., and Lowndes, N.F. (2014). The RSF1 histone-remodelling factor facilitates DNA double-strand break repair by recruiting centromeric and Fanconi Anaemia proteins. PLoS Biol *12*, e1001856.

Pfister, S.X., Ahrabi, S., Zalmas, L.P., Sarkar, S., Aymard, F., Bachrati, C.Z., Helleday, T., Legube, G., La Thangue, N.B., Porter, A.C.*, et al.* (2014). SETD2-dependent histone H3K36 trimethylation is required for homologous recombination repair and genome stability. Cell Rep *7*, 2006-2018.

Pierce, A.J., Johnson, R.D., Thompson, L.H., and Jasin, M. (1999). XRCC3 promotes homology-directed repair of DNA damage in mammalian cells. Genes & development *13*, 2633-2638.

Pinato, S., Scandiuzzi, C., Arnaudo, N., Citterio, E., Gaudino, G., and Penengo, L. (2009). RNF168, a new RING finger, MIU-containing protein that modifies chromatin by ubiquitination of histones H2A and H2AX. BMC Mol Biol *10*, 55.

Pinkel, D., Landegent, J., Collins, C., Fuscoe, J., Segraves, R., Lucas, J., and Gray, J. (1988). Fluorescence in situ hybridization with human chromosome-specific libraries: detection of trisomy 21 and translocations of chromosome 4. Proceedings of the National Academy of Sciences of the United States of America *85*, 9138-9142.

Pinto, C., Kasaciunaite, K., Seidel, R., and Cejka, P. (2016). Human DNA2 possesses a cryptic DNA unwinding activity that functionally integrates with BLM or WRN helicases. Elife *5*.

Pittman, D.L., and Schimenti, J.C. (2000). Midgestation lethality in mice deficient for the RecA-related gene, Rad51d/Rad51l3. Genesis *26*, 167-173.

Polo, S.E. (2015). Reshaping chromatin after DNA damage: the choreography of histone proteins. Journal of molecular biology *427*, 626-636.

Polo, S.E., Kaidi, A., Baskcomb, L., Galanty, Y., and Jackson, S.P. (2010). Regulation of DNA-damage responses and cell-cycle progression by the chromatin remodelling factor CHD4. The EMBO journal *29*, 3130-3139.

Polo, S.E., Roche, D., and Almouzni, G. (2006). New histone incorporation marks sites of UV repair in human cells. Cell *127*, 481-493.

Postow, L., Ghenoiu, C., Woo, E.M., Krutchinsky, A.N., Chait, B.T., and Funabiki, H. (2008). Ku80 removal from DNA through double strand break-induced ubiquitylation. The Journal of cell biology *182*, 467-479.

Price, B.D., and D'Andrea, A.D. (2013). Chromatin remodeling at DNA double-strand breaks. Cell *152*, 1344-1354.

Rai, R., Dai, H., Multani, A.S., Li, K., Chin, K., Gray, J., Lahad, J.P., Liang, J., Mills, G.B., Meric-Bernstam, F.*, et al.* (2006). BRIT1 regulates early DNA damage response, chromosomal integrity, and cancer. Cancer cell *10*, 145-157.

Rai, R., Hu, C., Broton, C., Chen, Y., Lei, M., and Chang, S. (2017). NBS1 Phosphorylation Status Dictates Repair Choice of Dysfunctional Telomeres. Molecular cell *65*, 801-817 e804.

Rao, S.S., Huntley, M.H., Durand, N.C., Stamenova, E.K., Bochkov, I.D., Robinson, J.T., Sanborn, A.L., Machol, I., Omer, A.D., Lander, E.S.*, et al.* (2014). A 3D map of the human genome at kilobase resolution reveals principles of chromatin looping. Cell *159*, 1665-1680.

Rass, E., Grabarz, A., Plo, I., Gautier, J., Bertrand, P., and Lopez, B.S. (2009). Role of Mre11 in chromosomal nonhomologous end joining in mammalian cells. Nature structural & molecular biology *16*, 819-824.

Rass, U., Ahel, I., and West, S.C. (2007). Defective DNA repair and neurodegenerative disease. Cell *130*, 991-1004.

Renkawitz, J., Lademann, C.A., Kalocsay, M., and Jentsch, S. (2013). Monitoring homology search during DNA double-strand break repair in vivo. Molecular cell *50*, 261-272.

Riballo, E., Woodbine, L., Stiff, T., Walker, S.A., Goodarzi, A.A., and Jeggo, P.A. (2009). XLF-Cernunnos promotes DNA ligase IV-XRCC4 re-adenylation following ligation. Nucleic acids research *37*, 482-492.

Robert, I., Dantzer, F., and Reina-San-Martin, B. (2009). Parp1 facilitates alternative NHEJ, whereas Parp2 suppresses IgH/c-myc translocations during immunoglobulin class switch recombination. J Exp Med *206*, 1047-1056.

Roberts, S.A., Strande, N., Burkhalter, M.D., Strom, C., Havener, J.M., Hasty, P., and Ramsden, D.A. (2010). Ku is a 5'-dRP/AP lyase that excises nucleotide damage near broken ends. Nature *464*, 1214-1217.

Rodrigue, A., Lafrance, M., Gauthier, M.C., McDonald, D., Hendzel, M., West, S.C., Jasin, M., and Masson, J.Y. (2006). Interplay between human DNA repair proteins at a unique double-strand break in vivo. The EMBO journal *25*, 222-231.

Rogakou, E.P., Boon, C., Redon, C., and Bonner, W.M. (1999). Megabase chromatin domains involved in DNA double-strand breaks in vivo. The Journal of cell biology *146*, 905-916.

Rogakou, E.P., Pilch, D.R., Orr, A.H., Ivanova, V.S., and Bonner, W.M. (1998). DNA double-stranded breaks induce histone H2AX phosphorylation on serine 139. The Journal of biological chemistry *273*, 5858-5868.

Rossetto, D., Avvakumov, N., and Cote, J. (2012). Histone phosphorylation: a chromatin modification involved in diverse nuclear events. Epigenetics *7*, 1098-1108.

Roth, D.B., and Wilson, J.H. (1986). Nonhomologous recombination in mammalian cells: role for short sequence homologies in the joining reaction. Molecular and cellular biology *6*, 4295-4304.

Rothkamm, K., Kruger, I., Thompson, L.H., and Lobrich, M. (2003). Pathways of DNA double-strand break repair during the mammalian cell cycle. Molecular and cellular biology *23*, 5706-5715.

Roukos, V., and Misteli, T. (2014). The biogenesis of chromosome translocations. Nature cell biology *16*, 293-300.

Roukos, V., Voss, T.C., Schmidt, C.K., Lee, S., Wangsa, D., and Misteli, T. (2013). Spatial dynamics of chromosome translocations in living cells. Science *341*, 660-664.

Roux, K.J., Kim, D.I., Raida, M., and Burke, B. (2012). A promiscuous biotin ligase fusion protein identifies proximal and interacting proteins in mammalian cells. The Journal of cell biology *196*, 801-810.

Roy, S., Andres, S.N., Vergnes, A., Neal, J.A., Xu, Y., Yu, Y., Lees-Miller, S.P., Junop, M., Modesti, M., and Meek, K. (2012). XRCC4's interaction with XLF is required for coding (but not signal) end joining. Nucleic acids research *40*, 1684-1694.

Rulten, S.L., Fisher, A.E., Robert, I., Zuma, M.C., Rouleau, M., Ju, L., Poirier, G., Reina-San-Martin, B., and Caldecott, K.W. (2011). PARP-3 and APLF function together to accelerate nonhomologous end-joining. Molecular cell *41*, 33-45.

Ryu, T., Bonner, M.R., and Chiolo, I. (2016). Cervantes and Quijote protect heterochromatin from aberrant recombination and lead the way to the nuclear periphery. Nucleus *7*, 485-497.

Ryu, T., Spatola, B., Delabaere, L., Bowlin, K., Hopp, H., Kunitake, R., Karpen, G.H., and Chiolo, I. (2015). Heterochromatic breaks move to the nuclear periphery to continue recombinational repair. Nature cell biology *17*, 1401-1411.

Saito, S., Goodarzi, A.A., Higashimoto, Y., Noda, Y., Lees-Miller, S.P., Appella, E., and Anderson, C.W. (2002). ATM mediates phosphorylation at multiple p53 sites, including Ser(46), in response to ionizing radiation. The Journal of biological chemistry *277*, 12491-12494.

Saksouk, N., Simboeck, E., and Dejardin, J. (2015). Constitutive heterochromatin formation and transcription in mammals. Epigenetics Chromatin *8*, 3.

San Filippo, J., Sung, P., and Klein, H. (2008). Mechanism of eukaryotic homologous recombination. Annu Rev Biochem *77*, 229-257.

Sanders, S.L., Portoso, M., Mata, J., Bahler, J., Allshire, R.C., and Kouzarides, T. (2004). Methylation of histone H4 lysine 20 controls recruitment of Crb2 to sites of DNA damage. Cell *119*, 603-614.

Sartori, A.A., Lukas, C., Coates, J., Mistrik, M., Fu, S., Bartek, J., Baer, R., Lukas, J., and Jackson, S.P. (2007). Human CtIP promotes DNA end resection. Nature *450*, 509-514.

Savic, V., Yin, B., Maas, N.L., Bredemeyer, A.L., Carpenter, A.C., Helmink, B.A., Yang-Iott, K.S., Sleckman, B.P., and Bassing, C.H. (2009). Formation of dynamic gamma-H2AX domains along broken DNA strands is distinctly regulated by ATM and MDC1 and dependent upon H2AX densities in chromatin. Molecular cell *34*, 298-310.

Schatz, D.G., and Baltimore, D. (2004). Uncovering the V(D)J recombinase. Cell *116*, S103-106, 102 p following S106.

Schober, H., Ferreira, H., Kalck, V., Gehlen, L.R., and Gasser, S.M. (2009). Yeast telomerase and the SUN domain protein Mps3 anchor telomeres and repress subtelomeric recombination. Genes & development *23*, 928-938.

Sedelnikova, O.A., Horikawa, I., Zimonjic, D.B., Popescu, N.C., Bonner, W.M., and Barrett, J.C. (2004). Senescing human cells and ageing mice accumulate DNA lesions with unrepairable double-strand breaks. Nature cell biology *6*, 168-170.

Seeber, A., Dion, V., and Gasser, S.M. (2013). Checkpoint kinases and the INO80 nucleosome remodeling complex enhance global chromatin mobility in response to DNA damage. Genes & development *27*, 1999-2008.

Serra, H., Da Ines, O., Degroote, F., Gallego, M.E., and White, C.I. (2013). Roles of XRCC2, RAD51B and RAD51D in RAD51-independent SSA recombination. PLoS genetics *9*, e1003971.

Sexton, T., Yaffe, E., Kenigsberg, E., Bantignies, F., Leblanc, B., Hoichman, M., Parrinello, H., Tanay, A., and Cavalli, G. (2012). Three-dimensional folding and functional organization principles of the Drosophila genome. Cell *148*, 458-472.

Sfeir, A., and Symington, L.S. (2015). Microhomology-Mediated End Joining: A Back-up Survival Mechanism or Dedicated Pathway? Trends Biochem Sci *40*, 701-714.

Shahbazian, M.D., and Grunstein, M. (2007). Functions of site-specific histone acetylation and deacetylation. Annu Rev Biochem *76*, 75-100.

Shanbhag, N.M., Rafalska-Metcalf, I.U., Balane-Bolivar, C., Janicki, S.M., and Greenberg, R.A. (2010). ATM-dependent chromatin changes silence transcription in cis to DNA double-strand breaks. Cell *141*, 970-981.

Sharma, G.G., So, S., Gupta, A., Kumar, R., Cayrou, C., Avvakumov, N., Bhadra, U., Pandita, R.K., Porteus, M.H., Chen, D.J.*, et al.* (2010). MOF and histone H4 acetylation at lysine 16 are critical for DNA damage response and double-strand break repair. Molecular and cellular biology *30*, 3582-3595.

Sharma, N., Zhu, Q., Wani, G., He, J., Wang, Q.E., and Wani, A.A. (2014). USP3 counteracts RNF168 via deubiquitinating H2A and gammaH2AX at lysine 13 and 15. Cell cycle *13*, 106-114.

Sheu, J.J., Guan, B., Choi, J.H., Lin, A., Lee, C.H., Hsiao, Y.T., Wang, T.L., Tsai, F.J., and Shih Ie, M. (2010). Rsf-1, a chromatin remodeling protein, induces DNA damage and promotes genomic instability. The Journal of biological chemistry *285*, 38260-38269.

Shim, E.Y., Hong, S.J., Oum, J.H., Yanez, Y., Zhang, Y., and Lee, S.E. (2007). RSC mobilizes nucleosomes to improve accessibility of repair machinery to the damaged chromatin. Molecular and cellular biology *27*, 1602-1613.

Shimazaki, N., Tsai, A.G., and Lieber, M.R. (2009). H3K4me3 stimulates the V(D)J RAG complex for both nicking and hairpinning in trans in addition to tethering in cis: implications for translocations. Molecular cell *34*, 535-544.

Shinohara, A., Ogawa, H., and Ogawa, T. (1992). Rad51 protein involved in repair and recombination in S. cerevisiae is a RecA-like protein. Cell *69*, 457-470.

Shu, Z., Smith, S., Wang, L., Rice, M.C., and Kmiec, E.B. (1999). Disruption of muREC2/RAD51L1 in mice results in early embryonic lethality which can Be partially rescued in a p53(-/-) background. Molecular and cellular biology *19*, 8686-8693.

Shuman, S., and Glickman, M.S. (2007). Bacterial DNA repair by non-homologous end joining. Nat Rev Microbiol *5*, 852-861.

Silverman, J., Takai, H., Buonomo, S.B., Eisenhaber, F., and de Lange, T. (2004). Human Rif1, ortholog of a yeast telomeric protein, is regulated by ATM and 53BP1 and functions in the S-phase checkpoint. Genes & development *18*, 2108-2119.

Simandlova, J., Zagelbaum, J., Payne, M.J., Chu, W.K., Shevelev, I., Hanada, K., Chatterjee, S., Reid, D.A., Liu, Y., Janscak, P.*, et al.* (2013). FBH1 helicase disrupts RAD51 filaments in vitro and modulates homologous recombination in mammalian cells. The Journal of biological chemistry *288*, 34168-34180.

Simsek, D., Brunet, E., Wong, S.Y., Katyal, S., Gao, Y., McKinnon, P.J., Lou, J., Zhang, L., Li, J., Rebar, E.J.*, et al.* (2011). DNA ligase III promotes alternative nonhomologous end-joining during chromosomal translocation formation. PLoS genetics *7*, e1002080.

Singleton, B.K., Torres-Arzayus, M.I., Rottinghaus, S.T., Taccioli, G.E., and Jeggo, P.A. (1999). The C terminus of Ku80 activates the DNA-dependent protein kinase catalytic subunit. Molecular and cellular biology *19*, 3267-3277.

Sinha, M., Watanabe, S., Johnson, A., Moazed, D., and Peterson, C.L. (2009). Recombinational repair within heterochromatin requires ATP-dependent chromatin remodeling. Cell *138*, 1109-1121.

Sinha, S., Villarreal, D., Shim, E.Y., and Lee, S.E. (2016). Risky business: Microhomology-mediated end joining. Mutation research *788*, 17-24.

Smeenk, G., and Mailand, N. (2016). Writers, Readers, and Erasers of Histone Ubiquitylation in DNA Double-Strand Break Repair. Frontiers in genetics *7*, 122.

Smeenk, G., Wiegant, W.W., Marteijn, J.A., Luijsterburg, M.S., Sroczynski, N., Costelloe, T., Romeijn, R.J., Pastink, A., Mailand, N., Vermeulen, W.*, et al.* (2013). Poly(ADP-ribosyl)ation links the chromatin remodeler SMARCA5/SNF2H to RNF168-dependent DNA damage signaling. Journal of cell science *126*, 889-903.

Smeenk, G., Wiegant, W.W., Vrolijk, H., Solari, A.P., Pastink, A., and van Attikum, H. (2010). The NuRD chromatin-remodeling complex regulates signaling and repair of DNA damage. The Journal of cell biology *190*, 741-749.

Smith, E.A., Gole, B., Willis, N.A., Soria, R., Starnes, L.M., Krumpelbeck, E.F., Jegga, A.G., Ali, A.M., Guo, H., Meetei, A.R.*, et al.* (2017). DEK is required for homologous recombination repair of DNA breaks. Sci Rep *7*, 44662.

Smits, V.A., Reaper, P.M., and Jackson, S.P. (2006). Rapid PIKK-dependent release of Chk1 from chromatin promotes the DNA-damage checkpoint response. Current biology : CB *16*, 150-159.

So, S., Davis, A.J., and Chen, D.J. (2009). Autophosphorylation at serine 1981 stabilizes ATM at DNA damage sites. The Journal of cell biology *187*, 977-990.

Sommers, J.A., Rawtani, N., Gupta, R., Bugreev, D.V., Mazin, A.V., Cantor, S.B., and Brosh, R.M., Jr. (2009). FANCJ uses its motor ATPase to destabilize protein-DNA complexes, unwind triplexes, and inhibit RAD51 strand exchange. The Journal of biological chemistry *284*, 7505-7517.

Soria, G., Polo, S.E., and Almouzni, G. (2012). Prime, repair, restore: the active role of chromatin in the DNA damage response. Molecular cell *46*, 722-734.

Soutoglou, E., Dorn, J.F., Sengupta, K., Jasin, M., Nussenzweig, A., Ried, T., Danuser, G., and Misteli, T. (2007). Positional stability of single double-strand breaks in mammalian cells. Nature cell biology *9*, 675-682.

Spector, D.L. (2001). Nuclear domains. Journal of cell science *114*, 2891-2893.

Spector, D.L. (2006). SnapShot: Cellular bodies. Cell *127*, 1071.

Spycher, C., Miller, E.S., Townsend, K., Pavic, L., Morrice, N.A., Janscak, P., Stewart, G.S., and Stucki, M. (2008). Constitutive phosphorylation of MDC1 physically links the MRE11-RAD50-NBS1 complex to damaged chromatin. The Journal of cell biology *181*, 227-240.

Stanley, F.K., Moore, S., and Goodarzi, A.A. (2013). CHD chromatin remodelling enzymes and the DNA damage response. Mutation research *750*, 31-44.

Stephens, P.J., McBride, D.J., Lin, M.L., Varela, I., Pleasance, E.D., Simpson, J.T., Stebbings, L.A., Leroy, C., Edkins, S., Mudie, L.J.*, et al.* (2009). Complex landscapes of somatic rearrangement in human breast cancer genomes. Nature *462*, 1005-1010.

Stewart, G.S., Panier, S., Townsend, K., Al-Hakim, A.K., Kolas, N.K., Miller, E.S., Nakada, S., Ylanko, J., Olivarius, S., Mendez, M.*, et al.* (2009). The RIDDLE syndrome protein mediates a ubiquitin-dependent signaling cascade at sites of DNA damage. Cell *136*, 420-434.

Stiff, T., O'Driscoll, M., Rief, N., Iwabuchi, K., Lobrich, M., and Jeggo, P.A. (2004). ATM and DNA-PK function redundantly to phosphorylate H2AX after exposure to ionizing radiation. Cancer Res *64*, 2390-2396.

Stucki, M., Clapperton, J.A., Mohammad, D., Yaffe, M.B., Smerdon, S.J., and Jackson, S.P. (2005). MDC1 directly binds phosphorylated histone H2AX to regulate cellular responses to DNA double-strand breaks. Cell *123*, 1213-1226.

Sturzenegger, A., Burdova, K., Kanagaraj, R., Levikova, M., Pinto, C., Cejka, P., and Janscak, P. (2014). DNA2 cooperates with the WRN and BLM RecQ helicases to mediate long-range DNA end resection in human cells. The Journal of biological chemistry *289*, 27314-27326.

Su, X.A., Dion, V., Gasser, S.M., and Freudenreich, C.H. (2015). Regulation of recombination at yeast nuclear pores controls repair and triplet repeat stability. Genes & development *29*, 1006-1017.

Sugawara, N., Wang, X., and Haber, J.E. (2003). In vivo roles of Rad52, Rad54, and Rad55 proteins in Rad51-mediated recombination. Molecular cell *12*, 209-219.

Sun, Y., Jiang, X., Xu, Y., Ayrapetov, M.K., Moreau, L.A., Whetstine, J.R., and Price, B.D. (2009). Histone H3 methylation links DNA damage detection to activation of the tumour suppressor Tip60. Nature cell biology *11*, 1376-1382.

Sun, Y., Xu, Y., Roy, K., and Price, B.D. (2007). DNA damage-induced acetylation of lysine 3016 of ATM activates ATM kinase activity. Molecular and cellular biology *27*, 8502-8509.

Sung, P. (1997). Function of yeast Rad52 protein as a mediator between replication protein A and the Rad51 recombinase. The Journal of biological chemistry *272*, 28194-28197.

Symington, L.S. (2002). Role of RAD52 epistasis group genes in homologous recombination and double-strand break repair. Microbiol Mol Biol Rev *66*, 630-670, table of contents.

Symington, L.S., Rothstein, R., and Lisby, M. (2014). Mechanisms and regulation of mitotic recombination in Saccharomyces cerevisiae. Genetics *198*, 795-835.

Taccioli, G.E., Amatucci, A.G., Beamish, H.J., Gell, D., Xiang, X.H., Torres Arzayus, M.I., Priestley, A., Jackson, S.P., Marshak Rothstein, A., Jeggo, P.A.*, et al.* (1998). Targeted disruption of the catalytic subunit of the DNA-PK gene in mice confers severe combined immunodeficiency and radiosensitivity. Immunity *9*, 355-366.

Taccioli, G.E., Rathbun, G., Oltz, E., Stamato, T., Jeggo, P.A., and Alt, F.W. (1993). Impairment of V(D)J recombination in double-strand break repair mutants. Science *260*, 207-210.

Tadi, S.K., Tellier-Lebegue, C., Nemoz, C., Drevet, P., Audebert, S., Roy, S., Meek, K., Charbonnier, J.B., and Modesti, M. (2016). PAXX Is an Accessory c-NHEJ Factor that Associates with Ku70 and Has Overlapping Functions with XLF. Cell Rep *17*, 541-555.

Takata, M., Sasaki, M.S., Tachiiri, S., Fukushima, T., Sonoda, E., Schild, D., Thompson, L.H., and Takeda, S. (2001). Chromosome instability and defective recombinational repair in knockout mutants of the five Rad51 paralogs. Molecular and cellular biology *21*, 2858-2866.

Talbert, P.B., and Henikoff, S. (2017). Histone variants on the move: substrates for chromatin dynamics. Nature reviews Molecular cell biology *18*, 115-126.

Tang, J., Cho, N.W., Cui, G., Manion, E.M., Shanbhag, N.M., Botuyan, M.V., Mer, G., and Greenberg, R.A. (2013). Acetylation limits 53BP1 association with damaged chromatin to promote homologous recombination. Nature structural & molecular biology *20*, 317-325.

Taty-Taty, G.C., Chailleux, C., Quaranta, M., So, A., Guirouilh-Barbat, J., Lopez, B.S., Bertrand, P., Trouche, D., and Canitrot, Y. (2016). Control of alternative end joining by the chromatin remodeler p400 ATPase. Nucleic acids research *44*, 1657-1668.

Taty-Taty, G.C., Courilleau, C., Quaranta, M., Carayon, A., Chailleux, C., Aymard, F., Trouche, D., and Canitrot, Y. (2014). H2A.Z depletion impairs proliferation and viability but not DNA double-strand breaks repair in human immortalized and tumoral cell lines. Cell cycle *13*, 399-407.

Taylor, M.R., Spirek, M., Chaurasiya, K.R., Ward, J.D., Carzaniga, R., Yu, X., Egelman, E.H., Collinson, L.M., Rueda, D., Krejci, L.*, et al.* (2015). Rad51 Paralogs Remodel Pre-synaptic Rad51 Filaments to Stimulate Homologous Recombination. Cell *162*, 271-286.

Therizols, P., Fairhead, C., Cabal, G.G., Genovesio, A., Olivo-Marin, J.C., Dujon, B., and Fabre, E. (2006). Telomere tethering at the nuclear periphery is essential for efficient DNA double strand break repair in subtelomeric region. The Journal of cell biology *172*, 189-199.

Thompson, L.H., and Schild, D. (2001). Homologous recombinational repair of DNA ensures mammalian chromosome stability. Mutation research *477*, 131-153.

Thorslund, T., Ripplinger, A., Hoffmann, S., Wild, T., Uckelmann, M., Villumsen, B., Narita, T., Sixma, T.K., Choudhary, C., Bekker-Jensen, S.*, et al.* (2015). Histone H1 couples initiation and amplification of ubiquitin signalling after DNA damage. Nature *527*, 389-393.

Timinszky, G., Till, S., Hassa, P.O., Hothorn, M., Kustatscher, G., Nijmeijer, B., Colombelli, J., Altmeyer, M., Stelzer, E.H., Scheffzek, K.*, et al.* (2009). A macrodomain-containing histone rearranges chromatin upon sensing PARP1 activation. Nature structural & molecular biology *16*, 923-929.

Tjeertes, J.V., Miller, K.M., and Jackson, S.P. (2009). Screen for DNA-damage-responsive histone modifications identifies H3K9Ac and H3K56Ac in human cells. The EMBO journal *28*, 1878-1889.

Tkac, J., Xu, G., Adhikary, H., Young, J.T., Gallo, D., Escribano-Diaz, C., Krietsch, J., Orthwein, A., Munro, M., Sol, W.*, et al.* (2016). HELB Is a Feedback Inhibitor of DNA End Resection. Molecular cell *61*, 405-418.

Toiber, D., Erdel, F., Bouazoune, K., Silberman, D.M., Zhong, L., Mulligan, P., Sebastian, C., Cosentino, C., Martinez-Pastor, B., Giacosa, S.*, et al.* (2013). SIRT6 recruits SNF2H to DNA break sites, preventing genomic instability through chromatin remodeling. Molecular cell *51*, 454-468.

Tomimatsu, N., Mukherjee, B., and Burma, S. (2009). Distinct roles of ATR and DNA-PKcs in triggering DNA damage responses in ATM-deficient cells. EMBO reports *10*, 629-635.

Tomimatsu, N., Mukherjee, B., Catherine Hardebeck, M., Ilcheva, M., Vanessa Camacho, C., Louise Harris, J., Porteus, M., Llorente, B., Khanna, K.K., and Burma, S. (2014). Phosphorylation of EXO1 by CDKs 1 and 2 regulates DNA end resection and repair pathway choice. Nature communications *5*, 3561.

Torres-Rosell, J., Sunjevaric, I., De Piccoli, G., Sacher, M., Eckert-Boulet, N., Reid, R., Jentsch, S., Rothstein, R., Aragon, L., and Lisby, M. (2007). The Smc5-Smc6 complex and SUMO modification of Rad52 regulates recombinational repair at the ribosomal gene locus. Nature cell biology *9*, 923-931.

Tremethick, D.J. (2007). Higher-order structures of chromatin: the elusive 30 nm fiber. Cell *128*, 651-654.

Trojer, P., and Reinberg, D. (2007). Facultative heterochromatin: is there a distinctive molecular signature? Molecular cell *28*, 1-13.

Truong, L.N., Li, Y., Shi, L.Z., Hwang, P.Y., He, J., Wang, H., Razavian, N., Berns, M.W., and Wu, X. (2013). Microhomology-mediated End Joining and Homologous Recombination share the initial end resection step to repair DNA double-strand breaks in mammalian cells. Proceedings of the National Academy of Sciences of the United States of America *110*, 7720-7725.

Tsouroula, K., Furst, A., Rogier, M., Heyer, V., Maglott-Roth, A., Ferrand, A., Reina-San-Martin, B., and Soutoglou, E. (2016). Temporal and Spatial Uncoupling of DNA Double Strand Break Repair Pathways within Mammalian Heterochromatin. Molecular cell *63*, 293-305.

Tsukuda, T., Lo, Y.C., Krishna, S., Sterk, R., Osley, M.A., and Nickoloff, J.A. (2009). INO80-dependent chromatin remodeling regulates early and late stages of mitotic homologous recombination. DNA repair *8*, 360-369.

Tuzon, C.T., Spektor, T., Kong, X., Congdon, L.M., Wu, S., Schotta, G., Yokomori, K., and Rice, J.C. (2014). Concerted activities of distinct H4K20 methyltransferases at DNA double-strand breaks regulate 53BP1 nucleation and NHEJ-directed repair. Cell Rep *8*, 430-438.

Typas, D., Luijsterburg, M.S., Wiegant, W.W., Diakatou, M., Helfricht, A., Thijssen, P.E., van den Broek, B., Mullenders, L.H., and van Attikum, H. (2015). The de-ubiquitylating enzymes USP26 and USP37 regulate homologous recombination by counteracting RAP80. Nucleic acids research *43*, 6919-6933.

van Attikum, H., Fritsch, O., and Gasser, S.M. (2007). Distinct roles for SWR1 and INO80 chromatin remodeling complexes at chromosomal double-strand breaks. The EMBO journal *26*, 4113-4125.

van Attikum, H., Fritsch, O., Hohn, B., and Gasser, S.M. (2004). Recruitment of the INO80 complex by H2A phosphorylation links ATP-dependent chromatin remodeling with DNA double-strand break repair. Cell *119*, 777-788.

Van Bortle, K., and Corces, V.G. (2012). Nuclear organization and genome function. Annual review of cell and developmental biology *28*, 163-187.

van Sluis, M., and McStay, B. (2015). A localized nucleolar DNA damage response facilitates recruitment of the homology-directed repair machinery independent of cell cycle stage. Genes & development *29*, 1151-1163.

van Steensel, B., and Belmont, A.S. (2017). Lamina-Associated Domains: Links with Chromosome Architecture, Heterochromatin, and Gene Repression. Cell *169*, 780-791.

Vazquez, B.N., Thackray, J.K., Simonet, N.G., Kane-Goldsmith, N., Martinez-Redondo, P., Nguyen, T., Bunting, S., Vaquero, A., Tischfield, J.A., and Serrano, L. (2016). SIRT7 promotes genome integrity and modulates non-homologous end joining DNA repair. The EMBO journal *35*, 1488-1503.

Vempati, R.K., Jayani, R.S., Notani, D., Sengupta, A., Galande, S., and Haldar, D. (2010). p300-mediated acetylation of histone H3 lysine 56 functions in DNA damage response in mammals. The Journal of biological chemistry *285*, 28553-28564.

Vidi, P.A., Liu, J., Salles, D., Jayaraman, S., Dorfman, G., Gray, M., Abad, P., Moghe, P.V., Irudayaraj, J.M., Wiesmuller, L*., et al.* (2014). NuMA promotes homologous recombination repair by regulating the accumulation of the ISWI ATPase SNF2h at DNA breaks. Nucleic acids research *42*, 6365-6379.

Wakeman, T.P., Wang, Q., Feng, J., and Wang, X.F. (2012). Bat3 facilitates H3K79 dimethylation by DOT1L and promotes DNA damage-induced 53BP1 foci at G1/G2 cell-cycle phases. The EMBO journal *31*, 2169-2181.

Walker, J.R., Corpina, R.A., and Goldberg, J. (2001). Structure of the Ku heterodimer bound to DNA and its implications for double-strand break repair. Nature *412*, 607-614.

Wang, B., Matsuoka, S., Ballif, B.A., Zhang, D., Smogorzewska, A., Gygi, S.P., and Elledge, S.J. (2007). Abraxas and RAP80 form a BRCA1 protein complex required for the DNA damage response. Science *316*, 1194-1198.

Wang, H., Guan, J., Wang, H., Perrault, A.R., Wang, Y., and Iliakis, G. (2001). Replication protein A2 phosphorylation after DNA damage by the coordinated action of ataxia telangiectasia-mutated and DNA-dependent protein kinase. Cancer Res *61*, 8554-8563.

Wang, H., and Xu, X. (2017). Microhomology-mediated end joining: new players join the team. Cell Biosci *7*, 6.

Wang, M., Wu, W., Wu, W., Rosidi, B., Zhang, L., Wang, H., and Iliakis, G. (2006). PARP-1 and Ku compete for repair of DNA double strand breaks by distinct NHEJ pathways. Nucleic acids research *34*, 6170-6182.

Wang, S., Su, J.H., Beliveau, B.J., Bintu, B., Moffitt, J.R., Wu, C.T., and Zhuang, X. (2016). Spatial organization of chromatin domains and compartments in single chromosomes. Science *353*, 598-602.

Wang, Y.G., Nnakwe, C., Lane, W.S., Modesti, M., and Frank, K.M. (2004). Phosphorylation and regulation of DNA ligase IV stability by DNA-dependent protein kinase. The Journal of biological chemistry *279*, 37282-37290.

Warmerdam, D.O., van den Berg, J., and Medema, R.H. (2016). Breaks in the 45S rDNA Lead to Recombination-Mediated Loss of Repeats. Cell Rep *14*, 2519-2527.

Weissman, L., de Souza-Pinto, N.C., Stevnsner, T., and Bohr, V.A. (2007). DNA repair, mitochondria, and neurodegeneration. Neuroscience *145*, 1318-1329.

Weller, G.R., Kysela, B., Roy, R., Tonkin, L.M., Scanlan, E., Della, M., Devine, S.K., Day, J.P., Wilkinson, A., d'Adda di Fagagna, F*., et al.* (2002). Identification of a DNA nonhomologous end-joining complex in bacteria. Science *297*, 1686-1689.

Wilson, J.H., Berget, P.B., and Pipas, J.M. (1982). Somatic cells efficiently join unrelated DNA segments end-to-end. Molecular and cellular biology *2*, 1258-1269.

Wilson, M.D., Benlekbir, S., Fradet-Turcotte, A., Sherker, A., Julien, J.P., McEwan, A., Noordermeer, S.M., Sicheri, F., Rubinstein, J.L., and Durocher, D. (2016). The structural basis of modified nucleosome recognition by 53BP1. Nature *536*, 100-103.

Wilson, T.E., Grawunder, U., and Lieber, M.R. (1997). Yeast DNA ligase IV mediates non-homologous DNA end joining. Nature *388*, 495-498.

Wu, J., Huen, M.S., Lu, L.Y., Ye, L., Dou, Y., Ljungman, M., Chen, J., and Yu, X. (2009). Histone ubiquitination associates with BRCA1-dependent DNA damage response. Molecular and cellular biology *29*, 849-860.

Wu, S., Shi, Y., Mulligan, P., Gay, F., Landry, J., Liu, H., Lu, J., Qi, H.H., Wang, W., Nickoloff, J.A*., et al.* (2007). A YY1-INO80 complex regulates genomic stability through homologous recombination-based repair. Nature structural & molecular biology *14*, 1165-1172.

Xiao, A., Li, H., Shechter, D., Ahn, S.H., Fabrizio, L.A., Erdjument-Bromage, H., Ishibe-Murakami, S., Wang, B., Tempst, P., Hofmann, K.*, et al.* (2009). WSTF regulates the H2A.X DNA damage response via a novel tyrosine kinase activity. Nature *457*, 57-62.

Xie, A., Kwok, A., and Scully, R. (2009). Role of mammalian Mre11 in classical and alternative nonhomologous end joining. Nature structural & molecular biology *16*, 814-818.

Xu, C., Xu, Y., Gursoy-Yuzugullu, O., and Price, B.D. (2012a). The histone variant macroH2A1.1 is recruited to DSBs through a mechanism involving PARP1. FEBS Lett *586*, 3920-3925.

Xu, Y., Ayrapetov, M.K., Xu, C., Gursoy-Yuzugullu, O., Hu, Y., and Price, B.D. (2012b). Histone H2A.Z controls a critical chromatin remodeling step required for DNA double-strand break repair. Molecular cell *48*, 723-733.

Xu, Y., Sun, Y., Jiang, X., Ayrapetov, M.K., Moskwa, P., Yang, S., Weinstock, D.M., and Price, B.D. (2010). The p400 ATPase regulates nucleosome stability and chromatin ubiquitination during DNA repair. The Journal of cell biology *191*, 31-43.

Yamane, A., Robbiani, D.F., Resch, W., Bothmer, A., Nakahashi, H., Oliveira, T., Rommel, P.C., Brown, E.J., Nussenzweig, A., Nussenzweig, M.C.*, et al.* (2013). RPA accumulation during class switch recombination represents 5'-3' DNA-end resection during the S-G2/M phase of the cell cycle. Cell Rep *3*, 138-147.

Yan, C.T., Boboila, C., Souza, E.K., Franco, S., Hickernell, T.R., Murphy, M., Gumaste, S., Geyer, M., Zarrin, A.A., Manis, J.P.*, et al.* (2007). IgH class switching and translocations use a robust non-classical end-joining pathway. Nature *449*, 478-482.

Yan, Q., Dutt, S., Xu, R., Graves, K., Juszczynski, P., Manis, J.P., and Shipp, M.A. (2009). BBAP monoubiquitylates histone H4 at lysine 91 and selectively modulates the DNA damage response. Molecular cell *36*, 110-120.

Yan, W., Shao, Z., Li, F., Niu, L., Shi, Y., Teng, M., and Li, X. (2011). Structural basis of gammaH2AX recognition by human PTIP BRCT5-BRCT6 domains in the DNA damage response pathway. FEBS Lett *585*, 3874-3879.

Yoo, S., and Dynan, W.S. (1999). Geometry of a complex formed by double strand break repair proteins at a single DNA end: recruitment of DNA-PKcs induces inward translocation of Ku protein. Nucleic acids research *27*, 4679-4686.

Yu, A.M., and McVey, M. (2010). Synthesis-dependent microhomology-mediated end joining accounts for multiple types of repair junctions. Nucleic acids research *38*, 5706-5717.

Yu, X., Fu, S., Lai, M., Baer, R., and Chen, J. (2006). BRCA1 ubiquitinates its phosphorylation-dependent binding partner CtIP. Genes & development *20*, 1721-1726.

Yu, Y., Mahaney, B.L., Yano, K., Ye, R., Fang, S., Douglas, P., Chen, D.J., and Lees-Miller, S.P. (2008). DNA-PK and ATM phosphorylation sites in XLF/Cernunnos are not required for repair of DNA double strand breaks. DNA repair *7*, 1680-1692.

Yun, M.H., and Hiom, K. (2009). CtIP-BRCA1 modulates the choice of DNA double-strand-break repair pathway throughout the cell cycle. Nature *459*, 460-463.

Zarebski, M., Wiernasz, E., and Dobrucki, J.W. (2009). Recruitment of heterochromatin protein 1 to DNA repair sites. Cytometry Part A : the journal of the International Society for Analytical Cytology *75*, 619-625.

Zeitlin, S.G., Baker, N.M., Chapados, B.R., Soutoglou, E., Wang, J.Y., Berns, M.W., and Cleveland, D.W. (2009). Double-strand DNA breaks recruit the centromeric histone CENP-A. Proceedings of the National Academy of Sciences of the United States of America *106*, 15762-15767.

Zha, S., Guo, C., Boboila, C., Oksenych, V., Cheng, H.L., Zhang, Y., Wesemann, D.R., Yuen, G., Patel, H., Goff, P.H.*, et al.* (2011). ATM damage response and XLF repair factor are functionally redundant in joining DNA breaks. Nature *469*, 250-254.

Zhang, F., Bick, G., Park, J.Y., and Andreassen, P.R. (2012). MDC1 and RNF8 function in a pathway that directs BRCA1-dependent localization of PALB2 required for homologous recombination. Journal of cell science *125*, 6049-6057.

Zhang, H., Liu, H., Chen, Y., Yang, X., Wang, P., Liu, T., Deng, M., Qin, B., Correia, C., Lee, S.*, et al.* (2016). A cell cycle-dependent BRCA1-UHRF1 cascade regulates DNA double-strand break repair pathway choice. Nature communications *7*, 10201.

Zhang, Y., Hefferin, M.L., Chen, L., Shim, E.Y., Tseng, H.M., Kwon, Y., Sung, P., Lee, S.E., and Tomkinson, A.E. (2007). Role of Dnl4-Lif1 in nonhomologous end-joining repair complex assembly and suppression of homologous recombination. Nature structural & molecular biology *14*, 639-646.

Zhang, Y., and Jasin, M. (2011). An essential role for CtIP in chromosomal translocation formation through an alternative end-joining pathway. Nature structural & molecular biology *18*, 80-84.

Zhang, Y., and Rowley, J.D. (2006). Chromatin structural elements and chromosomal translocations in leukemia. DNA repair *5*, 1282-1297.

Zhou, C.Y., Johnson, S.L., Gamarra, N.I., and Narlikar, G.J. (2016). Mechanisms of ATP-Dependent Chromatin Remodeling Motors. Annu Rev Biophys *45*, 153-181.

Zhu, C., Bogue, M.A., Lim, D.S., Hasty, P., and Roth, D.B. (1996). Ku86-deficient mice exhibit severe combined immunodeficiency and defective processing of V(D)J recombination intermediates. Cell *86*, 379-389.

Zhu, C., Mills, K.D., Ferguson, D.O., Lee, C., Manis, J., Fleming, J., Gao, Y., Morton, C.C., and Alt, F.W. (2002). Unrepaired DNA breaks in p53-deficient cells lead to oncogenic gene amplification subsequent to translocations. Cell *109*, 811-821.

Zierhut, C., and Diffley, J.F. (2008). Break dosage, cell cycle stage and DNA replication influence DNA double strand break response. The EMBO journal *27*, 1875-1885.

Ziv, Y., Bielopolski, D., Galanty, Y., Lukas, C., Taya, Y., Schultz, D.C., Lukas, J., Bekker-Jensen, S., Bartek, J., and Shiloh, Y. (2006). Chromatin relaxation in response to DNA double-strand breaks is modulated by a novel ATM- and KAP-1 dependent pathway. Nature cell biology *8*, 870-876.

Zou, L., and Elledge, S.J. (2003). Sensing DNA damage through ATRIP recognition of RPA-ssDNA complexes. Science *300*, 1542-1548.

Zou, L., Liu, D., and Elledge, S.J. (2003). Replication protein A-mediated recruitment and activation of Rad17 complexes. Proceedings of the National Academy of Sciences of the United States of America *100*, 13827-13832.

APPENDIX

Kring Hansen, R.*[1], Mund, A.*[1], Lund Poulsen*[1], S., Sandoval, M., Klement, K., **Tsouroula, K.,** Tollenaere, M., Räschle, M., Soria, R., Offermanns, S., Worzfeld, T., Grosse, R., Brandt, D.T., Rozell, B., Mann, M., Cole, F., Soutoglou, E., Goodarzi, A.A., Daniel, J.A., Mailand, N., Bekker-Jensen, S. (2016). SCAI promotes DNA double-strand break repair in distinct chromosomal contexts. *Nature Cell Biology* 18, 1357-1366. doi: 10.1038/ncb3436.

Lemaitre, C., Grabarz, A.*[2], **Tsouroula, K.***[2], Andronov, L., Furst, A., Pankotai, T., Heyer, V., Rogier, M., Attwood, K.M., Kessler, P., Dellaire, G., Klaholz, B., Reina-San-Martin, B., Soutoglou, E. (2014). Nuclear position dictates DNA repair pathway choice. *Genes & development*. doi: 10.1101/gad.248369.114.

nature cell biology

LETTERS

SCAI promotes DNA double-strand break repair in distinct chromosomal contexts

Rebecca Kring Hansen[1,12], Andreas Mund[2,12], Sara Lund Poulsen[1,12], Maria Sandoval[3], Karolin Klement[4], Katerina Tsouroula[5], Maxim A. X. Tollenaere[1,6], Markus Räschle[7], Rebeca Soria[2], Stefan Offermanns[8], Thomas Worzfeld[8,9], Robert Grosse[9], Dominique T. Brandt[9], Björn Rozell[10], Matthias Mann[11], Francesca Cole[3], Evi Soutoglou[5], Aaron A. Goodarzi[4], Jeremy A. Daniel[2,13], Niels Mailand[1,13] and Simon Bekker-Jensen[1,6,13]

DNA double-strand breaks (DSBs) are highly cytotoxic DNA lesions, whose accurate repair by non-homologous end-joining (NHEJ) or homologous recombination (HR) is crucial for genome integrity and is strongly influenced by the local chromatin environment[1,2]. Here, we identify SCAI (suppressor of cancer cell invasion) as a 53BP1-interacting chromatin-associated protein that promotes the functionality of several DSB repair pathways in mammalian cells. SCAI undergoes prominent enrichment at DSB sites through dual mechanisms involving 53BP1-dependent recruitment to DSB-surrounding chromatin and 53BP1-independent accumulation at resected DSBs. Cells lacking SCAI display reduced DSB repair capacity, hypersensitivity to DSB-inflicting agents and genome instability. We demonstrate that SCAI is a mediator of 53BP1-dependent repair of heterochromatin-associated DSBs, facilitating ATM kinase signalling at DSBs in repressive chromatin environments. Moreover, we establish an important role of SCAI in meiotic recombination, as SCAI deficiency in mice leads to germ cell loss and subfertility associated with impaired retention of the DMC1 recombinase on meiotic chromosomes. Collectively, our findings uncover SCAI as a physiologically important component of both NHEJ- and HR-mediated pathways that potentiates DSB repair efficiency in specific chromatin contexts.

In response to genotoxic insults such as DNA double-strand breaks (DSBs), eukaryotic cells mount a coordinated DNA damage response that activates DNA repair pathways to mitigate the deleterious consequences of DNA lesions[1,2]. DSBs can be repaired by non-homologous end-joining (NHEJ) or homologous recombination (HR)[3]. Dysfunctions in DSB repair pathways cause severe hereditary disorders with symptoms including cancer predisposition, neurodegeneration, subfertility and immunodeficiency[4].

The state and organization of chromatin fundamentally influences DSB repair efficiency and pathway choice, and major compositional and structural changes are imposed onto chromatin during DSB formation and repair[5,6]. DNA damage-induced modifications of chromatin-associated proteins near the lesions enable the accumulation of DNA repair factors at the damage sites[3,5]. The ATM kinase is a master organizer of this response, phosphorylating substrates including histone H2AX, and this phosphorylation product (γ-H2AX) triggers events that lead to recruitment of the E3 ubiquitin ligases RNF8 and RNF168. Ubiquitin-dependent modification of histones at DSB sites by these ligases then promotes accumulation of DSB repair factors including BRCA1 and 53BP1 to the DSB-surrounding chromatin areas[7]. However, the structure of chromatin can present a substantial barrier to efficient DSB repair. In particular, compacted, transcriptionally inert heterochromatin interferes with the accessibility of repair factors to DNA lesions, and heterochromatin-associated DSBs are generally repaired with slower kinetics than euchromatic

[1]Ubiquitin Signaling Group, Protein Signaling Program, The Novo Nordisk Foundation Center for Protein Research, Faculty of Health and Medical Sciences, University of Copenhagen, Blegdamsvej 3B, DK-2200 Copenhagen, Denmark. [2]Chromatin Structure and Function Group, Protein Signaling Program, The Novo Nordisk Foundation Center for Protein Research, Faculty of Health and Medical Sciences, University of Copenhagen, Blegdamsvej 3B, DK-2200 Copenhagen, Denmark. [3]Epigenetics and Molecular Carcinogenesis Department, The University of Texas MD Anderson Cancer Center, Smithville, Texas 78957, USA. [4]Robson DNA Science Centre, Arnie Charbonneau Cancer Institute, Departments of Biochemistry & Molecular Biology and Oncology, Cumming School of Medicine, University of Calgary, Calgary, Alberta T2N 4N1, Canada. [5]Institut de Génétique et de Biologie Moléculaire et Celullaire (IGBMC), University of Strasbourg, 67404 Illkirch, France. [6]Department of Cellular and Molecular Medicine, Center for Healthy Aging, University of Copenhagen, DK-2200 Copenhagen, Denmark. [7]Department of Molecular Genetics, TU Kaiserslautern, Paul-Ehrlich Str. 24, 67663 Kaiserslautern, Germany. [8]Max-Planck-Institute for Heart and Lung Research, Department of Pharmacology, 61231 Bad Nauheim, Germany. [9]Institute of Pharmacology, University of Marburg, 35032 Marburg, Germany. [10]Department of Experimental Medicine, Faculty of Health and Medical Sciences, University of Copenhagen, Blegdamsvej 3B, DK-2200 Copenhagen, Denmark. [11]Department of Proteomics and Signal Transduction, Max Planck Institute of Biochemistry, Am Klopferspitz 18, D-82152 Martinsried, Germany. [12]These authors contributed equally to this work.
[13]Correspondence should be addressed to J.A.D., N.M. or S.B.-J. (e-mail: jeremy.daniel@cpr.ku.dk or niels.mailand@cpr.ku.dk or simon.bekker-jensen@cpr.ku.dk)

Received 26 May 2016; accepted 5 October 2016; published online 7 November 2016; DOI: 10.1038/ncb3436

© 2016 Macmillan Publishers Limited, part of Springer Nature. All rights reserved.

breaks[6]. Cells therefore possess multiple factors that remodel chromatin structure to enhance the targeting of DNA repair factors to lesions in heterochromatic regions[6].

The chromatin-associated protein 53BP1 is an HR-inhibitory factor that mediates end-joining of unprotected telomeres and other toxic DNA repair reactions[8]. 53BP1 is also crucial for long-range end-joining during V(D)J recombination and immunoglobulin heavy-chain (IgH) class-switch recombination (CSR) in developing lymphocytes; consequently *53BP1*$^{-/-}$ B cells are severely impaired for CSR[9,10]. These functions of 53BP1 are, to a large extent, mediated by the 53BP1-binding factors RIF1 and PTIP[11–15]. Finally, 53BP1 has an established, but less well understood, role in promoting ATM-dependent repair of DSBs in heterochromatin. This involves localized phosphorylation of the transcriptional co-repressor KAP1 at Ser824 in heterochromatin by ATM, which triggers the release of the chromatin remodeller CHD3.1 to enable chromatin relaxation and efficient lesion repair[16–18]. Here, we identified the poorly characterized protein SCAI as a mediator of 53BP1-dependent repair of heterochromatin-associated DSBs.

Using the CHROMASS (chromatin mass spectrometry) method for systems-wide profiling of protein recruitment to chromatin templates incubated in *Xenopus* egg extracts that we recently described[19], we observed prominent enrichment of SCAI at DNA damage-containing chromatin along with multiple known DNA damage response components (Fig. 1a and Supplementary Fig. 1a,b). SCAI is highly conserved among vertebrates and has been implicated in transcriptional regulation[20,21], but has no annotated domains and shares little sequence homology with other proteins. Using cells expressing GFP-tagged human SCAI at near-physiological levels, we found that SCAI is recruited to microlaser- and ionizing radiation (IR)-generated DSB sites (Fig. 1b,c), suggesting that it is involved in DSB repair processes. To gain insight into this function, we used quantitative mass spectrometry to identify SCAI-interacting proteins, revealing 53BP1 as well as heterochromatin-associated factors (including the HP1 proteins HP1β (CBX1) and HP1α (CBX5)) among prominently enriched, prospective SCAI-binding proteins (Fig. 1d). Consistently, biochemical fractionation experiments showed that SCAI is predominantly associated with chromatin (Supplementary Fig. 1c). In co-immunoprecipitation assays, SCAI interacted with 53BP1 in an IR- and ATM-stimulated manner, and purified SCAI and 53BP1 interacted *in vitro* (Fig. 1e,f and Supplementary Fig. 1d), suggesting that their interaction is direct and functionally relevant in the context of DSB repair. Knockdown of 53BP1 or its upstream recruitment factor RNF8 (ref. 7) strongly attenuated SCAI accumulation at microlaser-generated DSBs, but not vice versa (Fig. 1b and Supplementary Fig. 1e–i), suggesting that SCAI is recruited to DSB-surrounding chromatin via direct binding to 53BP1, downstream of RNF8/RNF168-mediated histone ubiquitylation. Like ATM inhibition, RNF8 depletion suppressed IR-induced SCAI–53BP1 interaction (Fig. 1g), suggesting that the SCAI-53BP1 complex is stabilized once recruited to DSBs.

Reconstitution of *53BP1*$^{-/-}$ mouse embryonic fibroblasts (MEFs) with different 53BP1 constructs showed that its amino-terminal half, which undergoes multi-site phosphorylation by ATM to provide binding sites for RIF1 and PTIP[11–15], was required for SCAI recruitment to DSB sites (Fig. 2a and Supplementary Fig. 2a). Within this 53BP1 region we mapped the SCAI-binding site to amino acids 900–1230, which form part of its ATM phosphorylation domain (Fig. 2b). However, unlike RIF1 and PTIP, SCAI was recruited to damaged DNA independently of ATM-dependent 53BP1 phosphorylation, as expression of a 53BP1 28A mutant refractory to phosphorylation by ATM[22] in *53BP1*$^{-/-}$ cells restored SCAI recruitment to DSBs as efficiently as wild-type (WT) 53BP1 (Fig. 2a and Supplementary Fig. 2a). Also, downstream effectors of 53BP1, such as RIF1, accumulated at DSB sites independently of SCAI (Supplementary Fig. 2b). Interestingly, while 53BP1 depletion markedly impaired SCAI retention at DSB sites, we noted that a subset of cells displayed residual SCAI recruitment to punctate foci along microlaser-generated DNA damage tracks, which co-localized with RPA (Fig. 2a,c and Supplementary Fig. 2c). On the basis of our previous findings on compartmentalization of nuclear areas flanking DSBs[3,23], we surmised that the 53BP1-independent SCAI microfoci might co-localize with RPA-coated single-stranded DNA (ssDNA) regions generated by DSB end resection (Supplementary Fig. 2c). Indeed, these SCAI microfoci in 53BP1 knockdown cells were eliminated following co-depletion of the key resection factor CtIP, but not by downstream HR factors including BRCA1 and BRCA2 (Fig. 2d and Supplementary Fig. 2d). The mechanism underlying SCAI recruitment to resected DSBs may involve its direct binding to ssDNA stretches, as SCAI interacted with ssDNA oligonucleotides but not RPA (Fig. 1d and Supplementary Fig. 2e). We conclude from these findings that SCAI undergoes enrichment at both the chromatin and ssDNA regions surrounding DSBs, an unusual recruitment pattern observed so far only for BRCA1 and the MRE11-NBS1-RAD50 (MRN) complex[23], key factors in HR.

To understand how SCAI functions in DSB repair, we employed CRISPR/Cas9 technology to generate human cell lines with targeted *SCAI* knockout (KO). While deletion of SCAI did not significantly impact cell cycle distribution, *SCAI* KO cells showed reduced cell survival following exposure to IR (Fig. 2e,f and Supplementary Fig. 3a,b), consistent with a role for SCAI in promoting DSB repair. Reconstitution of *SCAI* KO cells with full-length ectopic SCAI at near-physiological levels fully rescued this defect (Fig. 2e and Supplementary Fig. 3b), demonstrating that it was a specific consequence of *SCAI* ablation. Notably, while 53BP1 loss also sensitized cells to IR as expected, we observed no additive effect of co-depleting SCAI and 53BP1 (Fig. 2f and Supplementary Fig. 3c), suggesting that they operate in a common DSB repair pathway. Using quantitative image analysis to monitor DSB repair kinetics through enumeration of γ-H2AX and 53BP1 foci, we observed a significant increase in persistent γ-H2AX and 53BP1 foci in *SCAI* KO cells, which was restored to WT levels by reintroduction of ectopic SCAI (Fig. 2g and Supplementary Fig. 3b,d). Using established reporter assays for NHEJ- and HR-mediated repair of DSBs[24], we found that SCAI deficiency in human cells led to a pronounced reduction in NHEJ efficiency, while overall HR activity as measured by this system, as well as RAD51 foci formation in response to IR, was not significantly impaired (Supplementary Fig. 3e–i). However, as described below, we obtained evidence that SCAI is important for HR in specific chromosomal contexts.

To characterize the physiological consequences of SCAI loss, we generated *SCAI* knockout mice and verified complete loss of SCAI protein expression in MEFs from *SCAI*$^{-/-}$ animals (Fig. 3a). *SCAI*$^{-/-}$ mice were born at the expected Mendelian frequency (Supplementary Table 1) and showed no overt developmental or survival defects,

© 2016 Macmillan Publishers Limited, part of Springer Nature. All rights reserved.

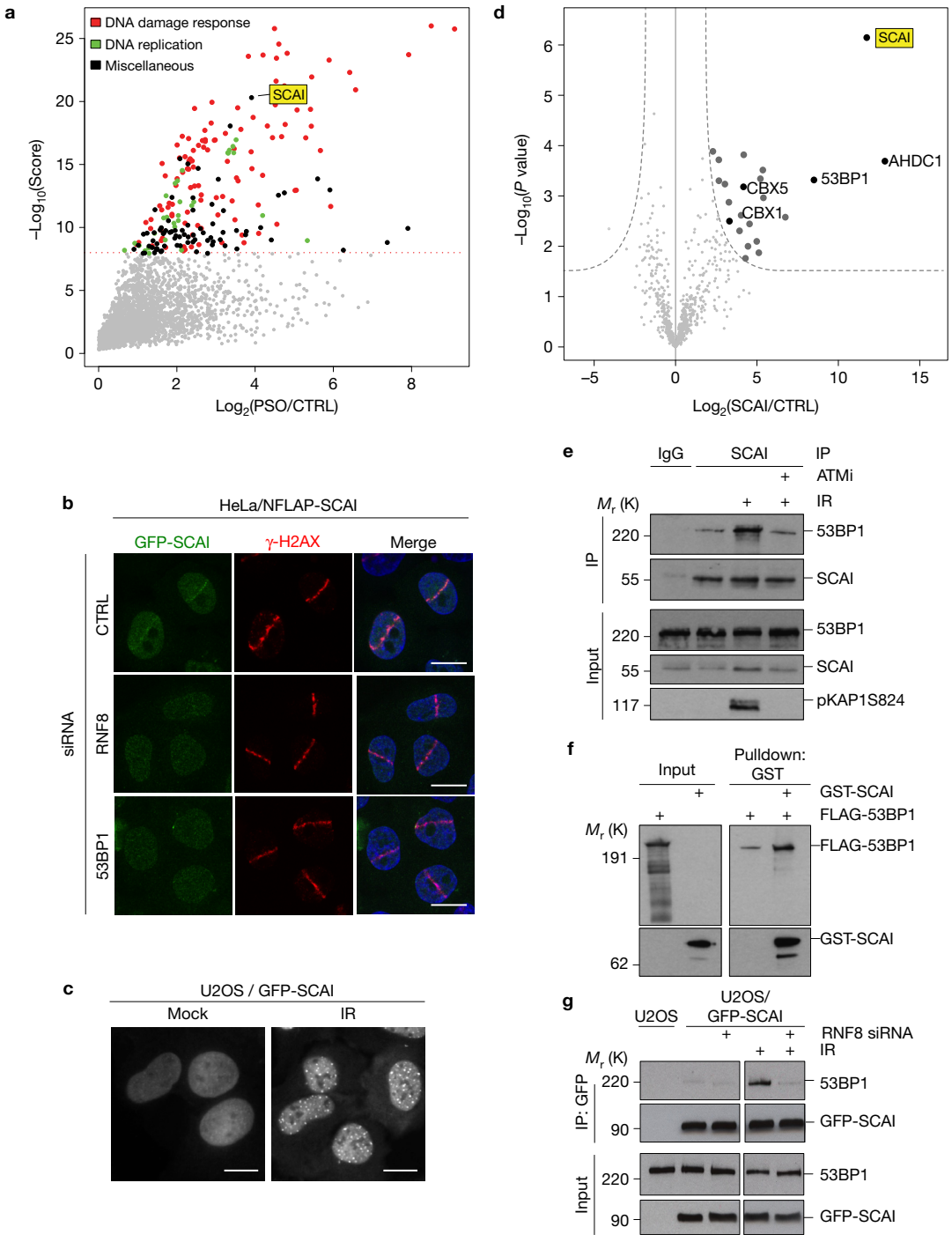

Figure 1 SCAI is recruited to DSB-surrounding chromatin via interaction with 53BP1. (**a**) Analysis of protein recruitment to psoralen-crosslinked chromatin (PSO) compared with undamaged control (CTRL). Chromatin templates were replicated in repair-proficient *Xenopus* egg extracts. After chromatin re-isolation, associated proteins were analysed by mass spectrometry. Maximal protein intensity is plotted against an overall score determined from several independent experiments. The dotted line indicates the significance threshold ($q < 0.01$). Data were replotted from ref. 19. (**b**) HeLa cells stably expressing GFP-tagged human SCAI at endogenous levels from a BAC (NFLAP-SCAI) were transfected with control, RNF8 or 53BP1 siRNAs. Cells were subsequently subjected to laser micro-irradiation, fixed 1 h later, immunostained with γ-H2AX antibody and counterstained with DAPI. (**c**) U2OS cells stably expressing GFP-SCAI were exposed to ionizing radiation (IR, 5 Gy) and fixed 4 h later. (**d**) GFP-SCAI was affinity-purified on GFP-Trap beads from HeLa/NFLAP-SCAI cells, and co-purifying proteins were analysed by QUBIC (quantitative BAC-GFP interactomics) mass spectrometry. Intensities and *P* values for interacting proteins are shown in a volcano plot. (**e**) Chromatin-enriched fractions of U2OS cells exposed to IR and/or ATM inhibitor (ATMi) were subjected to SCAI immunoprecipitation (IP) followed by immunoblotting with antibodies against 53BP1, SCAI and phospho-KAP1. (**f**) Interaction between recombinant full-length FLAG-tagged 53BP1 and GST-tagged SCAI was analysed by GST pulldown followed by immunoblotting with antibodies against FLAG and GST. (**g**) U2OS cells stably expressing GFP-SCAI were transfected with control or RNF8 siRNA and exposed to IR where indicated. Chromatin-enriched fractions were subjected to GFP immunoprecipitation followed by immunoblotting with antibodies against 53BP1 and GFP. All scale bars, 10 μm. Unprocessed original scans of blots (**e**–**g**) are shown in Supplementary Fig. 6.

© 2016 Macmillan Publishers Limited, part of Springer Nature. All rights reserved.

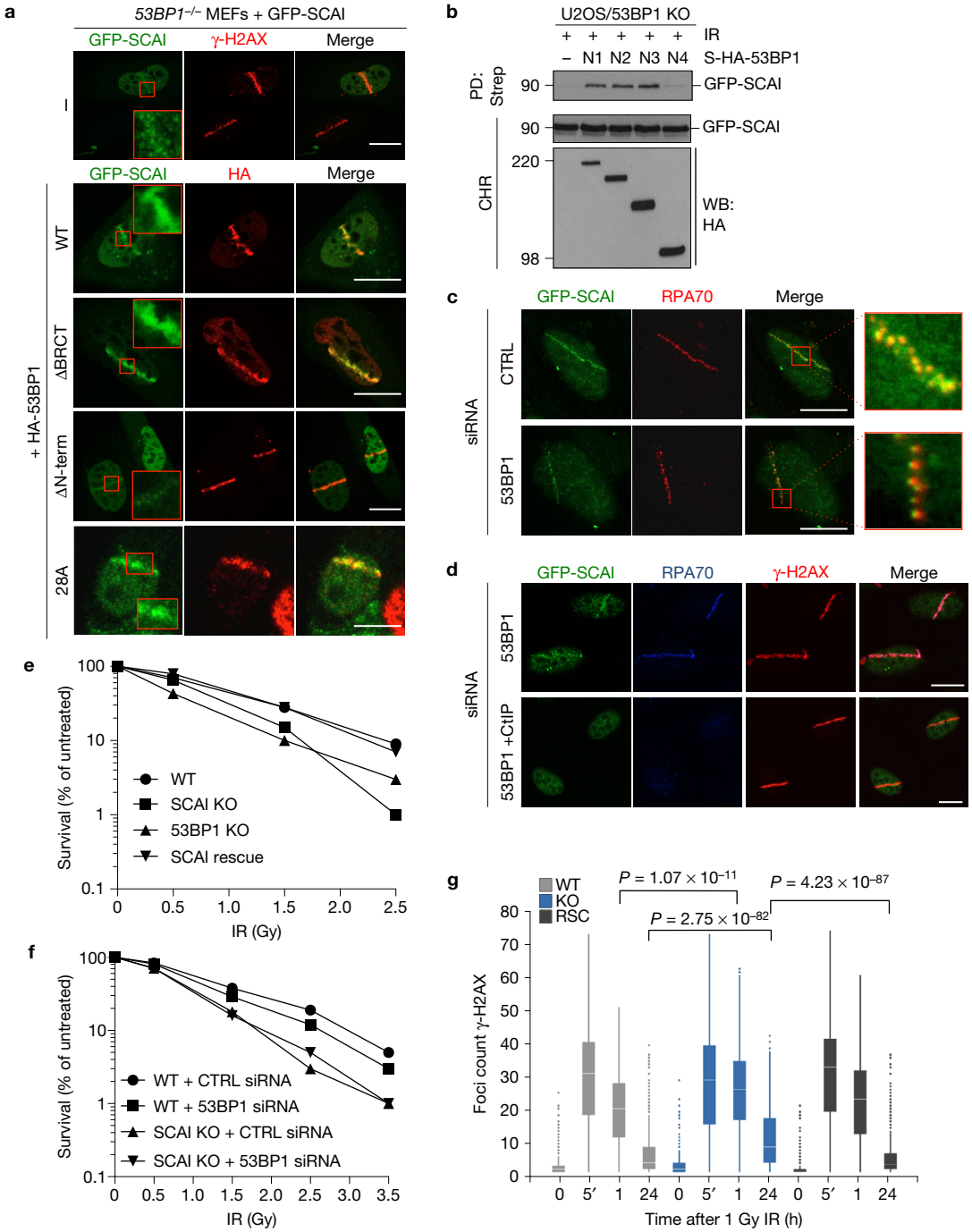

Figure 2 SCAI is required for optimal DSB repair. (**a**) *53BP1*$^{-/-}$ MEFs were co-transfected with GFP-SCAI and the indicated WT or deletion constructs of HA-tagged 53BP1 (Supplementary Fig. 2a), subjected to laser micro-irradiation, fixed 1 h later, and immunostained with γ-H2AX or HA antibody. Insets show larger magnifications of the highlighted regions. (**b**) U2OS cells with targeted knockout of 53BP1 were co-transfected with GFP-SCAI construct and plasmids encoding indicated Strep-HA-tagged fragments of 53BP1. To analyse SCAI-53BP1 interaction, chromatin-enriched fractions were subjected to Strep pulldown followed by immunoblotting with GFP antibody. N1, 53BP1 residues 250–1972; N2, 600–1972; N3, 900–1972; N4, 1230–1972. Unprocessed original scans of blots are shown in Supplementary Fig. 6. (**c**) U2OS cells stably expressing GFP-SCAI were transfected with control or siRNA targeting 53BP1 and treated as in **a**. One hour later, cells were pre-extracted and immunostained with RPA antibody. Insets show larger magnifications of the highlighted regions. (**d**) Cells from **c** transfected with the indicated siRNAs were processed as in **c** and co-immunostained with RPA70 and γ-H2AX antibodies. All scale bars, 10 μm. (**e**) U2OS WT, 53BP1 KO and SCAI KO cells (Supplementary Fig. 3b,c) were exposed to increasing doses of ionizing radiation (IR) and plated for clonogenic survival assays. After 14 days, colonies were fixed, stained and counted. Data points indicate the mean from three observations. (**f**) The indicated U2OS cell lines (Supplementary Fig. 3b) were transfected with control or 53BP1 siRNAs and were treated and analysed as in **e**. (**g**) U2OS cells and derivative cell lines in **e** were fixed at the indicated times after exposure to IR (1 Gy) and stained with γ-H2AX antibody. The number of foci per cell was measured by high-content microscopy. The centre indicates the median and whiskers the borders of the 95% quantiles. 1,000 cells ($n = 1{,}000$ independent measurements) were measured per condition and P values were calculated from a non-parametric two-tailed Mann–Whitney U-test.

© 2016 Macmillan Publishers Limited, part of Springer Nature. All rights reserved.

demonstrating that *SCAI* is not an essential gene. Moreover, *SCAI*$^{-/-}$ primary MEFs proliferated similarly to WT littermate controls (Supplementary Fig. 4a). To test whether loss of SCAI compromises DSB repair capacity in murine cells, we exposed G2 phase WT and *SCAI*$^{-/-}$ MEFs to low doses of IR and monitored 53BP1 foci clearance over time. Similar to human *SCAI* KO cells, we observed a pronounced persistence of 53BP1 foci at late time points across independent *SCAI*$^{-/-}$ primary MEF lines compared with WT lines (Supplementary Fig. 4b,c). Following exposure of WT and *SCAI*$^{-/-}$ mice to whole-body IR, we found that *SCAI*$^{-/-}$ animals died more quickly, ultimately showing an approximately twofold survival decrease in both males and females, compared with controls (Fig. 3b and Supplementary Fig. 4d,e). Together, these data suggest that SCAI has a physiologically important role in promoting DSB repair efficiency and survival after DNA damage in mammals.

While 53BP1 is a key DSB repair factor promoting CSR in B cells[9,10], we found that SCAI has no obvious role in facilitating this function of 53BP1. Specifically, *SCAI*$^{-/-}$ and control mice displayed comparable splenic B cell numbers and frequencies; moreover, proliferation and class-switching to IgG1 and IgG3 was indistinguishable between *SCAI*$^{-/-}$ and control B cells stimulated *ex vivo* (Supplementary Fig. 4f–i). In addition, *SCAI*$^{-/-}$ mice showed no differences in levels of IgG1, IgG3 or IgM in blood serum compared to control mice (Supplementary Fig. 4j). Instead, full-body necropsies showed that male *SCAI*$^{-/-}$ mice had markedly reduced testis size (Fig. 3c,d), suggesting that, unlike 53BP1 knockout[25,26], ablation of SCAI might result in defective spermatogenesis and subfertility. Indeed, while histological examination of *SCAI*$^{-/-}$ testes showed normal distributions of seminiferous tubules at different stages of spermatogenesis, the lumina of the seminiferous tubules were largely devoid of maturing sperm, with some tubules displaying a Sertoli-cell-only phenotype and concomitant expansion of extra-tubular Leydig cells (Fig. 3e (I–IV)). As a consequence of these defects, the caudal epididymis of *SCAI*$^{-/-}$ males contained few if any mature spermatids (Fig. 3e (V–VI)). Ovaries from *SCAI*$^{-/-}$ and control females were similar in size and shape and both contained fully developed corpora lutea (Fig. 3f (I–II)), indicating that overall development of ovary structure and hormonal signalling *per se* were not affected by SCAI loss. However, ovaries from *SCAI*$^{-/-}$ mice contained few or no developing primary follicles (Fig. 3f (I–IV)). Consistent with these germ cell maturation defects, we observed substantial reductions in fertility rates of both male and female *SCAI*$^{-/-}$ mice (nearly threefold and sevenfold, respectively) compared with controls (Supplementary Table 2). Moreover, the few litters generated by *SCAI*$^{-/-}$ female breeding cages were smaller compared with control cages (Supplementary Fig. 4k). We conclude that, unlike loss of 53BP1, SCAI deficiency leads to germ cell development defects and subfertility in both males and females.

To investigate the underlying cause of defective germ cell development associated with SCAI deficiency, we analysed spermatocyte spreads from *SCAI*$^{-/-}$ and control testes stained for meiosis-specific synaptonemal complex markers (SYCP1 and SYCP3). The frequencies of meiotic prophase I spermatocytes in leptonema, early zygonema, late zygonema and diplonema were indistinguishable from controls (Fig. 3g). However, *SCAI*$^{-/-}$ testes showed reduced levels of spermatocytes in pachynema and a concomitant increase in aberrant pachynema-like cells characterized by irregular synaptic behaviour including gaps, breaks and entangled chromosomes (Fig. 3g-i). These data suggest that loss of SCAI leads to impaired meiotic recombination of DNA breaks. Consistently, while the meiosis-specific recombinase DMC1 was loaded normally onto meiotic chromosomes at early stages, DMC1 foci were reduced in late zygonema, early pachynema and on the sex chromosomes of pachynema *SCAI*$^{-/-}$ spermatocytes (Fig. 3j and Supplementary Fig. 4l). Nevertheless, *SCAI*$^{-/-}$ spermatocytes form a proper sex body and show normal numbers of diplonema spermatocytes (Fig. 3g,i). This suggests that while *SCAI*$^{-/-}$ spermatocytes have a reduced ability to synapse homologues, most are capable of progressing through the mid-pachynema checkpoint. Additionally, late pachynema *SCAI*$^{-/-}$ spermatocytes show a normal frequency of MLH1 foci (Fig. 3k), marking sites of future crossovers. Intriguingly, we observed a dramatic reduction in the number of metaphase I cells in *SCAI*$^{-/-}$ testis (Fig. 3l). Metaphase I spermatocytes are lost through apoptosis as a consequence of lagging chromosomes, which are primarily caused by the absence of crossing over between homologues[27]. Our observations suggest that, while crossover designation may be normal in the absence of SCAI, crossing over itself is disrupted. Thus, loss of SCAI may cause impaired accumulation and/or retention of the HR recombinase DMC1 on meiotic chromosomes and aberrant progression through pachynema, ultimately leading to loss of spermatocytes at metaphase I. These results demonstrate that the germ cell developmental defects and subfertility of *SCAI*$^{-/-}$ mice are at least partially due to aberrant meiotic recombination although relatively mild compared with fully HR-deficient spermatocytes (*SPO11*$^{-/-}$ or *DMC1*$^{-/-}$) showing severe synapsis and/or pairing defects[28]. Further supporting a role of SCAI in HR, we observed an increase in chromosomal aberrations in primary *SCAI*$^{-/-}$ B cells compared with controls treated with olaparib, an established sensitizer of HR-compromised cells (Fig. 3m and Supplementary Fig. 4m and Supplementary Table 3)[29–31]. We conclude that SCAI deficiency gives rise to common features of compromised HR-mediated DSB repair in both meiotic and mitotically growing cells.

While SCAI is dispensable for 53BP1-dependent CSR, we reasoned that it might mediate other 53BP1 functions in DSB repair. The SCAI interactome (Fig. 1d) revealed an enrichment of heterochromatin-associated factors including HP1 proteins, which we confirmed biochemically (Supplementary Fig. 5a,b). This raised the possibility that SCAI promotes the function of 53BP1 in repair of heterochromatin-associated DSBs relying on localized, ATM-dependent phosphorylation of KAP1 (pKAP1) in heterochromatin[6,16]. Indicative of a heterochromatin-associated NHEJ defect[16], SCAI deficiency in MEFs arrested in G0/G1 phase gave rise to an increase in persistent 53BP1 foci after IR (Fig. 4a and Supplementary Fig. 5c). Moreover, epistasis experiments using WT and *SCAI*$^{-/-}$ MEFs treated with 53BP1 short interfering RNA (siRNA) or ATM inhibitor showed that loss of SCAI did not exacerbate the DSB repair defect observed following impaired 53BP1 or ATM function (Fig. 4b and Supplementary Fig. 5d), suggesting that SCAI and 53BP1 operate in a common pathway to mediate ATM-dependent repair of heterochromatin-associated DSBs. SCAI was recently found to be enriched in pull-downs with histone H3 tail peptides containing trimethylated Lys9 (H3K9me3)[32], the main repressive histone mark in heterochromatin. Indeed, a heterochromatin correlation analysis confirmed that most unrepaired DSBs at late time points in *SCAI*$^{-/-}$ MEFs were associated

© 2016 Macmillan Publishers Limited, part of Springer Nature. All rights reserved.

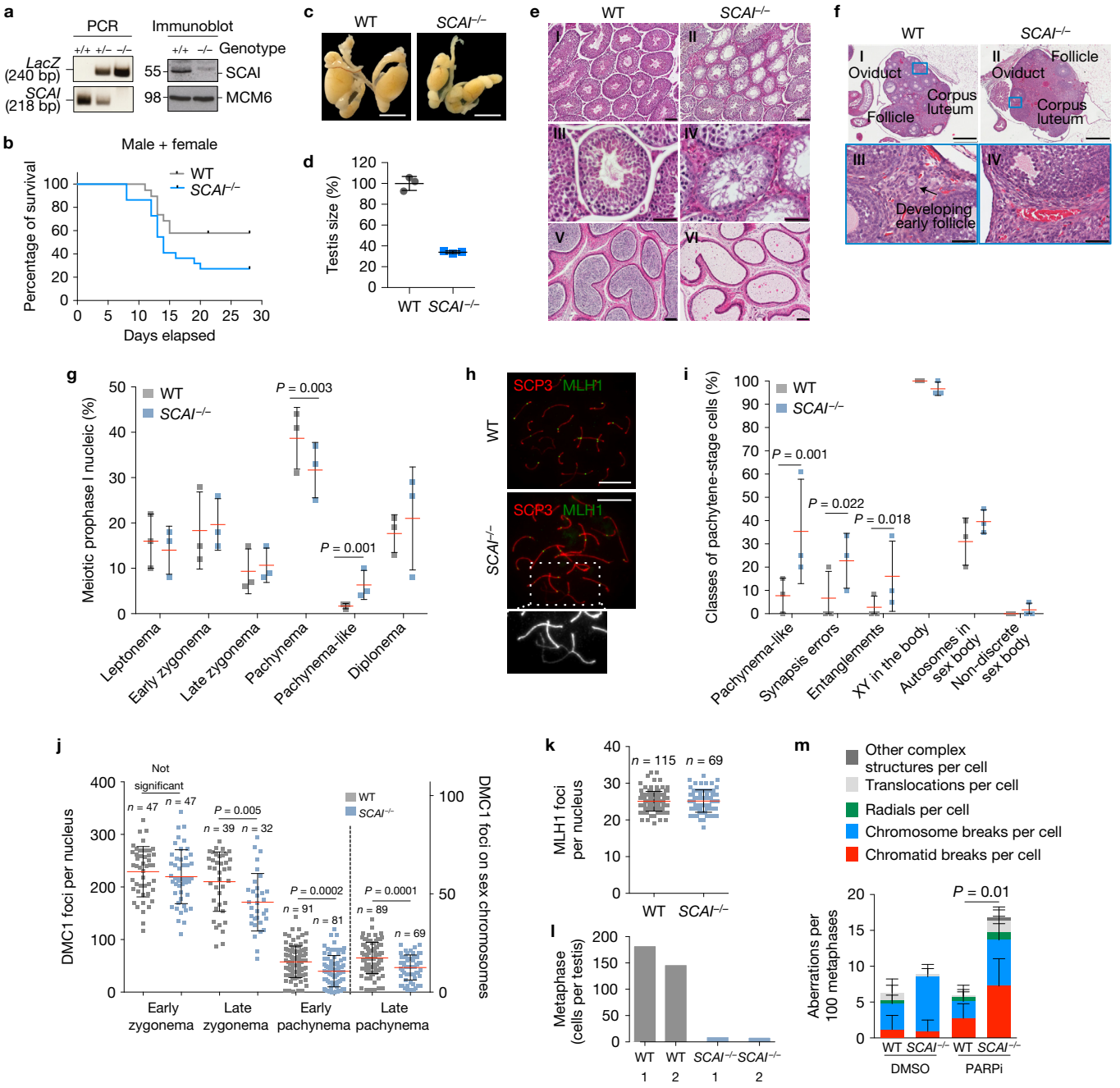

Figure 3 *SCAI* deficiency leads to meiotic recombination defects, germ cell loss and subfertility in mice. (**a**) Confirmation of SCAI gene disruption by PCR on mouse tails (WT = 218 bp, KO = 240 bp) and immunoblotting of MEFs with the indicated antibodies. Unprocessed original scans of blots are shown in Supplementary Fig. 6. (**b**) 8 Gy whole-body gamma irradiation of 19 age-matched WT and 22 *SCAI*$^{-/-}$ mice. Sex-separated data are in Supplementary Fig. 4d,e. (**c**) Testes from 8-week-old WT and *SCAI*$^{-/-}$ mice. Scale bars, 10 mm. (**d**) Sizes of $n = 3$ independent testes from **c**. (**e**) Haematoxylin and eosin (H&E)-stained sections of testes (I–IV) and caudal epididymis (V–VI) from 8-week-old mice. Scale bars I, II, V and VI, 100 μm; III–IV, 50 μm. (**f**) H&E-stained sections of ovaries from 14-week-old mice. Scale bars I and II, 500 μm; III and IV, 50 μm. (**g**) Spermatocyte spreads from WT and *SCAI*$^{-/-}$ mice stained with SYCP1 and SYCP3 antibodies. One hundred cells each from $n = 3$ independent animals were scored and the percentage of cells at each stage plotted. Data were analysed by Fisher's exact test, two-tailed. (**h**) Representative images of spermatocytes stained for MLH1 and SYCP3 showing a pachynema WT cell and a pachynema-like *SCAI*$^{-/-}$ cell. Inset: magnification of the boxed area with entangled chromosomes and loss of synapsis indicated by weaker SYCP3 staining. Scale bars, 10 μm. (**i**) Spermatocytes from **h** were stained for SYCP3 and γ-H2AX to identify chromosome entanglements and sex body. $n = 3$ independent animals were examined and a total of 52 and 58 cells analysed for WT and *SCAI*$^{-/-}$, respectively. Statistical analysis was performed as in **g**. (**j**) DMC1 foci were counted at the indicated stages of meiotic prophase I. Pooled cells from three independent animals. *P* values were calculated from a Mann–Whitney test. (**k**) MLH1 foci counts were plotted as in **j**. Pooled cells from three independent animals. (**l**) Total number of metaphase cells from one testis. (**m**) Metaphase spreads of primary B cells from WT and *SCAI*$^{-/-}$ mice treated with dimethylsulfoxide (DMSO) or PARP inhibitor (PARPi) for 16 h were FISH-stained for telomeric DNA and analysed for chromosomal aberrations. See Supplementary Table 3 and Supplementary Fig. 4m. *P* value was calculated as in **j** ($n = 6$ independent mice of each genotype). All data points are represented as mean ± s.d.

© 2016 Macmillan Publishers Limited, part of Springer Nature. All rights reserved.

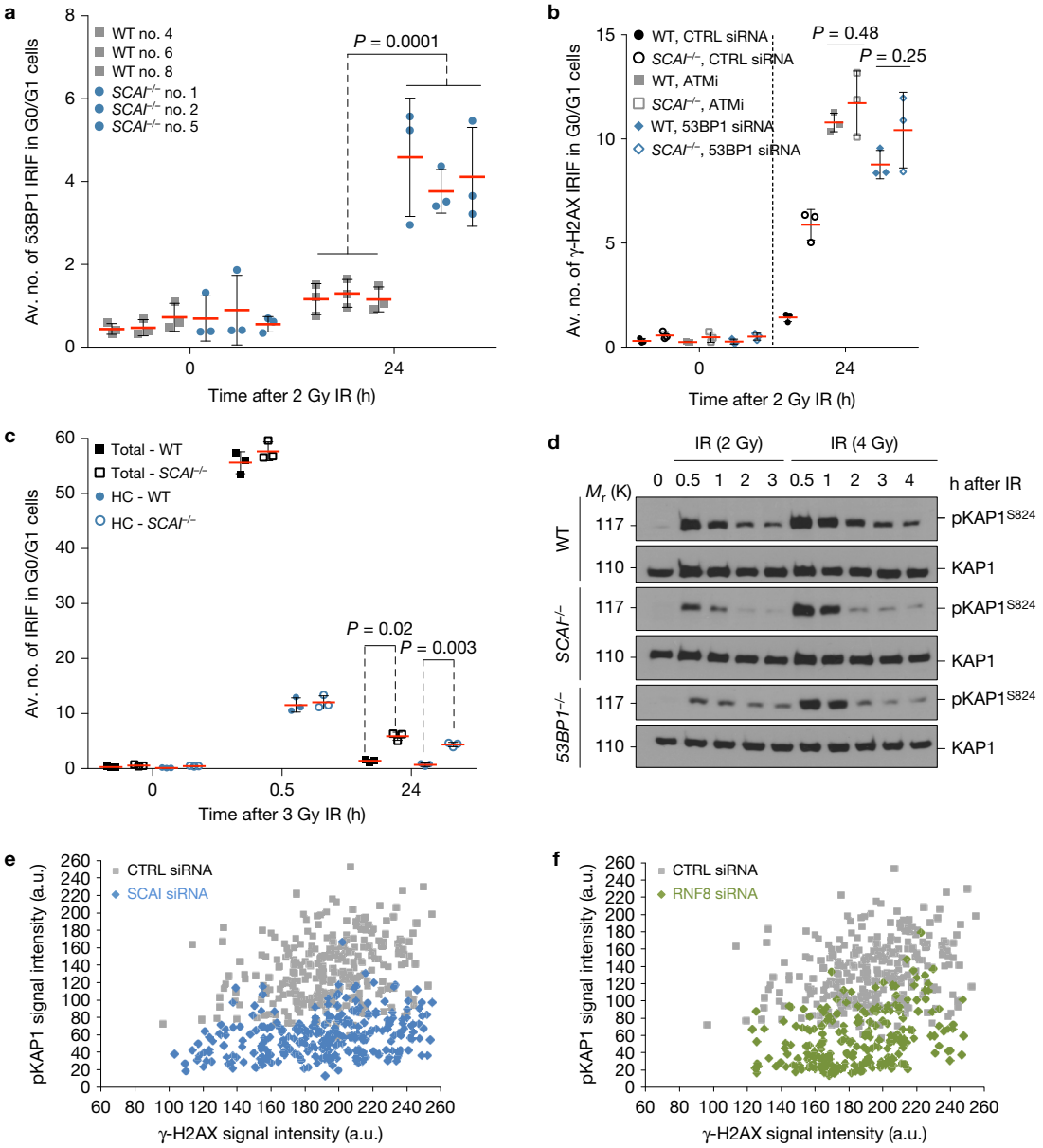

Figure 4 ATM, 53BP1 and SCAI operate in a common pathway to mediate repair of heterochromatin-associated DSBs. (**a**) Independent, immortalized WT and *SCAI*$^{-/-}$ MEF cell lines were arrested in G0/G1 by growing to full confluency. Cultures were mock-treated or exposed to IR (2 Gy), fixed 24 h later and stained with 53BP1 antibody. Images were acquired as *Z*-stacks and the number of 53BP1 foci per cell was counted through the entire nuclear volume. *P* value was calculated from a one-tailed *t*-test using Welch correction ($n = 9$ independent measurements across 3 MEF lines). Bars indicate mean ± s.d. See Supplementary Fig. 5c for the full data set including a 0.5 h time point. IRIF, ionizing radiation-induced foci. (**b**) Immortalized WT and *SCAI*$^{-/-}$ MEFs were grown to full confluency while transfecting with 53BP1 siRNA for 72 h or incubating with ATM inhibitor (ATMi) for 1 h prior to irradiation. Cells were treated and analysed as in **a**, except that they were immunostained for γ-H2AX as a marker of unrepaired DSB ($n = 3$ biologically independent samples). See Supplementary Fig. 5d for the full data set including a 0.5 h time point. (**c**) Immortalized WT and *SCAI*$^{-/-}$ MEFs were treated as in **a**, except that cells were co-stained with antibodies against γ-H2AX and the heterochromatin marker H3K9me3 to determine chromatin context ($n = 3$ biologically independent samples). HC, heterochromatin. See Supplementary Fig. 5e for analysis of ATM inhibitor-treated samples. (**d**) Immortalized WT, *SCAI*$^{-/-}$ and *53BP1*$^{-/-}$ MEFs were grown to confluency, exposed to IR (2 or 4 Gy) and harvested at the indicated time points. Lysates were analysed by immunoblotting with antibodies against total and phosphorylated KAP1. Unprocessed original scans of blots are shown in Supplementary Fig. 6. (**e**) Quiescent 48BR primary human fibroblasts were transfected with control or SCAI siRNAs, irradiated with IR and fixed after 24 h. Cells were immunostained with antibodies against γ-H2AX and phosphorylated KAP1 (pKAP1), and the relative fluorescence intensities were measured by high-content microscopy. Each data point represents one individual IRIF. See Supplementary Fig. 5f for representative images. (**f**) As in **e**, except that cells were transfected with control or RNF8 siRNAs. See Supplementary Fig. 5f for representative images.

with H3K9me3-positive chromocentres (Fig. 4c and Supplementary Fig. 5e). Similar to *53BP1*$^{-/-}$ MEFs, immediate IR-induced pKAP1, a marker of productive DSB repair in heterochromatin[16], was markedly reduced after low IR doses in quiescent *SCAI*$^{-/-}$ MEFs (Fig. 4d). This effect was partly masked on increasing IR doses (Fig. 4d), as seen also in 53BP1-deficient cells[16]. The pKAP1 defect was also evident at

© 2016 Macmillan Publishers Limited, part of Springer Nature. All rights reserved.

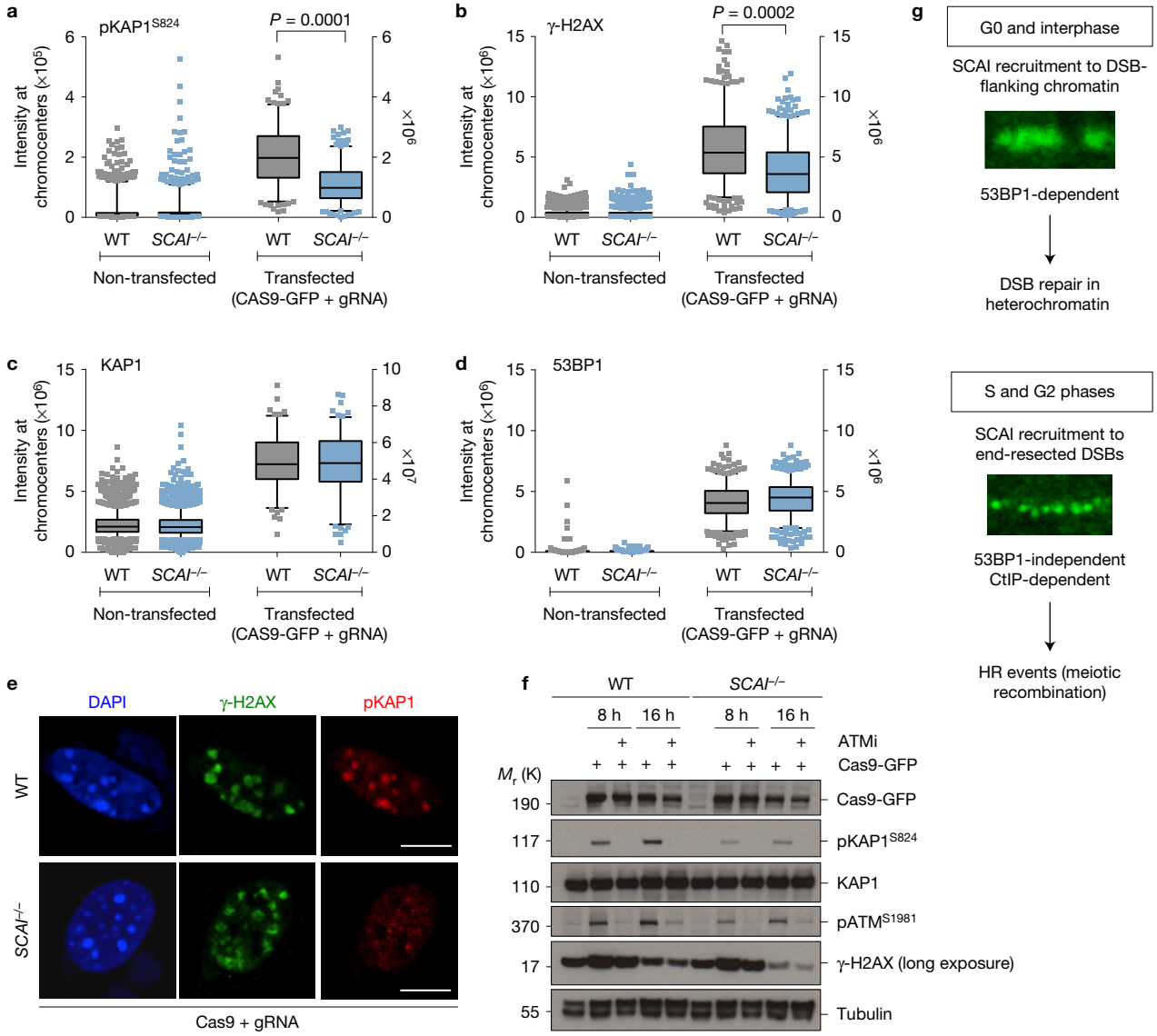

Figure 5 SCAI mediates ATM signalling from DSBs in heterochromatin. (**a**) Immortalized WT and *SCAI*$^{-/-}$ MEFs were transfected with Cas9-GFP and guide RNAs (gRNAs) targeting the major satellite repeats to induce CRISPR-mediated DSBs in heterochromatin-containing chromocentres. After 8 h cells were fixed and immunostained with antibodies against phosphorylated KAP1 (pKAP1). Cells were analysed by high-content microscopy using DAPI signal as a mask for chromocentres. *P* values were calculated from two-tailed *t*-tests using Welch correction. The centre indicates the median and whiskers the borders of the 95% quantiles. The *y* axis on the left side corresponds to the non-transfected conditions, while the *y* axis on the right side corresponds to the transfected conditions. ($n = 200$ independent measurements). (**b**) As in **a**, except cells were immunostained with γ-H2AX antibodies ($n = 430$ independent measurements). (**c**) As in **a**, except cells were immunostained with KAP1 antibodies ($n = 125$ independent measurements). (**d**) As in **a**, except cells were immunostained with 53BP1 antibodies ($n = 550$ independent measurements). (**e**) Representative images from the experiments in **a**,**b**. Scale bars, 10 μm. (**f**) Immortalized WT and *SCAI*$^{-/-}$ MEFs were transfected as in **a** while treated with ATM inhibitor (ATMi) where indicated. Cell extracts were analysed by immunoblotting with the indicated antibodies. Unprocessed original scans of blots are shown in Supplementary Fig. 6. (**g**) Model of SCAI function in DSB repair. SCAI is recruited to DSB-proximal chromatin throughout interphase through direct interaction with 53BP1, promoting 53BP1- and ATM-mediated repair of heterochromatic DSBs. Notably, SCAI is dispensable for other 53BP1-dependent functions, such as immunoglobulin class-switching. During the S and G2 phases of the cell cycle, SCAI also accumulates at CtIP-resected ssDNA regions in a 53BP1-independent manner. From this locale, SCAI supports a subset of HR events, and its deficiency is associated with defects in meiotic recombination and germ cell development.

persistent heterochromatin-associated breaks, as SCAI knockdown in quiescent 48BR primary human fibroblasts strongly reduced the decoration of γ-H2AX foci with pKAP1 after IR (Fig. 4e and Supplementary Fig. 5f). Knockdown of RNF8, an essential mediator of 53BP1 accumulation at DSB sites[7], phenocopied the effect of SCAI depletion (Fig. 4f and Supplementary Fig. 5f). Collectively, these data suggest that SCAI functions downstream of 53BP1 in heterochromatin-associated DSB repair to mediate ATM-dependent KAP1 phosphorylation in repressive chromatin environments.

To further characterize the DSB repair function of SCAI in heterochromatin, we employed a CRISPR/Cas9-based system using guide RNAs (gRNAs) targeting major satellite repeats to induce

© 2016 Macmillan Publishers Limited, part of Springer Nature. All rights reserved.

heterochromatin-specific DSBs in murine cells[33]. The resulting breaks caused rapid accumulation of 53BP1 and GFP-SCAI in DAPI-rich chromocentres corresponding to heterochromatin (Supplementary Fig. 5g). Employing this system to assay signalling from heterochromatin-associated DSBs in WT and *SCAI*$^{-/-}$ MEFs, we found that SCAI deficiency specifically compromised ATM-dependent phosphorylation of KAP1 and H2AX following DSB formation in heterochromatin, while it had no effect on total levels of KAP1 or 53BP1 accumulation at these structures (Fig. 5a–f). Moreover, loss of SCAI did not significantly impact the size and composition of DSB-containing chromocentres, as evidenced by markers such as DAPI, HP1 and H3K9me3 (Supplementary Fig. 5h–k). Consistent with a role for SCAI in promoting overall ATM signalling at heterochromatin-associated DSBs, overexpression of SCAI enhanced ATM-mediated phosphorylations following formation of such breaks (Supplementary Fig. 5l). Importantly, *SCAI*$^{-/-}$ MEFs did not display obvious ATM signalling defects after IR-induced DSBs, which mostly target euchromatic regions of the genome[34] (Supplementary Fig. 5m). Together, these results demonstrate that SCAI functions downstream of 53BP1 to mediate ATM-dependent signalling after DSBs specifically in heterochromatin. 53BP1 promotes repair of heterochromatin-associated DSBs via both NHEJ (in G0/G1 phase cells) and HR (in G2 phase cells)[16,35,36]. As SCAI deficiency gives rise to a DSB repair defect in both G0 and G2 phase cells, it is possible that SCAI mediates productive DSB repair in compacted heterochromatin via either of these major DSB repair pathways through chromatin remodelling events that facilitate the access of the repair machinery to the lesions.

Collectively, our data establish SCAI as a physiologically important chromatin-associated component of the cellular machinery that mediates DSB repair in different chromosomal contexts. This involvement minimally includes roles of SCAI in promoting 53BP1-dependent DSB repair in heterochromatin and 53BP1-independent crossover/DSB repair reactions on resected DNA ends during meiotic recombination, probably reflecting its unusual, dual presence at chromatin and end resection-dependent ssDNA regions flanking DSBs, respectively (Fig. 5g). Whether SCAI promotes these processes via common or distinct mechanisms, and precisely how it exerts its DSB repair functions at the molecular level, are important future areas of study. □

METHODS

Methods, including statements of data availability and any associated accession codes and references, are available in the online version of this paper.

Note: Supplementary Information is available in the online version of the paper

ACKNOWLEDGEMENTS

We thank C. Obuse (University of Hokkaido, Japan) and H. Kimura (University of Osaka, Japan) for sharing unpublished data, A. Nussenzweig (National Institutes of Health, USA), J. Rouse (University of Dundee, UK), V. Gorbunova (University of Rochester, USA), A. Hyman and I. Poser (both Max Planck Institute of Cell Biology and Genetics, Germany) for providing reagents, G. Karemore for statistical analysis support and J. Bulkescher (both University of Copenhagen, Denmark) for technical assistance with imaging. Work in the laboratory of N.M. was supported by grants from the Novo Nordisk Foundation (Grants no. NNF14CC0001 and NNF15OC0016926), European Research Council (ERC), The Danish Cancer Society, Danish Medical Research Council, and the Lundbeck Foundation. Work in the laboratory of M.M. was supported by the Center for Integrated Protein Research Munich (CIPSM). Work in the laboratory of J.A.D. was supported by grants from the Novo Nordisk Foundation (Grant no. NNF14CC0001) and the Danish Medical Research Council, and A.M. is supported by a Marie Curie Intra-European Fellowship for Career Development (Project no. 627187). The laboratory of A.A.G. is supported by the Canadian Institutes of Health Research. A.A.G is currently the Canada Research Chair for Genome Damage and Instability Disease and this work was undertaken, in part, thanks to funding from the Canada Research Chairs programme. Work in the laboratory of F.C. is supported by the Cancer Prevention and Research Institute of Texas (R1213), the Jeanne F. Shelby Scholarship Fund for the R. Lee Clark Fellowship, and the National Institutes of Health (DP2HD087943). Work in the laboratory of R.G. is supported by the German Research Foundation (Grant GR 2111/2-2). All experiments were performed in full compliance with the ethical guidelines for biological research in Denmark. Work with all animals has been approved by the Department of Experimental Medicine (University of Copenhagen), the Danish Working Environment Authority, the Danish Animal Experiment Inspectorate, the MDACC Institutional Animal Care and Use Committee (IACUC) and the Regierungspräsidia Karlsruhe and Darmstadt.

AUTHOR CONTRIBUTIONS

R.K.H., A.M., S.L.P., K.T. and K.K. performed the biochemical and cell biological experiments. R.S., A.M. and M.S. carried out mouse experiments. B.R. performed and analysed the mouse histology experiments. M.R. performed and analysed the proteomics experiments. R.K.H. and M.T. designed and generated CRISPR-based knockout cell lines. S.O., T.W., R.G. and D.T.B. generated the SCAI knockout mouse. M.R., M.M., F.C., E.S., A.A.G., J.A.D., N.M. and S.B.-J. designed the experiments, and N.M. and S.B.-J. conceived the project and wrote the manuscript. All authors discussed the results and commented on the manuscript.

COMPETING FINANCIAL INTERESTS

The authors declare no competing financial interests.

Published online at http://dx.doi.org/10.1038/ncb3436
Reprints and permissions information is available online at www.nature.com/reprints

1. Kastan, M. B. & Bartek, J. Cell-cycle checkpoints and cancer. *Nature* **432,** 316–323 (2004).
2. Ciccia, A. & Elledge, S. J. The DNA damage response: making it safe to play with knives. *Mol. Cell* **40,** 179–204 (2010).
3. Bekker-Jensen, S. & Mailand, N. Assembly and function of DNA double-strand break repair foci in mammalian cells. *DNA Repair* **9,** 1219–1228 (2010).
4. Jackson, S. P. & Bartek, J. The DNA-damage response in human biology and disease. *Nature* **461,** 1071–1078 (2009).
5. Lukas, J., Lukas, C. & Bartek, J. More than just a focus: the chromatin response to DNA damage and its role in genome integrity maintenance. *Nat. Cell Biol.* **13,** 1161–1169 (2011).
6. Lemaitre, C. & Soutoglou, E. Double strand break (DSB) repair in heterochromatin and heterochromatin proteins in DSB repair. *DNA Repair* **19,** 163–168 (2014).
7. Schwertman, P., Bekker-Jensen, S. & Mailand, N. Regulation of DNA double-strand break repair by ubiquitin and ubiquitin-like modifiers. *Nat. Rev. Mol. Cell Biol.* **17,** 379–394 (2016).
8. Bunting, S. F. & Nussenzweig, A. End-joining, translocations and cancer. *Nat. Rev. Cancer* **13,** 443–454 (2013).
9. Manis, J. P. *et al.* 53BP1 links DNA damage-response pathways to immunoglobulin heavy chain class-switch recombination. *Nat. Immunol.* **5,** 481–487 (2004).
10. Ward, I. M. *et al.* 53BP1 is required for class switch recombination. *J. Cell Biol.* **165,** 459–464 (2004).
11. Callen, E. *et al.* 53BP1 mediates productive and mutagenic DNA repair through distinct phosphoprotein interactions. *Cell* **153,** 1266–1280 (2013).
12. Di Virgilio, M. *et al.* Rif1 prevents resection of DNA breaks and promotes immunoglobulin class switching. *Science* **339,** 711–715 (2013).
13. Escribano-Diaz, C. *et al.* A cell cycle-dependent regulatory circuit composed of 53BP1-RIF1 and BRCA1-CtIP controls DNA repair pathway choice. *Mol. Cell* **49,** 872–883 (2013).
14. Chapman, J. R. *et al.* RIF1 is essential for 53BP1-dependent nonhomologous end joining and suppression of DNA double-strand break resection. *Mol. Cell* **49,** 858–871 (2013).
15. Zimmermann, M., Lottersberger, F., Buonomo, S. B., Sfeir, A. & de Lange, T. 53BP1 regulates DSB repair using Rif1 to control 5' end resection. *Science* **339,** 700–704 (2013).
16. Noon, A. T. *et al.* 53BP1-dependent robust localized KAP-1 phosphorylation is essential for heterochromatic DNA double-strand break repair. *Nat. Cell Biol.* **12,** 177–184 (2010).
17. Goodarzi, A. A., Kurka, T. & Jeggo, P. A. KAP-1 phosphorylation regulates CHD3 nucleosome remodeling during the DNA double-strand break response. *Nat. Struct. Mol. Biol.* **18,** 831–839 (2011).
18. Klement, K. *et al.* Opposing ISWI- and CHD-class chromatin remodeling activities orchestrate heterochromatic DNA repair. *J. Cell Biol.* **207,** 717–733 (2014).
19. Raschle, M. *et al.* Proteomics reveals dynamic assembly of repair complexes during bypass of DNA cross-links. *Science* **348,** 1253671 (2015).
20. Brandt, D. T., Xu, J., Steinbeisser, H. & Grosse, R. Regulation of myocardin-related transcriptional coactivators through cofactor interactions in differentiation and cancer. *Cell Cycle* **8,** 2523–2527 (2009).

© 2016 Macmillan Publishers Limited, part of Springer Nature. All rights reserved.

21. Brandt, D. T. *et al.* SCAI acts as a suppressor of cancer cell invasion through the transcriptional control of β1-integrin. *Nat. Cell Biol.* **11,** 557–568 (2009).
22. Bothmer, A. *et al.* Regulation of DNA end joining, resection, and immunoglobulin class switch recombination by 53BP1. *Mol. Cell* **42,** 319–329 (2011).
23. Bekker-Jensen, S. *et al.* Spatial organization of the mammalian genome surveillance machinery in response to DNA strand breaks. *J. Cell Biol.* **173,** 195–206 (2006).
24. Gunn, A. & Stark, J. M. I-SceI-based assays to examine distinct repair outcomes of mammalian chromosomal double strand breaks. *Methods Mol. Biol.* **920,** 379–391 (2012).
25. Ward, I. M., Minn, K., van Deursen, J. & Chen, J. p53 binding protein 53BP1 is required for DNA damage responses and tumor suppression in mice. *Mol. Cell Biol.* **23,** 2556–2563 (2003).
26. Broering, T. J. *et al.* BRCA1 establishes DNA damage signaling and pericentric heterochromatin of the X chromosome in male meiosis. *J. Cell Biol.* **205,** 663–675 (2014).
27. Svetlanov, A. & Cohen, P. E. Mismatch repair proteins, meiosis, and mice: understanding the complexities of mammalian meiosis. *Exp. Cell Res.* **296,** 71–79 (2004).
28. Hunter, N. Meiotic recombination: the essence of heredity. *Cold Spring Harb. Perspect. Biol.* **7,** a016618 (2015).
29. Jackson, S. P. The DNA-damage response: new molecular insights and new approaches to cancer therapy. *Biochem. Soc. Trans.* **37,** 483–494 (2009).
30. Farmer, H. *et al.* Targeting the DNA repair defect in BRCA mutant cells as a therapeutic strategy. *Nature* **434,** 917–921 (2005).
31. Bryant, H. E. *et al.* Specific killing of BRCA2-deficient tumours with inhibitors of poly(ADP-ribose) polymerase. *Nature* **434,** 913–917 (2005).
32. Eberl, H. C., Spruijt, C. G., Kelstrup, C. D., Vermeulen, M. & Mann, M. A map of general and specialized chromatin readers in mouse tissues generated by label-free interaction proteomics. *Mol. Cell* **49,** 368–378 (2013).
33. Tsouroula, K. *et al.* Temporal and spatial uncoupling of DNA double strand break repair pathways within mammalian heterochromatin. *Mol. Cell* **63,** 293–305 (2016).
34. Cowell, I. G. *et al.* γH2AX foci form preferentially in euchromatin after ionising-radiation. *PLoS ONE* **2,** e1057 (2007).
35. Goodarzi, A. A. *et al.* ATM signaling facilitates repair of DNA double-strand breaks associated with heterochromatin. *Mol. Cell* **31,** 167–177 (2008).
36. Kakarougkas, A. *et al.* Opposing roles for 53BP1 during homologous recombination. *Nucleic Acids Res.* **41,** 9719–9731 (2013).

© 2016 Macmillan Publishers Limited, part of Springer Nature. All rights reserved.

METHODS

Plasmids and siRNAs. Full-length *SCAI* cDNA was amplified by PCR and inserted into pEGFP-C1 (Clontech) and pcDNA4/TO (Life Technologies) containing an N-terminal Strep-HA-tag to generate mammalian expression plasmids for GFP-tagged and Strep-HA-tagged SCAI, respectively. The CMK6-HA-53BP1 plasmid was described previously[19]. 53BP1 N-terminal deletion constructs (N1–N4) were amplified by PCR and inserted into pcDNA4/TO-Strep-HA. Plasmid transfections were performed using GeneJuice (Novagen) or FuGene 6 (Promega) according to the manufacturer's instructions. siRNA transfections were done using RNAiMAX (Life Technologies) according to the manufacturer's instructions. siRNA target sequences used in this study were: control (5'-GGGAUACCUAGACGUUCUA-3'), SCAI (no. 9) (5'-GAGGCGGAUCCUGUAAUGGUA-3'); SCAI (no.10) (5'-GGACAG ACCUGAAUUGGUA-3'); 53BP1 (5'-GGACUCCAGUGUUGUCAUUUU-3'), RNF8 (5'-UGCGGAGUAUGAAUAUGAA-3'); CtIP (5'-GCUAAAACAGGAAC GAAUCTT-3'); BRCA1 (5'-GGAACCUGUCUCCACAAAGTT-3'); RNF8 (5'-U GCGGAGUAUGAAUAUGAATT-3'); and RNF168 (5'-GGCGAAGAGCGAUG GAGGATT-3'). BRCA2 siRNA was an siGENOME SMARTpool from Dharmacon (M-003462-01).

Plasmids for generation of *SCAI* knockout cells by CRISPR/Cas9 were generated as described previously[37]. Briefly, SCAI gRNA sequences were introduced into pEsgRNA by PCR-based insertion mutagenesis. gRNA sequences used were: SCAI no. 2: 5'-GTCTAATAGTGTTGCGTATAAGG-3' (chr9: 127757212-127757234); SCAI no. 4: 5'-GGCTTGAAGCGCTGGCAAATAGG-3' (chr9: 127790713-127790735); 53BP1 no. 1: 5'-GCCAGCTCCTGCTCGAAGCTGGG-3' (chr15: 43701875-43701897); and 53BP1 no. 2: 5'-GTTGACTCTGCCTGATTGTATG G-3' (chr15: 43724790-43724812). gRNA targeting major satellite repeats was cloned into vector containing U6 promoter plus followed by a gRNA scaffold. Sequence: Ma-sat no. 3: 5'-GAAATGTCCACTGTAGGACG-3' . Cas9 cDNA was amplified from pX330-U6-Chimaeric_BB-CBh-hSpCas9 (gift from F. Zhang, Massachusetts Institute of Technology, USA) and cloned using golden gate cloning into pCX5-CMVp-Cas9-EGFP-SV40p-Puro-pA and pX-86-U6p-gRNA(Ma-sat no. 3)-CMVp-Cas9-mCherry-SV40p-HygroR-pA plasmids to generate EGFP-tagged and mCherry-tagged Cas9 expression constructs, respectively.

Cell culture and reagents. All standard cell lines were obtained from ATCC and regularly tested for mycoplasma infection. The cell lines were not further authenticated and are not found in the database of commonly misidentified cell lines that is maintained by ICLAC and NCBI Biosample. Human U2OS, HeLa and 48BR cells were cultured in DMEM (GIBCO) containing 10% fetal bovine serum. Mouse NIH-3T3 cells were cultured in DMEM containing 10 % newborn calf serum. To generate cell lines stably expressing GFP-tagged SCAI, U2OS cells were co-transfected with pEGFP-C1-SCAI and pBabe.puro plasmids and positive single-cell clones were expanded in the presence of puromycin (1 μg ml^{-1}, Sigma). Doxycycline-induced Strep-HA-tagged SCAI cell lines were obtained by co-transfection of pcDNA4/TO-Strep-HA-SCAI and pcDNA6/TR (Life Technologies) and expansion of single-cell clones under Zeocin (0.2 μg ml^{-1}, Life Technologies) and blasticidin S (5 μg ml^{-1}, InVivoGen) selection. The HeLa/NFLAP-SCAI BAC cell line was a gift from A. Hyman (Max Planck Institute of Molecular Cell Biology and Genetics, Germany). *53BP1*$^{-/-}$ MEFs and reconstituted cell lines were a gift from A. Nussenzweig (National Institutes of Health, USA). For B cell cultures, resting splenic B cells were isolated from 8–14-week-old WT or *SCAI*$^{-/-}$ mice with anti-CD43 microbeads (anti-Ly48; Miltenyi Biotech no. 130-049-801) and stimulated to undergo class-switching with either LPS (25 μg ml^{-1}), α-IgD-dextran (2.5 ng ml^{-1}) and RP105 (0.5 μg ml^{-1}) for CSR to IgG3 or LPS (25 μg ml^{-1}), IL4 (5 ng ml^{-1}) and RP105 (0.5 μ g ml^{-1}) for CSR to IgG1, as described previously[38]. B cell proliferation was analysed by CFSE-like labelling using CellTrace Violet proliferation kit (no. C34557, Life Technologies) according to the manufacturer's instructions. Primary MEFs derived from E13.5 were obtained by intercrossing mice following standard procedures. For immortalization, MEFs were subjected to retroviral infections with SV40LT at passage 2 and cultured in DMEM supplemented with 15% fetal bovine serum (GIBCO), 100 U ml^{-1} penicillin and 0.1 mg ml^{-1} streptomycin (Sigma). Fibroblast proliferative capacities were assayed by plating passage 2 primary MEF lines (P2). Every 2 days, cells from each dish were trypsinized, counted and replated. Cells were treated with inhibitors targeting ATM kinase (KU60019 (10 μM, Selleckchem) or KU55933 (10 μM, Selleckchem)), proteasome (MG132 (20 μM, AH Diagnostics)) and PARP-1 (olaparib (1 μM, AZD2281, Selleckchem)). To induce DSBs, cells were exposed to the indicated doses of X-rays using a Y.SMART tube (YXLON A/S) at 6 mA and 160 kV through a 3-mm aluminium filter. For high-content imaging of RAD51 foci, cells were exposed to IR from a caesium irradiator.

CRISPR/Cas9 genome editing. SCAI or 53BP1 CRISPR knockout cell lines were generated as described previously[37]. Briefly, gRNA plasmids were co-transfected with pBabe.Puro in Cas9-FLAG U2OS SEC-C cells (a gift from J. Rouse, University of Dundee, UK)[37]. Cells were grown in DMEM in the presence of doxycycline to induce Cas9-FLAG expression. Subsequently, cells were grown in the presence of puromycin during clonal selection for 7–10 days. Knockdown efficiency was validated by qPCR and immunoblotting. Generation of heterochromatin-specific DSBs by Cas9 was achieved by transfecting cells with major satellite-specific gRNA and GFP-mCherry-Cas9 for 8 or 16 h, before pre-extraction in 0.1% Triton/PBS for 30 s followed by fixation in 4% paraformaldehyde/PBS for 10 min.

Mass spectrometry. Analysis of replication-dependent recruitment of proteins to damaged chromatin by means of the CHROMASS method was performed as described previously[19]. In brief, psoralen-crosslinked chromatin was incubated in repair-proficient *Xenopus* egg extracts. Chromatin was isolated by sedimentation through a sucrose cushion and analysed by mass spectrometry.

SCAI-interacting proteins were identified by QUBIC, as described previously[39]. HeLa BAC cells expressing GFP-tagged SCAI (NFLAP-SCAI) under the control of the endogenous promoter were cultured in DMEM. Pellets from ~10^7 cells were resuspended in 1 ml lysis buffer (50 mM Tris, pH 7.5; 150 mM NaCl; 5% glycerol; 1% NP-40; 1 mM $MgCl_2$) containing 200 U Benzonase (Merck) and EDTA-free complete protease inhibitor cocktail (Roche) and incubated for 30 min on ice. Cell lysates were cleared by centrifugation and GFP-tagged proteins were bound to 50 μl magnetic beads coupled to monoclonal mouse GFP antibody (Miltenyi Biotec, no. 130-091-125) for 15 min on ice. Bound proteins were washed three times with 800 μl ice-cold wash buffer I (50 mM Tris, pH 7.5; 150 mM NaCl; 5% glycerol; 0.05% NP-40) and two times with 500 μl wash buffer II (50 mM Tris, pH 7.5; 150 mM NaCl; 5% glycerol). Purified proteins were digested on beads at room temperature by adding 25 μl digestion buffer (50 mM Tris, pH 7.5; 2 M urea) containing 150 ng trypsin (Promega) and 1 mM dithiothreitol. After 30 min, peptides were eluted by adding twice 50 μl digestion buffer containing 5 mM chloracetamid. After overnight digestion at room temperature, peptides were acidified by addition of 1 μl trifluoroacetic acid and purified on C18 material. Peptides were separated on RP ReproSil-Pur C18-AQ 3 μm resin (Maisch) columns (15 cm) and directly injected into an LTQ-Orbitrap mass spectrometer (Q Exactive, Thermo Scientific)[39]. Raw data were analysed with MaxQuant using the label-free algorithm[40]. ProteinGroups were filtered to have at least three valid values in the LFQ intensities of the SCAI replicates and to be identified by at least two peptides. Missing values in the control pulldowns were imputed by values simulating noise around the detection limit. SCAI interactors were identified by comparing the LFQ intensities in the SCAI and mock pulldowns using a modified two-sided *t*-test (FDR < 0.01, S0 = 1, see www.maxquant.org for details).

Immunoblotting, immunoprecipitation and antibodies. For whole-cell extracts, cells were lysed in EBC buffer (50 mM Tris, pH 7.5; 150 mM NaCl; 1 mM EDTA; 0.5% NP-40) or RIPA buffer (1% NP-40, 0.5% sodium deoxycholate, 0.1% SDS, 150 mM NaCl, 50 mM TRIS pH 8.0) supplemented with protease and phosphatase inhibitors. To obtain chromatin-enriched fractions, cells were lysed in low-salt buffer (10 mM HEPES, pH 7.4; 10 mM KCl; 0.05% NP-40) supplemented with protease and phosphatase inhibitors, and chromatin-associated proteins were released from the pellet by treatment with micrococcal nuclease. Strep pulldowns were done with Strep-Tactin sepharose (IBA) and GFP immunoprecipitation was performed with GFP-Trap agarose (Chromotek). Bound material was resolved on SDS–PAGE and transferred to nitrocellulose membranes. Antibodies used in this study included: rabbit polyclonals against 53BP1 (sc-22,760, Santa Cruz, 1:5,000 (western blotting (WB))/1:1,000 (immunofluorescence (IF))), RAD51 (sc-8,349, Santa Cruz, 1:150 (IF)), DMC1 (sc-22,768, Santa Cruz, 1:200 (IF)), RIF1 (A300-569A, Bethyl, 1:200 (IF)), tubulin (ab6046, Abcam, 1:10.000 (WB)), histone H3K9me3 (ab8898, Abcam, 1:500 (IF)), 53BP1 (ab21083 and ab36823, Abcam, 1:1,000 (IF); NB100-304, Novus Biologicals, 1:1,000 (IF)), SYCP3 (sc-33195, Santa Cruz, 1:200 (IF)), SYCP1 (ab15090, Abcam, 1:200 (IF)), KAP1 (A300-274A, Bethyl, 1:500 (WB)) and phospho-KAP1 (Ser824) (A300-767A, Bethyl, 1:1,000 (WB and IF)); mouse monoclonal antibodies against GFP (sc-9,996 (clone B-2), Santa Cruz, 1:500 (WB)), FLAG (F-1804 (clone M2), Sigma, 1:100 (IF)/1:500 (WB)), HA (sc-7,392 (clone F-7), Santa Cruz, 1:500 (WB)/1:1,000 (IF)), γ-H2AX (Ser139) (05-636 (clone JBW301) Millipore, 1:1,000 (IF); ab22551 (clone 3F2) Abcam, 1:1,000 (IF and WB)), SYCP3 (sc-74569 (clone D-1) Santa Cruz, 1:200 (IF)), MLH1 (51-1327GR (clone G168-15) BD Pharmingen, 1:20 (IF)), BRCA1 (sc-6954 (clone D-9), Santa Cruz, 1:100 (IF)), HP1γ (MAB3450 (clone 2MOD-1G6), Millipore, 1:1,000 (WB)), HP-β(MAB3448 (clone 1MOD-1A9), Millipore, 1:1,000 (WB)), H3K9me2+3 (ab71604 (clone 6F12-H4), Abcam, 1:1,000 (IF)), ATM pSer1981 (200-301-400 (clone 10H11.E12), Rockland, 1:500 (IF)/1:1,000 (WB)) and phospho-H3 (Ser13) (ab14955 (clone mAbcam 14955), Abcam, 1:1,000 (IF)); rabbit monoclonal against RPA70 (ab79398 (clone EPR3472), Abcam, 1:1,000 (IF)); goat polyclonal against MCM6 (sc-9843, Santa Cruz, 1:500 (WB)). A sheep polyclonal antibody against SCAI was generated by immunization with a full-length GST-fusion protein produced in bacteria (μg μl^{-1} for IP). Rat monoclonal antibody against SCAI (IH2) was described (1:50 (WB)) previously[21].

© 2016 Macmillan Publishers Limited, part of Springer Nature. All rights reserved.

DOI: 10.1038/ncb3436

Immunofluorescence, confocal microscopy and laser micro-irradiation. Cells were fixed in 4% formaldehyde, permeabilized or pre-extracted prior to fixation with PBS containing 0.2% Triton X-100 for 5 min or 1 min, respectively, and incubated with primary antibodies diluted in DMEM for 1 h at room temperature. Following staining with secondary antibodies (Alexa Fluor 488 and 568; Life Technologies) for 30 min, coverslips were mounted in Vectashield mounting medium (Vector Laboratories) containing the nuclear stain DAPI. For detection of nucleotide incorporation during DNA replication, an EdU labelling kit (Life Technologies) was used according to the manufacturer's instructions. Confocal images were acquired on an LSM-780 (Carl Zeiss) mounted on a Zeiss-AxioObserver Z1 equipped with a Plan-Neofluar 40×/1.3 oil immersion objective. Dual- and triple-colour confocal images were acquired with standard settings for excitation of DAPI, Alexa Fluor 488, Alexa Fluor 568, and Alexa Fluor 647 dyes (Molecular Probes, Life Technologies), respectively. Image acquisition and analysis was carried out with LSM-ZEN software. Laser micro-irradiation of cells was performed essentially as described previously[41]. Imaging of Cas9-induced heterochromatin damage at chromocentres was acquired on Confocal Laser Scanning Microscope TCS SP8 (Leica), using a 63× objective. Spermatocyte spreads were prepared, stained, and scored as previously reported[42]. Images were acquired on a Zeiss Axio Imager M2 with a Plan-Apochromat 100×/1.4 oil immersion objective. Regarding animals used in spermatocyte spread analyses, age-matched animals were between 18 and 27 weeks of age, no statistical method was used to predetermine sample size, experiments were not randomized, nor were the investigators blinded to allocation during the experiments or outcome assessment.

Flow cytometry and ELISA. Cells were stained with antibodies and measured with an LSR Fortessa cell analyser (BD Pharmingen) using a DAPI negative live lymphocyte gate. Data were analysed using FlowJo X 10 software. Antibodies used for flow cytometric analysis included B220 (RA3-6B2), CD19 (1D3), IgM (II/41), IgG1 (A85-1) and IgG3 (R40-82) (BD and eBiosciences). To measure Ig in the blood serum by ELISA, plates were coated with anti-mouse IgM (no. 406501) or IgG (no. 1030-01) (Southern Biotechnology Associates), and Ig was detected with horseradish peroxidase (HRP)-conjugated goat anti-mouse IgG1 (no. 1070-05), IgG3 (no. 1100-05) or IgM (no. 1020-05) (Southern Biotechnology Associates). In all cases, wells were developed with the Ultra TMB peroxidase substrate system (Thermo Scientific) and OD was measured at 450 nm using a Fluostar Omega microplate reader (BMG-Labtech). Regarding animals used in FACS and ELISA experiments, animals were between 8 and 12 weeks of age, no statistical method was used to predetermine sample size, experiments were not randomized, nor were the investigators blinded to allocation during the experiments or outcome assessment.

Chromosome metaphase spreads. For genome instability analysis, B cells isolated from animals between 8 and 12 weeks of age were harvested after 3 days in culture stimulated to undergo class-switching to IgG1. Metaphase spreads were prepared and processed for FISH analysis as previously described[11,43–45]. The PARP inhibitor olaparib (2 μM, AZD2281, Selleckchem) was added to cells stimulated *ex vivo* for 16 h and colcemid (100 ng ml^{-1}, Roche) was added 1 h before preparation of metaphase spreads, and imaging as described below using a high-content microscope. Experiments were performed with the investigator blinded to the group allocation. An assistant labelled the slides and/or dissected spleen/cultured cells before analysis by the investigator, and the data were subsequently related to the identity of the specimens. A total of 165 (WT) and 189 (*SCAI*$^{-/-}$) metaphase spreads from DMSO-treated cells and 452 (WT) and 453 (*SCAI*$^{-/-}$) spreads from PARPi-treated cells were analysed, across multiple mice, and detailed in Supplementary Table 3. Spermatocyte metaphase spreads were prepared as previously described[46], except a 2.9% isotonic sodium citrate dihydrate solution was used and the slides were stained with Giemsa. Spermatocyte metaphase spread images were acquired on a Zeiss Axio Scope.A1 LED with a Plan-Apochromat 100×/1.4 oil immersion objective.

Generation of SCAI KO mice and histology. To generate *SCAI*$^{-/-}$ mice, embryonic stem cells carrying a targeted allele of the Scai gene were obtained from EUCOMM (allele name: SCAI (tm1a(EUCOMM)Hmgu); clone ID: HEPD0516_1_G04). Correct targeting was verified by PCR using primers spanning the homology arms. PCR fragments from the 5′ and 3′ end of the targeting construct were cloned into pCR4-TOPO (Invitrogen) and sequenced. Following blastocyst injection, chimaeras were mated with C57Bl/6 WT mice and germline transmission of the targeted allele was achieved. The resulting mouse line was crossed with E2A-Cre to remove floxed sequences. Cycling conditions for genotyping PCR were: 94 °C (60 s), 60 °C (90 s), 72 °C (120 s), 32 cycles, 72 °C (10 m). Primers LacZ_EUCOMM_for03 (5'-ccagttcaacatcagccgctacagtc-3') and SV40_EUCOMM_rev01 (5'-ctag agcttagatcccccctgcc-3') yield a 240-bp product specific for the targeted allele and primers mSCAI_for01 (5'-ccagcacttgggaggcagagac-3') and mSCAI_rev01 (5'-gcagctaaggatagacgatcatagcag-3') yield a 218-bp product for the WT allele.

All animal experiments were approved by the Department of Experimental Medicine (University of Copenhagen), the Danish Working Environment Authority, the Danish Animal Experiment Inspectorate, and the MDACC Institutional Animal Care and Use Committee (IACUC).

Testes and ovaries from WT and *SCAI*$^{-/-}$ mice were fixed in 10% formalin, and paraffin sections were stained with haematoxylin and eosin. Images were acquired with an inverted microscope (Axiovert 200M; Carl Zeiss) equipped with a 10× NA 0.45 objective lens (Plan-Apochromat; Nikon) and a colour charge-coupled device (CCD) camera (Axiocam MRc5; Carl Zeiss) using AxioVision software (version 4.6.3.0; Carl Zeiss). Male animals used for histology were 8 weeks old and female animals were 14 weeks old. At least three mice from each genotype were used, and similar results were obtained. For histological analyses, no statistical method was used to predetermine sample size, experiments were not randomized, nor were the investigators blinded to allocation during the experiments or outcome assessment.

Whole-body irradiation of mice. Age-matched male and female WT and *SCAI*$^{-/-}$ mice were subjected to whole-body gamma irradiation with a one-time dose of 8 Gy of gamma rays from a Gammacell 40 Exactor Cs137 source and were carefully monitored every day to assess survival. Post-irradiation, the mice were put on antibiotic water for the duration of the study (0.1 mg ml^{-1} Ciproxin). The experiment with male mice was performed twice with a reproducible result (Supplementary Fig. 4d) and the experiment with females was performed once (Supplementary Fig. 4e). Figure 3b represents the total data of all three experiments. A scoring sheet used by the animal caretaker was generated to carefully monitor weight loss, abnormal posture, and lack of movement/lethargy on a daily basis. Animals were euthanized by the caretaker before severe distress/suffering was observed, as determined by the scoring system. As such, the caretakers were blinded to allocation of the genotypes during the experiments and informed the investigator of the data. All remaining animals in the experiment were euthanized by day 28 post-irradiation. WT and *SCAI*$^{-/-}$ mice were age-matched (male experiment 1: 17–27 weeks of age, male experiment 2: 14–42 weeks of age, female experiment: 17–64 weeks of age), no statistical method was used to predetermine sample size, and experiments were not randomized.

High-content microscopy and image analysis. Quantitative image-based cytometry (QIBC) for measurement of fluorescence intensities was done as described previously[47,48]. The images were obtained with a 40 × 0.95 NA, FN 26.5 (UPLSAPO40×) dry objective, a quadruple-band filter set for DAPI, FITC, Cy3 and Cy5 fluorescent dyes, a MT20 Illumination system and a digital monochrome Hamamatsu C9100 electron-multiplying CCD camera. Camera resolution is 200 nm × 200 nm per pixel (binning 1, 40×). Image analysis was performed with Olympus ScanR automated image and data analysis software using standard algorithms for detection of nuclei and sub-objects within nuclei. Typically, 49 images (corresponding to 1,500–3,000 sub-objects) were acquired under non-saturating conditions for each data point, allowing robust measurements of experimental parameters such as intensities. Automated unbiased image acquisition was carried out with the ScanR acquisition software. Automated detection and imaging of high-resolution images of metaphase spreads were obtained using Olympus ScanR image analysis and Xcellence software. Images for quantification of 53BP1 and γ-H2AX foci were acquired with Olympus ScanR image analysis and Xcellence software. Twenty-five images were acquired and at least 2,500 cells were analysed per sample. High-throughput analysis of chromocentres and heterochromatin marker intensities after Cas9 damage induction were obtained using the IN Cell Analyzer 1000 Cellular Imaging System, followed by analysis using Cellomics Cell-Insight software. Briefly, cells were selected on the basis of DAPI-dense regions and cells expressing Cas9-EGFP-gRNA yielding a damage-induced 53BP1/γ-H2AX pattern at chromocentres were chosen for intensity analysis.

DSB repair by IR-induced foci enumeration. Immunofluorescence and DSB repair analysis was carried out as described previously[16,17,35]; briefly, cells were fixed in 3% paraformaldehyde containing 2% sucrose for 10 min, permeabilized for 3 min in 0.2% Triton X-100 in PBS and immunostained for 1 h with primary antibody (diluted in PBS containing 2% BSA), then 30 min with 1:200 dilutions of secondary antibodies (in PBS containing 2% BSA). Cells were counterstained with 0.1 μg ml^{-1} DAPI to visualize nuclei and were mounted using Polymount G. Samples were imaged with a Zeiss Axio Observer Z1 platform microscope, with a Plan-Apochromat 20×/0.8, an EC Plan-Neofluar 40×/0.75 or a Plan-Apochromatin 63×/1.4 (oil immersion) objective and an AxioCam MRm Rev.3 camera. Acquisition and analysis was done with Zen Pro (Zeiss) software. All error bars on DSB repair graphs indicate the standard deviation. DSB repair analysis within regions of heterochromatin was performed as described previously[16].

© 2016 Macmillan Publishers Limited, part of Springer Nature. All rights reserved.

Clonogenic survival assays. Between 250 and 3,000 cells were seeded in 6 cm dishes followed by X-ray irradiation the next day as indicated. After 10–14 days, cells were stained with crystal violet solution (0.5% crystal violet, 25% methanol) and colonies containing >100 cells were scored. The experiments were carried out in triplicates and the fraction of surviving cells was normalized to the untreated control.

HR and NHEJ reporter assays. NHEJ or HR reporter constructs (gift from V. Gorbunova, University of Rochester, USA) were digested *in vitro* with HindIII endonuclease. SCAI CRISPR WT or KO cells were co-transfected with RFP and either circular (negative control) or linearized reporter plasmids. Cells were collected three days after transfection and analysed by FACS as described previously[49].

Statistics and reproducibility. All western blots and microscopy experiments shown in the figures were successfully repeated at least three times. For statistical testing of parameters where normal distributions and equal variance could be assumed we calculated *P* values by the standard Student's *t*-test (Supplementary Figs 3e,f and 4k). In cases where equal variance could not be assumed, we used a *t*-test with Welch correction (Fig. 4a–c and Fig. 5a–d and Supplementary Figs 4b and 5c–e,h–k). For data sets where normal distribution could not be assumed, we employed the non-parametrical Mann–Whitney *U*-test (Fig. 2g and Fig. 3j,k,m and Supplementary Fig. 3d) or Fisher's exact test (Fig. 3g,i).

Data availability. The entire CHROMASS mass spectrometry data set has been deposited to the ProteomeXchange Consortium via the PRIDE[50] partner repository with the data set identifier PXD000490, and was previously published[19]. The SCAI interactome recorded by label-free quantification (Fig. 1d) has been deposited with the data set identifier PXD004912. All other data supporting the findings of this study are available from the corresponding authors on request.

37. Munoz, I. M., Szyniarowski, P., Toth, R., Rouse, J. & Lachaud, C. Improved genome editing in human cell lines using the CRISPR method. *PLoS ONE* **9,** e109752 (2014).
38. Daniel, J. A. *et al.* PTIP promotes chromatin changes critical for immunoglobulin class switch recombination. *Science* **329,** 917–923 (2010).
39. Hubner, N. C. *et al.* Quantitative proteomics combined with BAC TransgeneOmics reveals *in vivo* protein interactions. *J. Cell Biol.* **189,** 739–754 (2010).
40. Cox, J. *et al.* Accurate proteome-wide label-free quantification by delayed normalization and maximal peptide ratio extraction, termed MaxLFQ. *Mol. Cell. Proteomics* **13,** 2513–2526 (2014).
41. Mosbech, A., Lukas, C., Bekker-Jensen, S. & Mailand, N. The deubiquitylating enzyme USP44 counteracts the DNA double-strand break response mediated by the RNF8 and RNF168 ubiquitin ligases. *J. Biol. Chem.* **288,** 16579–16587 (2013).
42. Cole, F. *et al.* Homeostatic control of recombination is implemented progressively in mouse meiosis. *Nat. Cell Biol.* **14,** 424–430 (2012).
43. Bunting, S. F. *et al.* 53BP1 inhibits homologous recombination in Brca1-deficient cells by blocking resection of DNA breaks. *Cell* **141,** 243–254 (2010).
44. Callen, E. *et al.* ATM prevents the persistence and propagation of chromosome breaks in lymphocytes. *Cell* **130,** 63–75 (2007).
45. Daniel, J. A. *et al.* Loss of ATM kinase activity leads to embryonic lethality in mice. *J. Cell Biol.* **198,** 295–304 (2012).
46. Evans, E. P., Breckon, G. & Ford, C. E. An air-drying method for meiotic preparations from mammalian testes. *Cytogenetics* **3,** 289–294 (1964).
47. Gudjonsson, T. *et al.* TRIP12 and UBR5 suppress spreading of chromatin ubiquitylation at damaged chromosomes. *Cell* **150,** 697–709 (2012).
48. Toledo, L. I. *et al.* ATR prohibits replication catastrophe by preventing global exhaustion of RPA. *Cell* **155,** 1088–1103 (2013).
49. Seluanov, A., Mao, Z. & Gorbunova, V. Analysis of DNA double-strand break (DSB) repair in mammalian cells. *J. Vis. Exp.* (2010).
50. Vizcaino, J. A. *et al.* 2016 update of the PRIDE database and its related tools. *Nucleic Acids Res.* **44,** D447–D456 (2016).

© 2016 Macmillan Publishers Limited, part of Springer Nature. All rights reserved.

Downloaded from genesdev.cshlp.org on May 8, 2015 - Published by Cold Spring Harbor Laboratory Press

Nuclear position dictates DNA repair pathway choice

Charlène Lemaître,[1,2,3,4] Anastazja Grabarz,[1,2,3,4,7] Katerina Tsouroula,[1,2,3,4,7] Leonid Andronov,[1,2,3,4] Audrey Furst,[1,2,3,4] Tibor Pankotai,[1,2,3,4] Vincent Heyer,[1,2,3,4] Mélanie Rogier,[1,2,3,4] Kathleen M. Attwood,[5,6] Pascal Kessler,[1,2,3,4] Graham Dellaire,[5,6] Bruno Klaholz,[1,2,3,4] Bernardo Reina-San-Martin,[1,2,3,4] and Evi Soutoglou[1,2,3,4]

[1]Institut de Génétique et de Biologie Moléculaire et Cellulaire (IGBMC), 67404 Illkirch CEDEX, France; [2]U964, Institut National de la Santé et de la Recherche Médicale (INSERM), 67404 Illkirch CEDEX, France; [3]UMR7104, Centre National de Recherche Scientifique (CNRS), 67404 Illkirch CEDEX, France; [4]Université de Strasbourg (UDS), 67404 Illkirch CEDEX, France; [5]Department of Pathology, [6]Department of Biochemistry and Molecular Biology, Dalhousie University, Halifax, Nova Scotia B3H 4R2, Canada

Faithful DNA repair is essential to avoid chromosomal rearrangements and promote genome integrity. Nuclear organization has emerged as a key parameter in the formation of chromosomal translocations, yet little is known as to whether DNA repair can efficiently occur throughout the nucleus and whether it is affected by the location of the lesion. Here, we induce DNA double-strand breaks (DSBs) at different nuclear compartments and follow their fate. We demonstrate that DSBs induced at the nuclear membrane (but not at nuclear pores or nuclear interior) fail to rapidly activate the DNA damage response (DDR) and repair by homologous recombination (HR). Real-time and superresolution imaging reveal that DNA DSBs within lamina-associated domains do not migrate to more permissive environments for HR, like the nuclear pores or the nuclear interior, but instead are repaired in situ by alternative end-joining. Our results are consistent with a model in which nuclear position dictates the choice of DNA repair pathway, thus revealing a new level of regulation in DSB repair controlled by spatial organization of DNA within the nucleus.

[*Keywords*: alternative end-joining; DNA repair; nuclear lamina; nuclear organization]

Supplemental material is available for this article.

Received July 2, 2014; revised version accepted October 14, 2014.

Cells continuously experience stress and damage from exogenous sources, such as UV light or irradiation, and endogenous sources, such as oxidative by-products of cellular metabolism (Jackson and Bartek 2009). To avoid subsequent genomic instability, several pathways evolved to detect DNA damage, signal its presence, and mediate its repair (Misteli and Soutoglou 2009). The two main pathways for double-strand break (DSB) repair are homologous recombination (HR) and nonhomologous end-joining (NHEJ) (Chapman et al. 2012).

DNA repair occurs in the highly compartmentalized nucleus, and emerging evidence suggests an important role of nuclear organization in the maintenance of genome integrity (Misteli and Soutoglou 2009). Observations in yeast suggest that distinct, dedicated DNA repair centers exist as preferential sites of repair (Lisby et al. 2003). Further evidence for spatially restricted repair in yeast comes from the observation that persistent DSBs migrate from their internal nuclear positions to the nuclear periphery, where they associate with nuclear pores (Therizols et al. 2006; Nagai et al. 2008; Oza et al. 2009). In mammalian cells, multiple DSBs on several chromosomes are repaired individually and do not meet on shared repair centers or move toward the nuclear periphery (Soutoglou et al. 2007). In line with these observations, spatial proximity of DSBs in the nucleus is a key parameter that affects the frequency of formation of chromosomal translocations in mammals (Roukos et al. 2013; Roukos and Misteli 2014). Therefore, in mammals, although nuclear organization has emerged as a key parameter in the formation of chromosomal translocations (for review, see Roukos and Misteli 2014), very little is known about how nuclear compartmentalization contributes to genome stability and whether DNA repair occurs throughout the nucleus with the same robustness and accuracy.

[7]**These two authors contributed equally to this work.**
Corresponding author: evisou@igbmc.fr
Article published online ahead of print. Article and publication date are online at http://www.genesdev.org/cgi/doi/10.1101/gad.248369.114. Freely available online through the *Genes & Development* Open Access option.

© 2014 Lemaître et al. This article, published in *Genes & Development*, is available under a Creative Commons License (Attribution 4.0 International), as described at http://creativecommons.org/licenses/by/4.0.

Downloaded from genesdev.cshlp.org on May 8, 2015 - Published by Cold Spring Harbor Laboratory Press

Here, we used an inducible system to create temporally and spatially defined DSBs in chromatin within different nuclear compartments and followed their fate. We show that the presence of heterochromatin at the nuclear lamina delays DNA damage response (DDR) and impairs HR. We further used live-cell imaging and superresolution microscopy to probe the spatial dynamics of these DSBs. We show that, contrary to what was observed in yeast, DNA DSBs within lamina-associated domains (LADs) do not migrate to more permissive environments for HR, like the nuclear pores or the nuclear interior. Instead, they are repaired in situ by NHEJ or alternative end-joining (A-EJ). Our data reveal a new level of regulation in DSB repair pathway choice controlled by spatial organization of DNA in the nucleus.

Results

To investigate the impact of nuclear compartmentalization on DNA repair, we induced DSBs in chromatin associated with the inner nuclear membrane and then tested the consequences of nuclear position in DDR kinetics and DNA repair efficiency. We generated I-U2OS19 cells that contain a stably integrated I-SceI restriction site flanked by 256 repeats of the lac operator DNA sequences (lacO) (Supplemental Fig. S1A). This cell line was also engineered to express the I-SceI endonuclease under the control of a doxycycline (Dox)-inducible promoter (pTRE-tight), allowing us to temporally control the induction of a DSB at the lacO/I-SceI locus (Supplemental Fig. S1A). Stable expression of the GFP lac repressor (lacI) enables the visualization of the lacO/I-SceI locus in the nucleus. We induced specific tethering of the lacO locus at the inner nuclear membrane by the expression of an Emerin C-terminal deletion (ΔEMD), which localizes at the nuclear lamina, fused to GFP-lacI (GFP-lacI-ΔEMD) (Supplemental Fig. S1A) as described in Reddy et al. (2008).

Consistent with previous results (Reddy et al. 2008), ΔEMD is sufficient to target the GFP-lacI-ΔEMD fusion protein to the nuclear membrane and relocate the lacO/I-SceI-containing chromosome at the nuclear lamina after one mitotic cycle (Supplemental Fig. S1B,C). Indeed, in cells expressing GFP-lacI-ΔEMD, we observed 70% of colocalization of the lacO array with laminB by immuno-FISH in the absence or presence of I-SceI, whereas in cells expressing GFP-lacI, this colocalization is as low as 10% (Supplemental Fig. S1B,C).

To determine whether tethering of the lacO/I-SceI locus to the nuclear lamina has an effect on the accessibility of the I-SceI endonuclease, we performed ligation-mediated PCR (LM-PCR) in cells expressing GFP-lacI or GFP-lacI-ΔEMD. We found that the cutting efficiency is equivalent in both environments (Supplemental Fig. S1D), demonstrating that the I-SceI endonuclease is able to recognize its target sequence and cleave its substrate regardless of its nuclear localization.

DSBs activate the DDR, which allows recognition of breaks and the activation of checkpoints. Consequently, cell cycle progression is paused, which allows time for the cell to repair the lesions before dividing (Misteli and Soutoglou 2009). DDR involves a megabase-wide spreading of a phosphorylated form of the histone variant H2AX (γ-H2AX) around them (Rogakou et al. 1998; Misteli and Soutoglou 2009).

To assess the impact of repositioning the lacO/I-SceI locus at the nuclear lamina compartment on DDR efficiency, we compared the kinetics of induction of γ-H2AX at the I-SceI break in cells expressing GFP-lacI or GFP-lacI-ΔEMD by immuno-FISH. Although repositioning of the lacO/I-SceI break at the nuclear lamina did not affect the maximal percentage of γ-H2AX, cells expressing GFP-lacI showed the highest percentage of γ-H2AX colocalization with the lacO/I-sceI locus 14 h after Dox addition, whereas GFP-lacI-ΔEMD cells only achieved the same level 24 h after Dox was added (Fig. 1A, B). This observation was further confirmed by chromatin immunoprecipitation (ChIP) experiments (Fig. 1C). We also investigated the recruitment of another DDR factor, 53BP1, which has been implicated in the choice of the DSB repair pathway (Bunting et al. 2010; Panier and Boulton 2014). Similarly to γ-H2AX, the recruitment of 53BP1 was also delayed and showed a maximal accumulation at 24 h after I-SceI expression in GFP-lacI-ΔEMD cells compared with 20 h in GFP-lacI cells (Fig. 1D,E). A similar difference was observed in a lacO/I-SceI system integrated in the I-Hela111 cell line (Supplemental Fig. S2A,B), suggesting that the effect is not tissue-specific but rather is a general mechanism. Taken together, these results reveal a general delay in DDR in lesions occurring in chromatin associated with the nuclear lamina and suggest that this compartment is a repressive microenvironment for DDR.

To rule out the possibility that this defect was due to the expression of the ΔEMD in the context of the GFP-lacI-ΔEMD fusion protein, we performed an immuno-FISH experiment in the presence of IPTG. Under these conditions, the GFP-lacI-ΔEMD fusion protein is expressed but does not bind to the lacO array, and the array is not relocalized at the nuclear lamina, which was confirmed by the markedly reduced colocalization of the array and laminB (Supplemental Fig. S3A–C). As shown in Supplemental Figure S3B and quantified in Supplemental Figure S3D, there was no difference in the degree of γ-H2AX at the I-SceI break in cells expressing either GFP-lacI or GFP-lacI-ΔEMD in the presence of IPTG and 14 h after Dox where there was the maximal difference in DDR between the two compartments (Fig. 1B), confirming that the decreased phosphorylation of H2AX is a consequence of a lesion induced at the nuclear lamina.

In light of the above observations, we investigated whether the delay in DDR at the I-SceI lesion at the nuclear membrane impacts on its repair. To evaluate the effect of the I-SceI break repositioning at the inner nuclear membrane on NHEJ, we compared the degree of colocalization of Ku80 (Britton et al. 2013) with the lacO/I-SceI array by immuno-FISH and the recruitment of XRCC4 by ChIP in cells expressing GFP-lacI and GFP-lacI-ΔEMD, two main proteins of the NHEJ pathway (Lieber 2010). We observed no difference in the recruitment of KU80 in I-U2OS19 (Fig. 2A; Supplemental Fig. S4A) and I-Hela111 (Supplemental

Downloaded from genesdev.cshlp.org on May 8, 2015 - Published by Cold Spring Harbor Laboratory Press

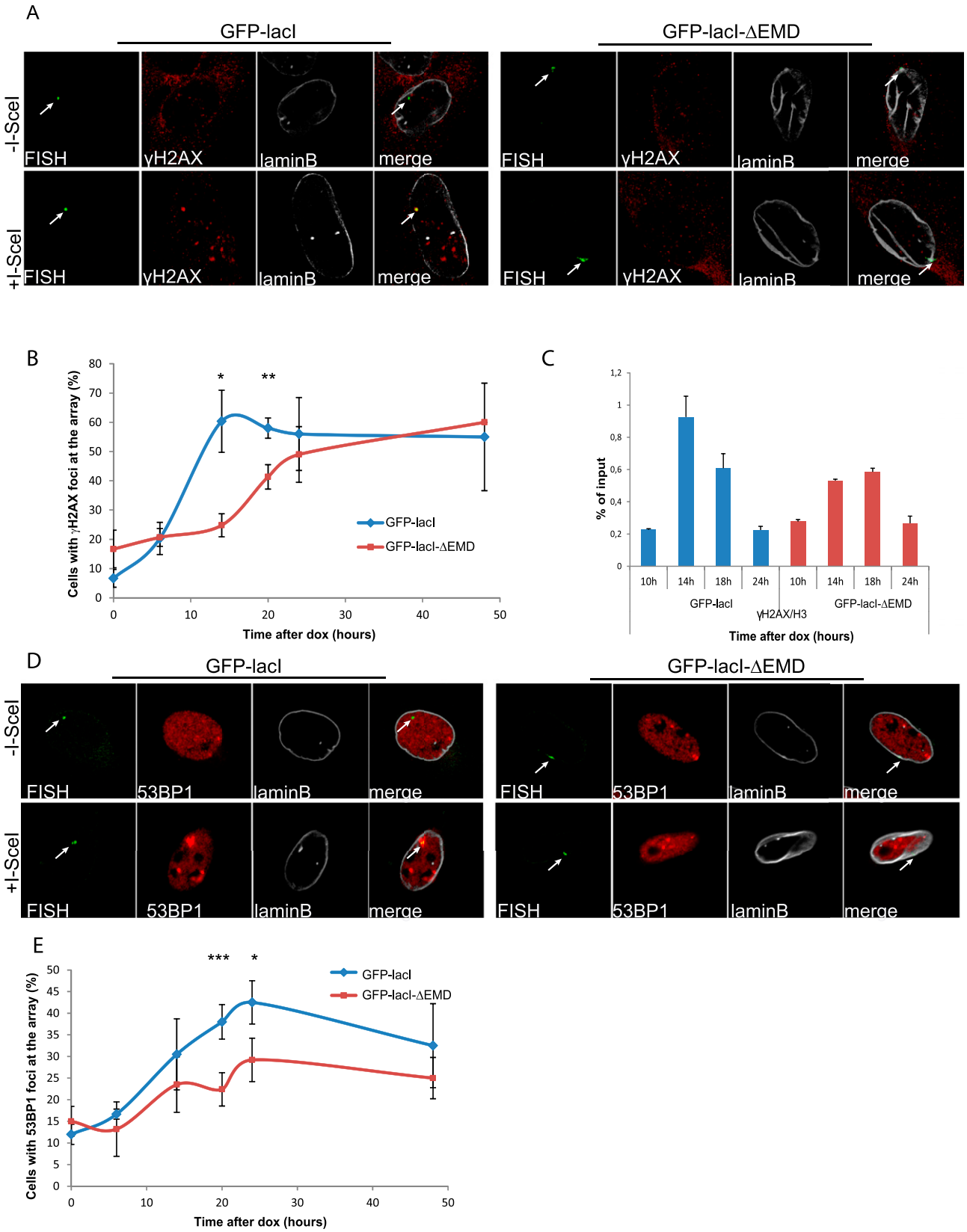

Figure 1. The DDR is delayed at the nuclear lamina. (*A*) Immuno-FISH single-Z confocal images of the lacO array (green), γ-H2AX (red), and laminB (gray) in I-U2OS19 cells expressing GFP-lacI or GFP-lacI-ΔEMD and treated or not with Dox for 14 h. (*B*) Time course of the percentage of colocalization of the lacO array with γ-H2AX. (*C*) γ-H2AX ChIP at the indicated time points after Dox addition in cells expressing GFP-lacI or GFP-lacI-ΔEMD. Values were normalized to input DNA and H3 ChIP and are representative of three independent experiments. (*D*) Immuno-FISH single-Z confocal images of the lacO array (green), 53BP1 (red), and laminB (gray) in I-U2OS19 cells expressing GFP-lacI or GFP-lacI-ΔEMD and treated or not with Dox for 20 h. (*E*) 53BP1 after Dox addition in I-U2OS19 cells expressing GFP-lacI or GFP-lacI-ΔEMD. Values represent mean ± SD of three independent experiments with $n > 50$ cells. For statistical analysis, a *t*-test was performed. (*) $P < 0.05$; (**) $P < 0.01$; (***) $P < 0.001$. In all figures, the arrow depicts the position of the lacO array.

Downloaded from genesdev.cshlp.org on May 8, 2015 - Published by Cold Spring Harbor Laboratory Press

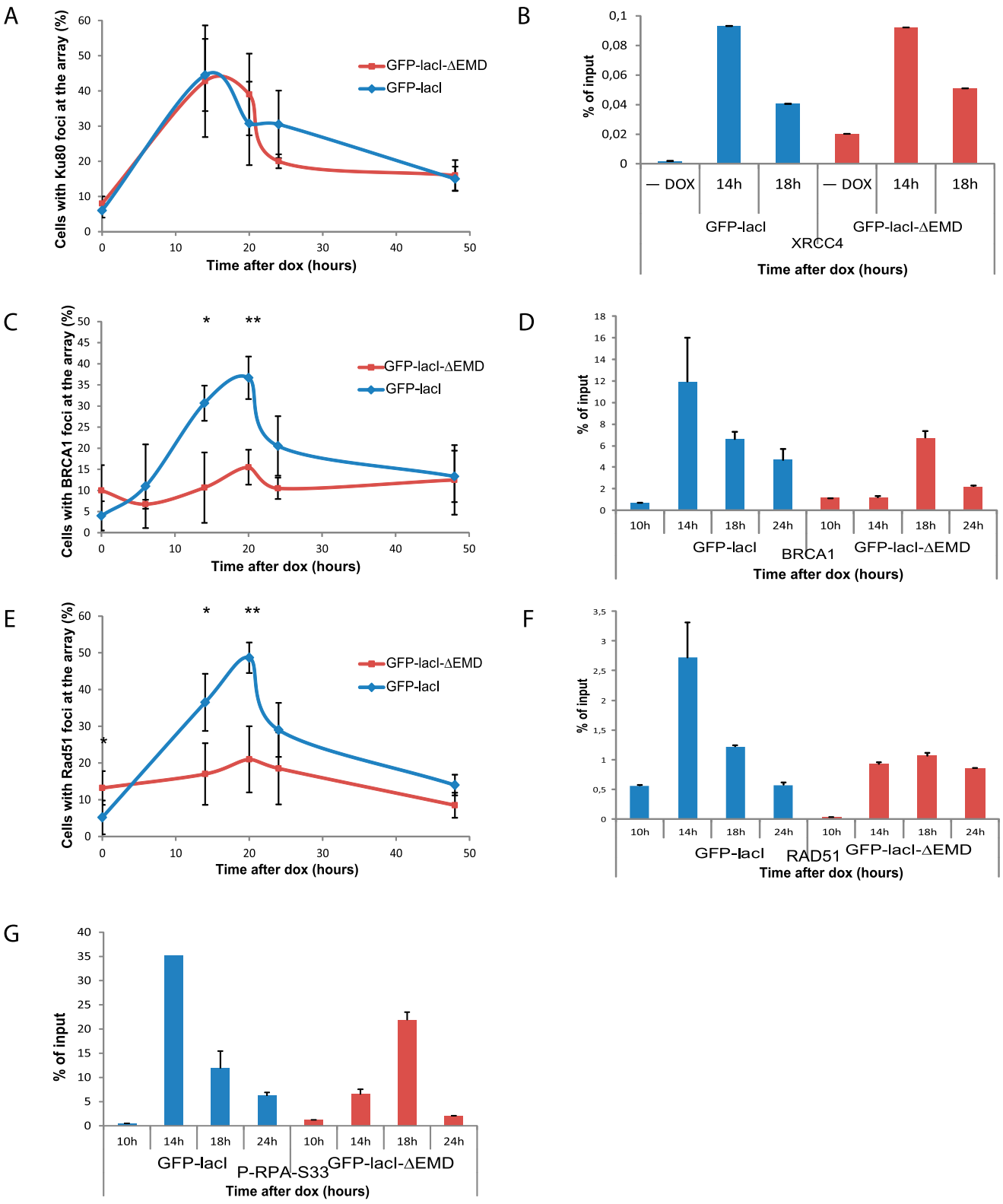

Figure 2. Recruitment of HR factors is impaired at the nuclear lamina. (*A*) Time course of the percentage of colocalization of the lacO array with Ku80 after Dox addition in I-U2OS19 cells expressing GFP-lacI or GFP-lacI-ΔEMD. Values represent mean ± SD of three independent experiments with $n > 50$ cells. ChIP for XRRC4 (*B*), BRCA1 (*D*), RAD51 (*F*), or P-RPAS33 (*G*) at the indicated times upon Dox addition in I-Hela111 cells (XRCC4) or I-U2OS19 cells expressing GFP-lacI or GFP-lacI-ΔEMD is shown. Values were normalized to input DNA and are representative of three independent experiments. The percentage of colocalization of the lacO array with BRCA1 (*C*) and Rad51 (*E*) at the indicated times after Dox addition in I-U2OS19 cells expressing GFP-lacI or GFP-lacI-ΔEMD is shown. Values represent mean ± SD of three independent experiments with $n > 50$ cells. For statistical analysis, a *t*-test was performed. (*) $P < 0.05$; (**) $P < 0.01$.

Downloaded from genesdev.cshlp.org on May 8, 2015 - Published by Cold Spring Harbor Laboratory Press

Fig. S5A–D) cells or XRCC4 at I-Hela111 (Fig. 2B) at the I-SceI break induced at the nuclear lamina compared with the nuclear interior, suggesting that NHEJ can occur efficiently in both compartments. Interestingly, the recruitment of NHEJ factors was not delayed, which is indicative of an uncoupling of DDR and repair by NHEJ.

HR is mainly active during the S phase of the cell cycle and uses the homologous sister chromatid as a template for error-free repair (San Filippo et al. 2008). Contrary to what was observed for NHEJ proteins, the recruitment of HR factors such as BRCA1, Rad51 (Fig. 2C–F; Supplemental Figs. S4B,C, S5B,C,E,F), and Rad54 (Supplemental Fig. S6A) at the broken lacO residing at the inner nuclear membrane was markedly decreased. Interestingly, the phosphorylation of RPA was delayed and less robust but not entirely abolished, suggesting a semifunctional resection pathway (Fig. 2G) and a more dramatic effect specific to late HR factors. To verify that this difference was not due to an impaired cell cycle progression in the cells expressing GFP-lacI-ΔEMD, we compared the cell cycle profiles of the two cell lines by flow cytometry and observed no difference (Supplemental Fig. S6B). Our results suggest that the nuclear lamina is a repressive environment for HR.

In the mammalian nucleus, chromatin is organized into structural domains by association with distinct nuclear compartments (Parada and Misteli 2002; Bickmore 2013). To gain insight into the cause of the DDR delay and HR repression promoted by the nuclear lamina environment, we considered the possibility that the repressive chromatin structure associated with the nuclear lamina (Padeken and Heun 2014) is involved in this phenomenon (Goodarzi and Jeggo 2012; Lemaître and Soutoglou 2014).

To test this hypothesis, we treated cells with an inhibitor of histone deacetylases, trichostatin A (TSA). This treatment resulted in an increase in histone acetylation (Supplemental Fig. S7A) and loss of heterochromatin in the nucleus, including perinuclear heterochromatin, leading to a homogenous chromatin state, as visualized by electron microscopy (Supplemental Fig. S7B–D). TSA treatment did not perturb the repositioning of the lacO/I-SceI locus at the inner nuclear membrane (Supplemental Fig. S7E,F). Interestingly, TSA treatment rescued the defect in γ-H2AX and recruitment of BRCA1 and RAD51 observed after the lacO locus relocalization at the inner nuclear membrane, pointing to an inhibitory role of chromatin compaction in DDR and HR (Fig. 3A–C; Supplemental Figs. S8, S9A,B). Our results are in line with previous studies that showed that reduced gene expression around the nuclear periphery after repositioning of the lacO array depends on the activity of histone deacetylases (Finlan et al. 2008).

To further confirm that the perinuclear heterochromatin in contact with the nuclear membrane is responsible for delayed DDR and repressed HR, we induced decondensation of the lacO/I-SceI chromatin by direct tethering of the chromatin remodeler BRG1. To this end, we expressed cherry-lacI-BRG1 in cells expressing GFP-lacI or GFP-lacI-ΔEMD (Supplemental Fig. S10A). As shown in Supplemental Figure S10B and quantified in Supplemental Figure S10C, tethering of BRG1 at the lacO array resulted in local chromatin decondensation, as visualized by an increased size of the array.

Similar to what we observed after global chromatin decondensation, local chromatin opening by BRG1 rescued the defect in γ-H2AX and the recruitment of BRCA1 and RAD51 upon lacO repositioning at the lamina (Fig. 3D–G; Supplemental Fig. S11A,B). Altogether, these results strongly suggest that the decreased recruitment of HR factors at the nuclear lamina is due to the highly compacted state of the surrounding chromatin.

To further examine whether the localization of a DSB within a nuclear compartment in relation to the state of the chromatin that surrounds the compartment can influence the DNA repair pathway choice, we assessed DSB repair at the nuclear pores, which are subcompartments of the nuclear periphery that represent a permissive environment for gene expression and other DNA-dependent nuclear transactions (Taddei et al. 2006; Ptak et al. 2014). To position the lacO/I-SceI locus at the nuclear pore compartment, we expressed GFP-lacI fused to the nucleoporin Pom121 (Supplemental Fig. S12A). We found that repositioning of the lacO array to the nuclear pores did not affect DDR, as visualized by H2AX phosphorylation and 53BP1 recruitment (Fig. 4A–C; Supplemental Fig. S12B). Furthermore, the recruitment of HR factors was similar in cells expressing GFP-lacI and GFP-lacI-Pom121 (Fig. 4D,E; Supplemental Fig. S12C,D). These observations suggest that in contrast to the nuclear lamina, nuclear pores represent a permissive microenvironment for DDR and DSB repair by HR. Therefore, although the nuclear lamina and nuclear pores are in very close proximity in the nuclear periphery, the difference in chromatin compaction associated with the two compartments regulates the choice of the repair pathway that will be prevalent in lesions occurring in each compartment.

It was previously shown that breaks inflicted at pericentric heterochromatin in *Drosophila* migrate at the periphery of the heterochromatin domain for HR repair in order to avoid recombination between repetitive sequences (Chiolo et al. 2011). Given that tethering of the lacO/I-SceI locus at the nuclear membrane using the GFP-lacI-ΔEMD might limit its potential mobility toward activating environments for DDR and repair, such as the nucleoplasm or the nuclear pores, we asked whether the lacO/I-SceI locus acquires mobility after break induction in the presence of IPTG when the lacI is not bound to the lacO array and cannot constrain its movement (Supplemental Fig. S13A). Surprisingly, we did not detect any migration of I-SceI breaks away from the compartment (Supplemental Fig. S13B).

To further investigate whether breaks occurring at the lamina migrate away from the lamina compartment toward the adjacent pores or the interior of the nucleus, we used an experimental system previously developed to visualize chromatin domains associated with laminB in single cells (Kind et al. 2013). This system uses DNA adenine methylation as a tag to visualize and track LADs

Downloaded from genesdev.cshlp.org on May 8, 2015 - Published by Cold Spring Harbor Laboratory Press

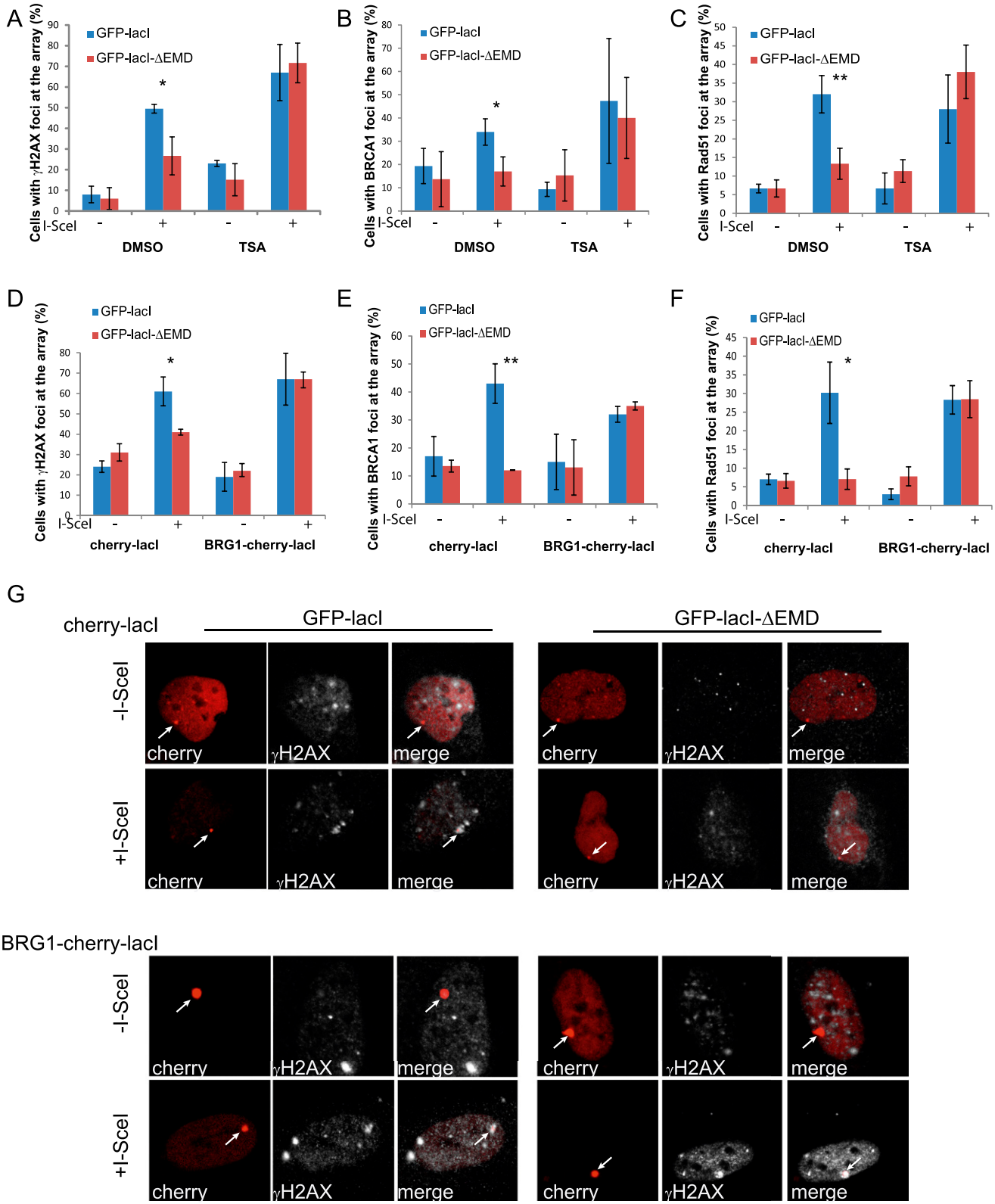

Figure 3. Chromatin decompaction restores DDR and the recruitment of HR factors at the nuclear lamina. Colocalization of the lacO array with γ-H2AX (*A*), BRCA1 (*B*), or RAD51 (*C*) in I-U2OS19 cells expressing GFP-lacI or GFP-lacI-ΔEMD and pretreated for 4 h with DMSO or TSA in the absence or presence of Dox for 14 h or 20 h is shown. The percentage of colocalization of the lacO array with γ-H2AX (*D*), BRCA1 (*E*), or RAD51 (*F*) in I-U2OS19 cells expressing GFP-lacI or GFP-lacI-ΔEMD and cherry-LacI or BRG1-cherry-lacI and treated or not with Dox for 14 h or 20 h is shown. (*G*) Immunofluorescence single-Z confocal images of γ-H2AX (gray) in I-U2OS19 cells expressing GFP-lacI or GFP-lacI-ΔEMD transfected with cherry-lacI or BRG1-cherry-lacI (red) and treated or not with Dox for 14 h. For statistical analysis, a *t*-test was performed. (*) $P < 0.05$; (**) $P < 0.01$.

Downloaded from genesdev.cshlp.org on May 8, 2015 - Published by Cold Spring Harbor Laboratory Press

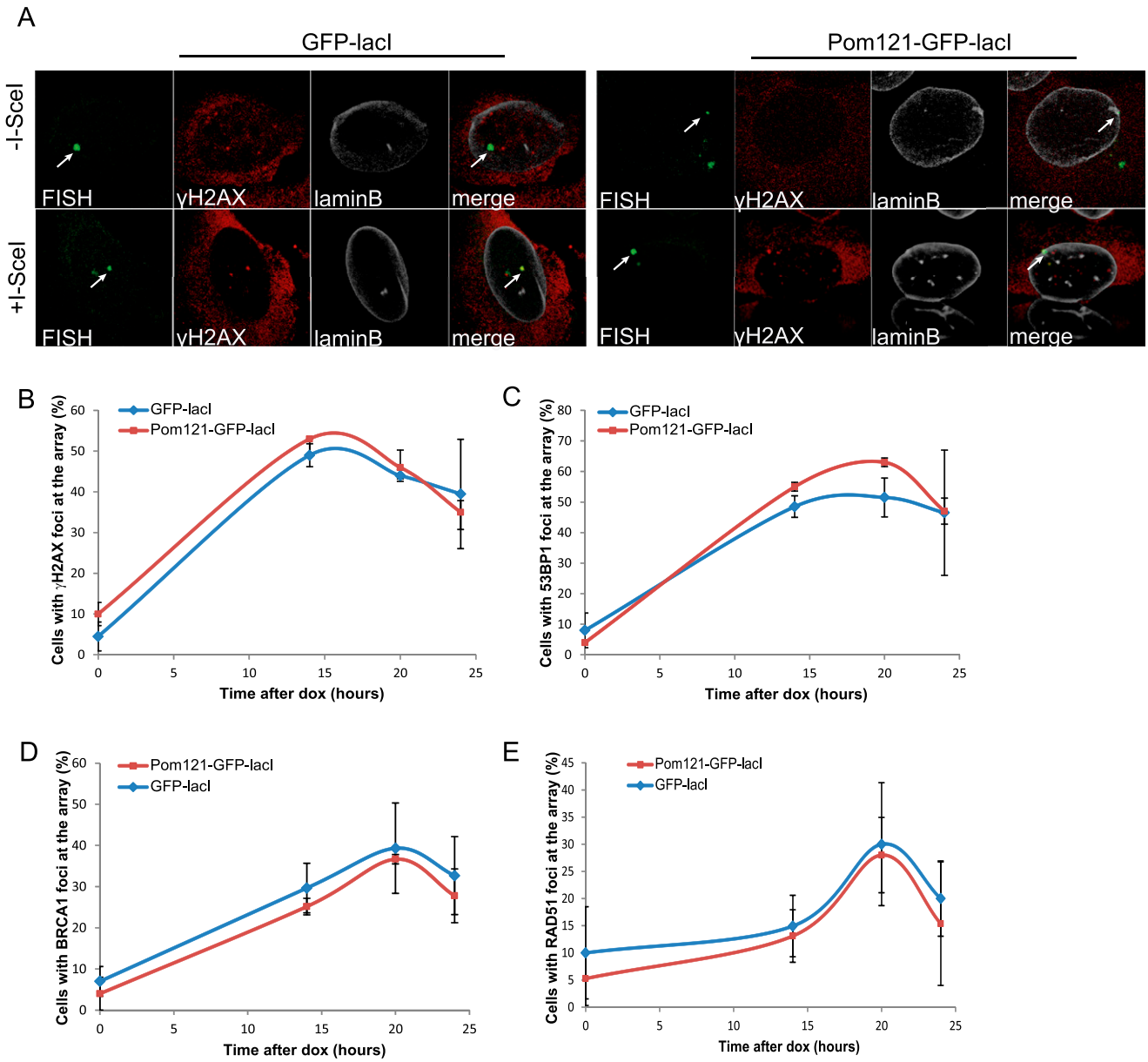

Figure 4. DDR and HR are not affected by tethering at the nuclear pores. (*A*) Immuno-FISH single-Z confocal images of the lacO array (green), γ-H2AX (red), and laminB (gray) in I-U2OS19 cells expressing GFP-lacI or Pom121-GFP-lacI and treated or not with Dox for 14 h. Time course of the percentage of colocalization of the lacO array with γ-H2AX (*B*), 53BP1 (*C*), BRCA1 (*D*), or RAD51 (*E*) in I-U2OS19 cells expressing GFP-lacI or Pom121-GFP-lacI cells after Dox addition is shown. Values represent mean ± SD of three independent experiments with $n > 50$ cells.

using a truncated version of the DpnI enzyme fused to GFP (m6a-Tracer), which recognizes methylated LADs in cells expressing LaminB-Dam (Kind et al. 2013). To probe the behavior of LADs in the presence of DNA damage, we followed the m6a-Tracer localization using live-cell imaging (Supplemental Fig. S13C) or confocal (Fig. 5A,B) or superresolution (Fig. 5C) microscopy. The infliction of DNA damage in the LADs was verified by γ-H2AX (Fig. 5A; Supplemental Fig. S13D). Interestingly, the partition of the LADs between the nuclear membrane and the nucleoplasm did not notably change before and after global DNA damage (Fig. 5A–C; Supplemental Fig. S13C), suggesting that DNA lesions do not lead to massive rearrangements of LADs within the nucleus.

In yeast, persistent DSBs migrate from their internal nuclear positions to the nuclear periphery, where they associate with nuclear pores (Therizols et al. 2006; Nagai et al. 2008; Oza et al. 2009). To more precisely assess the spatial proximity of LADs with laminB and nucleoporin of the nuclear basket TPR before and after DNA damage, we used two-color dSTORM superresolution microscopy (Folling et al. 2008). As expected, we observed juxtaposition and a certain degree of colocalization of LADs with LaminB but not with TPR

Downloaded from genesdev.cshlp.org on May 8, 2015 - Published by Cold Spring Harbor Laboratory Press

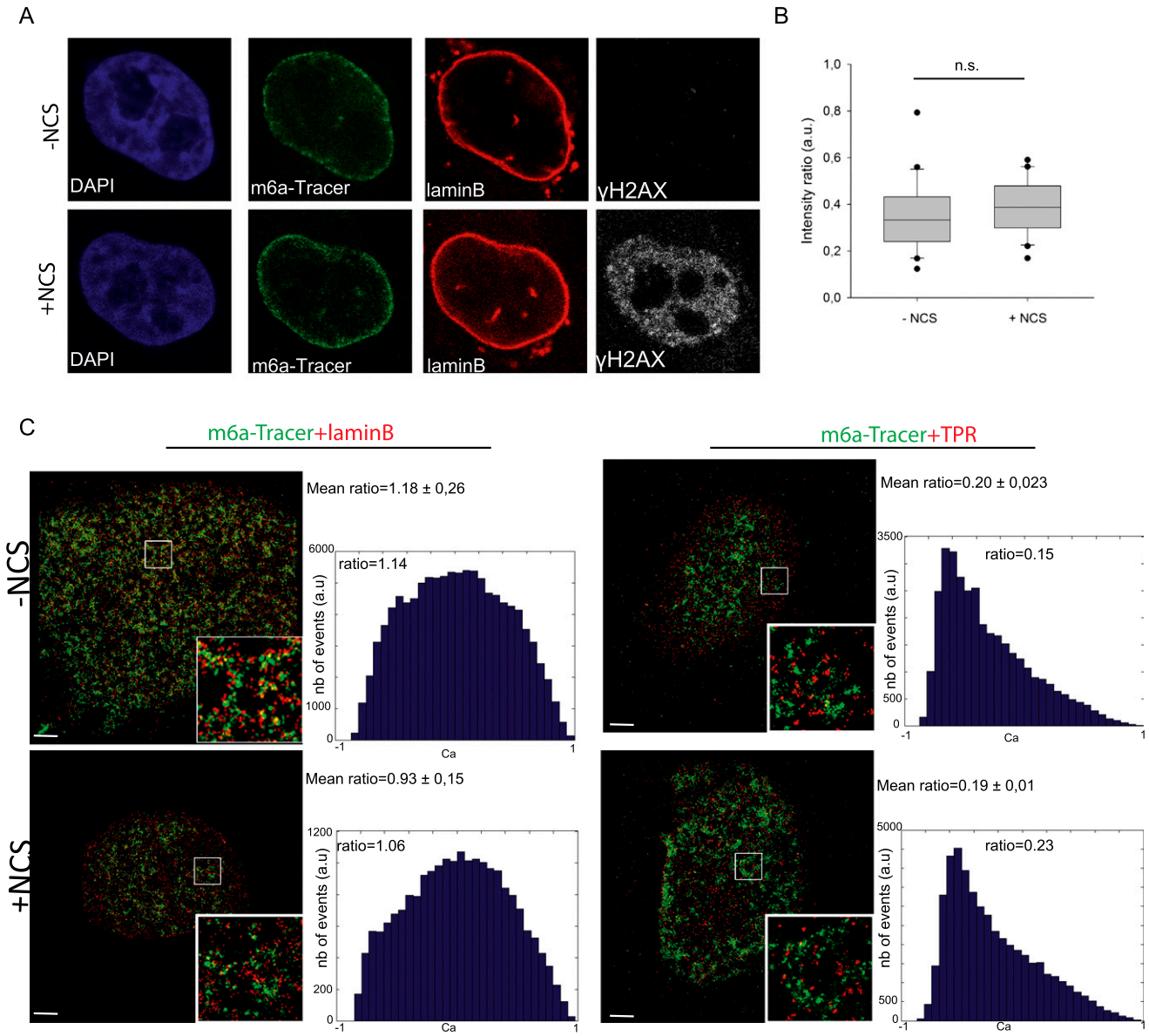

Figure 5. DSBs at the nuclear lamina are positionally stable. (*A*) Immunofluorescence of HT1080 cells expressing Dam-LaminB1 and m6A-Tracer 2 h after treatment (or not) with 50 ng/mL neocarzinostatin (NCS) for 15 min. (*B*) Box plot of GFP intensity ratios of the signal in the nucleoplasm versus the signal at the nuclear envelope in a HT1080-derived clonal cell line expressing a Dam-LaminB1 and the m6A-Tracer. The number of cells analyzed per condition was 20. For statistical analysis, χ^2 tests were performed. (n.s.) Nonsignificant. (*C*) dSTORM microscopy images of LADs (green) and laminB (*left* panel; red) or TPR (*right* panel; red) in the absence (*top* panel) or presence (*bottom* panel) of DNA damage (100 ng/mL NCS for 15 min and released for 2 h) in HT1080 cells expressing Dam-LaminB1 and m6A-Tracer. Images were taken from the bottom of the cells to allow better resolution of nuclear pores. Corresponding colocalization and the ratio of positive over negative colocalization events are displayed at the *right*. The mean ratios for all nuclei analyzed ($n \geq 8$) are displayed *above*.

(Fig. 5A). Interestingly, DNA damage did not induce changes in the proximity of LADs toward both compartments, which further pointed to the positional stability of LADs upon DNA damage (Fig. 5A). Taken together, these results suggest that contrary to what has been shown in yeast, breaks occurring on chromosomes that associate with the nuclear membrane do not travel and seek an environment permissive to HR repair, such as the nuclear pores.

To further investigate the contribution of NHEJ and HR in repairing the I-SceI breaks at the lamina or the nuclear interior, we assessed the degree of persistent breaks in GFP-lacI or GFP-lacI-ΔEMD cells depleted of XRCC4 and RAD51 (knockdown efficiencies verified in Supplemental Fig. S14A). Interestingly, in control cells, breaks were efficiently repaired in both nuclear compartments, which was exemplified by the decrease in γ-H2AX signal at the lacO array 24 h after break

Downloaded from genesdev.cshlp.org on May 8, 2015 - Published by Cold Spring Harbor Laboratory Press

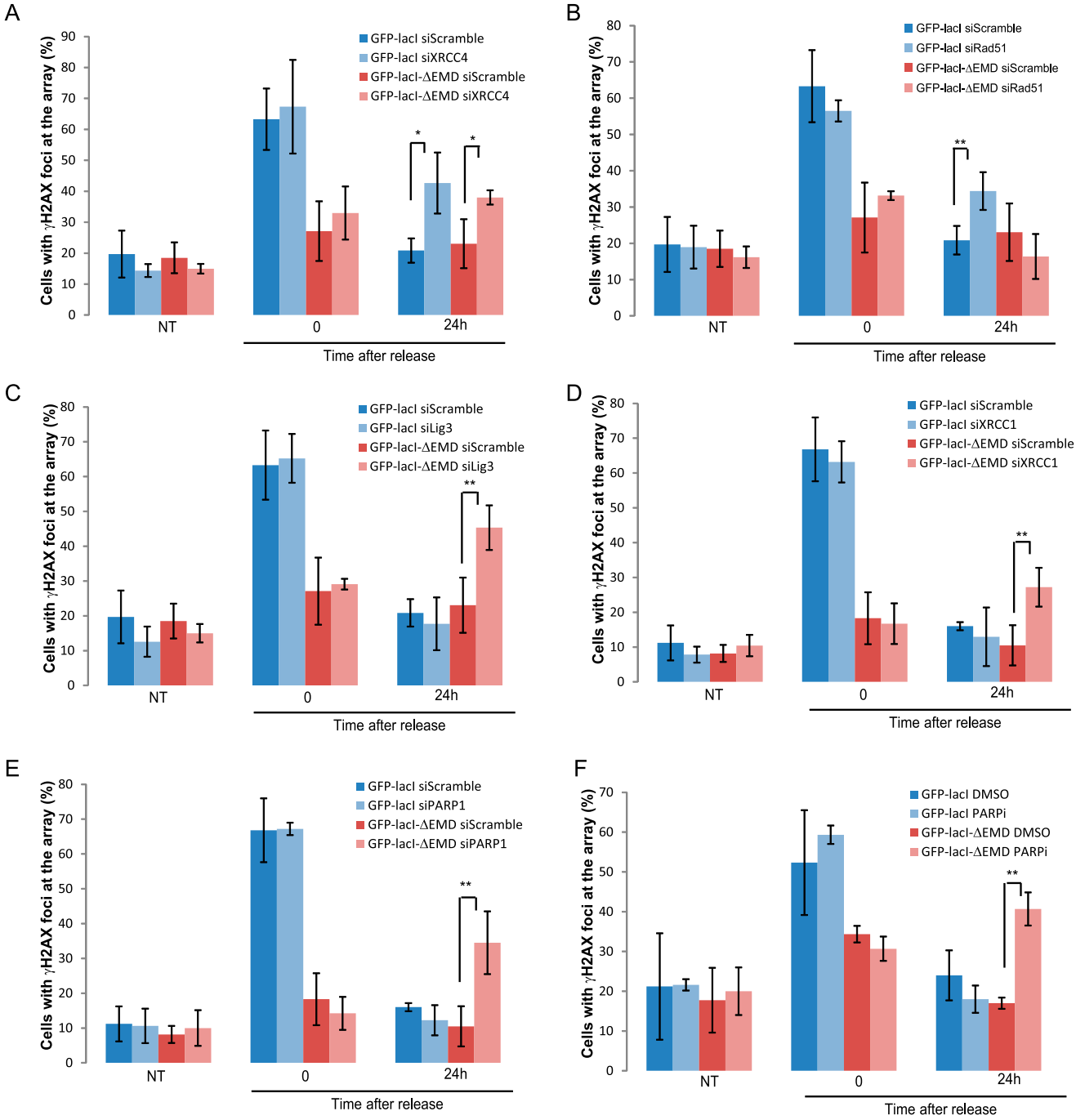

Figure 6. DSBs at the nuclear lamina are repaired by NHEJ or A-EJ. The percentage of colocalization of the lacO array with γ-H2AX in untreated cells (NT) or after 14 h of Dox (time point 0) and subsequent release for 24 h in I-U2OS19 cells expressing GFP-lacI or GFP-lacI-ΔEMD and transfected with XRCC4 (*A*), RAD51 (*B*), ligase 3 (*C*), XRCC1 (*D*), or PARP1-specific siRNAs (*E*) is shown. (*F*) The percentage of colocalization of the lacO array with γ-H2AX upon Dox treatment or release in I-U2OS19 cells expressing GFP-lacI or GFP-lacI-ΔEMD and treated with DMSO or a PARP inhibitor (PARPi, during the entire course of the experiment) is shown. Values represent mean ± SD of three independent experiments with $n > 50$ cells. For statistical analysis, a *t*-test was performed. (*) $P < 0.05$; (**) $P < 0.01$.

induction by a short pulse of Dox (Fig. 6A–E). Although depletion of XRCC4 led to persistent damage in both compartments (Fig. 6A), depletion of RAD51 did not affect the repair of breaks at the lamina (Fig. 6B). These results suggest that lesions at LADs do not depend on HR for their repair.

To test whether repositioning of the lacO/I-SceI break at the nuclear membrane affects the kinetics of repair, we performed LM-PCR in GFP-lacI and GFP-lacI-ΔEMD cells after a short pulse of Dox followed by release for 36 h. We found that breaks at both nuclear locations were efficiently repaired based on the marked decrease in PCR

Downloaded from genesdev.cshlp.org on May 8, 2015 - Published by Cold Spring Harbor Laboratory Press

signal (Supplemental Fig. S14B). These results strongly suggest that efficient DNA repair takes place at the lamina-associated I-SceI breaks even in the absence of functional HR.

Since resection is not abolished at lacO/I-SceI breaks when associated with the nuclear lamina, we sought to determine the fate of the lesions whereby resection has occurred but complete DNA repair by HR cannot occur. To answer this question, we assessed the contribution of the A-EJ pathway in the repair of breaks at the periphery. To this end, we quantified persistent γ-H2AX at the lacO/I-SceI locus 24 h after break induction in GFP-lacI and GFP-lacI-ΔEMD cells where ligase 3, XRCC1, or PARP1 had been depleted (knockdown efficiencies verified in Supplemental Fig. S14A,C) or PARP was inhibited. Interestingly, inhibition of the A-EJ pathway resulted in a repair delay for only breaks that were associated with the nuclear membrane (Fig. 6C–F; Supplemental Fig. S14D). These findings indicate that NHEJ and A-EJ, but not HR, are the most prevalent pathways of DNA repair for lesions occurring at nuclear membrane-associated chromatin and reveal for the first time that A-EJ takes place as a main pathway and not as a backup pathway activated solely in instances where there is a DNA repair factor deficiency (Frit et al. 2014).

Taken together, we showed that breaks occurring in chromatin that surrounds the nuclear membrane do not migrate to other regions of the nucleus, not even to other domains within the nuclear periphery, but rather are repaired within the lamina, where the break occurred by NHEJ and A-EJ.

Discussion

To preserve genomic integrity, different DNA repair pathways have evolved, and multiple layers of regulation like the cell cycle, specific proteins, or chromatin structure exist to ensure the tight balance between these pathways (Kass and Jasin 2010). Here, we propose another layer of regulation of DNA repair pathway choice imposed by nuclear compartmentalization. We show that the nuclear lamina restricts HR and allows NHEJ and A-EJ. These observations are in agreement with data in yeast showing that distinct nuclear compartments of the nuclear periphery like the nuclear pore or the inner nuclear membrane favor different repair outcomes (Nagai et al. 2008; Khadaroo et al. 2009; Oza et al. 2009; Horigome et al. 2014). Similar to what we observed, it was shown that binding of DSBs to Nup84 in yeast facilitates recombination through SUMO protease Ulp1 and the SUMO-dependent ubiquitin ligase Slx5/Slx8 (Nagai et al. 2008) using BIR and microhomology-mediated recombination. On the contrary, binding to the inner nuclear membrane protein Mps3 has two different outcomes: In the case of telomere tethering, it inhibits recombination by sequestering the DSBs from nonspecific interactions with chromatin (Oza et al. 2009; Schober et al. 2009), while in the case of persistent DSBs, it triggers repair by the classical HR pathway (Horigome et al. 2014).

We also found that the chromatin structure at the inner nuclear lamina is mainly responsible for inhibiting HR. This is in keeping with recent studies, which found that HR is activated at DSBs located within actively transcribed genes that reside in euchromatin (Aymard et al. 2014; Pfister et al. 2014). Given that the lacO locus is promoterless and not transcribed, our results indicate that HR is not regulated solely by the transcriptional status. Instead, the exact nature of the chromatin environment and chromatin accessibility appear to be major determinants of HR regulation (Jha and Strahl 2014; Pai et al. 2014). Indeed, other studies have shown that HR is a main pathway in repairing breaks within heterochromatin (Beucher et al. 2009; Geuting et al. 2013; Kakarougkas et al. 2013). However, our data point to the fact that not all heterochromatin domains within the nucleus behave in the same manner and that the specific type of heterochromatin at the nuclear lamina has distinct functions.

In most of the above studies, chromatin structure and histone modifications affect the very first step of the HR pathway that is DNA end resection. Aymard et al. (2014) show that H3K36me3 is essential for the recruitment of CtIP through LEDGF. On the other hand, H3K36me3 in yeast induces chromatin compaction and inhibits resection, as visualized by increased RPA foci when the methyltransferase responsible for this modification is absent (Pai et al. 2014). Here we observed that phosphorylation of RPA at S33 is delayed and not mounted properly at lesions occurring in chromatin associated with the inner nuclear membrane. We also show that BRCA1 recruitment is dramatically affected. Since BRCA1 is acting with CtIP to activate long-term resection (Chen et al. 2008), it is possible that DNA ends are not appropriately resected to create a proper template for recombination, and the short resection channels lesions to A-EJ as was proposed earlier (Zhang and Jasin 2011; Deng et al. 2014). The fact that resection at the lamina is not as dramatically affected as late steps of HR might also suggest that nuclear position dictates the DNA repair pathway choice by regulating only the recruitment of late HR proteins to DSBs.

The use of A-EJ, which is considered a highly mutagenic pathway, instead of the error-free HR pathway might seem dangerous for the maintenance of genomic stability. However, LADs are relatively gene-poor, have a repressive chromatin signature, and are demarcated by repetitive and AT-rich sequences (Meuleman et al. 2013). The inhibition of HR may represent a means to avoid genomic instability provoked by recombination between repetitive sequences, which is a mechanism that has been proposed for the repair of DSBs that form in heterochromatic regions in *Drosophila* (Chiolo et al. 2011). Moreover, activation of A-EJ that is an error-prone pathway might have less impact given that most of the genes that reside in LADs are not transcribed (Meuleman et al. 2013).

In *Drosophila*, breaks induced in the heterochromatic domain rapidly relocate outside of the domain, where HR is completed (Chiolo et al. 2011). A similar DSB relocation

Downloaded from genesdev.cshlp.org on May 8, 2015 - Published by Cold Spring Harbor Laboratory Press

was observed in mouse cells upon break induction by linear ion tracks in chromocenters (Jakob et al. 2011). On the contrary, we show that breaks occurring in chromatin associated with the inner nuclear lamina are positionally stable, suggesting that different heterochromatic compartments use different strategies to avoid recombination. One of the possible hypotheses to explain such a difference is a different chromatin composition or a difference in the regulation of chromatin mobility. Indeed, in yeast, DSBs were shown to have increased mobility (Dion and Gasser 2013). This mobility is facilitated by chromatin decompaction via chromatin remodelers (Neumann et al. 2012) and HR factors (Dion et al. 2012) and in turn allows the homology search step of HR (Mine-Hattab and Rothstein 2012). In mammalian cells, however, DSB mobility is limited and actively restricted by the NHEJ complex Ku70/Ku80 (Soutoglou et al. 2007; Roukos et al. 2013). In *Drosophila* cells, the relocation of DSBs outside of the heterochromatic domain is accompanied by decondensation of the domain (Chiolo et al. 2011), suggesting a mechanism similar to the one responsible for DSB mobility in yeast. At the nuclear lamina, however, this mechanism does not seem to be active, suggesting that an additional mechanism could repress DSB movement at the nuclear lamina. This hypothesis is in accordance with the observation that chromatin mobility is decreased for genomic loci associated with the nuclear lamina or the nucleoli (Chubb et al. 2002). Furthermore, laminA has recently been identified as a factor inhibiting DSB movement in mammalian cells (Mahen et al. 2013), further pointing to an active inhibition of DSB mobility at the nuclear lamina.

Another difference between our results and the results obtained in the heterochromatic compartment of *Drosophila* cells is the activation of DDR. In *Drosophila* cells, the activation of DDR was faster in heterochromatin compared with euchromatin (Chiolo et al. 2011). On the contrary, our results show a slower DDR activation at the nuclear lamina compared with the nuclear interior. Given the implication of the early steps of DDR in the initiation of resection by the ATM and MRN complexes, and the fact that resection facilitates DSB movement in yeast, one can hypothesize that the delayed DDR at the nuclear lamina inhibits DSB mobility.

Overall, our findings indicate that spatial positioning of a DSB is a new parameter to consider in the study of DSB repair, which has significant implications for our understanding of how the organization of repair in the highly compartmentalized nucleus contributes to maintaining genome stability and avoiding tumorigenesis.

Materials and methods

Cell lines, infections, transfections

I-U2OS19 GFP-lacI and GFP-lacI-ΔEMD cells were generated by infecting the U2OS19ptight13 cell line (Lemaître et al. 2012) with GFP-lacI (Soutoglou and Misteli 2008) and GFP-lacI-ΔEMD (Reddy et al. 2008) plasmids and after FACS sorting. Briefly, BOSC cells were transfected using FuGENE6 (Promega) according to the manufacturer's protocol with GFP-lacI or GFP-lacI-ΔEMD constructs and an amphotropic vector. Cell supernatants were harvested 48 h later and transferred to U2OS19ptight13 cells. Twenty-four hours after infection, cells were FACS-sorted for GFP-positive signal and cultured in the presence of 800 μg/mL G418 and 2 mM IPTG (inhibitor of the lacI/lacO interaction). Cells were plated in the absence of IPTG for 24 h prior to starting an experiment. To induce I-SceI expression, Dox was added to the cells at a concentration of 1 μg/mL. In Supplemental Figure S3, 2 mM IPTG was maintained during the whole experiment, and in Supplemental Figure S7, A and B, cells were plated in the absence of IPTG for 24 h and treated with Dox for 12 h. IPTG was then added for 2 h, while Dox was maintained until the end of the experiment.

Hela111 cells were obtained by transfection of lacO-I-SceI-hygro plasmid and subsequent clonal selection using 300 μg/mL hygromycin. I-HeLa111 cells were generated by transfection of Hela111 cells with pWHE320-HA-I-SceI and pWHE146-Tet activator plasmids and selection using 1 mg/mL G418. I-Hela111 GFP-lacI or GFP-lacI-ΔEMD cells were generated by infection of I-Hela111 cells with GFP-lacI and GFP-lacI-ΔEMD plasmids and FACS sorting for GFP-positive cells.

I-U2OS19 Pom121-GFP-lacI cells were obtained after infection of I-U2OS19 cells with Pom121-GFP-lacI and selection of GFP-positive cells using FACs sorting.

I-U2OS19 GFP-lacI and GFP-lacI-ΔEMD were transfected with cherry-lacI or BRG1-cherry-lacI by using FuGENE6 reagent according to the manufacturer's protocol. The cells were first plated in the absence of IPTG for 24 h and then transfected and treated with Dox 4 h after transfection.

I-U2OS19 GFP-lacI and GFP-lacI-ΔEMD cells were transfected with siRNA scramble (OnTarget Plus nontargeting pool siRNA; Dharmacon, D-001810-10-20), XRCC4 (Dharmacon, M-004494-02), Rad51 (Dharmacon, L-003530-00) or Lig3 (Dharmacon, L-009227-00) using oligofectamine reagent (Invitrogen) according to the manufacturer's protocol. Knockdown efficiency was analysed by Western blot or RT-qPCR. RNA was extracted using the RNeasy minikit (Qiagen) according to the manufacturer's protocol. RT-qPCRs were then processed as in (Pankotai et al. 2012). Proteins were extracted in RIPA buffer and analyzed by Western blot.

PARP inhibitor treatment

I-U2OS19 GFP-lacI and GFP-lacI-ΔEMD were plated in the absence of IPTG for 24 h and treated with PARPi (ABT-888, sc-202901A) at a 10 μM concentration or by DMSO.

TSA treatment

Cells were plated in the absence of IPTG for 24 h and subsequently treated with TSA at 0.5 μM or DMSO for control for 4 h. Dox was added after 4 h of treatment for the indicated time, while DMSO or TSA was maintained during the whole experiment.

Neocarzinostatin (NCS) treatment

Cells were plated in the presence of Shield for 20 h, treated for 15 min with 100 ng/mL NCS (N9162-100UG, Sigma), and fixed 2 h after treatment.

Cell cycle analysis

Cells were fixed in 70% EtOH overnight at −20°C and stained with 25 μg/mL propidium iodide. The acquisition was performed on a FACSCalibur. Results were analysed using FlowJo software.

Downloaded from genesdev.cshlp.org on May 8, 2015 - Published by Cold Spring Harbor Laboratory Press

LM-PCR

Cells were plated in the absence of IPTG for 24 h and subsequently treated with Dox for 14 h. DNA was then extracted with the DNeasy blood and tissue kit (Qiagen). Assymetric adaptator (S21, Phos-GCATCACTACGATGTAGGATG; and Lup, CATCCTACATCGTAGTGATGCTTAT) was annealed in TE for 5 min at 95°C and then allowed to reach room temperature slowly. One-hundred picomoles of assymetric adaptator was added to 1 μg of DNA extracted from cells. Ligation was performed using T4 DNA ligase overnight at 16°C. PCR was performed using Pfu enzyme (Agilent) with an annealing temperature of 58°C. The PCR primers used were LM-I-SceI (CAT CCTACATCGTAGTGATGC) and lacR (TTAATTAATCAAAC CTTCCTCT). The PCR product was then run on a 2% agarose gel.

Immunofluorescence, immuno-FISH, and microscopy

Cells were cultured on coverslips and fixed in 4% paraformaldehyde for 10 min, permeabilized in 0.5% Triton for 10 min, blocked in 1% BSA for 30 min, and incubated with primary antibody for 1 h (see the antibodies table in the Supplemental Material) and secondary antibodies for 45 min. Coverslips were incubated with DAPI and mounted on slides in Prolong Gold (Molecular Probes).

For Rad51 and Ku80 immunofluorescence or immuno-FISH, cells were pre-extracted in CSK buffer (10 mM Hepes at pH 7, 100 mM NaCl, 300 mM sucrose, 3 mM $MgCl_2$, 0.7% Triton X-100) containing 0.3 mg/mL RNase A prior to fixation (Britton et al. 2013).

For immuno-FISH, the same protocol was used, but after incubation with secondary antibodies, they were submitted to post-fixation in 4% formaldehyde for 20 min. Cells were washed for 5 min in 2× SSC and 45 min in 2× SSC with a increasing temperature from room temperature to 72°C. After one wash in 70% ethanol and two washes in absolute ethanol, coverslips were dried for 5 min at room temperature. They were subsequently incubated with 0.1 N NaOH for 10 min and washed in 2× SSC for 5 min. Coverslips were washed again in 70% ethanol and twice with absolute ethanol. After drying, cells were hybridized with DNA probe (see immuno-FISH probe preparation below) for 30 sec at 85°C and incubated overnight at 37°C.

The immuno-FISH probe was prepared by nick translation from the lacO-I-SceI plasmid that was used to create the I-Hela111 cell line. DNA probe (0.3 μg) was mixed with 9 μg of ssDNA and 3 μg of CotI human DNA (Roche) and precipitated with 2.5× vol of ethanol and 1/10 vol of 2.5 M sodium acetate for 30 min at −80°C. After 20 min of centrifugation, the supernatant was discarded, and the pellet was washed with 70% ethanol and centrifuged again for 5 min. The supernatant was discarded, and the pellet was dried. The pellet was resuspended in 20 μL of hybridization solution (50% formamide, 4× SSC, 10% dextran sulfate) per coverslip by vortexing for 1 h. The probe was denaturated for 5 min at 90°C and preannealed for at least 15 min at 37°C before hybridization with cells.

The day after hybridization, immuno-FISH was revealed. Coverslips were washed twice for 20 min at 42°C in 2× SSC and then incubated with secondary antibody and fluorescein anti-biotin (Vector Laboratories, SP-3040) at 1:100 dilution for 45 min. Coverslips were washed, incubated with DAPI, and mounted in Prolong Gold reagent (Molecular Probes).

Slides were observed, and colocalization counting was done in epifluorescence microscopy. Pictures were taken with confocal microscopy. For experiments with Pom121-GFP-lacI constructs, cells were always costained with laminB to evaluate relocalization of the lacO array at the nuclear pores. For experiments with BRG1-cherry-lacI or cherry-lacI transfections, colocalization was counted using confocal microscopy.

Time-lapse microscopy

Three-dimensional stacks were captured every 10 min for a total of 320 min upon NCS addition using the Leica DM6000 microscope with Leica CSU22 spinning disc and Andor Ixon 897 camera. Twenty different cells were imaged for each condition (±NCS).

Acknowledgements

We thank Harinder Singh (Genentech and University of California at San Francisco) for the ΔEMD-GFP-lacI plasmid, Naoko Imamoto for the POM121 plasmid (RIKEN Advanced Science Institute), Tom Misteli (National Cancer Institute, National Institutes of Health) for the cherry-lacI-BRG1 plasmid, Valérie Schreiber (École Supérieure de Biotechnologie de Strasbourg) for the XRCC1 and PARP1 antibodies, and Jop Kind (Hubrecht Institute) for the Dam-laminB/m6a-Tracer cell line. We thank Jiri and Claudia Lukas for critical reading of the manuscript, and the Soutoglou laboratory for helpful discussions. C.L. was supported by the Région Alsace and Fondation Association pour la Recherche sur le Cancer (ARC), K.T. received support from Marie Curie network address, and T.P. received support from Fondation pour la Recherche Médicale (FRM). Research in E.S.'s laboratory is supported by Agence Nationale de la Recherche (ANR), the Fondation Schlumberger pour l'Education et la Recherche (FSER), Fondation ARC (ARC fix), and La Ligue Contre le Cancer (Région). G.D.'s laboratory's contributions to this study were funded by a Discovery Grant (RGPIN 386049) from the Natural Sciences and Engineering Research Council (NSERC). K.M.A. is a recipient of a NSERC PGSD3 studentship and is a Killam Foundation Scholar. B.K.'s laboratory's contributions to this study were supported by the French Infrastructure for Integrated Structural Biology (FRISBI) (ANR-10-INSB-05-01) and Instruct as part of the European Strategy Forum on Research Infrastructures (ESFRI). B.R.-S.-M.'s laboratory's contributions to this study were supported by the FSER Fondation ARC and La Ligue Contre le Cancer.

References

Aymard F, Bugler B, Schmidt CK, Guillou E, Caron P, Briois S, Iacovoni JS, Daburon V, Miller KM, Jackson SP, et al. 2014. Transcriptionally active chromatin recruits homologous recombination at DNA double-strand breaks. *Nat Struct Mol Biol* **21:** 366–374.

Beucher A, Birraux J, Tchouandong L, Barton O, Shibata A, Conrad S, Goodarzi AA, Krempler A, Jeggo PA, Löbrich M. 2009. ATM and Artemis promote homologous recombination of radiation-induced DNA double-strand breaks in G2. *Embo J* **28:** 3413–3427.

Bickmore WA. 2013. The spatial organization of the human genome. *Annu Rev Genomics Hum Genet* **14:** 67–84.

Britton S, Coates J, Jackson SP. 2013. A new method for high-resolution imaging of Ku foci to decipher mechanisms of DNA double-strand break repair. *J Cell Biol* **202:** 579–595.

Bunting SF, Callén E, Wong N, Chen H-T, Polato F, Gunn A, Bothmer A, Feldhahn N, Fernandez-Capetillo O, Cao L, et al. 2010. 53BP1 inhibits homologous recombination in Brca1-deficient cells by blocking resection of DNA breaks. *Cell* **141:** 243–254.

Downloaded from genesdev.cshlp.org on May 8, 2015 - Published by Cold Spring Harbor Laboratory Press

Chapman JR, Taylor Martin RG, Boulton Simon J. 2012. Playing the end game: DNA double-strand break repair pathway choice. *Mol Cell* **47:** 497–510.

Chen L, Nievera CJ, Lee AY-L, Wu X. 2008. Cell cycle-dependent complex formation of BRCA1·CtIP·MRN is important for DNA double-strand break repair. *J Biol Chem* **283:** 7713–7720.

Chiolo I, Minoda A, Colmenares Serafin U, Polyzos A, Costes Sylvain V, Karpen Gary H. 2011. Double-strand breaks in heterochromatin move outside of a dynamic HP1a domain to complete recombinational repair. *Cell* **144:** 732–744.

Chubb JR, Boyle S, Perry P, Bickmore WA. 2002. Chromatin motion is constrained by association with nuclear compartments in human cells. *Curr Biol* **12:** 439–445.

Deng SK, Gibb B, de Almeida MJ, Greene EC, Symington LS. 2014. RPA antagonizes microhomology-mediated repair of DNA double-strand breaks. *Nat Struct Mol Biol* **21:** 405–412.

Dion V, Gasser SM. 2013. Chromatin movement in the maintenance of genome stability. *Cell* **152:** 1355–1364.

Dion V, Kalck V, Horigome C, Towbin BD, Gasser SM. 2012. Increased mobility of double-strand breaks requires Mec1, Rad9 and the homologous recombination machinery. *Nat Cell Biol* **14:** 502–509.

Finlan LE, Sproul D, Thomson I, Boyle S, Kerr E, Perry P, Ylstra B, Chubb JR, Bickmore WA. 2008. Recruitment to the nuclear periphery can alter expression of genes in human cells. *PLoS Genet* **4:** e1000039.

Folling J, Bossi M, Bock H, Medda R, Wurm CA, Hein B, Jakobs S, Eggeling C, Hell SW. 2008. Fluorescence nanoscopy by ground-state depletion and single-molecule return. *Nat Methods* **5:** 943–945.

Frit P, Barboule N, Yuan Y, Gomez D, Calsou P. 2014. Alternative end-joining pathway(s): Bricolage at DNA breaks. *DNA Repair* **17:** 81–97.

Geuting V, Reul C, Löbrich M. 2013. ATM release at resected double-strand breaks provides heterochromatin reconstitution to facilitate homologous recombination. *PLoS Genet* **9:** e1003667.

Goodarzi AA, Jeggo PA. 2012. The heterochromatic barrier to DNA double strand break repair: how to get the entry visa. *Int J Mol Sci* **13:** 11844–11860.

Horigome C, Oma Y, Konishi T, Schmid R, Marcomini I, Hauer MH, Dion V, Harata M, Gasser SM. 2014. SWR1 and INO80 chromatin remodelers contribute to DNA double-strand break perinuclear anchorage site choice. *Mol Cell* **55:** 626–639.

Jackson SP, Bartek J. 2009. The DNA-damage response in human biology and disease. *Nature* **461:** 1071–1078.

Jakob B, Splinter J, Conrad S, Voss KO, Zink D, Durante M, Löbrich M, Taucher-Scholz G. 2011. DNA double-strand breaks in heterochromatin elicit fast repair protein recruitment, histone H2AX phosphorylation and relocation to euchromatin. *Nucleic Acids Res* **39:** 6489–6499.

Jha DK, Strahl BD. 2014. An RNA polymerase II-coupled function for histone H3K36 methylation in checkpoint activation and DSB repair. *Nat Commun* doi: 1038/ncomms4965.

Kakarougkas A, Ismail A, Klement K, Goodarzi AA, Conrad S, Freire R, Shibata A, Lobrich M, Jeggo PA. 2013. Opposing roles for 53BP1 during homologous recombination. *Nucleic Acids Res* **41:** 9719–9731.

Kass EM, Jasin M. 2010. Collaboration and competition between DNA double-strand break repair pathways. *FEBS Lett* **584:** 3703–3708.

Khadaroo B, Teixeira MT, Luciano P, Eckert-Boulet N, Germann SM, Simon MN, Gallina I, Abdallah P, Gilson E, Geli V, et al. 2009. The DNA damage response at eroded telomeres and tethering to the nuclear pore complex. *Nat Cell Biol* **11:** 980–987.

Kind J, Pagie L, Ortabozkoyun H, Boyle S, de Vries SS, Janssen H, Amendola M, Nolen LD, Bickmore WA, van Steensel B. 2013. Single-cell dynamics of genome–nuclear lamina interactions. *Cell* **153:** 178–192.

Lemaître C, Soutoglou E. 2014. Double strand break (DSB) repair in heterochromatin and heterochromatin proteins in DSB repair. *DNA Repair* **19:** 163–168.

Lemaître C, Fischer B, Kalousi A, Hoffbeck AS, Guirouilh-Barbat J, Shahar OD, Genet D, Goldberg M, Betrand P, Lopez B, et al. 2012. The nucleoporin 153, a novel factor in double-strand break repair and DNA damage response. *Oncogene* **31:** 4803–4809.

Lieber MR. 2010. The mechanism of double-strand DNA break repair by the nonhomologous DNA end-joining pathway. *Annu Rev Biochem* **79:** 181–211.

Lisby M, Mortensen UH, Rothstein R. 2003. Colocalization of multiple DNA double-strand breaks at a single Rad52 repair centre. *Nat Cell Biol* **5:** 572–577.

Mahen R, Hattori H, Lee M, Sharma P, Jeyasekharan AD, Venkitaraman AR. 2013. A-type lamins maintain the positional stability of DNA damage repair foci in mammalian nuclei. *PLoS ONE* **8:** e61893.

Meuleman W, Peric-Hupkes D, Kind J, Beaudry JB, Pagie L, Kellis M, Reinders M, Wessels L, van Steensel B. 2013. Constitutive nuclear lamina–genome interactions are highly conserved and associated with A/T-rich sequence. *Genome Res* **23:** 270–280.

Mine-Hattab J, Rothstein R. 2012. Increased chromosome mobility facilitates homology search during recombination. *Nat Cell Biol* **14:** 510–517.

Misteli T, Soutoglou E. 2009. The emerging role of nuclear architecture in DNA repair and genome maintenance. *Nat Rev Mol Cell Biol* **10:** 243–254.

Nagai S, Dubrana K, Tsai-Pflugfelder M, Davidson MB, Roberts TM, Brown GW, Varela E, Hediger F, Gasser SM, Krogan NJ. 2008. Functional targeting of DNA damage to a nuclear pore-associated SUMO-dependent ubiquitin ligase. *Science* **322:** 597–602.

Neumann FR, Dion V, Gehlen LR, Tsai-Pflugfelder M, Schmid R, Taddei A, Gasser SM. 2012. Targeted INO80 enhances subnuclear chromatin movement and ectopic homologous recombination. *Genes Dev* **26:** 369–383.

Oza P, Jaspersen SL, Miele A, Dekker J, Peterson CL. 2009. Mechanisms that regulate localization of a DNA double-strand break to the nuclear periphery. *Genes Dev* **23:** 912–927.

Padeken J, Heun P. 2014. Nucleolus and nuclear periphery: velcro for heterochromatin. *Curr Opin Cell Biol* **28:** 54–60.

Pai CC, Deegan RS, Subramanian L, Gal C, Sarkar S, Blaikley EJ, Walker C, Hulme L, Bernhard E, Codlin S, et al. 2014. A histone H3K36 chromatin switch coordinates DNA double-strand break repair pathway choice. *Nat Commun* doi: 10.1038.ncomms5091.

Panier S, Boulton SJ. 2014. Double-strand break repair: 53BP1 comes into focus. *Nat Rev Mol Cell Biol* **15:** 7–18.

Pankotai T, Bonhomme C, Chen D, Soutoglou E. 2012. DNAPKcs-dependent arrest of RNA polymerase II transcription in the presence of DNA breaks. *Nat Struct Mol Biol* **19:** 276–282.

Parada LA, Misteli T. 2002. Chromosome positioning in the interphase nucleus. *Trends Cell Biol* **12:** 425–432.

Pfister SX, Ahrabi S, Zalmas LP, Sarkar S, Aymard F, Bachrati CZ, Helleday T, Legube G, La Thangue NB, Porter AC, et al.

Downloaded from genesdev.cshlp.org on May 8, 2015 - Published by Cold Spring Harbor Laboratory Press

2014. SETD2-dependent histone H3K36 trimethylation is required for homologous recombination repair and genome stability. *Cell Reports* **7:** 2006–2018.

Ptak C, Aitchison JD, Wozniak RW. 2014. The multifunctional nuclear pore complex: a platform for controlling gene expression. *Curr Opin Cell Biol* **28:** 46–53.

Reddy KL, Zullo JM, Bertolino E, Singh H. 2008. Transcriptional repression mediated by repositioning of genes to the nuclear lamina. *Nature* **452:** 243–247.

Rogakou EP, Pilch DR, Orr AH, Ivanova VS, Bonner WM. 1998. DNA double-stranded breaks induce histone H2AX phosphorylation on serine 139. *J Biol Chem* **273:** 5858–5868.

Roukos V, Misteli T. 2014. The biogenesis of chromosome translocations. *Nat Cell Biol* **16:** 293–300.

Roukos V, Voss TC, Schmidt CK, Lee S, Wangsa D, Misteli T. 2013. Spatial dynamics of chromosome translocations in living cells. *Science* **341:** 660–664.

San Filippo J, Sung P, Klein H. 2008. Mechanism of eukaryotic homologous recombination. *Annu Rev Biochem* **77:** 229–257.

Schober H, Ferreira H, Kalck V, Gehlen LR, Gasser SM. 2009. Yeast telomerase and the SUN domain protein Mps3 anchor telomeres and repress subtelomeric recombination. *Genes Dev* **23:** 928–938.

Soutoglou E, Misteli T. 2008. Activation of the cellular DNA damage response in the absence of DNA lesions. *Science* **320:** 1507–1510.

Soutoglou E, Dorn JF, Sengupta K, Jasin M, Nussenzweig A, Ried T, Danuser G, Misteli T. 2007. Positional stability of single double-strand breaks in mammalian cells. *Nat Cell Biol* **9:** 675–682.

Taddei A, Van Houwe G, Hediger F, Kalck V, Cubizolles F, Schober H, Gasser SM. 2006. Nuclear pore association confers optimal expression levels for an inducible yeast gene. *Nature* **441:** 774–778.

Therizols P, Fairhead C, Cabal GG, Genovesio A, Olivo-Marin JC, Dujon B, Fabre E. 2006. Telomere tethering at the nuclear periphery is essential for efficient DNA double strand break repair in subtelomeric region. *J Cell Biol* **172:** 189–199.

Zhang Y, Jasin M. 2011. An essential role for CtIP in chromosomal translocation formation through an alternative end-joining pathway. *Nat Struct Mol Biol* **18:** 80–84.

Aikaterini TSOUROULA

Double Strand Break Repair within constitutive heterochromatin

Résumé

L'hétérochromatine, de nature compacte et répétitive, limite l'accès à l'ADN et fait de la réparation des DSBs un processus difficile que les cellules doivent surmonter afin de maintenir leur intégrité génomique. Pour y étudier la réparation des DSBs, nous avons conçu un système CRISPR / Cas9 dans lequel les DSB peuvent être efficacement et spécifiquement induites dans l'hétérochromatine de fibroblastes de souris NIH3T3. En développant un système CRISPR / Cas9 hautement spécifique et robuste pour cibler l'hétérochromatine péricentrique, nous avons montré que les DSB en G1 sont positionnellement stables et réparés par NHEJ. En S / G2, ils se déplacent vers la périphérie de ce domaine pour être réparés par HR. Ce processus de relocalisation dépend de la résection et de l'exclusion de RAD51 du domaine central de l'hétérochromatine. Si ces cassures ne se relocalisent pas, elles sont réparées dans le cœur du domaine de l'hétérochromatine par NHEJ ou SSA. D'autre part, les DSBs dans l'hétérochromatine centromérique activent NHEJ et HR tout au long du cycle cellulaire. Nos résultats révèlent le choix de la voie de réparation différentielle entre l'hétérochromatine centromérique et péricentrique, ce qui régule également la position des DSBs.

Mots clés: Hétérochromatine, CRISPR/ Cas9, NHEJ, HR, RAD51, SSA

Résumé en anglais

Heterochromatin is the tightly packed form of repetitive DNA, essential for cell viability. Its highly compacted and repetitive nature renders DSB repair a challenging process that cells need to overcome in order to maintain their genome integrity. Developing a highly specific and robust CRISPR/Cas9 system to target pericentric heterochromatin, we showed that DSBs in G1 are positionally stable and repaired by NHEJ. In S/G2, they relocate to the periphery of this domain to be repaired by HR. This relocation process is dependent of resection and RAD51 exclusion from the core domain of heterochromatin. If these breaks fail to relocate, they are repaired within heterochromatin by NHEJ or SSA. On the other hand, DSBs in centromeric heterochromatin activate both NHEJ and HR throughout the cell cycle. Our results reveal the differential repair pathway choice between centromeric and pericentric heterochromatin that also regulates the DSB position.

Keywords: Heterochromatin, CRISPR/ Cas9, NHEJ, HR, RAD51, SSA